Natural product inhibitors of bacterial type-IV secretion systems and efflux pumps

AWO AFI KWAPONG

This thesis is submitted in partial fulfilment of the requirements for the degree of Doctor of Philosophy

2016

Department of Biological and Pharmaceutical Chemistry
UCL School of Pharmacy London

Thesis declaration form

This thesis describes research conducted in the UCL School of Pharmacy between October 2012 and April 2016 under the supervision of Prof. Simon Gibbons and Dr. Paul Stapleton. I certify that the work presented in this thesis is my own. Where information has been derived from other sources, I confirm that this has been clearly indicated in the thesis.

Signature:

Name: Awo Afi Kwapong

Date:

Dedication

This thesis is dedicated to my parents, Dr. & Mrs. Kwapong.

Acknowledgements

" For I know the plans I have for you," declares the LORD, "plans to prosper you and not to harm you, plans to give you hope and a future. Jeremiah 29:11." I thank the almighty God for His guidance and protection throughout this PhD. You are God and ever true to your word.

I thank my supervisors, Prof. Simon Gibbons and Dr. Paul Stapleton for their tutorship, support, encouragement, useful advice and discussions that have made this PhD a success. I am truly grateful.

To the School of Pharmacy, University of Ghana, Legon and Commonwealth Scholarship Commission, I say many thanks for granting me permission to pursue this PhD and for the financial support.

A huge thank you to Mr. Cory Beckwith for helping with the purchase of laboratory materials and maintenance of the laboratory equipment and to the members of the UCL School of Pharmacy: Student and Academic Support Office, Library, Stores, Computer Unit and the School Safety team. You all contributed in diverse ways to make my PhD project a reality.

Special thanks to Dr. Proma Khondkar (Postdoc), Sabine Heinrich (Departmental administrator) and to my PhD colleagues; Mansa, Arunotayanun, Blessing, Amaka, Jawal, Angela, Acom, Cynthia, Jeanne, Aljawharah, Andrea, Mukrish, Natchagorn, Cornelius, Tariq, Pedro, Sarah, Ihechi, Nattika, Stephen, Takahiro, Gizem and Vivek. You people made PhD fun and less stressful. To Mrs. Gugu Sibandze, a true friend, I say God bless you and your family. You stood by and supported me through it all, good and hard times. I am privileged to have met and worked with you in the same research group. My appreciation also goes to the MPharm and MSc students I was honoured to work with: Rebecca, Ify and Liying.

Finally, none of this would have been possible without the encouragement of my parents, Dr. & Mrs. Kwapong, my siblings: Mr. & Mrs. Gyan Kwapong, Dr. & Dr. (Mrs) Kyei and Mr. &

Mrs. Owusu-Nyamekye. I thank them for their understanding, listening ear and their steady love that supports me.

Abstract

Multidrug-resistance is a global health concern and in bacteria it may be conferred by the acquisition of multiple-drug resistance genes and/or by the action of multidrug-efflux pumps. The current study targeted these processes as a means to combat the spread of multidrug resistance genes among bacteria, and reinstate the efficacy of antibiotics against efflux-mediated drug-resistant strains. Our aim was therefore to isolate and characterise natural products that function by either inhibiting bacterial conjugation and/or by potentiating antibiotic activity against efflux-related multidrug-resistant (MDR) strains.

Selected medicinal plants, some of which have antibacterial properties (*Amoracia rusticana*, *Borago officinalis, Brassica oleracea*, *Lepidium sativum*, *Myristica lowiana*, *Sinapis alba*, *Uncaria tomentosa* and *Zingiber officinale*) were extracted with solvents of increasing polarity. The extracts were then screened against *Escherichia coli* conjugation pairs of donors (pKM101, IncN; TP114, $IncI_2$; pUB307, IncP; and R7K, IncW), and recipients (ER1793 and JM109), and *Staphylococcus aureus* strains expressing distinct efflux-related multidrug-resistance pumps; SA-1199B (NorA) and XU212 (TetK). The active extracts were further fractionated using various chromatographic techniques (Thin Layer Chromatography, Solid Phase Extraction, Vacuum Liquid Chromatography, Column Chromatography and High Performance Liquid Chromatography). The compounds, which were isolated from the bioactive fractions, were then characterized by the use of spectroscopic techniques (NMR, MS, IR and UV) and re-assessed for anti-conjugation and antibiotic potentiation activity.

The isolated glucosinolates from the *Brassica* plants showed moderate activity (10 - 50% reduction) against the conjugal transfer of the tested plasmids while the isothiocyanates, which are degradation products of the glucosinolates, showed better broad-range anti-conjugal activity. An amide, isolated from *M. lowiana*, showed significant anti-conjugal inhibitory activity (16.7 ± 2.0%) against the R7K plasmid. Its anti-conjugal activity was plasmid specific and non-toxic to human dermal fibroblasts, adult cells. In addition, a gingerol compound isolated from *Z. officinale*, the isolated amide from *M. lowiana*, and

benzyl isothiocyanate, significantly potentiated the activity of norfloxacin and tetracycline against SA-1199B (NorA) and XU212 (TetK), respectively. Their potentiation activity ranged from 2 to 512-fold.

In conclusion, the study identified natural product inhibitors of the type-IV secretion-related processes and efflux pump systems. Compounds with such anti-conjugative and antibiotic potentiation activity could help decrease the spread of multidrug resistance genes via conjugation and prolonging the efficacy of existing antibiotics.

Table of contents

Thesis declaration form ii

Dedication iii

Acknowledgements iv

Abstract vi

Table of contents viii

Table of figures xii

Table of tables xix

List of abbreviations xxi

Chapter 1 Introduction 1

1.1 Background 1

1.2 Antibiotic resistance 2

1.3 Genetic mechanisms of resistance 2

1.4 Biochemical mechanisms of resistance 4

1.5 The role of bacterial plasmid in antibiotic resistance 6

1.5.1 Bacterial conjugation 7

1.5.2 Inhibition of plasmid conjugation 10

1.6 Description of plasmids used in this study 12

1.7 The role of efflux pumps in antibiotic resistance 14

1.8 Importance of natural products in drug discovery 15

1.9 Description of plants used in this study 16

1.10 *Sinapis alba* L. 17

1.11 *Armoracia rusticana* G.Gaertn., B.Mey. & Scherb. 18

1.12 *Brassica oleracea* L. var. *italica* Plenck 20

1.13 *Lepidium sativum* L. 21

1.14 *Zingiber officinale* Roscoe 23

1.15 *Myristica lowiana* King 26

1.16 *Borago officinalis* L. 27

1.17 *Uncaria tomentosa* (Willd. ex Schult.) DC 29

1.18 Aims and objectives 31

Chapter 2 Materials and methods 33

2.1 Plant Material 33

2.2 Extraction 33

2.2.1 Soxhlet Extraction 33

2.2.2 Ultrasound-assisted Extraction (UAE) 35

2.2.3 Acid-base Extraction 35

2.2.4 Preparation of Dragendorff's reagent 36

2.3 Chromatographic Techniques 37

2.3.1 Thin Layer Chromatography (TLC) 37

2.3.2 Gravity Column Chromatography (CC) 38

2.3.3 Solid Phase Extraction (SPE) 40

2.3.4 Vacuum Liquid Chromatography (VLC) 41

2.3.5 High Performance Liquid Chromatography (HPLC) 42

2.4 Spectroscopic Methods 43

2.4.1 Nuclear Magnetic Resonance (NMR) Spectroscopy 43

2.4.2 Proton (^{1}H) NMR Spectroscopy 45

2.4.3 Carbon (^{13}C) NMR Spectroscopy 46

2.4.4 Distortionless Enhancement by Polarisation Transfer (DEPT-135) 47

2.4.5 Heteronuclear Multiple-Quantum Correlation (HMQC) Spectroscopy 47

2.4.6 Heteronuclear Multiple-Bond Correlation (HMBC) 52

2.4.7 Correlation Spectroscopy (COSY) 52

2.4.8 Nuclear Overhauser Effect Spectroscopy (NOESY) 52
2.5 Biological Methods 55
2.5.1 Bacterial and Fungal Strains 55
2.5.2 Minimum Inhibitory concentration assay 56
2.5.3 Antibiotic Potentiation Assay 57
2.5.4 Bacterial Plasmid Conjugation Inhibition Assay 58
2.5.5 Plasmid Elimination Assay 61
2.5.6 Cytotoxicity Testing 61

Chapter 3 Results and Discussion 63

3.1 Crude Extracts 63
3.2 Isolation and Structure Elucidation 65
3.2.1 Isolation from *S. alba* 65
3.2.2 Isolation from *A. rusticana* 79
3.2.3 Biosynthesis of glucosinolates 90
3.2.4 Isolation from *L. sativum* 92
3.2.5 Isolation from *Z. officinale* 103
3.2.6 Isolation from *B. officinalis* 112
3.2.7 Isolation from *U. tomentosa* 119
3.2.8 Isolation from *M. lowiana* 129
3.3 Biological evaluation 155
3.3.1 Antibacterial activity 155
3.3.2 Bacterial plasmid conjugation inhibition 168
3.3.3 Bacterial plasmid elimination studies 182
3.3.4 Antibiotic potentiation activity 184
3.3.5 Antifungal activity studies 185
3.3.6 Cytotoxicity studies of benzyl isothiocyanate and allyl isothiocyanate 186

Chapter 4 Conclusions 188

4.1 Conclusions and future work 188

References 192

Appendices 216

Appendix A: NMR and HRTOFESIMS spectra for **AK-5** 216

Appendix B: NMR and HRTOFESIMS spectra for **AK-6** 221

Appendix C: NMR and HRTOFESIMS spectra for **AK-7** 227

Appendix D: COSY and NOESY spectra for **AK-12** 232

Appendix E: COSY and NOESY spectra for **AK-13** 234

Appendix F: COSY and NOESY spectra for **AK-14** 236

Appendix G: MS spectra for the isolated compounds 238

Table of figures

Figure 1.1 Biochemical mechanisms of antibiotic resistance 6

Figure 1.2 Schematic diagram of bacterial conjugation 9

Figure 1.3 *Sinapis alba* seeds 17

Figure 1.4 *Armoracia rusticana* roots 19

Figure 1.5 *Brassica oleracea* var. *italica* plant 21

Figure 1.6 *Lepidium sativum* plant and seeds 22

Figure 1.7 *Zingiber officinale* rhizome 24

Figure 1.8 *Myristica lowiana* trunk and leaf 26

Figure 1.9 *Borago officinalis* plant 27

Figure 1.10 *Uncaria tomentosa* vine 29

Figure 2.1 Soxhlet extraction of *L. sativum* seeds 34

Figure 2.2 Liquid-liquid extraction of alkaloidal mixture from *U. tomentosa* methanol extract 36

Figure 2.3 Gravity column chromatograph of a *Z. officinale* chloroform extract 39

Figure 2.4 Solid phase extraction of a *M. lowiana* methanol extract 40

Figure 2.5 Vacuum liquid chromatography of *A. rusticana* chloroform extract 41

Figure 2.6 Structure for **AK-11** 44

Figure 2.7 ^{1}H NMR spectrum for **AK-11**, recorded in DMSO-d_6, 500 MHz 45

Figure 2.8 ^{13}C NMR spectrum for **AK-11** 48

Figure 2.9 DEPT-135 NMR spectrum for **AK-11** 49

Figure 2.10 HMQC NMR spectrum for **AK-11** 50

Figure 2.11 HMBC NMR spectrum for **AK-11** 51

Figure 2.12 COSY spectrum for **AK-11** 53

Figure 2.13 NOESY spectrum for **AK-11** 54

Figure 3.1 Structure for **AK-1** 65

Figure 3.2 ^{1}H NMR spectrum for **AK-1**, recorded in CD_3OD, 500 MHz 67

Figure 3.3 DEPT-135 NMR spectrum for **AK-1**, recorded in CD_3OD, 500 MHz 68

Figure 3.4 HMBC NMR spectrum for **AK-1** 69

Figure 3.5 COSY NMR spectrum for **AK-1** 70

Figure 3.6 HMBC (solid arrow) and NOESY (dotted arrow) correlations for **AK-1** 71

Figure 3.7 Structure for **AK-2** 72

Figure 3.8 ^{1}H NMR spectrum for **AK-2**, recorded in DMSO-d_6, 500 MHz 73

Figure 3.9 ^{13}C NMR spectrum for **AK-2**, recorded in DMSO-d_6, 500 MHz 74

Figure 3.10 HMQC NMR spectrum for **AK-2** 75

Figure 3.11 HMBC NMR spectrum for **AK-2** 76

Figure 3.12 COSY NMR spectrum for **AK-2** 77

Figure 3.13 Selected HMBC correlations for **AK-2** 78

Figure 3.14 Analytical TLC of VLC fractions from *A. rusticana* methanol extract 80

Figure 3.15 Structure for the alkenyl glucosinolate component of **AK-3** (compound **1**) 81

Figure 3.16 Structure for the aromatic glucosinolate component of **AK-3** (compound **2**) 81

Figure 3.17 ^{1}H NMR spectral comparison of **AK-3** (blue spectrum) with gluconasturtiin (green spectrum) and sinigrin (red spectrum) standards, recorded in methanol-d_4, 500 MHz 83

Figure 3.18 ESI-MS spectrum for the **AK-3** mixture in the negative ion mode 84

Figure 3.19 ^{1}H NMR spectrum for **AK-3** showing proton integration for compound **1** (labeled in black) and additional proton resonances for compound **2** (labeled in red) superimposed in the spectrum, recorded in CD_3OD, 500 MHz 85

Figure 3.20 DEPT-135 NMR spectrum for **AK-3**, with carbon resonances for compound **1** labeled in black and that of compound **2** in red 86

Figure 3.21 Selected HMBC correlations (solid arrows) for compound **1** of **AK-3** 87

Figure 3.22 Selected HMBC (solid arrows) correlations for compound **2** of **AK-3** 87

Figure 3.23 Biosynthetic pathway of glucosinolates 91

Figure 3.24 Analytical TLC of the column chromatography pool of fractions from *L. sativum* alkaloidal extract 92

Figure 3.25 Analytical TLC of the isolated imidazole alkaloids from pools D and E 93

Figure 3.26 Structure for **AK-4** and **AK-5** 93

Figure 3.27 Structure of **AK-6** and **AK-7** 95

Figure 3.28 ^{1}H NMR spectrum of the isolated imidazole alkaloids, recorded in CD_3OD, 500 MHz 97

Figure 3.29 ^{1}H NMR spectrum for **AK-4**, recorded in CD_3OD, 500 MHz 98

Figure 3.30 HMBC spectrum for **AK-4** 99

Figure 3.31 COSY NMR spectrum for **AK-4** 100

Figure 3.32 HMBC correlations for **AK-4** 101

Figure 3.33 Structures for the isolated gingerol compounds 104

Figure 3.34 ^{1}H NMR spectrum for **AK-8**, recorded in $CDCl_3$, 500 MHz 106

Figure 3.35 HMBC spectrum for **AK-8** 107

Figure 3.36 ^{1}H NMR spectrum for **AK-9**, recorded in CD_3OD, 500 MHz 109

Figure 3.37 ^{13}C NMR spectrum for **AK-9**, recorded in CD_3OD, 500 MHz 110

Figure 3.38 Selected HMBC correlations for **AK-9** 111

Figure 3.39 Structure for **AK-10** 113

Figure 3.40 ^{1}H NMR spectrum for **AK-10**, recorded in DMSO, 500 MHz 114

Figure 3.41 HMBC NMR spectrum for **AK-10** 115

Figure 3.42 NOESY NMR spectrum for **AK-10** 116

Figure 3.43 Selected HMBC (solid black arrow), COSY (solid red arrow) and NOESY (dotted black arrow) correlations for **AK-10** 117

Figure 3.44 Isolation scheme for *U. tomentosa* 119

Figure 3.45 The analytical HPLC chromatogram of UtSPE3-7CC3 120

Figure 3.46 Analytical TLC plates for the isolated oxindole compounds. 120

Figure 3.47 ^{1}H NMR spectrum for the isolated alkaloids, 500 MHz, **AK-11** to **-13** were recorded in DMSO and **AK-14** was recorded in CD_3OD 121

Figure 3.48 The core structure for the isolated oxindole alkaloids (**AK-11** to **-14**) 122

Figure 3.49 Selected HMBC correlations for **AK-11** 123

Figure 3.50 Structure for **AK-11** 126

Figure 3.51 Structure for **AK-12** 127

Figure 3.52 Structure for **AK-14** 128

Figure 3.53 Tentative structure for **AK-13** 129

Figure 3.54 Structure for **AK-15** 130

Figure 3.55 Selected HMBC correlations for **AK-15** 131

Figure 3.56 HMQC NMR spectrum for **AK-15**, recorded in CD_3OD, 500 MHz 133

Figure 3.57 Structure for **AK-16** 134

Figure 3.58 ^{1}H NMR spectrum for **AK-16**, recorded in CD_3OD, 500 MHz 136

Figure 3.59 HMBC NMR spectrum for **AK-16** 137

Figure 3.60 Selected HMBC correlations for **AK-16** 138

Figure 3.61 Structure for **AK-17** 139

Figure 3.62 ^{1}H NMR spectrum for **AK-17**, recorded in DMSO, 500 MHz 140

Figure 3.63 HMBC spectrum for **AK-17** 141

Figure 3.64 Structure for **AK-18** 143

Figure 3.65 ^{1}H NMR spectrum for **AK-18**, recorded in DMSO, 500 MHz 145

Figure 3.66 HMBC NMR spectrum for **AK-18** 146

Figure 3.67 NOESY NMR spectrum for **AK-18** 147

Figure 3.68 Selected HMBC correlations for **AK-18** 149

Figure 3.69 Amphipathic nature of *M. lowiana* hexane extract compound (**AK-17**) 155

Figure 3.70 Structure of quinolone molecule and the isolated gingerols 160

Figure 3.71 The core structure of a flavone with the substituent groups for the isolated flavones (**AK-10** and **AK-15**) indicated beneath 161

Figure 3.72 Structures showing the resemblance among the compounds, the isolated guaiacin, nor-isoguaiacin and dihydroguaiaretic acid (the red rings indicate the structural differences in comparison to guaiacin) 162

Figure 3.73 Chemical structures of selected isothiocyanates 163

Figure 3.74 Chemical structures of the other selected compounds 164

Figure 3.75 Generalised scheme for glucosinolate hydrolysis 165

Figure 3.76 Structures of the compounds, which actively inhibited the conjugal transfer of IncN plasmid pKM101 168

Figure 3.77 The influence of the natural products on the conjugal transfer of IncN plasmid pKM101 170

Figure 3.78 Structures of linoleic acid and novobiocin 171

Figure 3.79 Structure of coumermycin 171

Figure 3.80 Structures of the compounds, which actively inhibited the conjugal transfer of IncP plasmid pUB307 173

Figure 3.81 The influence of the natural products on the conjugal transfer of $IncI_2$ plasmid TP114 174

Figure 3.82 The influence of the natural products on the conjugal transfer of IncP plasmid pUB307 175

Figure 3.83 The influence of the natural products on the conjugal transfer of IncW plasmid R7K 176

Figure 3.84 Structures of the compounds, which showed appreciable inhibition against IncW plasmid R7K 177

Figure 3.85 The effect of varying concentrations of BITC on the conjugal transfer of plasmids pKM101 (IncN), TP114 (IncI$_2$) and pUB207 (IncP) 179

Figure 3.86 The effect of varying concentrations of 4-methoxyphenyl isothiocyanate on the conjugal transfer of IncP plasmid pUB207 180

Figure 3.87 The effect of varying concentrations of **AK-17** on the conjugal transfer of IncW plasmid R7K 181

Figure 3.88 Cytotoxicity study using HDFa cells 187

Figure A.1 ^{1}H NMR spectrum for **AK-5**, recorded in CD_3OD, 500 MHz 216

Figure A.2 DEPT-135 spectrum for **AK-5** 217

Figure A.3 HMQC spectrum for **AK-5** 218

Figure A.4 HMBC spectrum for **AK-5** 219

Figure A.5 HRTOFESIMS spectrum for **AK-5** 220

Figure A.6 ^{1}H NMR spectrum for **AK-6**, recorded in CD_3OD, 500 MHz 221

Figure A.7 DEPT-135 NMR spectrum for **AK-6** 222

Figure A.8 HMQC NMR spectrum for **AK-6** 223

Figure A.9 HMBC NMR spectrum for **AK-6** 224

Figure A.10 HRTOFESIMS spectrum for **AK-6** 225

Figure A.11 ESI-MS spectrum for **AK-6** 226

Figure A.12 ^{1}H NMR spectrum for **AK-7**, recorded in CD_3OD, 500 MHz 227

Figure A.13 DEPT-135 NMR spectrum for **AK-7** 228

Figure A.14 HMQC NMR spectrum for **AK-7** 229

Figure A.15 HMBC NMR spectrum for **AK-7** 230

Figure A.16 ESI-MS NMR spectrum for **AK-7** 231

Figure A.17 COSY NMR spectrum for **AK-12** 232

Figure A.18 NOESY NMR spectrum for **AK-12** 233

Figure A.19 COSY NMR spectrum for **AK-13** 234

Figure A.20 NOESY NMR spectrum for **AK-13** 235

Figure A.21 COSY NMR spectrum for **AK-14** 236

Figure A.22 NOESY NMR spectrum for **AK-14** 237

Figure A.23 HRTOFESIMS spectrum for **AK-1** 238

Figure A.24 HRTOFESIMS spectrum for **AK-2** 239

Figure A.25 ESI-MS spectrum for **AK-8** 240

Figure A.26 HRTOFESIMS spectrum for **AK-9** 241

Figure A.27 HRTOFESIMS spectrum for **AK-10** 242

Figure A.28 ESI-MS spectrum for **AK-11** 243

Figure A.29 ESI-MS spectrum for **AK-12** 244

Figure A.30 HRTOFESIMS spectrum for **AK-13** 245

Figure A.31 HRTOFESIMS spectrum for **AK-15** 246

Figure A.32 HRTOFESIMS spectrum for **AK-16** 247

Figure A.33 HRTOFESIMS spectrum for **AK-17** 248

Figure A.34 ESI-MS spectrum for **AK-18** 249

Table of tables

Table 2.1 Summary of the plants used, their source, part and voucher or batch number 33

Table 2.2 Chemical shifts of NMR solvent signals used in this study 44

Table 2.3 Summary of bacterial and fungal strains used 55

Table 2.4 Summary of *E. coli* strains and plasmids used 59

Table 3.1 The effects of plant extracts on the conjugal transfer of selected plasmids 64

Table 3.2 ^{1}H and ^{13}C NMR spectral data (ppm) and HMBC correlations of **AK-1**, recorded in methanol-d_4 71

Table 3.3 ^{1}H NMR (coupling constant, Hz) and ^{13}C NMR spectral data (ppm) and HMBC correlations of **AK-2,** recorded in DMSO-d_6 79

Table 3.4 ^{1}H and ^{13}C NMR spectral data (ppm) and HMBC correlations of **AK-3** compounds **1**, recorded in methanol-d_4 88

Table 3.5 ^{1}H and ^{13}C NMR spectral data (ppm) and HMBC correlations of **AK-3** compounds **2**, recorded in methanol-d_4 89

Table 3.6 ^{1}H NMR spectral data (ppm) and coupling constants (Hz) of the isolated dimeric imidazole alkaloids, recorded in methanol-d_4 101

Table 3.7 ^{13}C NMR spectral data (ppm) of the isolated dimeric imidazole alkaloids, recorded in methanol-d_4 102

Table 3.8 HMBC correlations (^{2}J, ^{3}J and ^{4}J) of the isolated dimeric imidazole alkaloids, recorded in methanol-d_4 103

Table 3.9 ^{1}H (coupling constants, Hz) and ^{13}C NMR spectral data (ppm) and HMBC correlations of **AK-8**, recorded in chloroform-*d* 108

Table 3.10 ^{1}H (coupling constants, Hz) and ^{13}C NMR spectral data (ppm) and HMBC correlations of **AK-9**, recorded in methanol-d_4 111

Table 3.11 ^{1}H (coupling constants, Hz) and ^{13}C NMR spectral data (ppm) and HMBC correlations of **AK-10**, recorded in DMSO-d_6 118

Table 3.12 ^{1}H (coupling constants, Hz) and ^{13}C NMR spectral data (ppm) and HMBC correlations of **AK-11**, recorded in DMSO-d_6 125

Table 3.13 ^{1}H (coupling constants, Hz) and ^{13}C NMR spectral data (ppm) and HMBC correlations of **AK-15**, recorded in methanol-d_4 132

Table 3.14 ^{1}H (coupling constants, Hz) and ^{13}C NMR spectral data (ppm) and HMBC correlations of **AK-16**, recorded in methanol-d_4 138

Table 3.15 ^{1}H (coupling constants, Hz) and ^{13}C NMR spectral data (ppm) and HMBC correlations of **AK-17**, recorded in DMSO-d_6 142

Table 3.16 ^{1}H (coupling constants, Hz) and ^{13}C NMR spectral data (ppm) and HMBC correlations of **AK-18**, recorded in DMSO-d_6 148

Table 3.17 The MIC values of the crude extract against *S. aureus* strains 156

Table 3.18 The MIC values of the isolated compounds against *S. aureus* and *E. coli*..... 158

Table 3.19 The MIC values of the selected isothiocyanates and other compounds against *S. aureus* and *E. coli*..... 164

Table 3.20 Plasmid elimination activity of selected compounds..... 182

Table 3.21 Antibiotic potentiation activity of selected compounds 184

Table 3.22 Antifungal activity of selected compounds..... 186

List of abbreviations

ABC	ATP-Binding Cassette
AMR	Antimicrobial Resistance
AITC	Allyl isothiocyanate
Cfu	Colony Forming Unit
$CHCl_3$	Chloroform
COSY	Correlation Spectroscopy
BITC	Benzyl isothiocyanate
d	Doublet
δ	Chemical Shift
1D	One Dimensional
2D	Two Dimensional
DEPT	Distortionless Enhancement by Polarisation Transfer
DHCA	Dehydrocrepenyic Acid
DMEM	Dulbecco's Modified Eagle's Medium
DMSO	Dimethylsulphoxide
DNA	Deoxyribonucleic Acid
ESBLs	Extended-Spectrum Beta-Lactamases
ESI	Electrospray Ionisation
EtOAc	Ethyl acetate
FBS	Fetal Bovine Serum
HDFa	Human Dermal Fibroblasts, adult
HMBC	Heteronuclear Multiple-Bond Correlation

HMQC	Heteronuclear Multiple-Quantum Correlation
HPLC	High Performance Liquid Chromatography
HRESIMS	High Resolution Electrospray Ionisation Mass Spectrometry
Hz	Hertz
Inc	Incompatibility
IR	Infrared
J	Coupling Constant
LB	Luria Bertani
m	Multiplet
MATE	Multidrug And Toxic-Compound Extrusion
MDR	Multidrug-Resistance
MeOH	Methanol
MFS	Major Facilitator Superfamily
MHB	Mueller Hinton Broth
MHz	Megahertz
MIC	Minimum Inhibitory Concentration
MRSA	Methicillin-Resistant *Staphylococcus aureus*
MS	Mass Spectrometry
MTT	3-(4,5-Dimethylthiazol-2-yl)-2,5- diphenyltetrazolium bromide
NEAA	Non-Essential Amino Acids
NMR	Nuclear Magnetic Resonance
NOESY	Nuclear Overhauser Effect Spectroscopy
OD	Optical Density

PBS	Phosphate Buffered Saline
PEITC	Phenylethyl isothiocyanate
ppm	Parts per million
q	Quartet
R*f*	Retention Factor
RNA	Ribonucleic Acid
RPMI	Roswell Park Memorial Institute
S	Singlet
SFN	Sulforaphane
SIC	Sub-Inhibitory Concentration
SMR	Small Multidrug-Resistance
SPE	Solid Phase Extraction
t	Triplet
TA	Toxin-Antitoxin
TCA	Trichloroacetic
T4SS	Type IV Secretion System
TLC	Thin Layer Chromatography
UV	Ultraviolet
VLC	Vacuum Liquid Chromatography
VRE	Vancomycin-Resistant enterococci
VRSA	Vancomycin-Resistant *Staphylococcus aureus*
XDR	Extensively Drug-Resistant

Chapter 1 Introduction

1.1 Background

One would expect that with the large number of available antibiotics, the fight against infectious diseases would be a thing of the past. Unfortunately that is not what we see in our world today; rather there is a continual rise of antibiotic-resistant infections and a decline in the development of new antimicrobials to curb this public health issue (Spellberg *et al*., 2008; Boucher *et al*., 2009; CDC, 2013). What makes this alarming is the rise of multidrug-resistant (MDR) strains for almost all pathogenic bacteria in our hospitals and communities, a clear indication that bacteria have evolved (Levy and Marshall, 2004; CDC, 2013). Notable examples of such evolved bacteria include MDR strains of *Acinetobacter baumanii*, *Enterococcus faecalis*, *Enterococcus faecium*, *Escherichia coli*, *Klebsiella pneumoniae*, *Mycobacterium tuberculosis*, *Neisseria gonorrhoeae*, *Pseudomonas aeruginosa*, and *Staphylococcus aureus* (Levy and Marshall, 2004; WHO, 2011; CDC, 2013).

In 2013, the Center for Disease Control and Prevention (CDC) released an epidemiological report which showed that more than 2 million people acquire antibiotic-resistant infections each year in the United States, and 23,000 of them die because the existing antibiotics are no longer effective against these infections (CDC, 2013). In Europe, antibiotic-resistant bacteria are estimated to cause 25,000 deaths each year (WHO, 2015). Although reliable estimates of deaths caused by antibiotic-resistant bacteria in the developing world are not available (Gelbrand *et al*., 2015), it has been predicted that by the year 2050, 300 million lives will be lost to antimicrobial-resistant infections if nothing is done about this public health issue (O'Neill, 2014). These facts show the gravity of antibiotic resistance in our world today and the urgent need for new classes of antibiotics with new modes of actions or new strategies to combat bacteria and drug resistance.

1.2 Antibiotic resistance

Antibiotic resistance is defined by World Health Organisation (WHO) as the ability of microorganisms to withstand the therapeutic effect of antibiotics to which they were originally susceptible (WHO, 2015). Bacteria acquire resistance genes through genetic mechanisms and achieve resistance through biochemical mechanisms. The genetic mechanisms include spontaneous mutation and acquisition of new DNA through horizontal gene transfer mechanism (Tenover, 2006). The biochemical mechanisms include antibiotic inactivation, decreased drug accessibility, alteration of antibiotic target, metabolic bypass and development of tolerance (Mcmanus, 1997).

Pathogenic bacteria are classified as multidrug-resistant when they are able to withstand the therapeutic effect of at least one agent in three or more antimicrobial classes, despite their earlier sensitivity to them (Magiorakos *et al.*, 2012). This type of resistance is generated by "the accumulation of multiple resistant genes on mobile genetic elements such as plasmids or transposons within a cell and/ or by the increased expression of genes that encode for multidrug-efflux pumps" (Nikaido, 2009). Although MDR is a natural phenomenon, its increased prevalence is due to the inappropriate use of antibiotics both in the clinical and agricultural sectors, and the use of antibacterial cleaning agents in our homes (Levy, 2002). The inappropriate use of antibiotics contributes to selective inhibition of susceptible microorganisms and the selection of resistant strains bearing antibiotic resistant genes and this is the major cause of today's antibiotic resistance crisis (Levy and Marshall, 2004).

1.3 Genetic mechanisms of resistance

Genetic mechanisms of bacterial resistance may be classified into two groups, intrinsic or acquired resistance. Intrinsic resistance is bestowed in bacteria by innate genes found on their chromosome (Alekshun and Levy, 2007). It is a stable genetic property, which is shared by all members of the genus (Mcmanus, 1997). Notable examples are chromosomal AmpC

β-lactamase genes of Gram-negative bacteria and the many multidrug-resistant efflux systems (Jacoby and Munoz-Price, 2005).

Acquired resistance involves mutational changes in the bacterial DNA and/ or the acquisition of resistance genes borne on genetic elements, which are mobile such as plasmids, bacteriophages and transposons (Alekshun and Levy, 2007). This type of resistance results in the bacteria expressing new phenotypic features such as resistance to antibiotics, to which they were originally sensitive (Mcmanus, 1997). The resistance acquired through mutations is less frequent as there are cellular mechanisms to repair chromosomal changes (Shafran, 1990). Examples of resistance acquired through mutations include fluoroquinolone resistance resulting from mutations within the drug's targets, DNA gyrase and topoisomerase IV (Hooper, 2000), rifampicin resistance through a point mutation in the rifampicin-binding region of RpoB (β subunit of RNA polymerase) in *Mycobacterium tuberculosis* (Sharma and Mohan, 2006) and tetracycline resistance through a point mutation in the 16S rRNA operon of *Propionibacterium* acnes (Ross *et al*., 1998) and *Helicobacter pylori* (Gerrits *et al*., 2002).

Bacteria acquire resistance genes through the horizontal gene transfer mechanisms such as conjugation, transduction and transformation (Amabile-Cuevas, 2013). In conjugation, resistance genes borne on plasmids (an extra-chromosomal element) are transferred through conjugative pili from one bacterium to another (Mcmanus, 1997; Alekshun and Levy, 2007). An example of this is the conjugative plasmid transfer of the tetracycline-resistance gene, *tetM* from enterococci and *Mycoplasma* species to gonococci (Neu, 1992). In transduction, a bacteriophage aids in the transfer of resistances genes of plasmid or chromosomal origin from one bacterium to another (Mcmanus, 1997; Alekshun and Levy, 2007). Transformation is the process in which the bacterium picks up resistance genetic material from the environment (Furuya and Lowy, 2006). This process is reported to be the underlying cause of penicillin-resistance in pneumococci and *Neisseria* species (Spratt, 1994). These resistance genes, when acquired, can be integrated into the bacterial chromosome or they can be maintained as extra chromosomal material on a bacterial plasmid and stably transferred from generation to generation.

1.4 Biochemical mechanisms of resistance

Antibiotic resistance can also be classified based on biochemical mechanisms. This is purely dependent on the mode of action exhibited by the resistant strains. Biochemical mechanisms of resistance can be grouped into five classes: antibiotic inactivation, decreased antibiotic accessibility, alteration of antibiotic target, metabolic bypass, and development of tolerance (Mcmanus, 1997).

Some bacterial strains resist antibiotics by producing enzymes that inactivate or degrade them. This has been demonstrated for some bacterial enzymes, examples are the β-lactamases, the aminoglycoside-modifying enzymes (*O*-adenyltransferases, *N*-acetyltransferases and *O*-phosphotransferases) and the chloramphenicol acetyltransferases (Giedraitienė *et al*., 2011). β-lactamases hydrolyse β-lactam antimicrobials, rendering these antibiotics inactive (Bradford, 2001). *N*-acetyltransferase catalyse acetyl CoA-dependent acetylation of the amino group of the 2-deoxystreptamine nucleus of aminoglycosides (Mingeot-Leclercq *et al*., 1999). While the *O*-adenyltransferase and *O*-phosphotransferase catalyse an ATP-dependent adenylation or phosphorylation of the hydroxyl group of the 2-deoxystreptamine nucleus of aminoglycosides, respectively (Cox and Serpersu, 1997; Mingeot-Leclercq *et al*., 1999). The action of these enzymes lead to the modification of the aminoglycoside nucleus which results in reduced binding affinity for their target site, the 30S ribosomal unit of the bacteria (Tolmasky, 2000; Giedraitienė *et al*., 2011). Chloramphenicol acetyltransferases on the other hand elicit their activity by covalently binding an acetyl group to chloramphenicol molecule (Giedraitienė *et al*., 2011). This decreases the binding ability of chloramphenicol for its target site, the 50S ribosomes and in doing so it renders chloramphenicol therapeutically ineffective.

By virtue of the membrane characteristics of bacteria, they are able to limit the access of certain antimicrobials (Delcour, 2009). The outer lipopolysaccharide membrane and cell membrane porins of the Gram-negative bacteria offer intrinsic resistance to the diffusion of hydrophilic solutes and penetration of hydrophobic solutes, respectively (Nikaido, 1985;

Hancock, 1997), while the Gram-positive bacteria have a thick peptidoglycan layer which offers little resistance to the diffusion of small molecules because of its coarse meshwork (Nikaido, 1994). Both Gram-negative and Gram-positive bacteria have efflux pumps interspersed in their outer membrane. The efflux pumps expel a wide variety of structurally unrelated drugs out of a bacterium, which contributes to their intrinsic resistance. Examples of this type of resistance is the expulsion of β-lactams, tetracyclines and aminoglycosides from Gram-negative through efflux pumps (McMurry *et al.*, 1980; Poole, 2004).

Other bacteria also achieve resistance by altering or modifying the target site of action. This is well demonstrated in macrolide-resistant *Streptococcus pneumoniae*, where the 23S mRNA subunit is altered by methylases leading to decreased binding affinity of the macrolides (Neu, 1992).

Metabolic bypass and tolerance are the last of the mentioned biochemical mechanisms of resistance. In metabolic bypass, bacteria produce new enzymes that are not susceptible to existing antibiotics for example, expression of a new dihydrofolate reductase or dihydropteroate synthetase that are not susceptible to trimethoprim-sulfamethoxazole and sulfonamides, respectively (Mcmanus, 1997; Giedraitienė *et al.*, 2011). Tolerance is the ability of bacteria to resist the therapeutic effect of antibiotics due to its physiological growth state so that bactericidal agent is no longer able to kill the bacteria but rather cause growth inhibition and upon withdrawal of the antibiotic the bacteria resume normal activity such as recurrence of infection. An example is the tolerance of non-growing pneumococci to β-lactams (Tuomanen and Tomasz, 1990). The various biochemical mechanisms of resistance are illustrated in Figure 1.1.

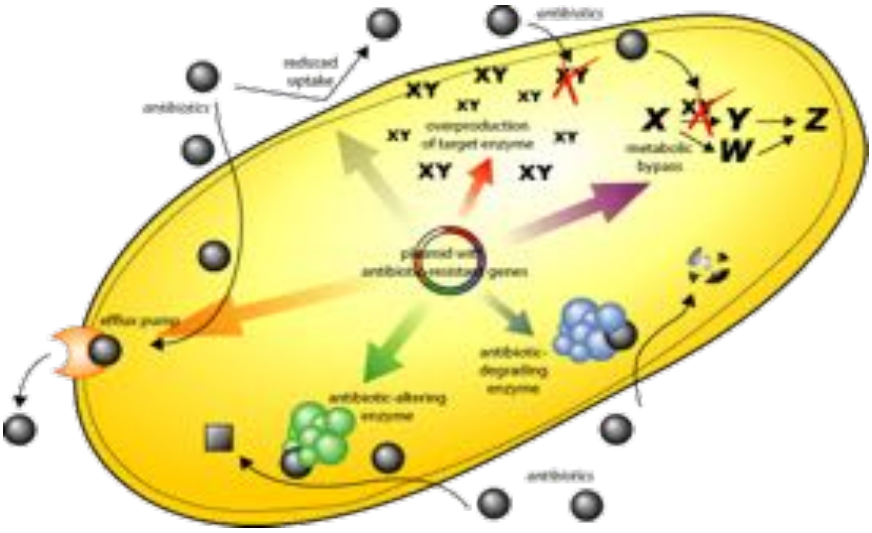

Figure 1.1 Biochemical mechanisms of antibiotic resistance (Sarawilcox, 2006)

1.5 The role of bacterial plasmid in antibiotic resistance

Bacterial plasmids are small genetic elements that exist and replicate independent of their host's chromosomal DNA (Bennett, 2008). Most plasmids are double-stranded DNA molecules and are usually circular, but some do exist in the linear form (Kinashi *et al.*, 1993; Bennett, 2008). Plasmids vary in size from 1 to more than 100 kilobase pairs and they serve as a platform for the assembling and re-assorting of genes (Bennett, 2008). The genes found on plasmids encode for antibiotic-resistance, bacterial conjugation, virulence and a variety of other functions (Bennett, 2008; Thomas and Summers, 2008). These plasmid-encoded functions promote the survival of the plasmid and their host cell in a wide range of hostile environments (Thomas and Summers, 2008).

Plasmid-mediated conjugation and the transfer of multidrug-resistant genes was first identified in the 1950s and 1960s in a recombination study of *E. coli* K12 (Summers, 2009). With time, this process has contributed to the rapid spread of antibiotic resistant genes among bacteria, and even from bacteria to yeast (Heinemann and Sprague Jr, 1989; Mazodier and Davies, 1991). Notable evidence of plasmid-mediated resistance in clinically

relevant pathogens include plasmid pMG252 transfer of low-level quinolone-resistant genes, qnr from *K. pneumoniae* to the Enterobacteriaceae and *P. aureginosa* (Rodriguez-Martinez *et al.*, 2003; Wang *et al.*, 2003; Wang *et al.*, 2004), plasmid pAT191 transfer of kanamycin-resistant genes from *E. faecalis* to *E. coli* (Doucet-Populaire *et al.,* 1992), the conjugative transfer of kanamycin, penicillin and tetracycline resistance genes among patient isolates of *Klebsiella* (as plasmid RK2) and *Pseudomonas* (as plasmid RP4) (Ingram *et al.*, 1973; Waters, 1999), and the conjugative transfer of multidrug-resistant plasmids from vancomycin-resistant enterococci to a clinical isolate of methicillin-resistant *S. aureus* (MRSA) (Weigel *et al.*, 2003; Weigel *et al.*, 2007). Other clinical examples of plasmid-mediated transfer of antibiotic resistance genes in pathogenic bacteria are the *K. pneumoniae* EK105 and *Yersinia pestis* 17/95 (Tolmasky *et al.*, 1986; Galimand *et al.*, 1997). Both of these microorganisms are multidrug-resistant and they cause infections leading to high mortality (Waters, 1999). The *K. pneumoniae* JHCK1 strain bears both mobilizable plasmid and a conjugative plasmid, and these encode for resistance to ampicillin, amikacin, gentamicin, mezlocillin, oxacillin, netilmicin, kanamycin, chloramphenicol, tobramycin and streptomycin (Tolmasky *et al.*, 1986). *Y. pestis* 17/95 carries plasmid pIP1202 which encodes for resistance to ampicillin, chloramphenicol, kanamycin, minocycline, spectinomycin, streptomycin, sulfonamides and tetracycline (Galimand *et al.*, 1997). These few examples show the extent and relevance of plasmid-mediated conjugation to the dissemination of antibiotic resistance genes and the need to inhibit this process as a strategy to curtail the spread and rise in antibiotic resistance.

1.5.1 Bacterial conjugation

Bacterial conjugation allows the transfer of genetic material from one bacterium to another through cell-cell contact (Waters, 1999; Alvarez-Martinez and Christie, 2009). This process is mediated by self-transmissible plasmids (also known as conjugative plasmids) and it occurs in both Gram-negative and Gram-positive bacteria, as well as in wall-less bacteria and the

members of the phylum *Crenarchaeota* of the *Archaea* (Frost *et al.*, 2005; Alvarez-Martinez and Christie, 2009). A plasmid is characterized as self-transmissible when it carries the essential genes for conjugation; the mobility (MOB) genes also known as DNA transfer and replication (Dtr) genes and the mating pair formation (MPF) genes (Smillie *et al.*, 2010). For the purpose of this study, discussion will be limited to conjugation systems of the Gram-negative bacteria, which primarily use the type-IV secretion systems (T4SS) for plasmid transfer.

Water (1999) conceptualized conjugation in Gram-negative bacteria into four sub-processes namely;

- contact between the donor and the recipient cell and the formation of the conjugation pilus,
- enzyme mediated nick within the *oriT* (origin of transfer) of one of the strands of the conjugative plasmid,
- conjugative replication and the transfer of the nicked DNA strand to the recipient and re-cirularization,
- formation of a complementary DNA strand in the recipient (Waters, 1999).

The conjugation process commences with a donor to recipient cell contact, transfer genes on the donor conjugative plasmid encodes for the formation of a conjugative pilus (a complex multi-protein structure) (Waters, 1999; Thomas and Summers, 2008; Alvarez-Martinez and Christie, 2009; Arutyunov and Frost, 2013). This conjugative pilus connects the cytoplasmic compartments of both the donor and recipient bacteria and serves as a transfer pore (Waters, 1999). The interaction between the cells then triggers the release of DNA transfer and replication (Dtr) proteins including a relaxase enzyme, which binds onto the origin of transfer (*oriT*) of the conjugative plasmid, this DNA-enzyme complex is known as the relaxosomes (Alvarez-Martinez and Christie, 2009). The relaxase enzyme then mediates a nick at the *oriT* of a single strand of the conjugative plasmid (Waters, 1999; Alvarez-Martinez and Christie, 2009; Arutyunov and Frost, 2013). The nicked strand (T-strand), still with the

relaxase enzyme covalently attached to its 5' terminus is unwound into a relaxed open DNA strand and transferred to the recipient cell through the conjugative pili (Waters, 1999; Alvarez-Martinez and Christie, 2009; Fronzes *et al.*, 2009). Re-circularization of the nicked strands then starts at the conjugative pili on the recipient side; this process is catalyzed by the relaxase (Alvarez-Martinez and Christie, 2009). The nicking of the conjugative pili supplies the 3' terminus end of the T-strand for the complete circularization (Waters, 1999). This then releases a circular form of single stranded DNA into the recipient cell. Finally, both donor and recipient cells synthesize complementary strands so that each cell would have a double stranded plasmid (Waters, 1999). Figure 1.2 shows the processes involve in bacterial conjugation.

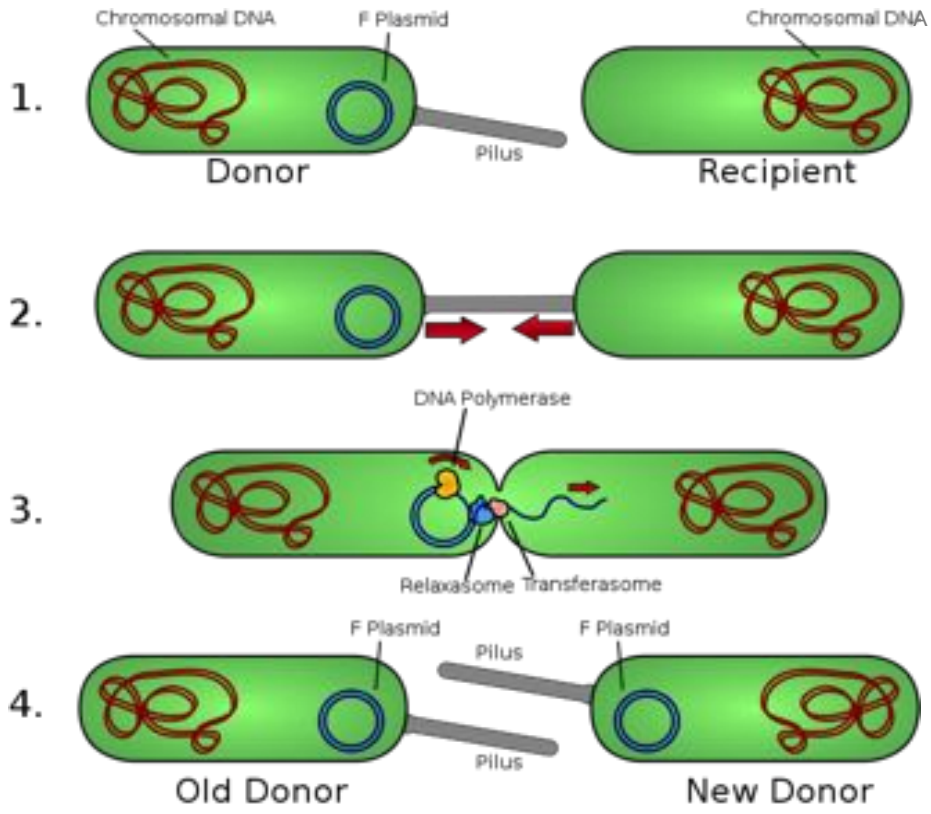

Figure 1.2 Schematic diagram of bacterial conjugation (en.wikipedia.org, 2010)

1.5.2 Inhibition of plasmid conjugation

Inhibition of plasmid conjugation is an approach that aims to prevent the spread of antibiotic resistance gene amongst bacteria (Fernandez-Lopez *et al.*, 2005; Smith and Romesberg, 2007). This approach would not necessarily kill resistant microorganisms but rather prevent an increase in the number of plasmid-containing cells in a bacterial population, a means to re-establish the antibiotic-susceptible populations and reinstate the efficacy of existing antibiotics.

This approach of plasmid conjugal inhibition has not received much attention but studies so far have led to the identification of two types of chemical compound inhibitors, the non-specific and the specific conjugal inhibitors. The specific inhibitors achieve anti-conjugal activity by targeting specific components (Lujan *et al.*, 2007) or the overall conjugation process (Fernandez-Lopez *et al.*, 2005; Getino *et al.*, 2015) while the non-specific inhibitors achieve activity by non-selective processes.

The non-specific conjugal inhibitors include nifurzide (**1**) a nitrofuran, which showed anti-conjugal activity against R plasmid transfer between *E. coli* strains for plasmids of nine different incompatibility groups (Michel-Briand and Laportf, 1985). Its conjugal inhibitory activity was attributed to its reduced -NO_2 group (Michel-Briand and Laportf, 1985). Nalidixic acid (**2**), norfloxacin (**3**) and pipemidic acid (**4**) have been reported to inhibit the conjugal transfer of R plasmids of different incompatibility groups of *P. aeruginosa* and *E. coli* (Nakamura *et al.*, 1976; Hirai *et al.*, 1984).

Novobiocin (**5**) and coumermycin (**6**) have been reported to inhibit the conjugal transfer of plasmids pKM101, TP114 and pUB307 (Maree *et al.*, 2014) and R64drd-11(Hooper *et al.*, 1989) in *E. coli* by targeting the DNA gyrase. Although these compounds do not specifically target the conjugation machinery, they are able to inhibit plasmid conjugation as they interact with the DNA and functioning DNA gyrase has been shown to be essential for bacterial conjugation hence the their anti-conjugal activity (Hooper *et al.*, 1989).

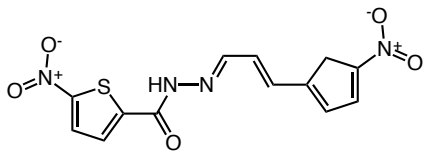

1

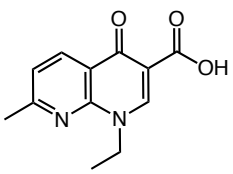

2

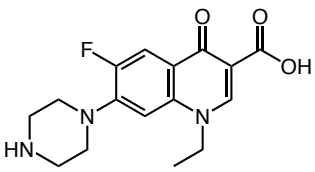

3

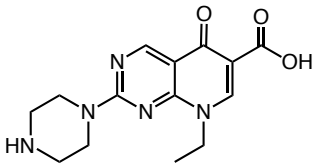

4

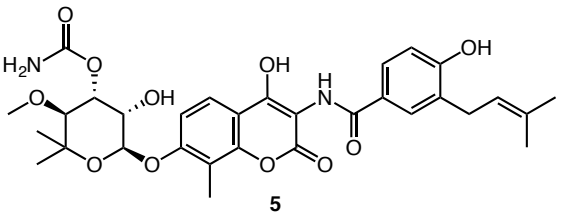

5

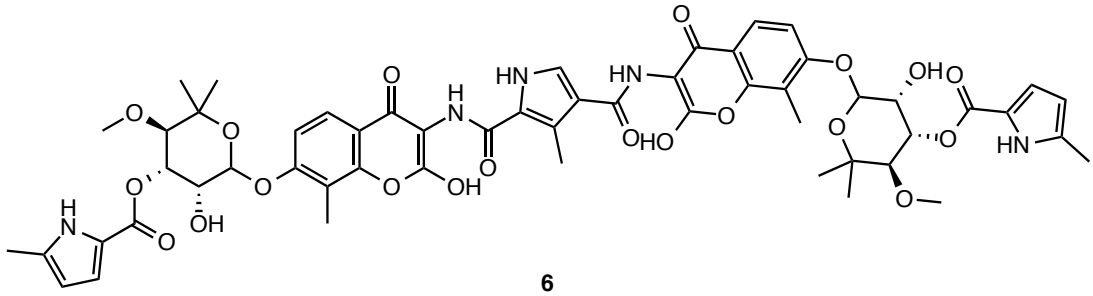

6

The specific conjugal inhibitors are a better alternative as they are expected to impose weak selective pressure, minimizing the possibility of resistance (Baron and Coombes, 2007; Smith and Romesberg, 2007), unfortunately only a few have been identified so far. These include dehydrocrepenynic acid (**7**) linoleic acid (**8**) and oleic acid (**9**), which were reported to have active inhibition against the conjugal transfer of plasmids F and R388 but not against plasmids RP4, RK6 and pKM101 (Fernandez-Lopez *et al.*, 2005). Synthetic fatty acids, 2-hexadecynoic acid (**10**) and 2-octadecynoic acid (**11**) have shown promising anti-conjugal activity against IncF, IncW and IncH plasmids but these compounds do have toxicity issues (Getino *et al.*, 2015). Quite recently two natural products, tanzawaic acids A (**12**) and B (**13**) have been added to the list of specific conjugal inhibitors (Getino *et al.*, 2016). These specifically inhibited the IncW and IncFII conjugative systems but were inactive against IncN and IncP plasmids (Getino *et al.*, 2016). Bisphosphonates, were initially reported to be specific inhibitors of the plasmid F relaxase (Lujan *et al.*, 2007) but recent studies have shown that this class of drugs are rather nonspecific chelating agents (Nash *et al.*, 2012).

This then leaves the mentioned fatty acids and polyketides as the only class of compounds identified as specific conjugal inhibitors, making it essential for research in this area. It is also worth mentioning that none of the identified conjugal inhibitors have progressed to the stage of clinical trials yet but the well-documented evidence of plasmids mediating antibiotic resistance in bacteria and the inability of current antibiotics to achieve therapeutic effect makes the targeting of bacteria conjugation a rational option (Smith and Romesberg, 2007; Williams and Hergenrother, 2008).

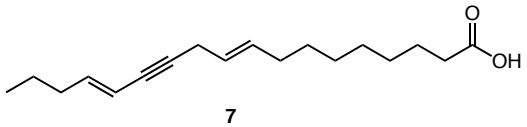

7

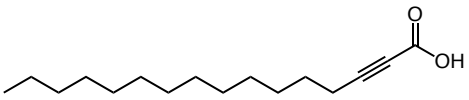

10

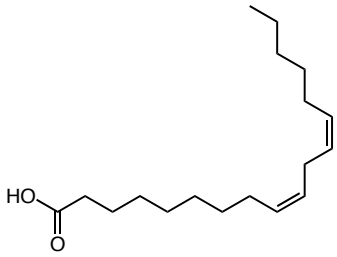

8

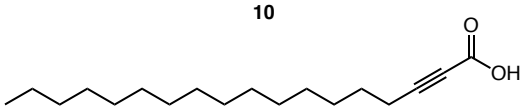

11

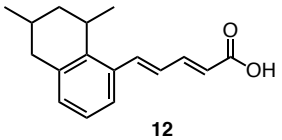

12

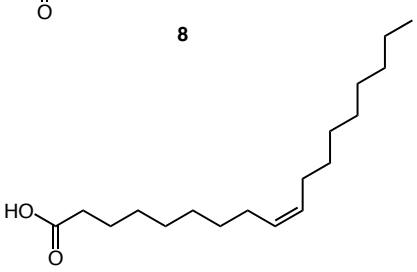

9

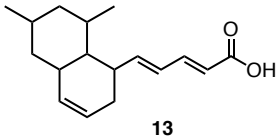

13

1.6 Description of plasmids used in this study

Plasmids are classified based on their stability during conjugation and their ability to stably co-exist in a cell, a phenomenon termed plasmid incompatibility (Inc) (Datta and Hedges, 1971; Carattoli, 2009). Incompatibility is “the inability of two plasmids to propagate stably in the same cell line, thus, only compatible plasmids can be found in transconjugants” (Couturier *et al.*, 1988; Carattoli, 2009). Incompatible plasmids cannot exist in a transconjugant because they have the same replication mechanisms (Frost *et al.*, 2005).

Based on the plasmid incompatibility classification, such plasmids which are incompatible to each other are assigned to the same group (Couturier *et al.*, 1988). At present, 26 incompatibility groups have been identified for the Enterobacteriaceae, 14 groups for the Pseudomonadaceae and about 18 groups for Staphylococci (Frost *et al.*, 2005). For this study four infective plasmids were used, namely plasmid pKM101 (IncN), TP114 ($IncI_2$), pUB307 (IncP) and R7K (IncW).

pKM101 is a 35.4 kilobase plasmid, which belongs to incompatibility group N (IncN). This plasmid was derived from the clinically isolated plasmid R46 (Langer *et al.*, 1981). Plasmid pKM101 has a *bla* gene, which encodes for a β-lactamase hence the host cell's resistance to the β-lactam antibiotics (Langer *et al.*, 1981). It has the *tra* genes, which enable it to encode for the conjugation and transfer of its genes (Langer *et al.*, 1981). In addition, it has the *muc* (mutagenesis: UV and chemical) genes, which are responsible for enhancing ultraviolet light and chemically induced mutagenesis in its host cell (Langer *et al.*, 1981). An example of this is the reported increase in sensitivity to mutagenesis and resistance to UV killing by *E. coli* and *Salmonellla typhimurium* cells which habour plasmid pKM101 (Langer *et al.*, 1981; Maron and Ames, 1983).

TP114 is a 65.1 kilobase I_2 incompatibility group ($IncI_2$) plasmid. This plasmid was isolated from *E. coli* (Grindley *et al.,* 1973). It is a self-transmissible plasmid with resistance genes for kanamycin (McConnell *et al.*, 1979).

pUB307 is an incompatibility group P (IncP) plasmid. It is a derivative of the plasmid RP1 (Bennett *et al.*, 1977). It is a self-transmissible plasmid, which encodes for kanamycin and tetracycline resistance (Bennett *et al.*, 1977). Studies on pUB307 have shown that this plasmid mobilizes gonococcal resistance plasmids from *E. coli* to *N. gonorrhoeae* (Piffaretti *et al.*, 1988).

R7K is a 30.3 kb plasmid belonging to the incompatibility group W (IncW). This plasmid was isolated form *Proteus rettgeri* (Coetzee *et al*., 1972). It is a self-transmissible plasmid with resistant markers for ampicillin, spectinomycin and streptomycin (Coetzee *et al*., 1972).

1.7 The role of efflux pumps in antibiotic resistance

Bacterial efflux pumps are trans-membrane proteins found in the cytoplasmic membrane of bacterial cells. They function by actively transporting toxic compounds including antibiotics from the bacterial cell to help maintain normal physiological processes of the cell (Lomovskaya *et al*., 2001). Bacterial efflux pumps expel a wide variety of structurally unrelated antibiotics from the cell, resulting in a sub-therapeutic concentration and hence reduced bacterial susceptibility (Gibbons *et al*., 2003). Genes located on the bacterial chromosome or numerous plasmids encode the expelling capabilities of bacterial efflux pumps, which could either be drug-specific or non-drug specific (Lomovskaya *et al*., 2001; Poole, 2005). The non-drug specific pumps are able to expel multiple drugs and this confers multidrug-resistance in the bacteria. Effluxing of substrates from the cell is energy dependent. The primary active transporters use adenosine triphosphate hydrolysis and the secondary active transporters (uniporters, symporter or antiporters) utilize the electrochemical potential difference created by ion exchange in the cell as a source of energy (Dimroth, 1997; Paulsen, 2006).

Bacterial efflux pumps have been categorized into five main families, based on their amino acid sequences and the energy source utilized to transport a substrate (Piddock, 2006; Schindler, 2013). The families: ATP-binding cassette (ABC) transporters, major facilitators superfamily (MFS), resistance-nodulation cell division (RND) superfamily, small multidrug-resistance (SMR) family, and multidrug and toxic compound extrusion (MATE) family (Li and Nikaido, 2004). ABC transporters are adenosine triphosphate (ATP) hydrolysis driven. The

MFS, RND, SMR and MATE are all secondary active transporters catalyzed by drug-ion (H^+) antiport except MATE, which is catalyzed by drug-ion (Na^+) antiport (Poole, 2005).

Documented evidence of efflux-mediated antibiotic resistance in clinically relevant pathogens include, a chromosome-encoded RND family multidrug efflux pump, MexXY, responsible for resistance of *P. aeruginosa* to tetracycline, aminoglycosides and macrolides (Masuda *et al*., 2000). The MF superfamily efflux pump, Tet proteins, which are responsible for resistance of *E. coli* (Maynard *et al.,* 2004), *S. aureus* (Truong-Bolduc *et al.,* 2005), *Mycobacterium smegmatis*, *Mycobacterium fortuitum* (Viveiros *et al.,* 2003), *Acinetobacter* spp. (Agerso and Guardabassi, 2005) and *Chlamydia* spp. (Dugan *et al*., 2004) to tetracycline have been reported. Given these examples and the significance of bacterial efflux pump in multidrug resistance, efflux inhibition is an essential process that must be considered in the approaches to combat bacteria and drug resistance.

1.8 Importance of natural products in drug discovery

Natural products have always been an important source of lead compounds in drug discovery. Historically, natural products were the main source of all medicinal preparations until the introduction of combinatorial chemistry, which led to a decrease in the focus on natural products by the pharmaceutical industries (Gibbons, 2008; Harvey *et al*., 2015). Despite this, natural products or their derivatives have continued to enter clinical trials particularly as anticancer and anti-infective agents, showing their potential as a source of drugs. A detailed analysis of new small molecules anticancer medicines approved between 1940 and 2014 revealed that 49% were either natural products or of natural product-based origin (Newman and Cragg, 2016). In addition, an analysis of new small molecules approved between 1981 and 2014 as anti-infective medicine showed that 55% of them were actually natural products or of natural product origin (Newman and Cragg, 2016).

Natural products are likely to produce more potential drugs and/or drug leads than synthetic chemistry because living organisms are in constant contact with the evolving pathogenic microorganisms. As such, living organisms tend to produce bioactive metabolites against these pathogens as a chemical defense mechanism (Gibbons, 2008). An example is the synthesis of phytoalexins; allixin (**14**), totarol (a conifer oleoresin, **15**) and capsidiol (**16**) by certain plants in response to pathogenic attack (Kodera *et al.*, 1989; Smith *et al.*, 2007; Maldonado-Bonilla *et al.*, 2008).

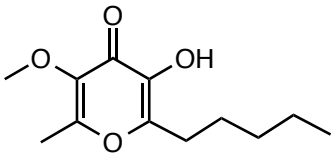

14

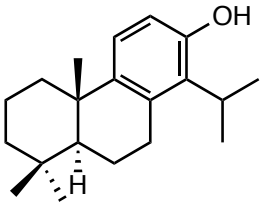

15

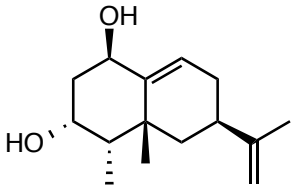

16

In addition, metabolites from natural products tend to have unique features that make them quite different from drugs of synthetic origin, such as oxygenated molecules, chiral centres, polycyclic carbon skeletons and extensive functional group chemistry (Ganesan, 2004; Gibbons, 2008). The structural diversity, unique features and the abundance of natural products marks them out as a valuable source of bioactive molecules, which are likely to have a different mode of action against multidrug-resistant microorganism from the existing antimicrobials (Gibbons, 2008). These facts are the very reasons why natural products, especially plants, should be exploited for potential new drugs.

1.9 Description of plants used in this study

In this study, six edible medicinal plants and two non-edible medicinal plants were screened for bioactive compounds against the bacterial conjugation in *E. coli* and bacterial efflux systems in *S. aureus*. The plants are *Amoracia rusticana*, *Borago officinalis, Brassica oleracea*, *Lepidium sativum*, *Myristica lowiana*, *Sinapis alba*, *Uncaria tomentosa* and

Zingiber officinale. A brief description of these plants is shown in the sections 1.10 -1.17, below.

1.10 *Sinapis alba* L.

Sinapis alba is a leafy annual plant of the family Brassicaceae. It grows up to about a meter in height with stalk-less pinnate leaves, yellow flowers, which produce oblong hairy seedpods. It is commonly known as white mustard. *S. alba* originates from Europe but it is now grown globally for its seeds (van Wyk and Wink, 2004). The seeds are hard and round, with a diameter size of 1 to 1.5 mm (Balke and Diosady, 2000). Although it is known as white mustard, the seeds usually appear as pale beige or light straw-yellow in colour (van Wyk and Wink, 2004).

Figure 1.3 *Sinapis alba* seeds

Credit: Photo by Awo Afi Kwapong, 2014, UCL School of Pharmacy.

Phytochemical studies on *S. alba* seeds have revealed the presence of essential oils, sterols, fatty acids, flavonoids, glucosinolates, isothiocyanates and antioxidants (Durkeet and Harborne, 1973; Appelqvist *et al.*, 1981; Fahey *et al.*, 2001). It is also a rich source of vitamins and minerals. Compounds isolated from *S. alba* seeds include; gluconapin (3-

butenyl glucosinolate; **17**), sinalbin (4-hydroxylbenzyl glucosinolate; **18**), which is responsible for its pungent taste, sinigrin (2-propenyl or allyl glucosinolate) (Fahey *et al*., 2001), sinalexin (**19**), a phytoalexin produced by *S. alba* under biotic or abiotic elicitation (Soledade *et al*., 1997), 4-hydroxy-3-nitrophenylacetic (**20**) and sinapic acids (Figure 3.73) (Tesaki *et al*., 1998).

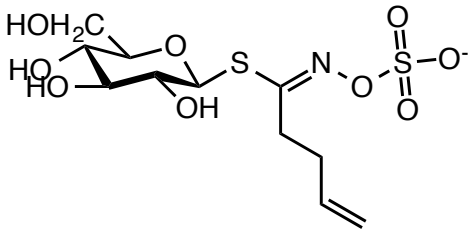

17

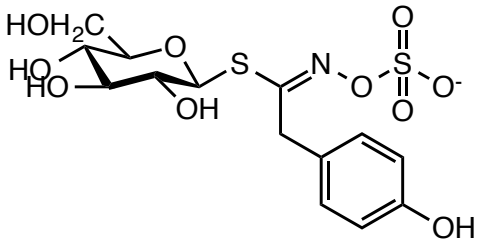

18

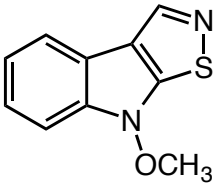

19

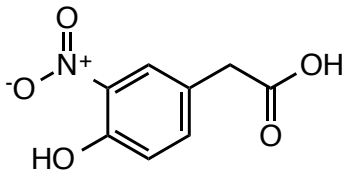

20

White mustard seed is used as a condiment and as an emulsifier in meat products. In traditional medicine, *S. alba* seed oil is used topically to relieve muscle pain, rheumatism, arthritic pain and chest congestion (Divakaran and Babu, 2016). It is also used in the treatment of dyspepsia and to increase peripheral blood flow by acting as a skin irritant (van Wyk and Wink, 2004).

1.11 *Armoracia rusticana* G.Gaertn., B.Mey. & Scherb.

Armoracia rusticana is a perennial plant of the family Brassicaceae. It grows up to about 1 to 4 ft in height (Foster and Hobbs, 2002). It has large oblong leaves, which grow directly from its taproot in a distinctive rosette pattern with small white flowers borne on long flower stalk

of up to 1m high (van Wyk and Wink, 2004). It is commonly known as horseradish and cultivated mostly for its fleshy roots, which are used as a spice. This plant is thought to have originated from Eastern Europe (van Wyk and Wink, 2004).

Figure 1.4 *Armoracia rusticana* roots (plantvillage.org, 2014)

The edible roots are known to contain glucosinolates (glucobrassicin (**21**), neoglucobrassicin (**22**)) and isothiocyanates (allyl isothiocyanate, phenylethyl isothiocyanate), which are common in most *Brassica* vegetables. Plastoqinone-9 (**23**), 6-*O*-acyl-*β*-D-glucosyl-*β*-sitosterol and 1,2-dilinolenoyl-3-galactosylglycerol have been reported for in the roots (Weil *et al.*, 2005). The plant is also known to contain flavonoids (kaempferol (**24**) and quercetin, and their glycosides, rutinoside, 3-*O*-*β*-D-glucosyl-*β*-D-kaempferol-xyloside, 3-*O*-*β*-D-glucosyl-*β*-D-quercetin-xyloside), asparagine, resin and vitamin C (Chevallier, 2001).

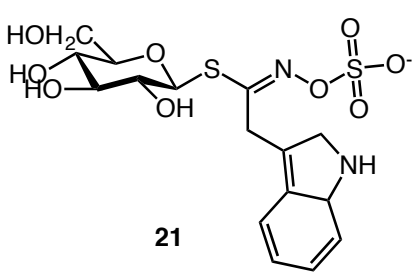

21

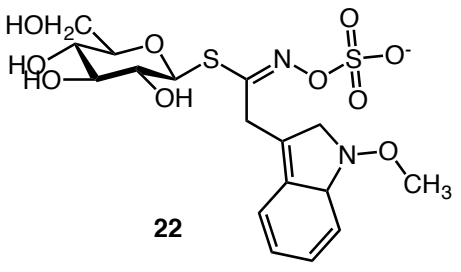

22

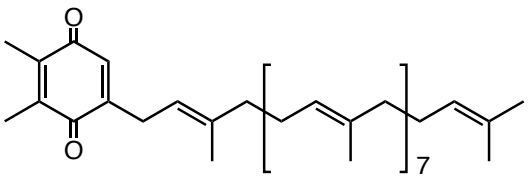

23

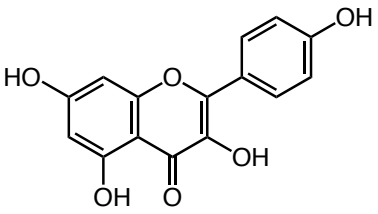

24

In herbal medicine, a decoction made from the roots is used as a weak diuretic, antiseptic and an expectorant (Chevallier, 2001; Foster and Hobbs, 2002). The roots are also used for the treatment of bronchitis, coughs and bronchial catarrh (Foster and Hobbs, 2002). The root poultice is used for the treatment of rheumatism and respiratory congestion (Foster and Hobbs, 2002). In Germany, extracts of the roots are used for the treatment of respiratory tract inflammation and urinary tract infections (Chevallier, 2001; Foster and Hobbs, 2002).

1.12 *Brassica oleracea* L. var. *italica* Plenck

Brassica oleracea is an herbaceous annual plant of the Brassicaceae family, commonly known as broccoli. It has thick green stalk, which gives rise to thick, leathery gray-blue to green coloured leaves and a large branching flower heads. This plant is cultivated for its edible unopened flower buds and tender flower stalks. Broccoli originated from the Mediterranean area and Asia Minor (Buck, 1956; Stephens, 2015).

Phytochemical studies on this plant revealed the presence of glucosinolates (3-methylsulphinylpropyl glucosinolate (**25**), 4-methylsulphinylbutyl glucosinolate) and the isothiocyanates (sulforaphane (**26**), indole-3-carbinol (**27**), glucoraphanin), anti-oxidants (quercetin, glutathione, beta carotene, vitamin C) (Giamoustaris and Mithen, 1996; Moreno *et al.*, 2006; Pérez-Balibrea *et al.*, 2008). It is also a rich source of flavonoids, minerals and vitamins (Giamoustaris and Mithen, 1996; Moreno *et al.*, 2006; Pérez-Balibrea *et al.*, 2008).

The main use of broccoli is for its health-promoting properties but in traditional medicine, the

Figure 1.5 *Brassica oleracea* var. *italica* plant (plantvillage.org, 2015a)

juice from the leaves of broccoli is used in the treatment of warts (Guarrera, 2005). A number of anti-cancer studies have also shown that high consumption of the *Brassica* vegetables especially broccoli, reduces the progression of lung, gastrointestinal tract and prostate cancers (Fahey *et al.*, 1997; Moreno *et al.*, 2006; Traka *et al.*, 2014; Wong *et al.*, 2014).

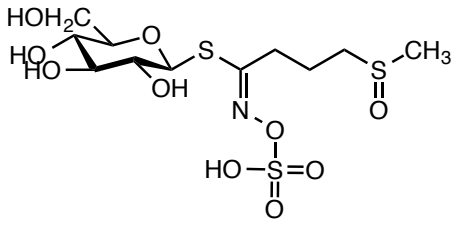

25

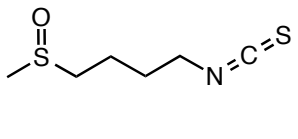

26

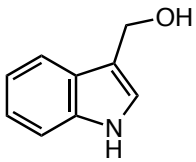

27

1.13 *Lepidium sativum* L.

Lepidium sativum is an annual herb of the family Brassicaceae and is commonly known as garden cress. It is an edible herb, which can grow to a height of 60 centimeters (Boswell and Sowerby, 1863). The whole plant is nearly glabrous (Ghante *et al.*, 2011). The upper part of the herb has many branches with radical leaves, white to pinkish flowers and it bears

elliptical shaped seeds, which are pale reddish brown in colour (Boswell and Sowerby, 1863; Ghante *et al.*, 2011). *L. sativum* is a native of Egypt and West Asia but it is now grown in temperate countries globally for its edible shoot and for medicinal purposes (Gokavi *et al.*, 2004; Nehdi *et al.*, 2012).

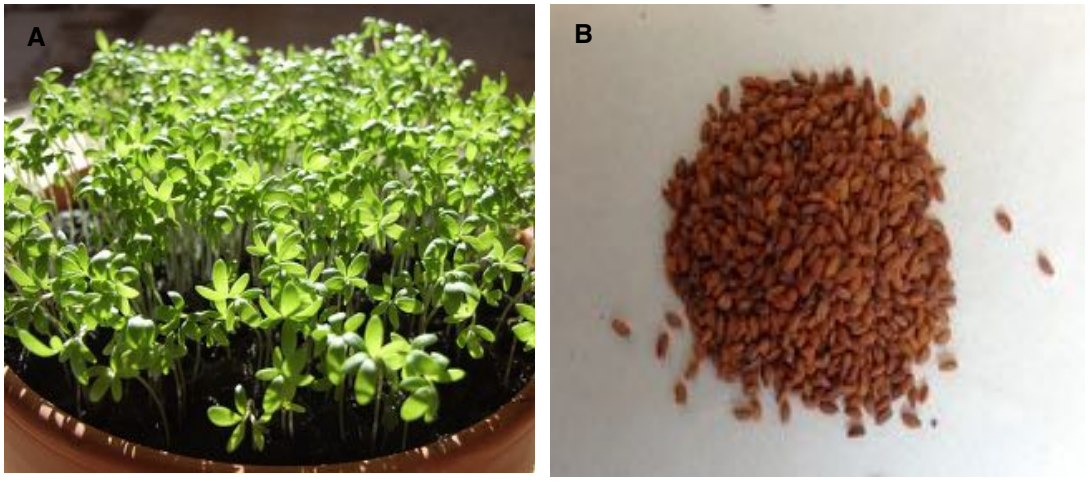

Figure 1.6 *Lepidium sativum* plant and seeds

A (plantvillage.org, 2015b); **B**, photo by Awo Afi Kwapong, 2014, UCL School of Pharmacy.

Phytochemical studies on *L. sativum* have shown the presence of essential oil, glucosinolates, alkaloids, sterols, cyanogenic glycosides (traces), flavonoids, tannins, saponins and triterpenes (Sharma and Agarwal, 2011; Ghante *et al.*, 2011). Glucotropaeolin (**28**), 2-phenylethyl glucosinolate (Figure 3.16), methyl glucosinolate (**29**) and butyl glucosinolate have been reported for this plant (Radwan *et al.*, 2007; Sharma and Agarwal, 2011).

Dimeric imidazole alkaloids such as the lepidines E and F (**30**), and the monomeric imidazole alkaloids semilepidinoside A and B (**31**) are some of the main alkaloids isolated from garden cress seeds (Maier *et al.*, 1998). The volatile products; phenylacetonitrile, benzyl isothiocyanate, 1,8-cincole and α-pinene of *L. sativum* have been reported to be responsible for its antibacterial activity (Sharma and Agarwal, 2011).

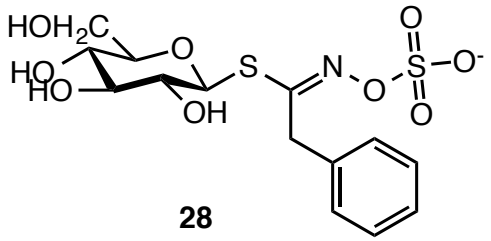

28

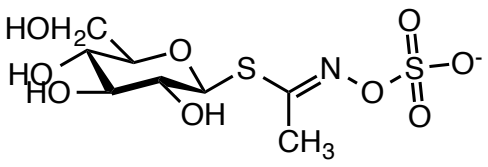

29

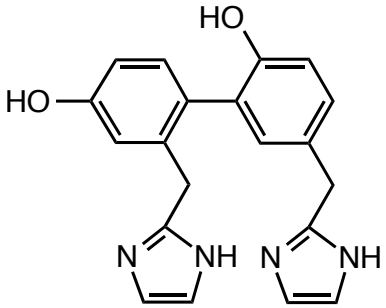

30

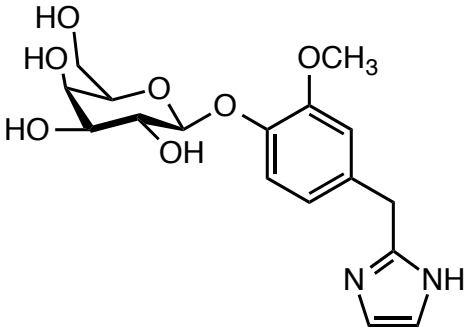

31

The leaves of *L. sativum* can be consumed raw as a salad or cooked for their health promoting properties. *L. sativum* has been implicated in the treatment and management of many pathological conditions. In China, garden cress seeds are used for the treatment of abdominal colic, asthma, pleurisy and dropsy (Sharma and Agarwal, 2011). In some countries in Africa, the seeds are chewed to cure throat diseases, asthma, headache, and bone fracture (Sharma and Agarwal, 2011). Both the seeds and leaves of *L. sativum* are used in the treatment of bronchitis, inflammation, rheumatism and muscular pain in the Unani system of medicine (Ghante *et al.*, 2011; Sharma and Agarwal, 2011). It is also used for the treatment of cough, bleeding piles, diabetes and hypertension (Eddouks *et al.*, 2005; Maghrani *et al.*, 2005; Juma, 2007; Mali *et al.*, 2007).

1.14 *Zingiber officinale* Roscoe

Zingiber officinale (ginger) is an herbaceous perennial plant of the family Zingiberaceae. It grows up to a meter in height bearing narrow, glossy, bright green ribbed leaves and

yellowish flowers (Chevallier, 2001). This plant is grown mostly for its edible rhizome, which is widely used as a spice or medicine. The rhizomes are rough, knotty and beige in appearance with a characteristic flavor and pungency. The young ginger rhizomes are

Figure 1.7 *Zingiber officinale* rhizome

Credit: Photo by Awo Afi Kwapong, 2014, UCL School of Pharmacy.

usually juicy and fleshy with a mild taste because of the high content of gingerol and water while the mature rhizomes are fibrous and nearly dried with an extremely pungent taste because of the high content of shogaols (Natarajan *et al.*, 1972; McGee, 2004). The shogaols are about twice as pungent as their precursors the gingerol and this explains why matured and dried ginger is more pungent than the fresh young ginger (McGee, 2004).

The main biochemical constituents of ginger rhizome are essential oils, oleoresins and crude fibre (Van-Beek *et al.*, 1987). In the oleoresin are found the essential oils and the nonvolatile phenylpropanoid-derived compounds, which are responsible for the pungent taste of ginger, particularly the gingerols, zingerone and shogaols (McGee, 2004; Lim, 2016). The reported essential oils of ginger include (-)-zingiberene (**32**), (-)-β-sesquiphellandrene (**33**), (+)-ar-curcumene, (*E*)(*E*)-α-farnesene, β-bisabolene, geranial, 1,8-cineole (Van-Beek *et al.*, 1987; Ekundayo *et al.*, 1988). These type of compounds, galanolactones (**34**), diarylheptanoids (5-hydroxy-1-(4-hydroxy-3-methoxyphenyl)-7-(4-hydroxyphenyl)heptan-3-one (**35**)), gingerdiols,

gingerdiones, and zingerines have also been reported in ginger (Harvey, 1981; Endo *et al.*, 1990; Huang *et al.*, 1991; Kikuzaki *et al.*, 1991; Kikuzaki *et al.*, 1992; Jiang *et al.*, 2007; Araya *et al.*, 2011; Ahn and Oh, 2012; Lv and She, 2012).

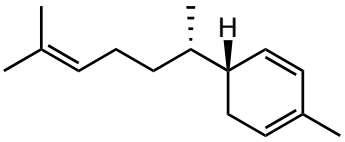

32

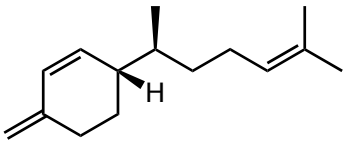

33

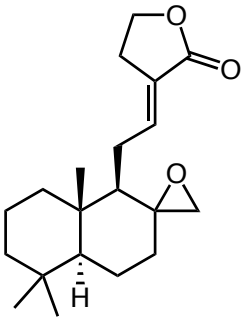

34

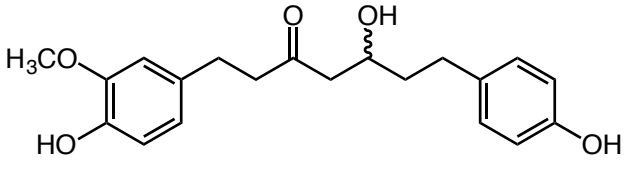

35

In traditional medicine, ginger is commonly used for the treatment of cold, coughs, fever, nausea and headaches (van Wyk and Wink, 2004; Semwal *et al.*, 2015). It is also used as a expectorant, carminative, anti-inflammatory agent, diaphoretic, antispasmodic, peripheral circulatory stimulant, diuretic, astringent, digestive aid and appetite stimulant in many countries (Chevallier, 2001; Semwal *et al.*, 2015). The use of ginger in traditional medicine is well supported by scientific research, which has shown that ginger has anti-allergenic (Yamahara *et al.*, 1995), immune-boosting (Lu *et al.*, 2011), anti-nausea (Pertz *et al.*, 2011), anti-gastric, analgesic, antipyretic and anti-inflammatory activities (Young *et al.*, 2005; Ueki *et al.*, 2008; Baliga *et al.*, 2011; Ahn *et al.*, 2009).

1.15 *Myristica lowiana* King

Myristica lowiana is a dioecious flowering tree of the family Myristicaceae. It is a native of Southeast Asia and it is largely found in the deep forest (de Wilde, 2000). It usually grows up to 7-25 metres in height with a dark chocolate or blackish coloured stem bark, lanceolate oliveacous or brown leaves, cream rusty coloured flowers and ellipsoidal shaped fruits (de Wilde, 2000). Its bark and wood exude a watery red sap on cutting, which is characteristic of this plant (de Wilde, 2000). There is no known medicinal use of this plant in literature; so far it is mainly used as wood for construction purposes. There are also no phytochemical reports on this plant but the Myristicaceae are known to contain essential oils, coumarins, flavonoids, lignans, acylphenols, alkaloids, polyketides and terpenoids compounds (Valderrama, 2000; van Wyk and Wink, 2004; Francis *et al.*, 2014; Cao *et al.*, 2015).

Figure 1.8 *Myristica lowiana* trunk and leaf

Credit: Photo by Stephen Teo, 2016, St Matang, Malaysia.

1.16 *Borago officinalis* L.

Borago officinalis is an easy growing annual herb of the Boraginaceae family. It is commonly known as borage, starflower or bee plant. It grows to a height of about 1.6 ft (van Wyk and Wink, 2004). The whole plant is covered with bristle or trichomes. The stem of borage is covered with alternate arranged wrinkled deep green leaves and bright blue coloured flowers (van Wyk and Wink, 2004; Franz *et al.*, 2007). Both the flowers and leaves are edible and are usually used to garnish food or as salads (Franz *et al.*, 2007). Borage is thought to have originated from southern Spain and Morocco (Chevallier, 2001). It is grown mostly as a garden herb and cultivated in large scale agriculture for its seed oil, which is commercially known as starflower oil (van Wyk and Wink, 2004).

Figure 1.9 *Borago officinalis* plant

Credit: Photo by Awo Afi Kwapong, 2014, UCL School of Pharmacy.

This plant contains tannins, flavonoids and trace amounts of several unsaturated pyrrolizidine alkaloids (van Wyk and Wink, 2004; Franz *et al.*, 2007). Some of the pyrrolizidine alkaloids are amabiline (**36**), supinidine (**37**), lycopsamine (**38**) and intermedine,

which are mostly found in the leaves of borage are known to be hepatotoxic as well as mutagenic and carcinogenic (Smith and Culvenor, 1981; Chevallier, 2001; Vacillotto *et al.*, 2013). Thesinine (**40**), a non-toxic pyrrolizidine alkaloid has been reported for this plant and it is responsible for the deep blue colour of the flowers (Dodson and Stermitz, 1986; Herrmann *et al.*, 2002). The seeds are rich in fatty acids, particularly gamma linoleic acid (Chevallier, 2001; van Wyk and Wink, 2004).

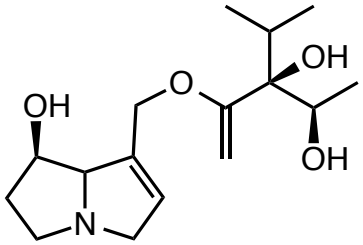

36

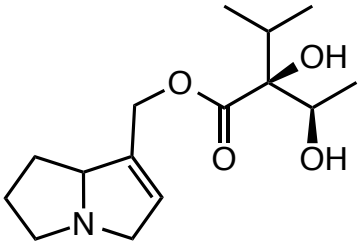

37

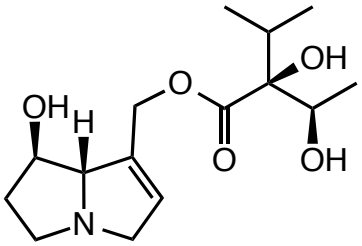

38

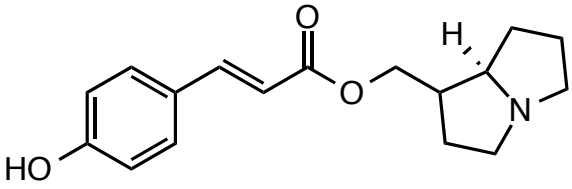

39

In traditional medicine, borage herb or the flowers are used as a diuretic, diaphoretic, expectorant, anti-inflammatory, demulcent, mild sedative and anti-depressant (Chevallier, 2001; van Wyk and Wink, 2004). Its seed oil is used in the treatment of rheumatic problems, eczema, premenstrual complaints and other chronic skin conditions (Chevallier, 2001). Additionally, scientific research has shown that borage oil has anti-allergic (Gu *et al.*, 1998), immune-modulatory (Harbige *et al.*, 2000) and blood pressure lowering activity (Engler and Engler, 1998) and these justify its use in traditional medicine.

1.17 *Uncaria tomentosa* (Willd. ex Schult.) DC.

Uncaria tomentosa is a woody climbing vine of the Rubiaceae family. It usually grows up 100 ft or more, its stem can grow up to 20 cm thick with opposite arranged leaves and sharp thorns (Chevallier, 2001). It is commonly called cat's claws because of its claw-shaped thorns (Chevallier, 2001). This plant is a native of the tropical rainforest of South and Central America (Chevallier, 2001).

Figure 1.10 *Uncaria tomentosa* vine (mb-med.it, 2013)

Phytochemical studies on this plant revealed the presence of pentacyclic oxindole alkaloids such as pteropodine, speciophylline, mitraphylline and tetracyclic oxindole alkaloids such as, rhynochophylline (**40**) and isorhychophylline (Shamma *et al.*, 1967; Seki *et al.*, 1993; Laus and Keplinger, 1994). In addition, triterpenoid glycosides, sterols, flavonoids, coumarins and tannins have also been reported for this plant (Chevallier, 2001; Heitzman *et al.*, 2005). The reported triterpenoids include 3β,6β,19α-trihydroxyurs-12-en-28-oic acid (**41**), 3β,6β,19α-trihydroxy-23-oxo-urs-12-en-28-oic acid (Aquino *et al.*, 1990), pyroquinovic acid 3β-*O*-β-D-glucopyranosyl-(1-4)-β-D-fucopyranosyl-28-*O*-β-D-glucopyranosyl ester (tomentoside A) and pyrocincholic acid 3β-*O*-β-D-glucopyranosyl-(1-4)-β-D-fucopyranosyl-28-*O*-β-D-glucopyranosyl ester (tomentoside B) (Kitajima *et al.*, 2003), the flavonoids include

epicatechin (**42**), catechin, kaempferol (Wirth and Wagner, 1997; Goncalves *et al*., 2005) and the flavono-lignans include cinchonain Ia (**43**) and cinchonain Ib (Wirth and Wagner, 1997).

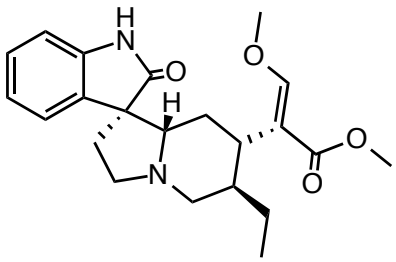

40

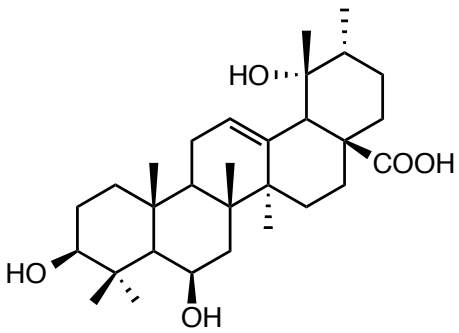

41

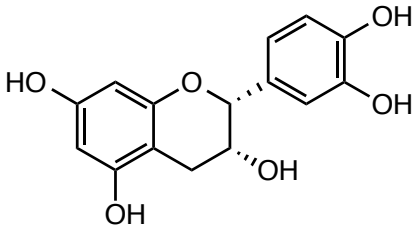

42

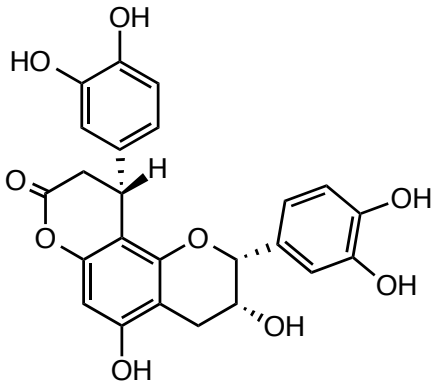

43

Native healers of South and Central America use *U. tomentosa* for the treatment of asthma, diabetes, arthritis, allergies, fever, gastric ulcers, haemorrhage, inflammation, menstrual irregularity, urinary tract infections and cancer (Chevallier, 2001; Heitzman *et al*., 2005). A decoction of the stem or root cuttings is used to boost the body's immune system against infections (Chevallier, 2001). The use of *U. tomentosa* in herbal medicine is well supported by research findings, which have shown that this plant has anti-inflammatory (Rizzi *et al*., 1993; Aguilar *et al*., 2002), antioxidant (Wirth and Wagner, 1997; Goncalves *et al*., 2005) and immune-stimulatory properties (Keplinger *et al*., 1999; Lemaire *et al*., 1999).

1.18 Aims and objectives

The main aims of this project was to isolate and characterise natural products that:

- inhibit bacterial plasmid conjugal transfer as a strategy to combat the spread of multi-drug resistance genes among bacteria.
- potentiate the activity of antibiotics against efflux-mediated multidrug-resistant strains as a strategy to restore the activity of existing antibiotics.

Five major objectives were set to help achieve the aims of the project. They are as follows:

1. To carry out a bioassay-guided isolation, this involved:
    - extraction of ground plant materials using solvents of different polarity
    - subsequent bioassay-guided fractionation of the identified anti-conjugal extracts and further isolation from the identified anti-conjugal fractions using chromatographic methods
    - structural elucidation of the isolated compounds using spectroscopic methods.
2. To screen for bacterial plasmid conjugation inhibitory activity, this involved:
    - the determination of antibacterial sensitivity of the plant extracts, fractions, isolated and purchased compounds against *E. coli* NCTC 10418,
    - subsequent screening of the plants extracts, fractions, isolated and purchased compounds at sub-inhibitory concentrations against the conjugal transfer of IncP plasmid pKM101, $IncI_2$ plasmid TP114, IncP plasmid pUB307 and IncW plasmid R7K,
    - concentration-dependent study of the identified conjugal inhibitors.
3. To determine the plasmid eliminating activity of the identified conjugal inhibitors.
4. To determine the cytotoxicity of the identified conjugal inhibitors against human dermal fibroblast adult cells.
5. To screen for antibiotic potentiation activity, this involved:

- the determination of antibacterial sensitivity of the plant extracts, isolated and purchased compounds against *S. aureus* strains, SA-1199B (NorA) and XU212 (TetK), which over expresses multidrug-resistance pumps, and
- subsequent testing of the isolated and purchased compounds at sub-inhibitory concentrations in combination with the relevant antibiotics against SA-1199B (NorA) and XU212 (TetK).

Chapter 2 Materials and methods

2.1 Plant Material

The plant material for this project was obtained as seeds, roots, florets, rhizomes, stem bark or whole plant as outlined in Table 2.1. The fresh rhizomes were cleaned, cut up into pieces and oven dried at 40°C for 3 days. The stem bark was sun dried for a week. The fresh flower heads were freeze-dried. The dried plant materials were finely milled and stored at room temperature. A voucher specimen of *Myristica lowiana* was deposited at the herbarium of the Department of Pharmaceutical and Biological Chemistry, UCL School of Pharmacy.

Table 2.1 Summary of the plants used, their source, part and voucher or batch number

SPECIES	SOURCE	PART USED	VOUCHER/ BATCH NUMBER
Sinapis alba	Holland & Barrett, UK	Seeds	79337
Armoracia rusticana	G Baldwin & Co., UK	Roots	0030
Brassica oleracea	Waitrose, UK	Florets	206MAE
Lepidium sativum	Seed Parade, UK	Seeds	900
Zingiber officinale	Waitrose, UK	Rhizome	-
Myristica lowiana	Stephen Teo, Forest Department Sarawak. Collected from St Matang, Malaysia, May 2014	Stem bark	ST001/14
Borago officinalis	Herb in a Bottle, Germany	Aerial part	139611
Uncaria tomentosa	G Baldwin & Co., UK	Woody vine	0043

2.2 Extraction

2.2.1 Soxhlet Extraction

Soxhlet extraction is a classical solid-liquid extraction procedure and can be carried out using organic solvents or heterogeneous solvent mixtures of different polarities to obtain extracts

of different chemistry. It has the advantage of large-scale extraction and high extraction yields. However, thermo-labile compounds might be degraded during the process because this extraction process is heat-dependent. This process was used for the extraction of *L. sativum* seeds (245 g), *Z. officinale* rhizome (200 g) and *U. tomentosa* vine cuttings (500 g).

The powdered plant material was packed into a cellulose thimble and placed into the extraction tube of the Soxhlet apparatus. The extraction tube packed with the plant material was then secured onto a 5 L round bottomed flask and placed on a heating mantle. The setup was filled with solvent (2.5 L) and a reflux condenser was secured above the extraction tube of the Soxhlet apparatus. The extraction was allowed to run at a heating temperature of 40°C to 60°C until extraction was completed. Extraction was carried out using solvents of increasing polarity (hexane or petroleum ether, chloroform and methanol). The resulting extracts were evaporated to dryness on a rotary evaporator at 40°C. Dried extracts were weighed and stored in the refrigerator until they were required for use.

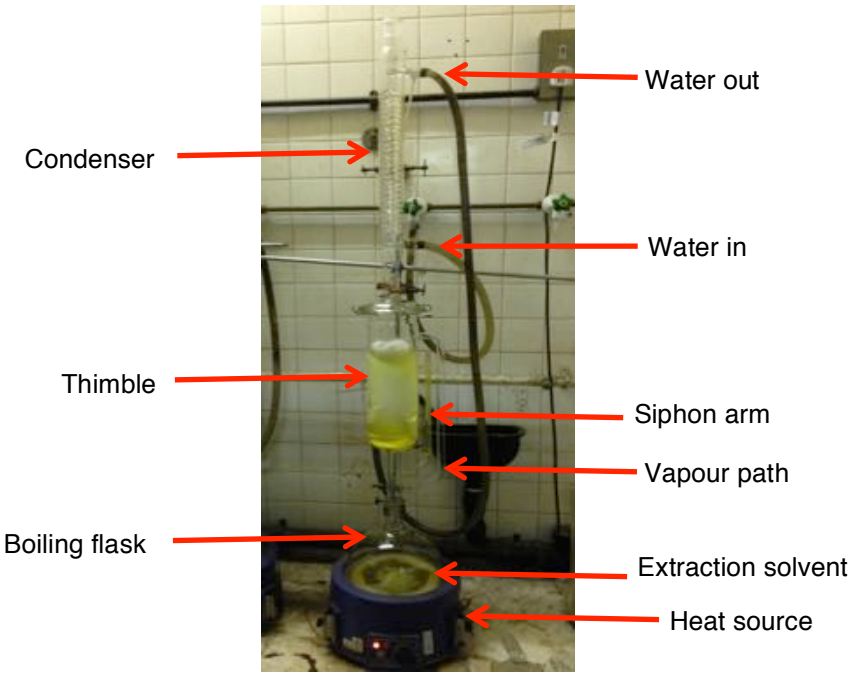

Figure 2.1 Soxhlet extraction of *L. sativum* seeds

2.2.2 Ultrasound-assisted Extraction (UAE)

Ultrasound-assisted extraction is a solvent extraction process, which is gradually gaining popularity (Bucar *et al.*, 2013). It can be carried out using organic solvents or heterogeneous solvent mixtures of different polarities to obtain extracts of different chemistry. Ultrasound-assisted extraction uses mechanical stress to induce cavitation and cellular breakdown of plant material that results in increased extraction yield. It has the advantage of decreased extraction time and improved temperature control of the water bath used in the process. *S. alba* seeds (1kg), *A. rusticana* roots (1 kg), *B. oleracea* florets (910 g), *M. lowiana* stem bark (592 g) and *B. officinalis* herb (200 g) were individually extracted using ultrasound-assisted extraction.

The powdered plant material was placed in a 5 L glass beaker and covered with the extracting solvent, hexane. This was then placed in an ultrasonic bath for 4 h. The resulting extract was filtered and dried under vacuum. Dried extracts were weighed and stored in the refrigerator until they required for use. The procedure was repeated with chloroform and finally with methanol to obtain extracts of increasing polarity.

2.2.3 Acid-base Extraction

Acid-base extraction is a liquid-liquid extraction process that achieves separation based on the solubility of compounds in two immiscible liquids (Figure 2.2). Water and an organic solvent are usually the solvent of choice for alkaloid extraction; the components of the analyte separate into either the aqueous or organic layer depending on their solubility and basicity of the compounds. This process helps to extract a mixture of alkaloids after which individual alkaloids can be separated by chromatography. The methanol extracts of *L. sativum* (40 g), *B. officinalis* (10 g) and *U. tomentosa* (48 g) were subjected to alkaloid extraction. Each extract was re-suspended in water, acidified with 2 mL concentrated hydrochloric acid (HCl) and extracted three times with 250 mL of ethyl acetate (EtOAc). The

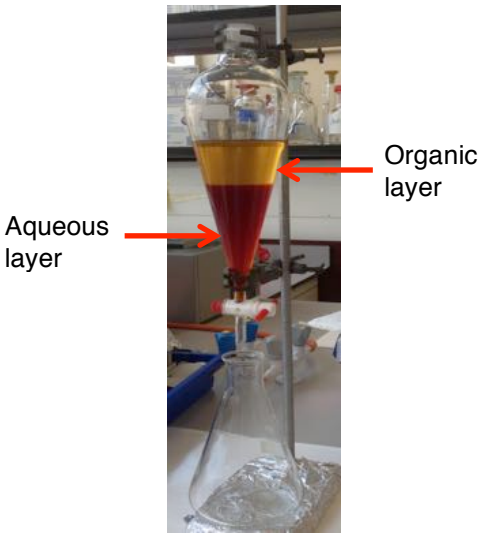

Figure 2.2 Liquid-liquid extraction of alkaloidal mixture from *U. tomentosa* methanol extract

remaining aqueous layer was basified with 2.5 mL concentrated aqueous ammonium solution and extracted again three times with 250 mL of EtOAc. The EtOAc layer (organic layer) was dried under vacuum and tested for the presence of alkaloids using Dragendorff's reagent. The extracts that tested positive to Dragendorff's reagent were further subjected to chromatographic methods to isolate the pure alkaloids. The isolation schemes for the various alkaloids are described in sections 3.2.4 and 3.2.7.

2.2.4 Preparation of Dragendorff's reagent

Equal volumes of a solution of 1.7 g bismuth nitrate, 20 mL glacial acetic acid in 80 mL water and a solution of 16 g potassium iodide in 40 mL water were mixed. Ten milliliter of this mixture was added to 20 mL glacial acetic acid and made up with 100 mL water to give the Dragendorff's reagent. All the reagents for this preparation were purchased from Sigma-Aldrich, UK.

2.3 Chromatographic Techniques

Chromatographic techniques are used to separate components of an analyte between two phases; this is the stationary and mobile phases. For this project liquid chromatographic methods with solid stationary phases were used for the fractionation and purification. The solid stationary phases were silica gel and octadecyl carbon chain (C18) bonded silica. Silica gel was used mostly for the separation of non-polar extracts and sometimes for polar extracts when hydrophilic-interaction chromatography (HILIC) was adopted. C18 silica gel was used for the separation of polar extracts.

For normal phase chromatography, a polar stationary phase and a non-polar mobile phase are used whilst in reversed phase chromatography, non-polar stationary phases with a polar mobile phase are used. Separation in normal and reversed phase chromatography is achieved mostly by adsorption and partition.

HILIC is used for the separation of polar compounds just like reversed phase chromatography but it uses polar stationary phase and mobile phase for elution. The elution order in HILIC is almost the reverse of that of reversed phase chromatography. It utilizes polar stationary phases such as silica gel, hybrid silica, zwitterion, amide and diol phases. The mobile phase is mostly a polar aprotic solvent with a small amount of water (3 - 30%). At least 3% water is necessary to produce hydrophilic partition, a separation mechanism for HILIC. A commonly used aprotic solvent is acetonitrile, although acetone can also be used.

2.3.1 Thin Layer Chromatography (TLC)

Thin layer chromatography is a separation method used for the separation of non-volatile mixtures. It is simple, fast and an inexpensive method for detection of a wide range of compounds. It is sometimes used in bioassay (bioautography) for rapid identification of

possible bioactive zones. The main disadvantage of this technique is the uncontrolled flow rates of the mobile phase, which distorts separation.

Analytical TLC was performed on all of the extracts and fractions, and depending on the polarity of the sample, normal or reverse phase chromatography was employed. For this purpose, a tiny amount of the sample was dissolved in a small amount of appropriate solvent and was spotted at a centimeter from the bottom edge of the plate, using a capillary tube. The plate was then lowered into a chromatography-developing tank containing a suitable solvent system, which migrated up the plate via capillary action, separating the mixture according to the polarity of the compounds. The mobile phase was allowed to travel up to 0.5 cm from the top part of the plate and after which the developed TLC plate was air dried and observed under UV-254 nm and 356 nm, in order to determine the absorbance and fluorescence properties of the compounds. The plates were then sprayed with appropriate detection reagents to visualize the characteristic compounds. To quantify the migration of the compounds on a particular plate and solvent system, the retention factor value was calculated as the ratio of the migration distance of compound and the migration distance of solvent front.

Preparative TLC was also employed for the further purification of some compounds. The procedure was same as analytical TLC. The only exceptions were that the analyte was applied as a thin line and separated compounds were scraped off the TLC plate. The scraped compounds were separated from the silica by desorbing with a suitable solvent, which was then filtered off. The filtrate was dried under vacuum. The dried compounds were weighed and stored in the refrigerator.

2.3.2 Gravity Column Chromatography (CC)

Gravity column chromatography is a separation technique used for the isolation or purification of compounds from fractions, mixtures of compounds or extracts. For a gravity

column, separation occurs as the mobile phase travels down the stationary phase under the influence of gravity. The main advantage of a gravity column is the relative low cost. It is time consuming to run gravity columns as the column runs slowly but gives good separation and pure compounds. There are two general methods of packing a gravity column: the dry method and the wet method. The difference between the two packing methods is that for the dry method, the column is first packed with stationary phase, which is dry and then flushed with the mobile phase whilst for the wet method, the column is filled with a prepared slurry of the stationary and mobile phase. For this project, the wet method was used for the separation of compounds.

The column was clamped vertically and half-filled with the mobile phase (solvent system). It was then filled with slurry of silica gel 60 (70 - 230 mesh; Merck) and the mobile phase. The stopcock was opened to allow excess solvent to drain and help the silica gel sediment. Upon packing of the silica gel with all necessary precautions taken to avoid disruption in the continuity of the packing, a final layer of sand (5-10 mm) was added to the column. This prevents disruption of the leveled packing, upon addition of fresh mobile phase. The solvent

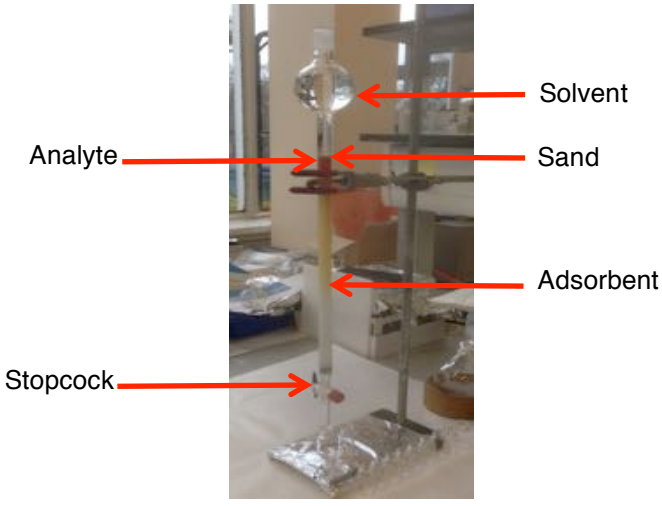

Figure 2.3 Gravity column chromatograph of a *Z. officinale* chloroform extract

was then allowed to drop just above the level of the sand before the dissolved analyte (not more than 5% of the packed silica gel 60) was introduced onto the column. The analyte was

allowed to adsorb onto the surface of the column before eluting with the mobile phase. Fractions were collected in a 7 mL glass vial.

2.3.3 Solid Phase Extraction (SPE)

Solid phase extraction is a chromatographic method used to separate compounds that are dissolved or suspended in a liquid. Separation of compounds is achieved by the adsorption of an analyte on to a solid phase (cartridge device containing a chromatographic packing material) and elution is by the application of a gradient system (mobile phase) of increasing eluting power in a stepwise manner under the influence of forced flow using a vacuum manifold. In this study, solid phase extraction was applied for the fractionation of extracts and purification of compounds.

The SPE cartridge was attached to the vacuum manifold and conditioned with 200 mL methanol after which it was solvated with 200 mL of deionized water for the reverse phase cartridge. For normal phase, the cartridge was just conditioned with hexane. The analyte (not more than 5% of the cartridge weight) was dissolved in a minimal amount of conditioning

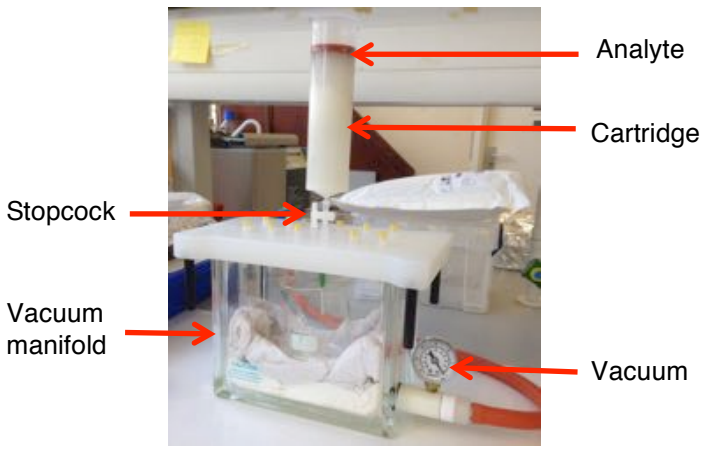

Figure 2.4 Solid phase extraction of a *M. lowiana* methanol extract

solvent and dispensed evenly onto the top of the column using a Pasteur pipette. The analyte was allowed to adsorb onto the surface of the column before eluting with 100 – 200 mL of appropriate solvent system. Fractions were collected in 250 mL round-bottom flasks.

Polar extracts were subjected to reverse-phase solid-phase extraction (Phenomenex® Strata Silica C18) using a step gradient system, 10% methanol increments in water. The methanol-water SPE fractions were dried under vacuum and freeze dried. Non-polar extracts were subjected to normal phase solid phase extraction (Phenomenex® Strata Silica S1) using a step gradient system with 10% increments of either chloroform or ethyl acetate in hexane. The resulting fractions were dried under vacuum.

2.3.4 Vacuum Liquid Chromatography (VLC)

Vacuum liquid chromatography is a column-based method that uses vacuum to increase the flow rate of the mobile phase. It is mostly used for fractionation of large amount of crude extracts.

The column (70 x 170 mm, 70 x 510 mm) was clamped vertically and attached to the vacuum and a 250 mL round-bottom flask (Figure 2.5). The column was two-thirds filled with

Figure 2.5 Vacuum liquid chromatography of *A. rusticana* chloroform extract

dry silica gel (230 – 400 mesh; Merck), the vacuum was turned on and the surface was pressed to allow compact packing of the silica gel. The column was flushed with the hexane to check for voids and channels. The extract (5-13 g) was dissolved in an appropriate organic solvent and pre-adsorbed on silica. This was then added as a thin uniform layer on top of the column and for compact packing of the analyte, vacuum was applied. A small piece of cotton wool was placed at the top of the packed column to protect the leveled surface from being disturbed when fresh solvent was introduced. The column was eluted with a gradient solvent system and fractions were collected in 250 mL round-bottom flasks.

2.3.5 High Performance Liquid Chromatography (HPLC)

High performance liquid chromatography is an automated chromatographic technique used to identify, quantify and separate components of a mixture. The principles of separation are the same like as other liquid-solid chromatographic techniques except that HPLC uses pressure to pass the mobile phase and analyte through a column filled with adsorbent (stationary phase). HPLC facilitates fast and efficient analysis. Its main disadvantage is that it is an expensive piece of equipment to purchase and maintain (Gibbons, 2012).

In this study both analytical and preparative HPLC were used for the isolation of compounds. Analytical work was run on an Agilent 1200 series using an Ascentis® column (C18, 25 cm x 4.6 mm, 5 μm). The preparative work was run on a Waters 2489 UV/Visible Detector using a Phenomenex® Prodigy™ column (ODS-3, 250 x 21.20 mm, 5 μm). The column was first washed with 100% methanol at 10 mL/min for 20 min to remove any unwanted material and then conditioned with the eluent. A gradient system from 10 to 100% acetonitrile or methanol in water and a flow rate 1 mL/min was used for the analytical work. Based on the separation of the compounds as shown in the chromatogram of the analytical HPLC run, a solvent system was chosen for the preparative HPLC run. An isocratic system was used for the

preparative HPLC runs with a flow rate of 10 mL/min and slight modification in the concentration of the analyte.

2.4 Spectroscopic Methods

Spectroscopic methods are useful tools that give structural information about a molecule, such as the hydrogens and their environment, carbons and their environment, functional groups, alternating single and double bonds (conjugation), mass of the molecule and the mass fragments. These pieces of information are useful for the structural elucidation of compounds and for the study of the behaviour of complex systems.

In this study, the spectroscopic identification of isolated compounds was carried out using Nuclear Magnetic Resonance (NMR) spectroscopy, Mass Spectrometry (MS), Infrared spectroscopy (IR) and Ultraviolet-visible spectroscopy (UV).

Low-resolution mass spectra were recorded on a Thermo Finnigan ThermoQuest Navigator instrument and accurate mass data was recorded on a Micromass Q-ToF Premier Tandem Mass Spectrometer. The measurement of the mass-to-charge (*m/z*) ratio and abundance of isolated compounds on the mass spectrometers were performed by Dr. Andrew Weston and Mr. Emmanuel Samuel at the Research Services, UCL School of Pharmacy.

IR spectra were recorded as a thin-film on a PerkinElmer Spectrum 100 FT-IR Spectrometer. The UV spectra were recorded on a Beckman Coulter Du® 720 UV/Vis Spectrophotometer with samples dissolved in methanol.

2.4.1 Nuclear Magnetic Resonance (NMR) Spectroscopy

Samples (≤ 5 mg) were dissolved in 0.7 mL of deuterated NMR solvents depending on their solubility and placed in NMR tubes. Full NMR spectra (^{1}H, ^{13}C, DEPT-135, HMQC, HMBC,

COSY, and NOESY) were acquired for the structure elucidation on a Bruker Avance 500 MHz spectrometer. The deuterated NMR solvents and tubes were purchased from Sigma-Aldrich and Cambridge Isotope Laboratories. All chemical shift values were given in parts per million (ppm) and calibration was achieved by reference to the solvent peaks. Coupling constants (*J* values) were reported in Hertz (Hz).

Table 2.2 Chemical shifts of NMR solvent signals used in this study

Solvent	^{1}H NMR Chemical shift (ppm)	^{13}C NMR Chemical shift (ppm)
Acetone-d_6	2.05	206.7, 29.9
Chloroform-*d*	7.26	77.2
Dimethyl sulfoxide-d_6	2.50	39.5
Methanol-d_4	3.31	49.1
Water (D_2O)	4.8	

The NMR spectra for **AK-11** (UtSPE 8*) (Figures 2.7 - 2.13), an oxindole alkaloid isolated from *U. tomentosa* will be used to illustrate the NMR experiments used in the structure elucidation of compounds throughout this project.

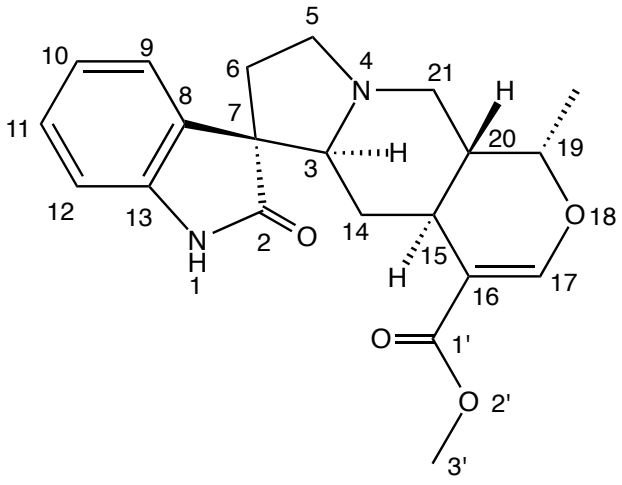

Figure 2.6 Structure for **AK-11**

2.4.2 Proton (^{1}H) NMR Spectroscopy

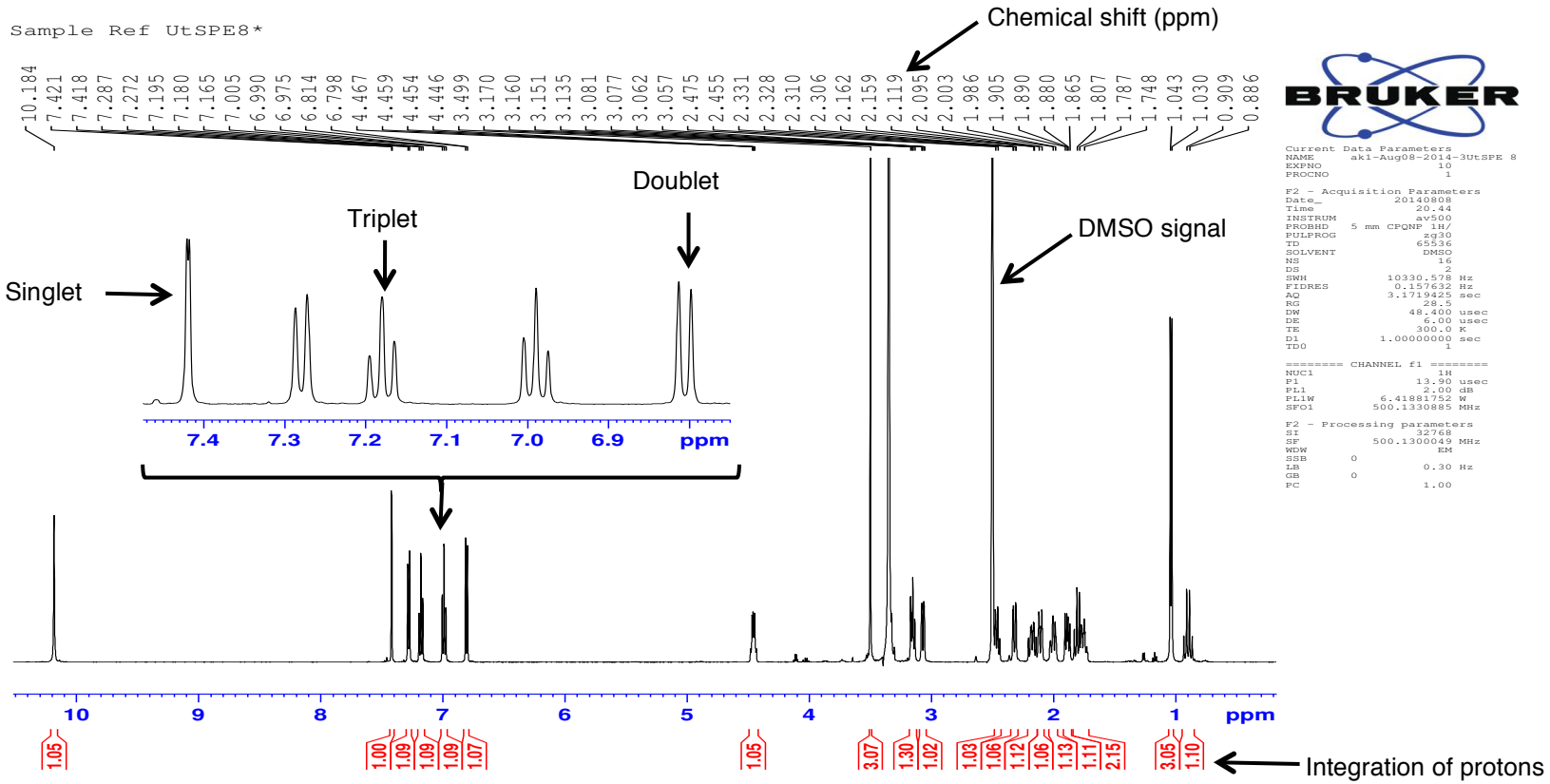

Figure 2.7 ^{1}H NMR spectrum for **AK-11**, recorded in DMSO-d_6, 500 MHz

The ^{1}H NMR spectrum provides information on the number of protons within a compound and the chemical environment of the protons (chemical shift (δ)). The chemical shift of a proton shows the shielding and deshielding effect of neighbouring electron donating or withdrawing groups, respectively. Shielded protons resonate at lower chemical shift values, whereas deshielded protons resonate at higher chemical shift values. Deshielding of protons is caused by electron withdrawing groups such as carbonyl groups, conjugated systems and heteroatoms (oxygen, fluorine and nitrogen). Integration shows the number of protons associated with a group in the same chemical environment. The splitting pattern (spin multiplicity) of a proton signal represents the number of neighbouring protons in a system, using the n+1 rule, where n is the number of neighbouring non-equivalent protons. A doublet or triplet split pattern of a proton indicates the presence of one or two neighbouring proton, respectively. An unsplit signal (singlet) is observed when there are no adjacent protons. Coupling constants (*J* values) give indication of how strongly a group couples to another. They are measured by the distance between two adjacent sub-peaks in a split signal multiplied by the field strength. For example, the doublet at 6.79 ppm (Figure 2.7) has a J = 8.0 Hz, it was calculated by finding the difference between the two sub-peaks, 6.798 and 6.814 ppm and the value was multiplied by the field strength of 500 MHz.

2.4.3 Carbon (^{13}C) NMR Spectroscopy

The ^{13}C broadband decoupled NMR spectrum provides information on the number of carbon nuclei within a compound and the chemical environment of the carbons. Like ^{1}H NMR spectra, shielded carbons resonate at lower chemical shift values and deshield carbons resonate at higher chemical shift values.

2.4.4 Distortionless Enhancement by Polarisation Transfer (DEPT-135)

DEPT-135 provides useful information on the type of carbon when compared to the ^{13}C broadband decoupled NMR spectrum. It tells whether the carbon signal is a methine (-CH), methyl ($-CH_3$), methylene ($-CH_2$) or quaternary carbon. In the DEPT spectrum, methine and methyl carbons appear as on one side while methylene carbons are shown on the other side. Quaternary carbons signals are absent in DEPT spectra so by comparison with the ^{13}C NMR spectrum, the quaternary carbon can be identified.

2.4.5 Heteronuclear Multiple-Quantum Correlation (HMQC) Spectroscopy

Heteronuclear multiple-quantum correlation spectra show the direct bonding between carbon and proton nuclei. The HMQC spectrum is two-dimensional spectrum with the ^{13}C spectrum displayed on the left axis and the ^{1}H spectrum displayed on the top axis. HMQC ^{1}H-^{13}C correlations are shown as cross peaks in the spectrum. Carbon atoms that have no attached protons and protons bonded to other heteroatoms do not show cross peaks.

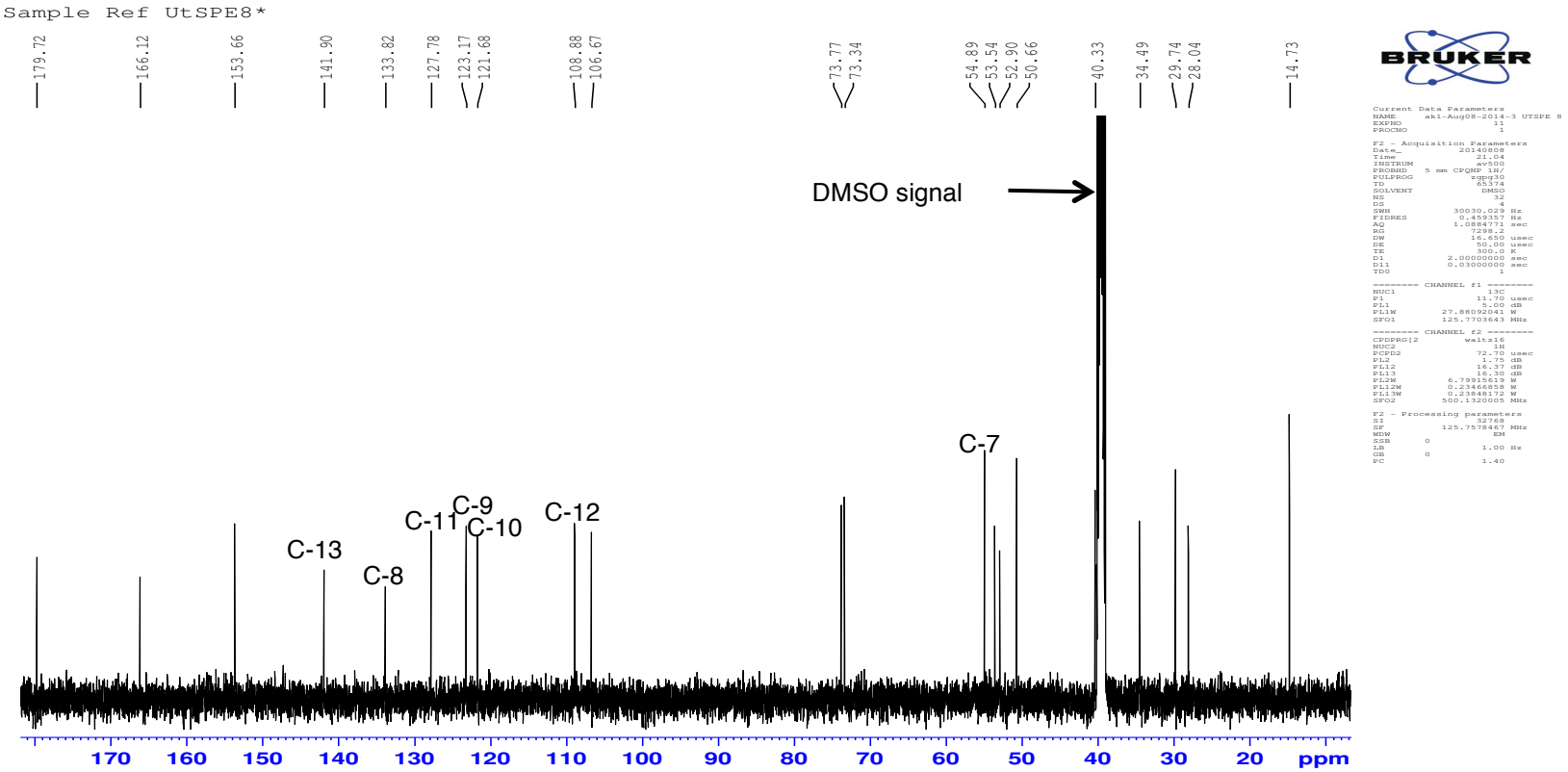

Figure 2.8 ^{13}C NMR spectrum for **AK-11**

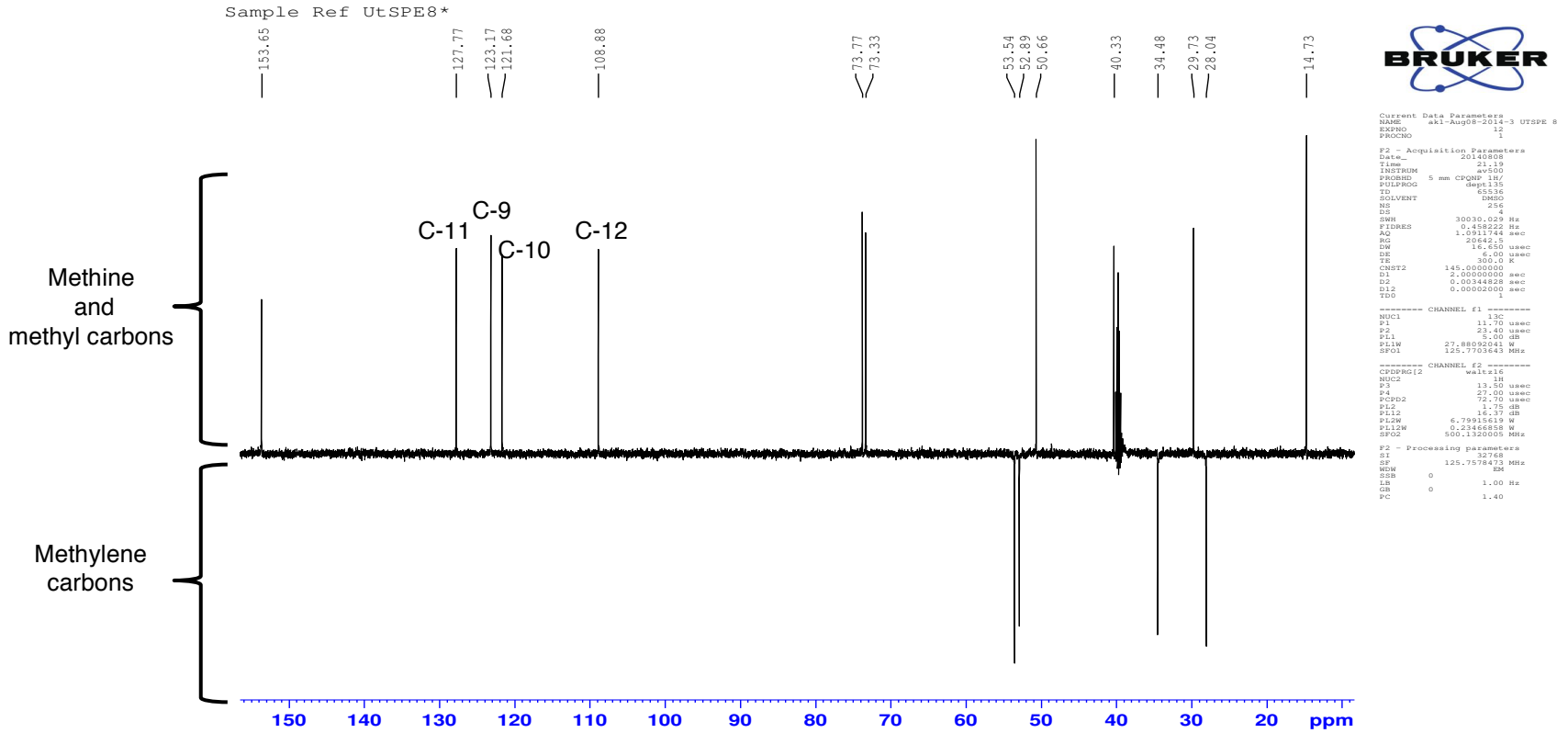

Figure 2.9 DEPT-135 NMR spectrum for **AK-11**

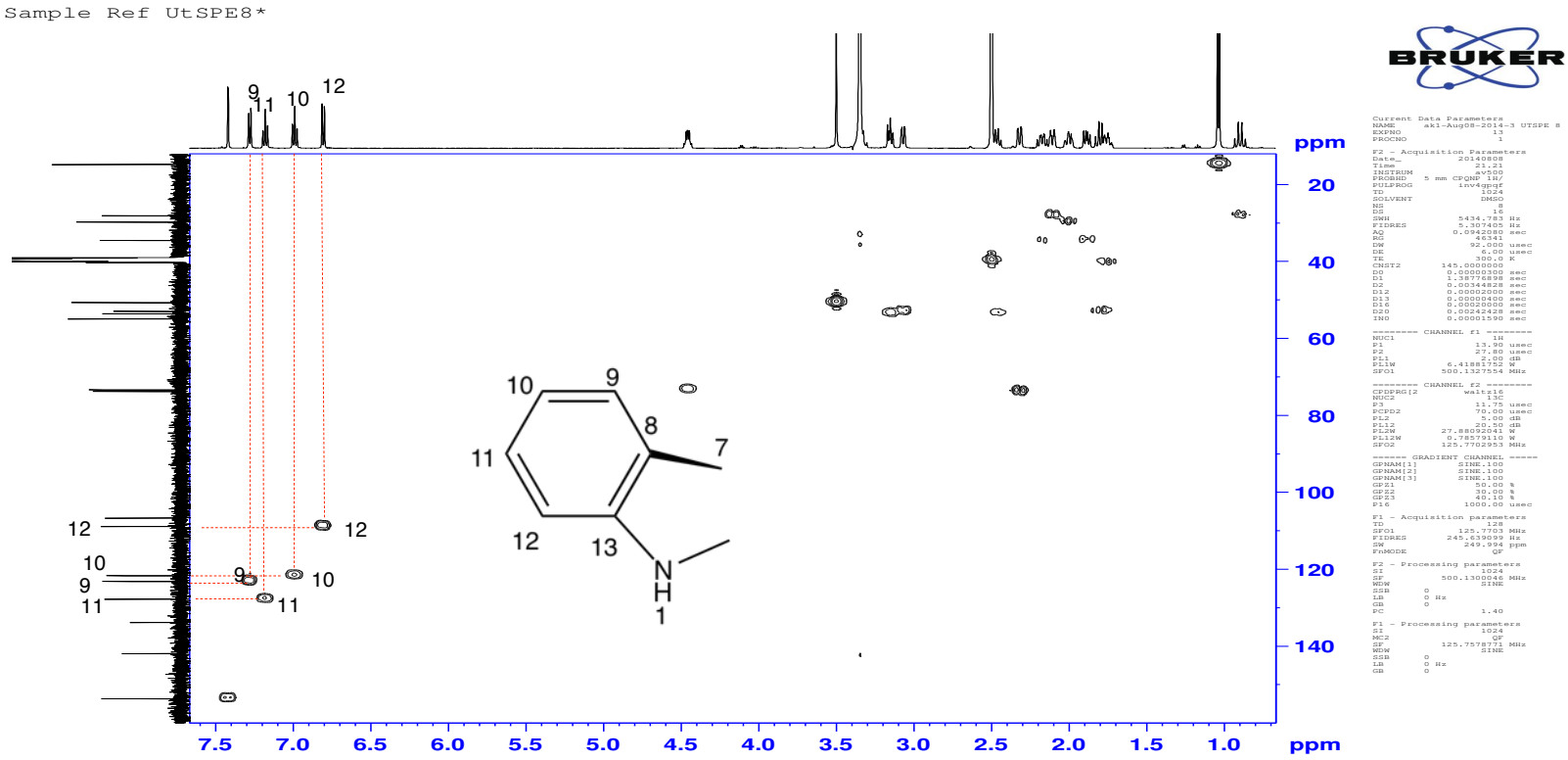

Figure 2.10 HMQC NMR spectrum for **AK-11**

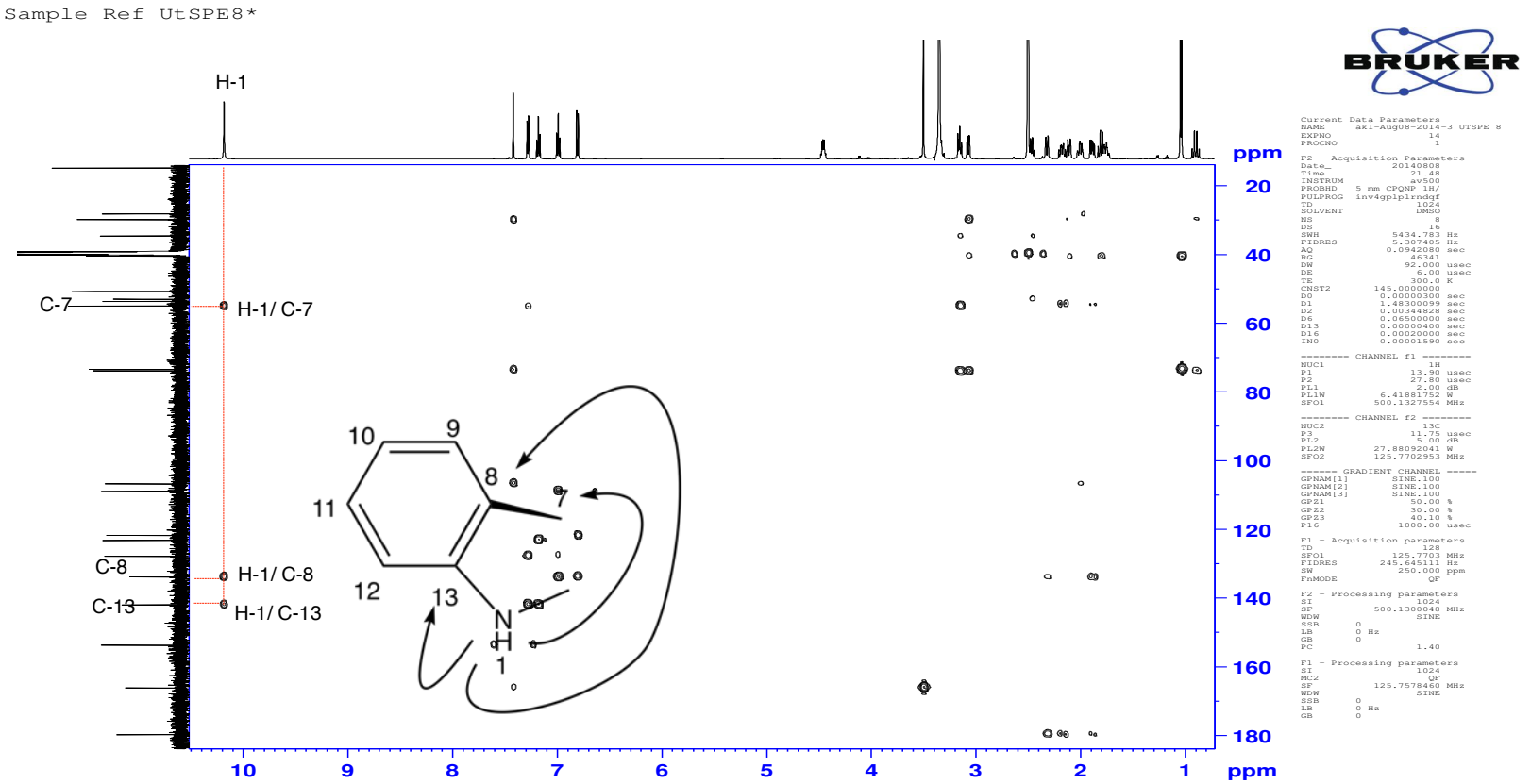

Figure 2.11 HMBC NMR spectrum for **AK-11**

2.4.6 Heteronuclear Multiple-Bond Correlation (HMBC)

Heteronuclear multiple-bond correlation spectra show long-range correlation between carbon and proton nuclei. The correlation could be over two to three bonds distant and it is sometimes referred to as ^{2}J and ^{3}J respectively. Like HMQC, its spectrum is presented with a ^{13}C NMR displayed on the left axis and ^{1}H NMR spectrum to the top axis. Information from this heteronuclear experiment allows structural fragments to be assembled.

2.4.7 Correlation Spectroscopy (COSY)

This experiment shows coupling between protons (^{1}H-^{1}H) over two to three bonds and sometimes four bonds distant. COSY spectra can also display long range coupling such as five bonds distant but these are rare. In the COSY spectrum, a ^{1}H NMR spectrum is plotted on both sides of the axes resulting in the display of two types of peaks, a diagonal and cross peaks. The diagonal peaks show the proton signals in the ^{1}H NMR, while the cross peaks indicate couplings between pairs of protons.

2.4.8 Nuclear Overhauser Effect Spectroscopy (NOESY)

Nuclear Overhauser Effect Spectroscopy shows through space coupling of protons (^{1}H-^{1}H) and it is important for the determination of the stereochemistry. The spectrum format is similar to that of the COSY experiment except that it displays both through space and bond coupling signals. It is therefore important to compare both COSY and NOESY spectra to be able to make a distinction between cross peaks indicative of through space coupling or bond coupling. Unlike the COSY spectrum however, the cross peak signals in NOESY spectra are not symmetrical.

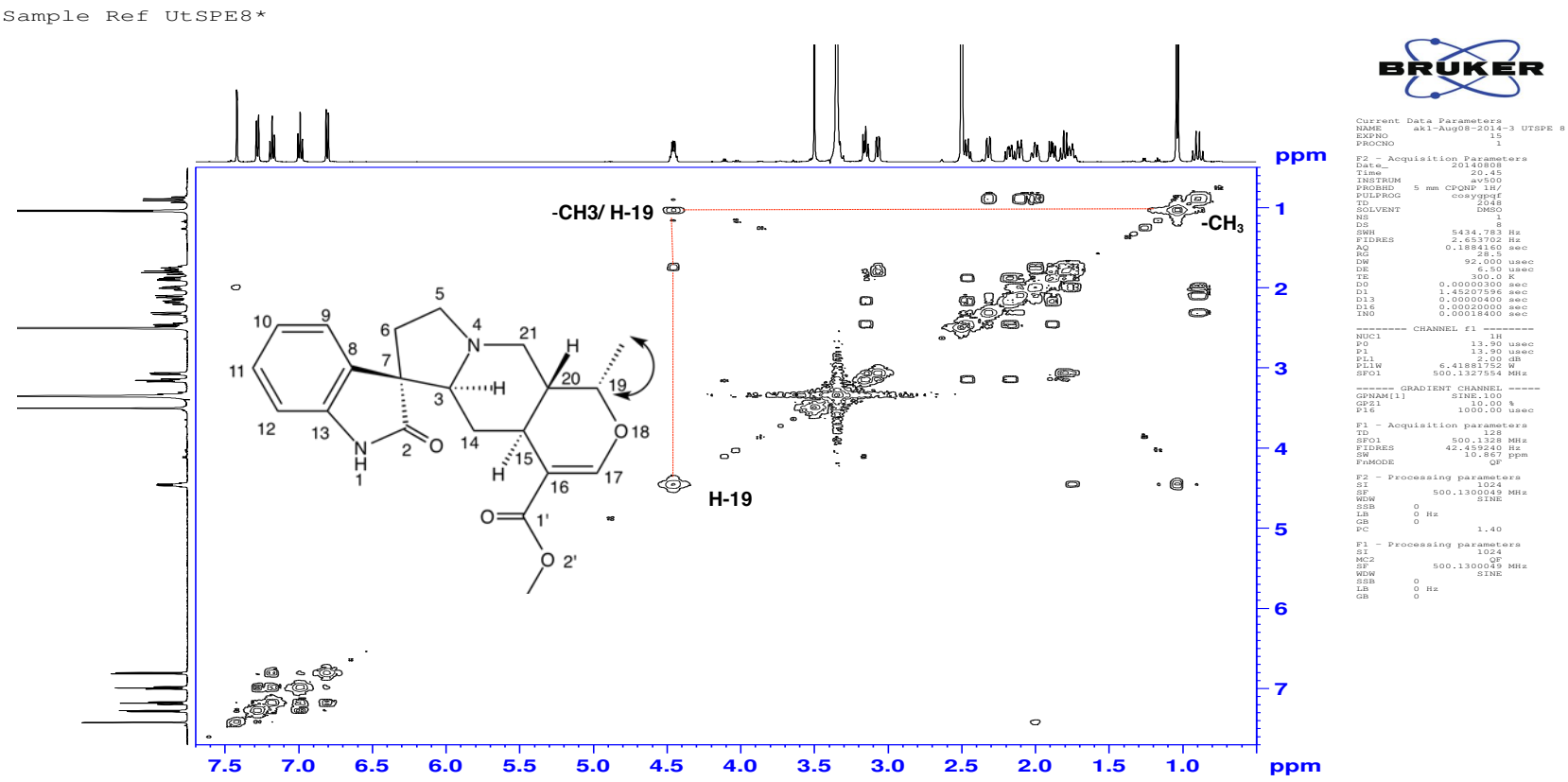

Figure 2.12 COSY spectrum for **AK-11**

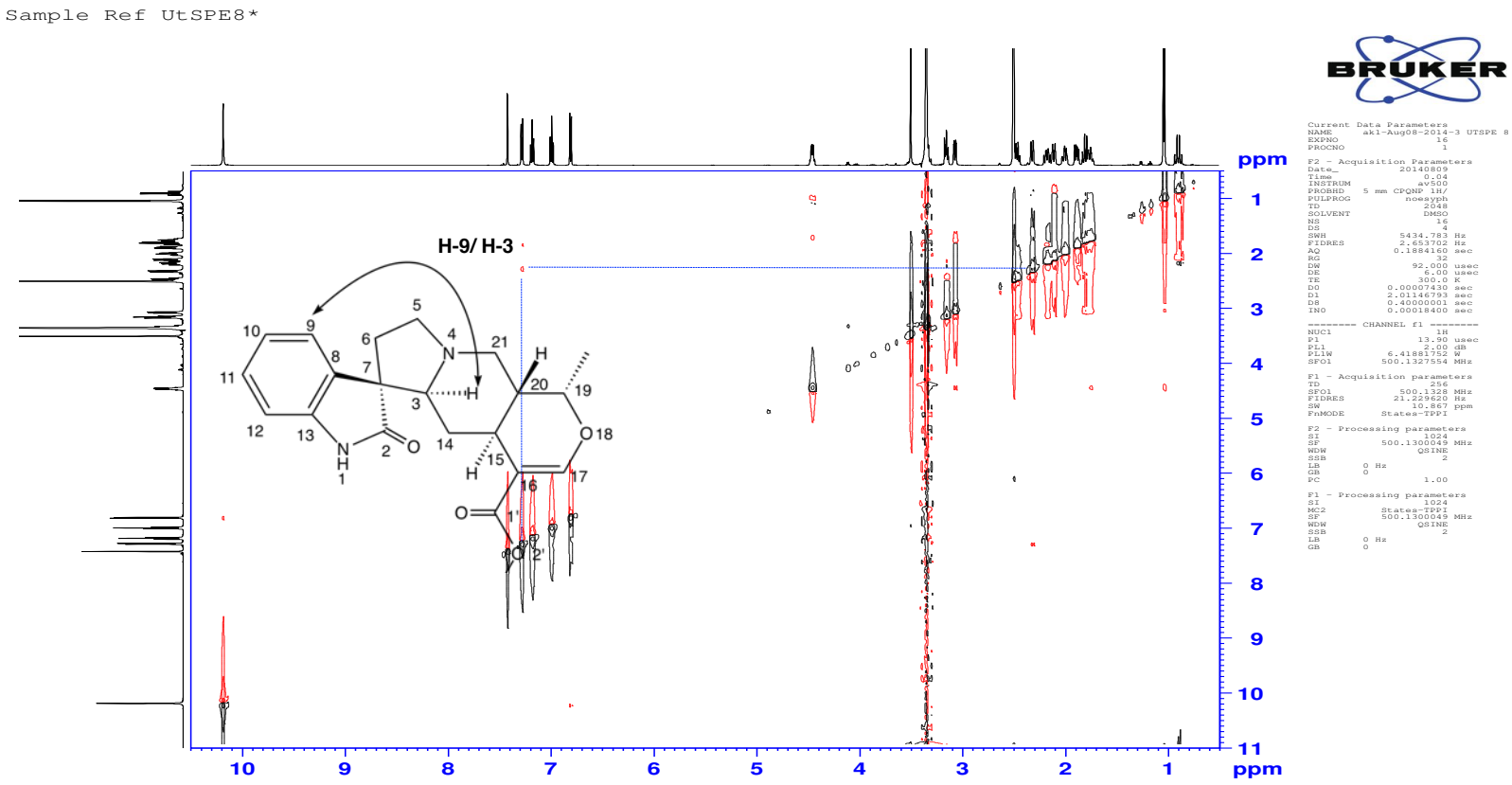

Figure 2.13 NOESY spectrum for **AK-11**

2.5 Biological Methods

2.5.1 Bacterial and Fungal Strains

The extracts, fractions, isolated compounds and some purchased compounds were screened against *Staphylococcus aureus, Escherichia coli* and *Candida spp* for antibacterial and antifungal activity. In addition antibiotic potentiation activity studies were conducted on the *S. aureus* strains expressing distinct efflux-related multidrug-resistance pumps. All bacterial and fungal strains used for the activity study are outlined in Table 2.3.

Table 2.3 Summary of bacterial and fungal strains used

STRAIN	SOURCE	NOTES
S. aureus 1199B	G. Kaatz (Kaatz *et al.*, 1993)	A multidrug-resistant *S. aureus* strain that over expresses the NorA efflux mechanism and possesses a gyrase mutation, both contribute to a high level of resistance to certain fluoroquinolones.
S. aureus XU212	E. Udo (Gibbons and Udo, 2000)	Tetracycline-resistant *S. aureus* strain XU212 possesses the TetK tetracycline efflux protein and mecA genes.
S. aureus RN4220	J. Cove (Reynolds and Cove, 2005)	A macrolide and type B streptogramin-resistant *S. aureus* strain possesses the Msr(A) genes.
S. aureus ATCC 25923	ATCC	Susceptibility testing control strain
E. coli NCTC 10418	NCTC	Control strain
C. albicans ATCC 66027	ATCC	Control strain
C. tropicalis ATCC750	ATCC	Control strain

ATCC – American Type Culture Collection, NCTC – National Collection of Type Cultures

2.5.2 Minimum Inhibitory concentration assay

2.5.2.1 Antibacterial testing

The *in vitro* antibacterial activity of extracts, fractions, isolated compounds and some purchased compounds was assessed by the broth microdilution method as described by Andrews (2001). All bacterial strains were sub-cultured on nutrient agar (Fluka Analytical) and incubated at 37°C for 24 h. An inoculum suspension of 1.0 x 10^8 cfu/mL was prepared in normal saline (0.9%$^{w}/_{v}$) by comparing with the 0.5 McFarland turbidity standard. This bacterial suspension was further diluted in normal saline and growth medium to yield a final 5 x 10^5 cfu/mL in the assay. Antibacterial agents (norfloxacin, tetracycline, erythromycin and ciprofloxacin; Sigma-Aldrich) were used as controls for the assay. Mueller Hinton Broth (MHB; Fluka Analytical) was used as the growth media. Calculated quantity of test samples and control antibiotics were prepared by dissolving in dimethylsulphoxide (DMSO; Panreac AppliChem) and further diluted in MHB. DMSO and diluents concentrations used in the experiment had no inhibitory activity against bacterial growth. Sterile MHB (100 μL) was dispensed into wells in columns 1 to 11 of a 96 well microtitre plate. Test sample (100 μL) or antibiotic (100 μL) were then introduced into wells in column 1 in their respective demarcated positions and serially diluted across the plate (from 512 to 1 μg/mL). The wells of column 11 were used as the growth control so no drug was introduced into these wells. The inoculum (100 μL) was then added to all wells except wells in column 12 which served as a sterile control. The assay plate was incubated at 37°C and results were determined at 24 h.

Results were determined by visual inspection after the addition of 20 μL of a 1 mg/mL methanolic solution of 3-[4,5-dimethylthiazol-2-yl]-2,5-diphenyltetrazolium bromide (MTT; Sigma-Aldrich) to the assay plate and incubated at 37°C for 20 min. A colour change from yellow to dark blue was indicative of bacterial growth. The MIC values were recorded as the lowest concentration at which no colour change was observed this is no bacterial growth. MIC values were determined in duplicate per plate and repeated in at least two independent experiments.

2.5.2.2 Antifungal testing

The *in vitro* antifungal activity of some isolated compounds was assessed by the broth microdilution method according to the guidelines of European Committee for Antimicrobial Susceptibility Testing (EUCAST) (Rodríguez-Tudela *et al.*, 2003). The fungal strains were sub-cultured on Sabouraud dextrose agar (Oxoid) and incubated for 24 h at 37°C prior to MIC determination. Antifungals (amphotericin B, itraconazole and ketoconazole; Sigma-Aldrich) were used as controls for the assay. The growth media for the assay was prepared by autoclaving a calculated quantity of Roswell Park Memorial Institute (RPMI)-1640 medium (AutoMod™), which was supplemented with glucose to a final concentration of 2% and with 0.165 M 3-(*N*-morpholino)-propanesulfonic acid (MOPS) as the buffer. Sodium hydroxide (10 M) was used to adjust the pH to 7.0 and thereafter L-glutamine (0.3 g/L) was sterile-filtered into the cooled autoclaved media. Materials for the preparation of the growth media were purchased from Sigma-Aldrich and Fischer Scientific. The preparation of test samples, control antifungals, an inoculum density of 5 x 10^5 cfu/mL, broth dilution plates and incubation conditions were done as per section 2.5.2.1 for antibacterial testing. Results were determined by visual inspection before and after the addition of MTT. The MIC of amphotericin B and test samples were recorded as the lowest concentration with no visible fungal growth. For the azole antifungals, the MIC was determined as the lowest concentration that resulted in an 80% reduction in turbidity as compared to the drug-free control. MIC values were determined in duplicate per plate and repeated in at least two independent experiments.

2.5.3 Antibiotic Potentiation Assay

All strains were cultured on nutrient agar at 37°C for 24 h prior to MIC determination. Bacterial suspension of 5 x 10^5 cfu/mL was prepared for each strain as per section 2.5.2.1 on antibacterial testing. Test samples, antibiotics (norfloxacin, tetracycline and erythromycin)

and reserpine (Sigma-Aldrich) were prepared by dissolving in DMSO. The concentration of the modulators (i.e. test samples and reserpine) remained the same throughout the experiment whereas the antibiotics were serially diluted across the plate. The MIC of antibiotics was determined in combination with the sub-inhibitory concentration of the test samples (i.e. a quarter of the MIC). 20 μg/mL of reserpine, a known modulator, was used as the control for comparison purposes. This method was adapted from Smith *et al.*, (2005).

100 μL of double strength test sample was introduced into wells of column 1 of a 96 well microtitre plate. 100 μL of single strength test sample was introduced into wells of column 2 to 10. Then 100 μL of antibiotic was dispensed into wells of column 1 and serially diluted across the assay plate. The wells of column 11 were used the as growth control, hence no drug was dispensed into these wells. The final volume from wells of column 10 was dispensed into wells of column 12. 100 μL of sterile MHB was dispensed into wells of column 11. The inoculum (100 μL) was then added to all wells except wells in column 12 which served as a sterile control. The assay plate was incubated at 37°C for 18 h. MIC was determined by visual inspection after the addition of MTT and incubation for 20 min. MIC values were determined in duplicate per plate and again repeated in at least two independent experiments.

2.5.4 Bacterial Plasmid Conjugation Inhibition Assay

Principle of Conjugal Transfer of Antibiotic Resistance

The goal of this experiment was to identify compounds that inhibited conjugal transfer of antibiotic resistance between two bacterial strains with disparate resistance determinants. The assay involves the mixture of a donor that possesses a transferable resistant determinant to be examined, and the recipient must be susceptible to the antibiotic to which

the transferable determinant confers. The recipient must also have one or more antibiotic-resistance markers to which the donor is susceptible. The resistant characteristics of the recipient should be chromosomally-encoded and non-transferable, to allow positive identification. These resistance traits allow growth of transconjugants in media with two antibiotics but inhibit the growth of both the recipient and the donor. Transconjugants are recipients that have acquired the transferable determinants from donors.

Bacterial strains and plasmids

E. coli cells harbouring plasmids used in this study have been outlined in Table 2.4.

Table 2.4 Summary of *E. coli* strains and plasmids used

Strain	Plasmid	Incompatibility (Inc) group	Resistance markers	Source
Donor				
WP2	pKM101	N	Ap	Deutsche Sammlung von Mikroorganismen und Zellkulturen (DSMZ)
K12 J53-2	TP114	I_2	Km	
K12 J53-2	R7K	W	Ap, Sm, Sp	
K12 JD173	pUB307	P	Km, Tc	Prof. Keith Derbyshire, Wadsworth Center, New York Department of Health
Recipient				
ER1793	-	-	Sm	New England BioLabs
JM109	-	-	Nal	

Ap, Ampicillin; Km, Kanamycin; Tc, Tetracycline; Sm, Streptomycin; Sp, Spectinomycin; Nal, Nalidixic acid. DSMZ is the German Collection of Microorganisms and Cell Cultures GmbH.

Assay

Five mL of Luria-Bertani broth (LB; Fisher Scientific) was inoculated with 2 - 3 single colonies from a recipient culture and the same procedure was repeated for the donor culture. Both recipient and donor inoculum were incubated overnight at 37°C. The overnight culture was serially diluted with phosphate buffered saline (PBS; Sigma-Aldrich) to determine the number of donor and recipient colony forming unit (cfu) prior to conjugation. Conjugation was performed as previously described by Rice and Bonomo (2005) with slight modifications. 20 μL of the donor and 20 μL of the recipient were dispensed into a 96 well microtitre plate with 160 μL of LB broth and a calculated quantity of the test sample. Test samples were assessed for anti-conjugative activity at sub-inhibitory concentrations (one-quarter the MIC). The assay plate was incubated overnight at 37°C. The overnight conjugation mixture was serially diluted and to determine the number of transconjugants and donors, 20 μL was plated onto antibiotic containing MacConkey agar (Sigma-Aldrich) plate. This was incubated overnight at 37°C. Novobiocin and linoleic acid (Sigma-Aldrich) were used as the positive plasmid transfer inhibitor control drugs at sub-inhibitory concentrations. Antibiotics and the concentrations used in MacConkey agar for positive identification of donors, recipients and transconjugants (μg/mL): amoxicillin (50), streptomycin sulphate (20), nalidixic acid (30), kanamycin sulphate (20 and 30) (Sigma-Aldrich). Donor cells with plasmids pKM101, TP114 and pUB307 were paired with the recipient ER1793 and plasmid R7K donor cells were paired with the recipient JM109 for the assay. Conjugation frequency was calculated as the ratio of total number of transconjugants (cfu/mL) to the total number of donor (cfu/mL) and expressed as a percentage relative to the negative control. This experiment was performed as duplicate in three independent experiments.

2.5.5 Plasmid Elimination Assay

The isolated compounds that showed promising anti-conjugative activity were further assessed for plasmid-eliminating activity by a slightly modified version of the agar plate method described by Hooper (1984). The *E. coli* donor strains in Table 2.5.4 were sub-cultured on MacConkey agar plates supplemented with the appropriate antibiotic, to ensure plasmid presence. LB (5 mL) was inoculated with 2-3 single colonies of the *E. coli* cells harbouring plasmids. This was incubated at 37°C for 24 h and the cfu determined prior to the assay. The overnight culture (20 μL) was then added to 180 μL LB and calculated quantity of test sample in a 96 well microtitre plate and incubated overnight (24 h) at 37°C. Test samples were evaluated for plasmid elimination activity at sub-inhibitory concentration (one-quarter of the MIC). The overnight mixture was serially diluted, 20 μL was then plated on antibiotic containing MacConkey agar and incubated at 37°C for 24 h. Promethazine (Sigma-Aldrich) a known anti-plasmid agent was used as the control drug to demonstrate plasmid elimination. Plasmid elimination was calculated as the difference between the total number of colonies without test sample and with test sample expressed as a percentage relative to the total number of colonies without test sample. Antibiotics and concentrations used in MacConkey agar for positive identification of *E. coli* cells harbouring plasmids (μg/mL): amoxicillin (50) and kanamycin sulphate (20 and 30). This experiment was performed as duplicate in three independent experiments.

2.5.6 Cytotoxicity Testing

Compounds that showed promising anti-conjugative activity without plasmid-eliminating activity were further screened for their cytotoxic effect on human dermal fibroblasts, adult (HDFa) cells (C-013-5C; Thermo Fisher Scientific). The Sulforhodamine B (SRB) assay as previously described by Skehan (1990) was adapted for the cytotoxicity screening. In this method, cell number was estimated by the determination of cell density

based on the staining of proteins with SRB. The HDFa cells were also grown in a 75 cm^2 culture flask and maintained in Dulbecco's Modified Eagle's Medium (DMEM; Gibco). The DMEM was supplemented with 10% FBS, 1% non-essential amino acids (NEAA; Gibco), 0.1% gentamicin and amphotericin B (Sigma-Aldrich) solution to prevent bacterial growth. The cells were maintained at 37°C in a humidified atmosphere of 5% carbon dioxide. The medium was also used for cell seeding and as a diluent for test samples. The cells were seeded in a 96 well microtitre plate and the calculated quantity of test samples were added and incubated at 37°C. At 72 h of incubation, 50 μL of cold 40%$^{w}/_{v}$ trichloroacetic acid (TCA; Sigma-Aldrich) solution was dispensed into the cell culture to promote cell fixation. The plate was then incubated at 4°C for an hour and washed four times with distilled water. The TCA-fixed cells were stained with 0.4% $^{w}/_{v}$ SRB solution (Sigma-Aldrich) and left at room temperature for an hour. Afterwards, the plate was rinsed four times with 1% acetic acid (Sigma-Aldrich), flicked to remove unbound dye and dried overnight (24 h). Prior to optical density determination, 100 μL of 10 mM Tris buffer (Sigma-Aldrich) solution was dispensed into the wells and agitated in an orbital shaker for 5 min, this allowed solubilisation of the SRB-protein complex. The optical density (OD) was then measured at 510 nm using a microtitre plate reader. Percentage change in cell growth was calculated as:

$$\text{Percentage of viable cell} = \frac{\text{OD}_{510} \text{ of test sample - OD}_{510} \text{of blank}}{\text{OD}_{510} \text{ of control - OD}_{510} \text{ of blank}} \times 100$$

This experiment was performed in triplicate in three independent experiments. Mohd Mukrish Mohd Hanafi at the Cell Culture Laboratory, Research Department of Pharmaceutical and Biological Chemistry, UCL School of Pharmacy kindly performed this cytotoxicity screening.

Data from each experiment, bacterial plasmid conjugation inhibition, plasmid elimination and cytotoxicity were expressed as the mean and respective standard deviation (SD). Differences between the control and the test samples were evaluated by Student's t-test (GraphPad software). Values of $p < 0.05$ were considered significant.

Chapter 3 Results and Discussion

3.1 Crude Extracts

Crude extracts were obtained from 0.2 - 1 kg of the powdered plant materials with hexane or petroleum ether, chloroform and methanol using either Soxhlet or ultrasound-assisted extraction method. The extracts were first assessed for antibacterial activity against *E. coli* NCTC 10418. All the extracts had no inhibitory activity against *E. coli* NCTC 10418 even at a concentration of 512 µg/mL. The extracts were further assessed for anti-conjugative activity against *E. coli* strains, as the aim of the project was to isolate compounds that inhibited the conjugal transfer of antibiotic resistance between bacterial strains but not kill the bacteria or inhibit its growth. Hence antibacterial activity of the extracts was not mandatory making all the extracts good candidates for this assay. Screening for antibacterial activity was necessary as the results informed the concentrations needed for the bacterial plasmid conjugation inhibition assay. Table 3.1 summarizes the conjugative activity for each extract at a sub-inhibitory concentration of 100 µg/mL against *E. coli* strains harbouring plasmids with antibiotic resistance makers. Low percentage transfer frequency was indicative of active inhibition of bacterial conjugation while high percentage transfer frequency was indicative of poor inhibition or promotion of bacterial conjugation. A transfer frequency of less than 10% was considered active, 10 - 50% was considered moderately active and greater than 50% was considered as poorly active. Extracts with a transfer frequency ≥ 120% was considered as inactive and to be promoters or enhancers of bacterial conjugation.

Table 3.1 The effects of plant extracts on the conjugal transfer of selected plasmids

Extracts		Transfer Frequency (%)			
		pKM101 IncN	**TP114 $IncI_2$**	**pUB307 IncP**	**R7K IncW**
S. alba	chloroform	13.5 ± 4.9	94.5 ± 2.1	64.0 ± 3.6	33.0 ± 4.4
	methanol	9.0 ± 2.8	66.5 ± 7.8	50.3 ± 6.8	> 120.0
A. rusticana	hexane	> 120.0	> 120.0	> 120.0	> 120.0
	chloroform	> 120.0	> 120.0	> 120.0	75.0 ± 4.0
	methanol	> 120.0	15.5 ± 7.2	15.1 ± 3.8	> 120.0
B. oleracea	hexane	> 120.0	> 120.0	42.5 ± 19.1	75.0 ± 2.7
	chloroform	> 120.0	> 120.0	69.5 ± 19.5	> 120.0
	methanol	> 120.0	38.0 ± 13.9	43.3 ± 18.5	> 120.0
L. sativum	Petroleum ether	13.5 ± 10.6	42.5 ± 6.4	> 120.0	> 120.0
	methanol	10.5 ± 6.4	72.0 ± 28.9	> 120.0	> 120.0
Z. officinale	hexane	3.5 ± 0.7	47.0 ± 7.1	71.9 ± 34.7	59.9 ± 10.0
	chloroform	44.5 ± 16.3	44.5 ± 5.0	> 120.0	> 120.0
	methanol	6.5 ± 0.7	42.0 ± 7.0	90.5 ± 37.1	> 120.0
M. lowiana	hexane	> 120.0	> 120.0	47.5 ± 4.2	11.4 ± 6.5
	chloroform	> 120.0	> 120.0	42.6 ± 4.2	> 120.0
	methanol	> 120.0	48.8 ± 7.7	13.5 ± 5.4	30.0 ± 0.5
B. officinalis	hexane	73. 5 ± 1.7	78.0 ± 17.0	> 120.0	> 120.0
	chloroform	27. 0 ± 4.2	45.5 ± 5.0	> 120.0	> 120.0
	methanol	6.0 ± 2.8	46.5 ± 3.5	> 120.0	> 120.0
U. tomentosa	hexane	> 120.0	> 120.0	69.6 ± 13.4	> 120.0
	chloroform	> 120.0	> 120.0	61.5 ±19.1	64.0 ± 4.2
	methanol	> 120.0	112.0 ± 27.6	> 120.0.0	54.0 ± 15.6
Positive control	Novobiocin 10 µg/mL	-	17.0 ± 4.2	27.5 ± 0.71	-
	Linoleic acid 200 µg/mL	-	-	-	16.3 ± 3.7
Negative control		100	100	100	100

The values represent the mean transfer frequency (%) ± SD of at least three independent experiments

From the anti-conjugation screening, activity was observed mostly for the methanol extracts and some chloroform extracts. Based on these results, extracts with promising anti-

conjugative activity of ≤15% were further worked on in an attempt to isolate the bioactive principles.

3.2 Isolation and Structure Elucidation

3.2.1 Isolation from *S. alba*

Powdered *S. alba* seeds (1kg) were successively extracted with hexane, chloroform and methanol; this gave a yield of 28.0%, 21.7% and 8.3%, respectively. The active methanol extract was subjected to silica gel gravity column chromatography and reversed-phased SPE, which gave two glucosinolate compounds, **AK-1** (7.5 mg) and **AK-2** (27.1 mg), respectively. **AK-1** was eluted with acetonitrile, methanol and water (7:2:1, v/v) from a 2.4 g methanol extract whilst **AK-2** was eluted with water and methanol (7:3, v/v) from a gram of methanol extract.

3.2.1.1 Characterisation of AK-1 as 3-butenyl glucosinolate

AK-1 was isolated as an amorphous greenish bluish solid from the methanol extract of *S. alba.* The accurate mass measurement gave an $[M-H]^-$ ion at *m/z* 372.0406 which suggested that its molecular formula was $C_{11}H_{18}NO_9S_2^-$. The ^1H NMR data were characteristic of an alkenyl glucosinolate, organic compounds commonly found in the *Brassica* species (Fahey *et al.*, 2001).

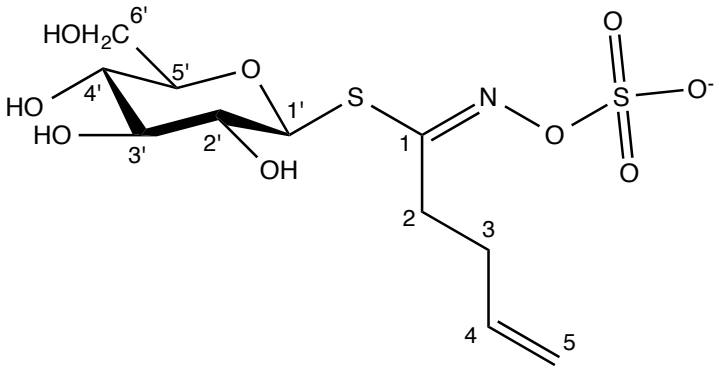

Figure 3.1 Structure for **AK-1**

The NMR and IR spectra data showed the presence of a β-thioglucoside *N*-hydroxysulfate moiety that carried an alkenyl side chain. The IR spectrum revealed a C=N (1641.19 cm^{-1}), an sulfonic acid group (916.68 – 877.15 cm^{-1}) and a C-S (642.89 cm^{-1}) absorption bands indicating of the presence of these functional groups. The ^{1}H NMR resonance spectral between δ_H 3.23 to 4.83 accounted for the oxymethine hydrogens of a glucose moiety (Figure 3.2). The proton signals at δ_H 2.70, 2.47, 4.99 and 5.89 accounted for the hydrogens on the alkyl chain. The ^{13}C and DEPT-135 NMR spectra (Figure 3.3) revealed the anomeric carbon (C-1', δ_C 83.8), oxymethines (C-2' to 5', δ_C 71.2 to 82.4) and the oxymethylene (C-6', δ_C 62.7) carbons for the glucose moiety. It also showed the methine (C-4, δ_C 138.5), methylenes (C-2 δ_C 33.1 and C-3 δ_C 32.6) and exomethylene (C-5, δ_C 115.9) carbons of the alkyl chain. The presences of the quaternary carbon (C-1, δ_C 161.0) bonded to a β-thioglucoside *N*–hydroxysulfate moiety was also confirmed by the ^{13}C and DEPT-135 NMR spectra. The glucose moiety and alkenyl chain were structurally assigned by the HMBC correlations as shown in Figure 3.6 and Table 3.2. The HMBC spectrum (Figure 3.4) revealed the thioglucosidic linkage of hydrogen H-1' (δ_H 4.81) to the quaternary carbon, C-1 (δ_C 161.0) of the sulphonated oxime by a ^{3}J correlation. The NOESY spectrum showed the correlation between the H-1' of the glucose moiety and the H-2 (δ_H 2.70) of the alkenyl chain. Compound **AK-1** was therefore identified as (*E*)-(1-((3,4,5-trihydroxy-6-(hydroxymethyl) tetrahydro-2*H*-pyran-2-yl)thio)pent-4-en-1-ylidene)aminosulfate commonly known as gluconapin or 3-butenyl glucosinolate. The ^{1}H and ^{13}C NMR data of this compound are in good agreement with published literature for the isolation of 3-butenyl glucosinolate from broccoli seeds (*Brassica oleracea* var. *italica*) and brown mustard seeds (*Brassica juncea*) (Du *et al.*, 2008; Wang *et al.*, 2014). Additionally, this compound has been reported for in *Brassica campestris* L. *ssp. Peckinensis,* (Chinese cabbage), *Brassica napus* L. var. *oleifera* (rapeseed) (Charpentier *et al.*, 1998; Kim *et al.*, 2004).

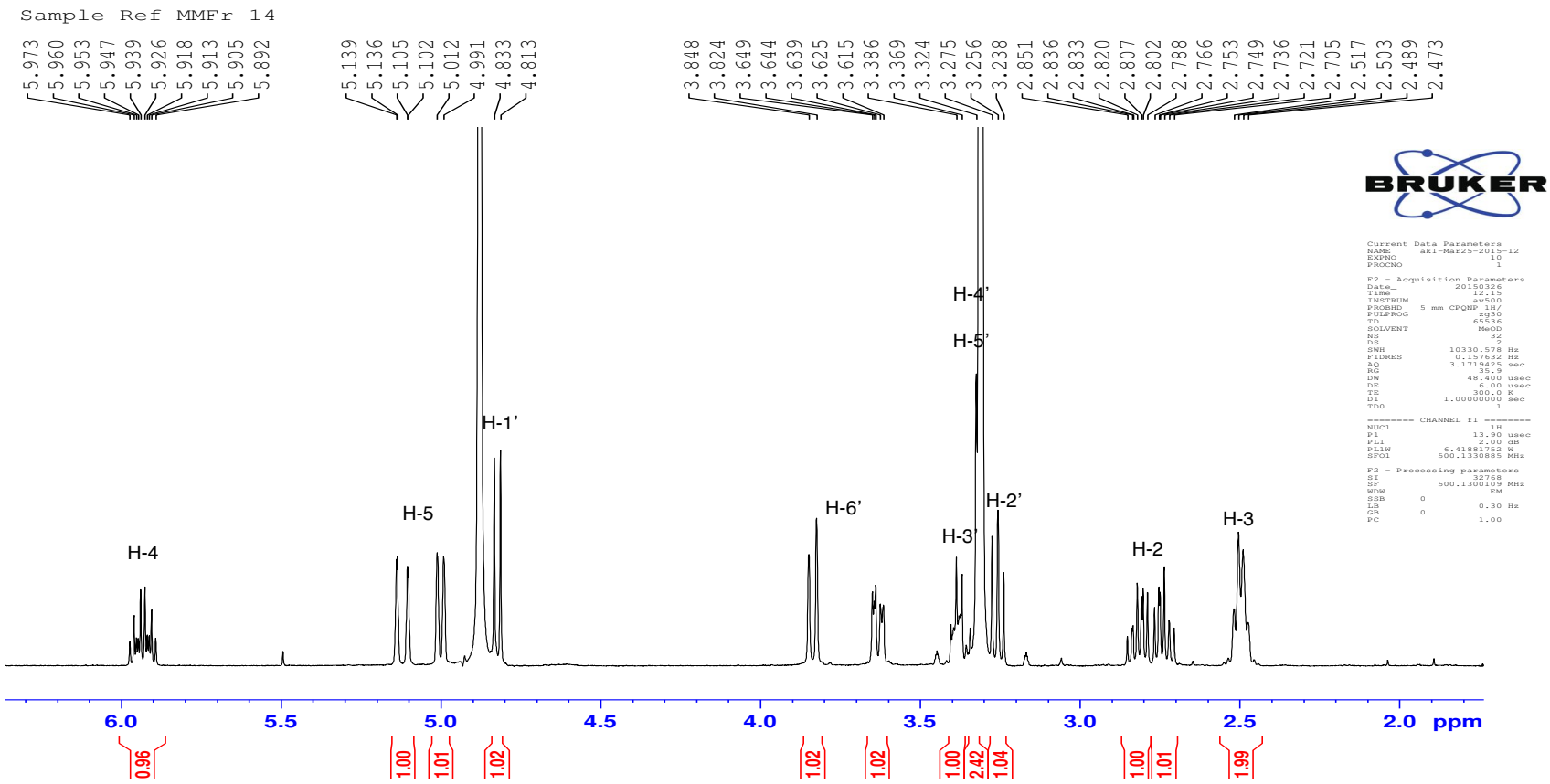

Figure 3.2 ^{1}H NMR spectrum for **AK-1**, recorded in CD_3OD, 500 MHz

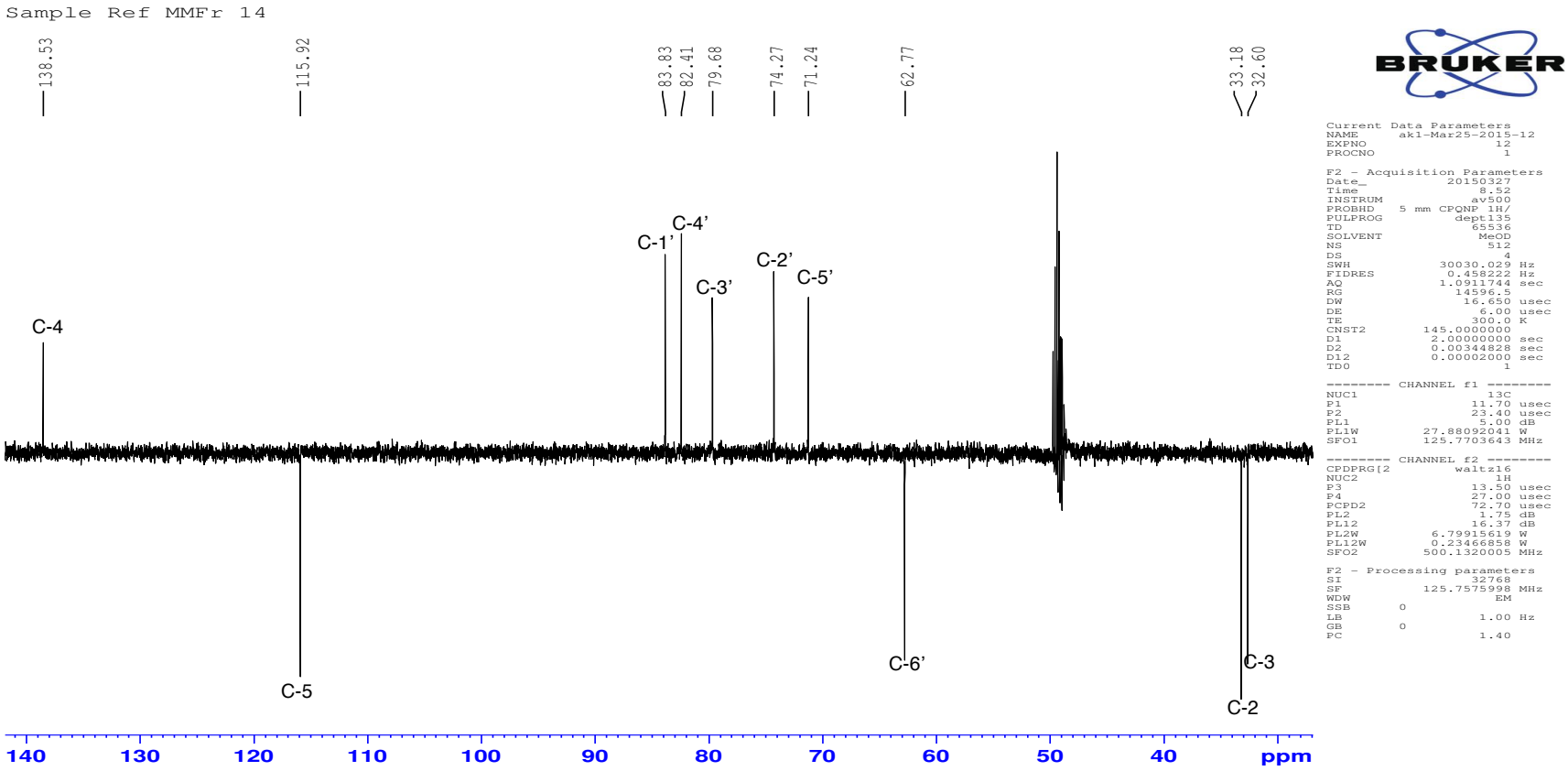

Figure 3.3 DEPT-135 NMR spectrum for **AK-1**, recorded in CD_3OD, 500 MHz

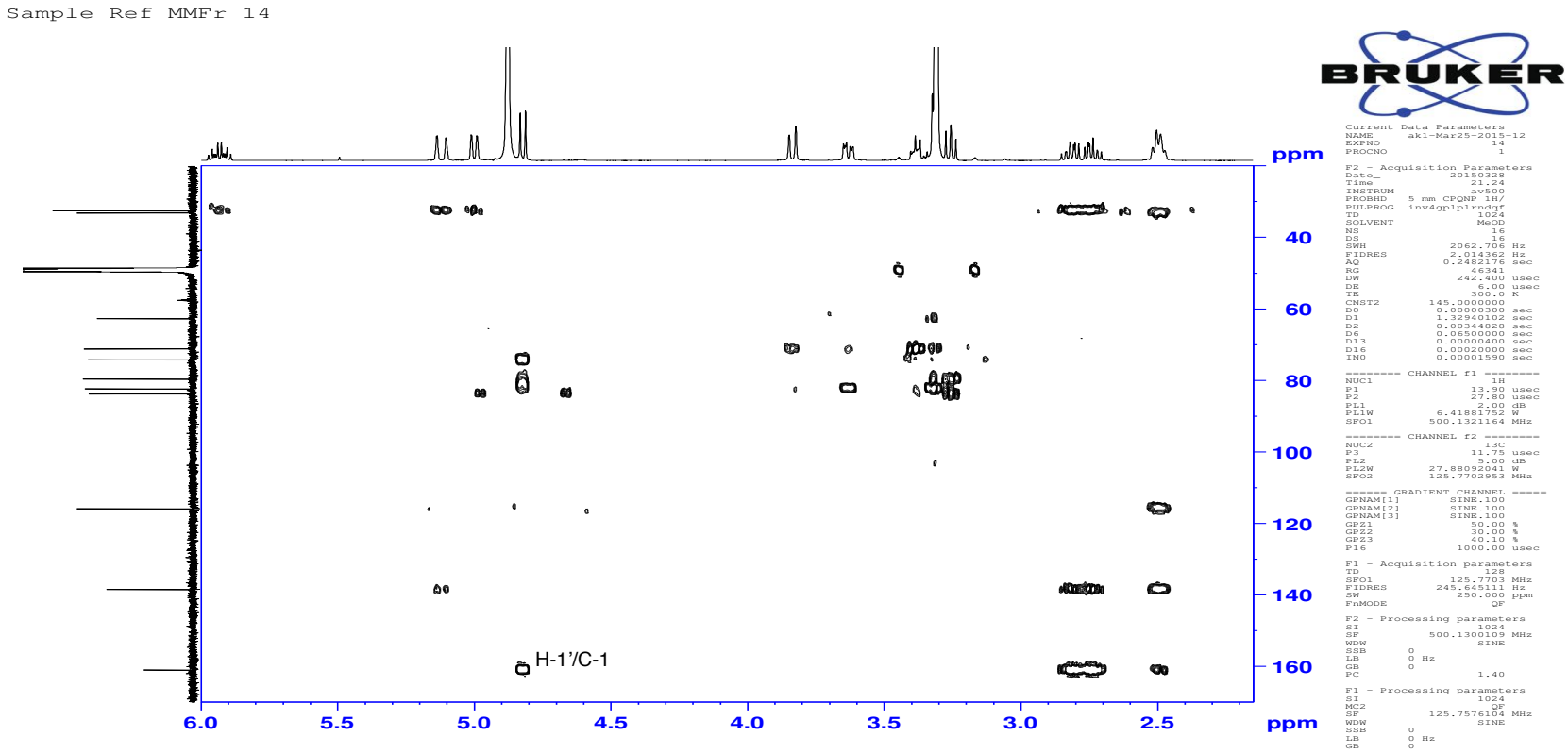

Figure 3.4 HMBC NMR spectrum for **AK-1**

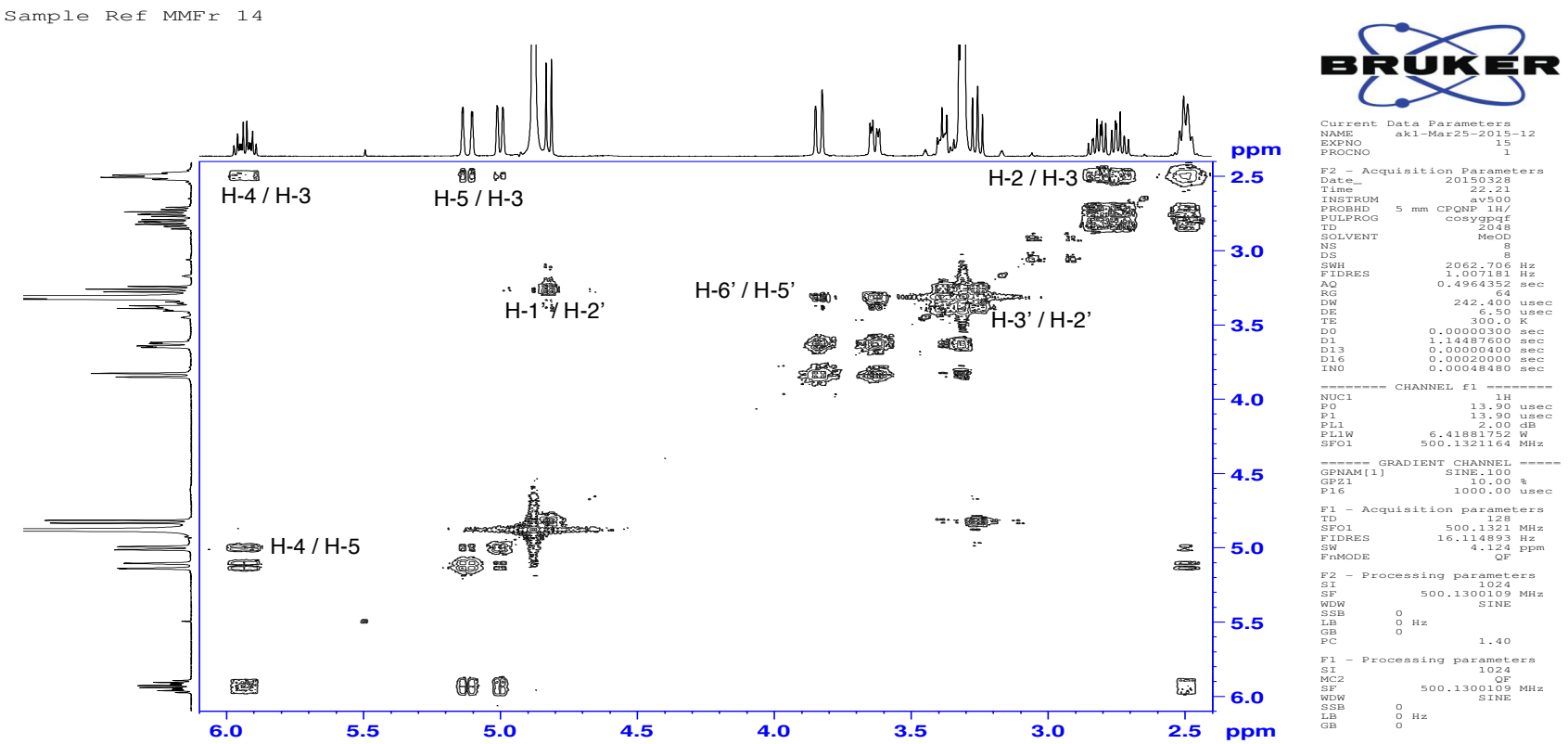

Figure 3.5 COSY NMR spectrum for **AK-1**

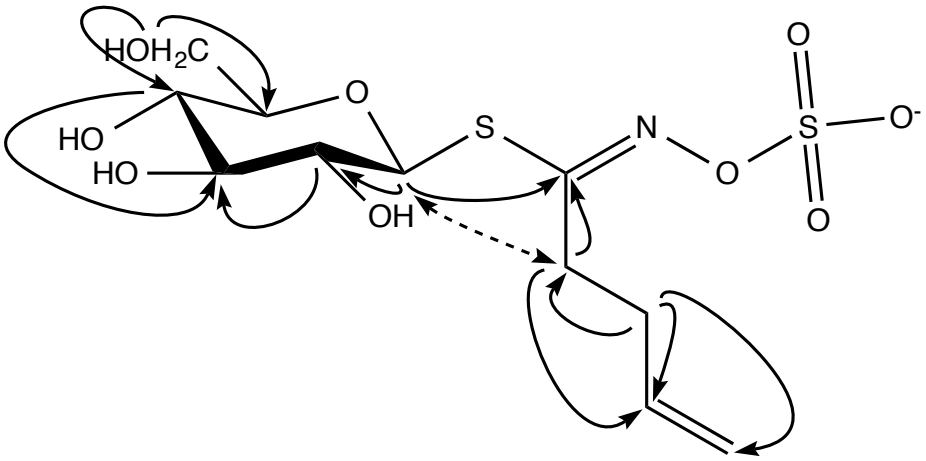

Figure 3.6 HMBC (solid arrow) and NOESY (dotted arrow) correlations for **AK-1**

Table 3.2 ^{1}H and ^{13}C NMR spectral data (ppm) and HMBC correlations of **AK-1**, recorded in methanol-d_4

Position	^{1}H	^{13}C	^{2}J	^{3}J	^{13}C Du *et al.*, 2008 (CD_3OD, 125 MHz)
1	-	161.0			161.6
2	2.70, 2.78 m	33.1	C1, C3	C4	33.0
3	2.47 (2H) q	32.6	C2, C4	C1, C5	32.9
4	5.89 m	138.5	C3		138.2
5	4.99, 5.10 dd	115.9		C3	116.0
1’	4.81 d	83.8	C2’	C1	83.6
2’	3.23 t	74.2	C1’, C3’		74.1
3’	3.61 d	79.6		C5’	79.5
4’	3.32 d	82.4	C3’		82.1
5’	3.32 d	71.2	C4’	C3’	71.1
6’	3.63, 3.84 dd	62.7	C5’	C4’	62.5

Multiplicities of proton signals: d - doublet, dd - doublet of doublets, t - triplet, q - quartet and m - multiplet

3.2.1.2 Characterization of AK-2 as 4-hydroxybenzyl glucosinolate

AK-2 was isolated as a straw coloured gummy liquid from the methanol extract of *S. alba.* The accurate mass measurement gave an $[M-H]^-$ ion at *m/z* 424.0363 suggesting a

molecular formula of $C_{14}H_{18}NO_{10}S_2^-$. The ^1H and ^{13}C NMR data were characteristic of an aromatic glucosinolate. The NMR and IR spectral data showed the presence of a β-thioglucoside *N*-hydroxysulfate moiety that carried a *p*-hydroxylbenzyl side chain. The IR spectrum revealed C=N (1653.04 cm^{-1}), a sulfonic acid group (951.11 cm^{-1}) and C-S (703.08 cm^{-1}) absorption bands indicating the presence of these groups. The ^1H resonance between δ_H 2.94 to 5.41 accounted for the oxymethine hydrogens positioned on the glucose moiety. The ^{13}C NMR (Figure 3.9) and DEPT spectra revealed the oxymethines and oxymethylene (C-6', δ_C 60.9) carbons of the glucose moiety. The proton signals at δ_H 3.70 and 3.99 accounted for the methylene hydrogens on the alkyl chain. The roofed hydrogens (δ_H 6.71 and 7.09, J = 8.0 Hz) and a hydroxyl group (δ_H 9.33) accounted for the positions on the

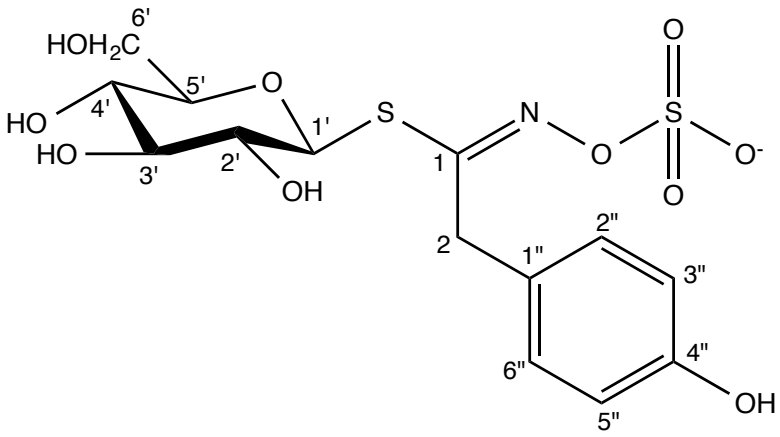

Figure 3.7 Structure for **AK-2**

p-hydroxylbenzyl aromatic ring of the side chain (Figure 3.8). The structural assignment of the β-thioglucoside *N*-hydroxysulfate moiety of compound **AK-2** was same as the previously described for compound **AK-1** in section 3.2.1.1. The HMBC revealed the thioglucosidic linkage of H-1' (δ_H 4.32) to the quaternary carbon, C-1 (δ_C 155.3) of the sulphonated oxime by a ^3J correlation (Figure 3.11). The methylene hydrogens (H_2-2, δ_H 3.70 and 3.99) showed a ^2J correlation to the quaternary carbon of the sulphonated oxime and the aromatic quaternary carbon, C-1" (δ_C 126.5) (Figure 3.11).

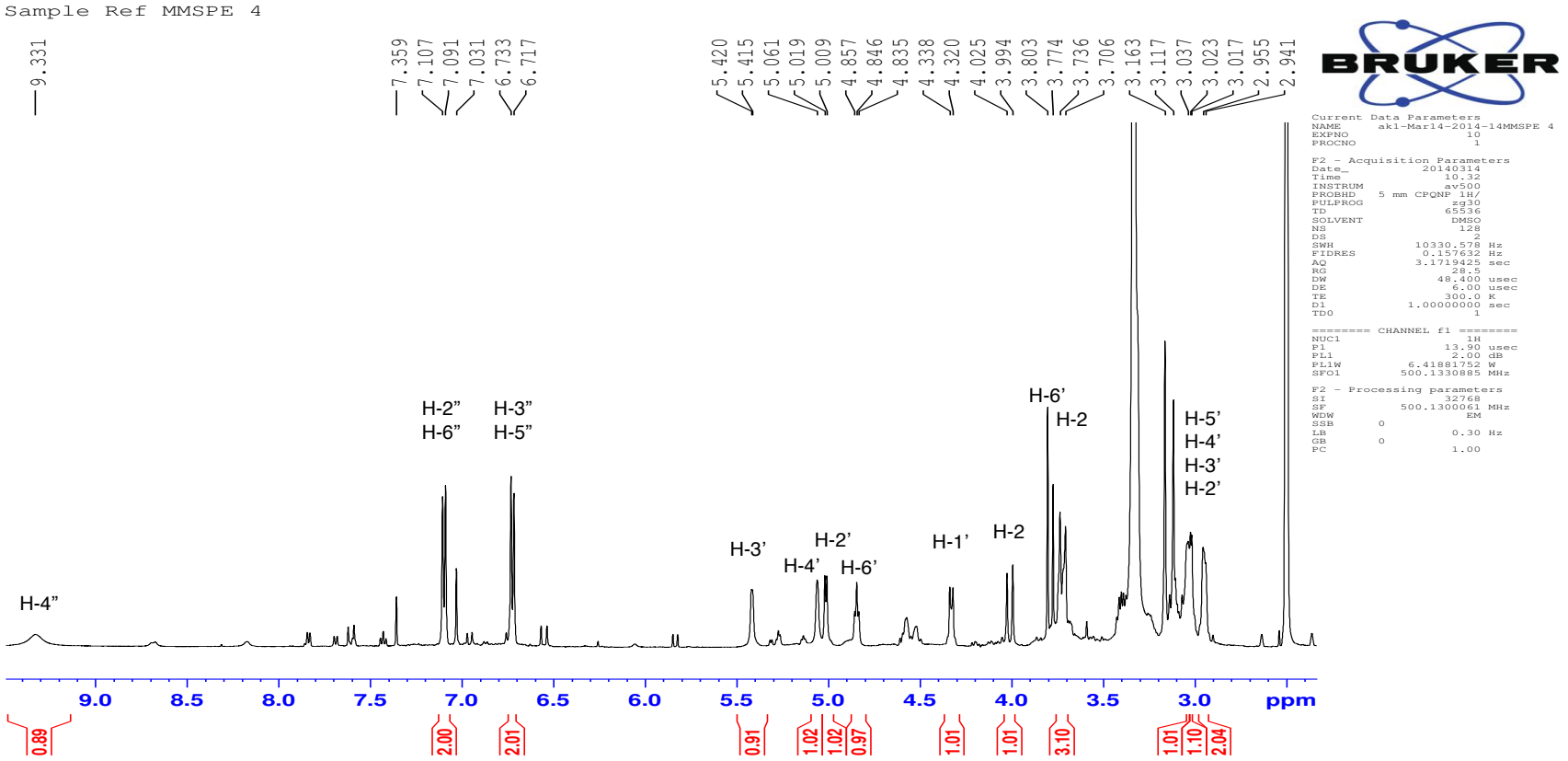

Figure 3.8 ^{1}H NMR spectrum for **AK-2**, recorded in DMSO-d_6, 500 MHz

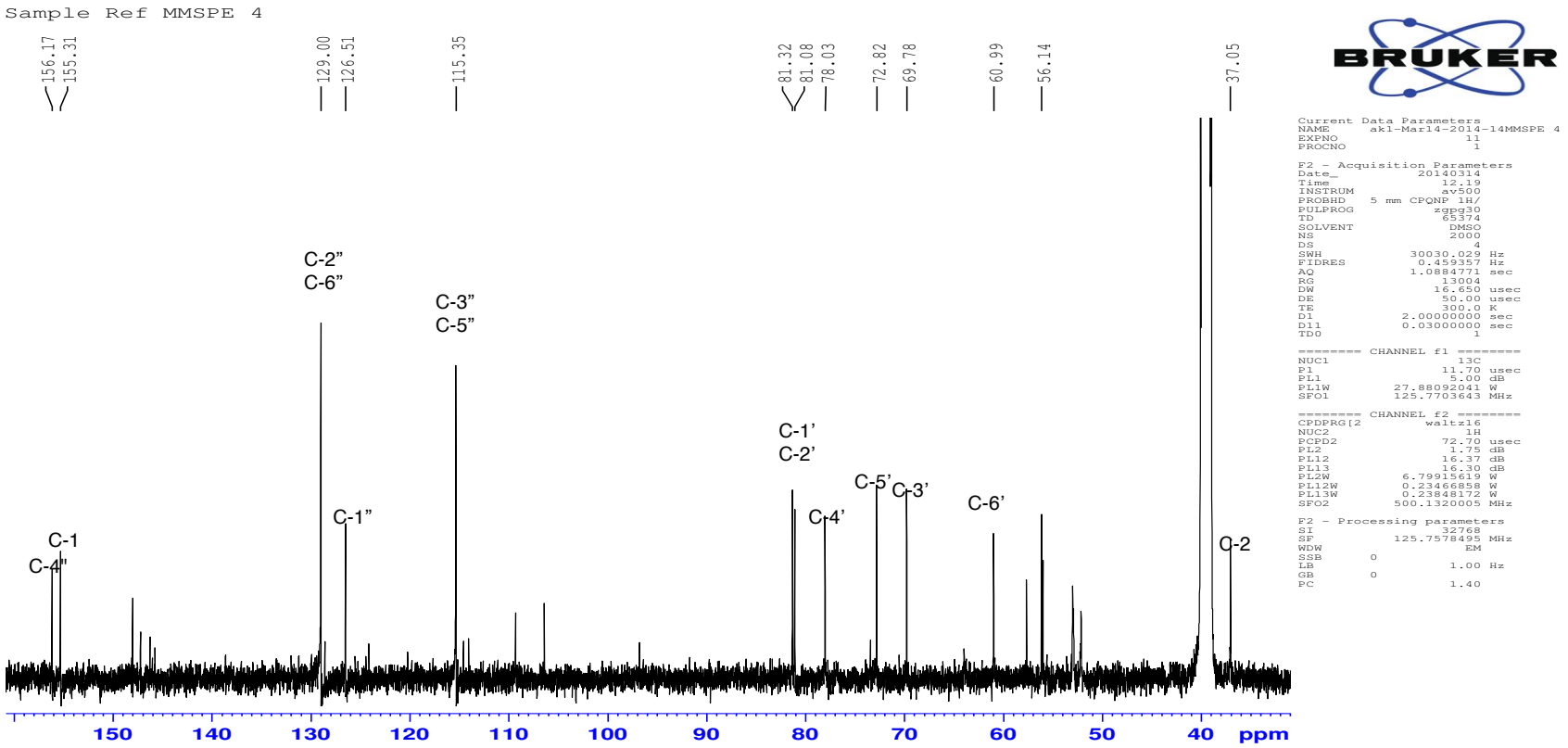

Figure 3.9 ^{13}C NMR spectrum for **AK-2**, recorded in DMSO-d_6, 500 MHz

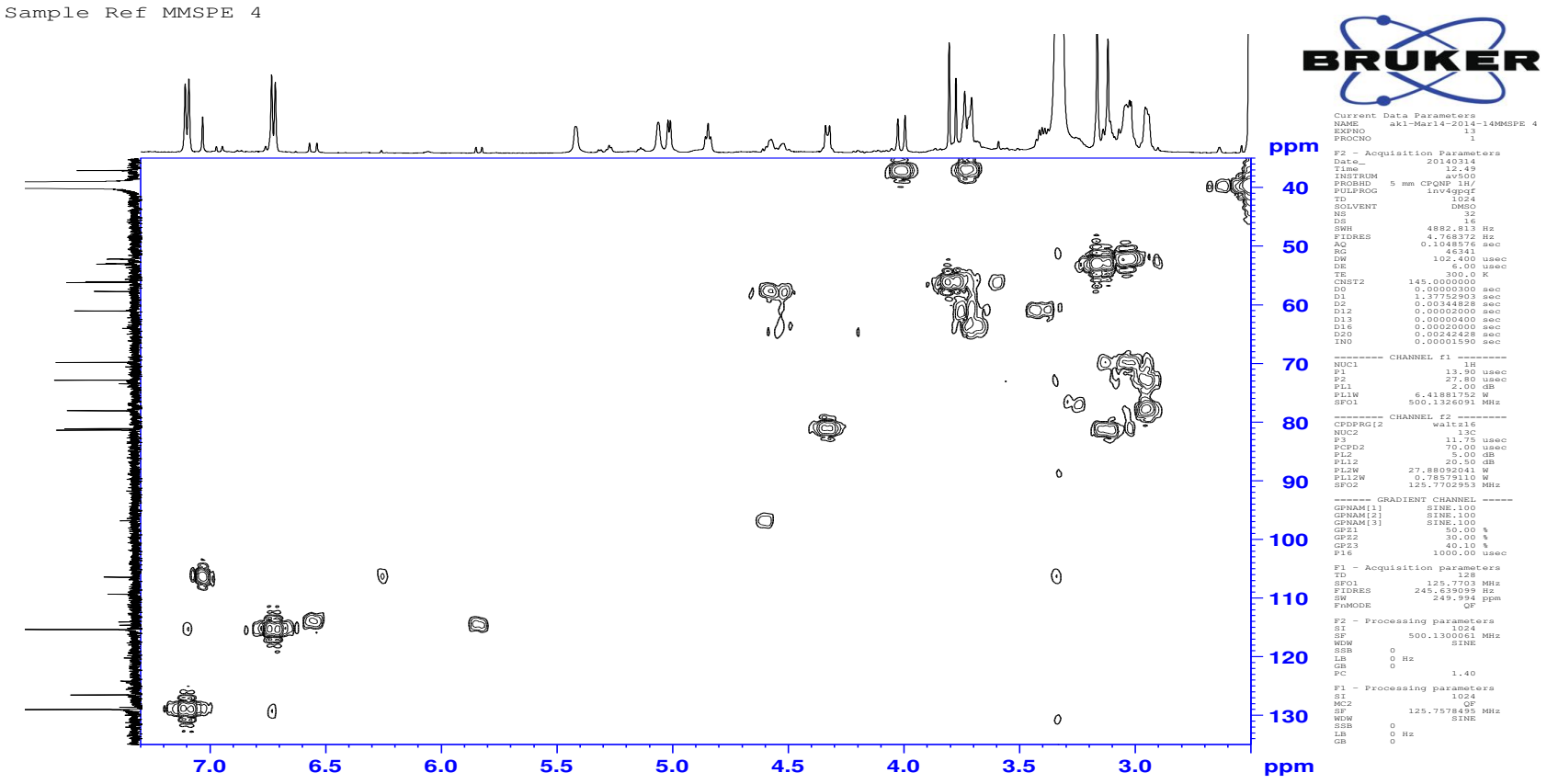

Figure 3.10 HMQC NMR spectrum for **AK-2**

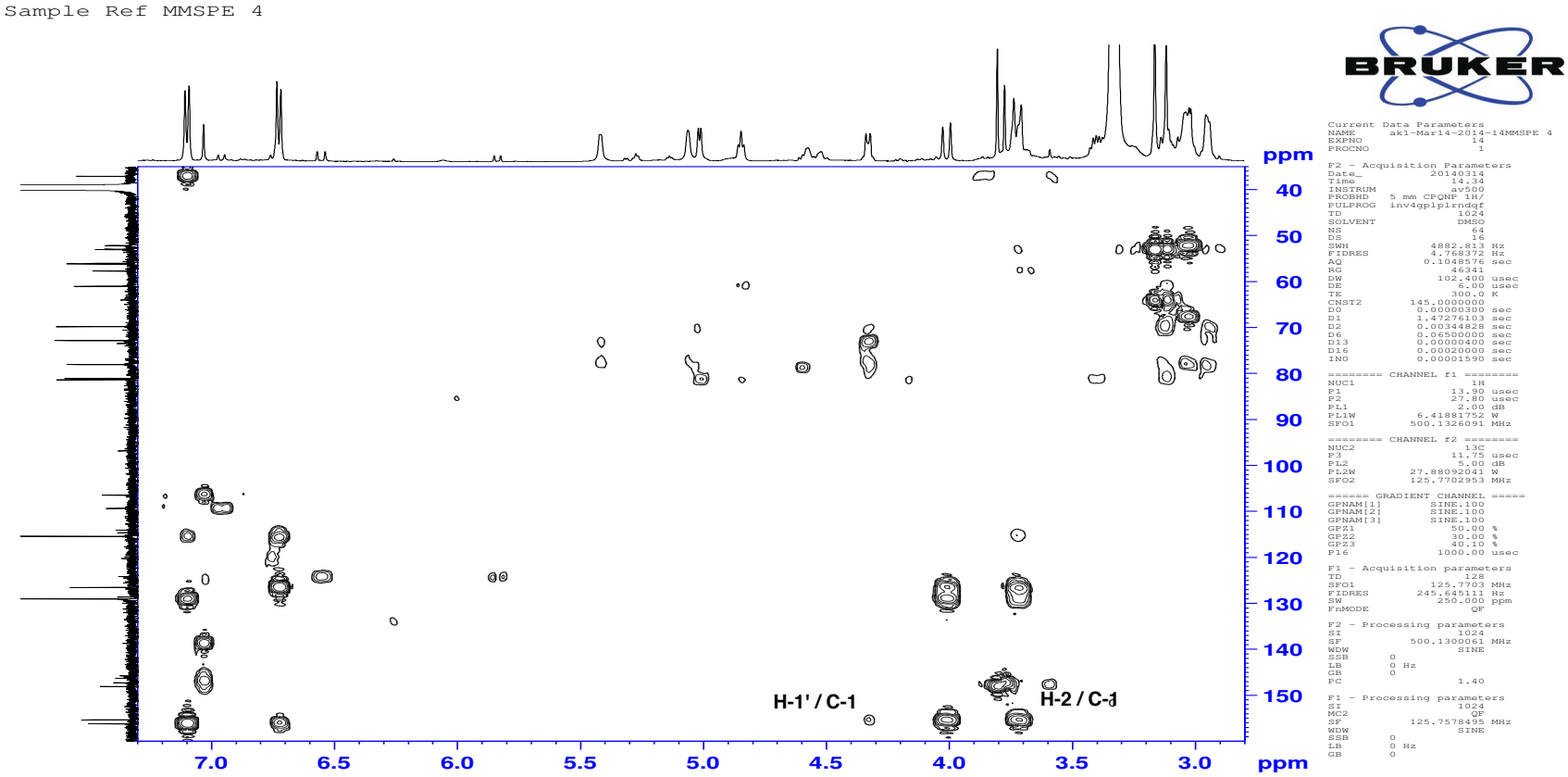

Figure 3.11 HMBC NMR spectrum for **AK-2**

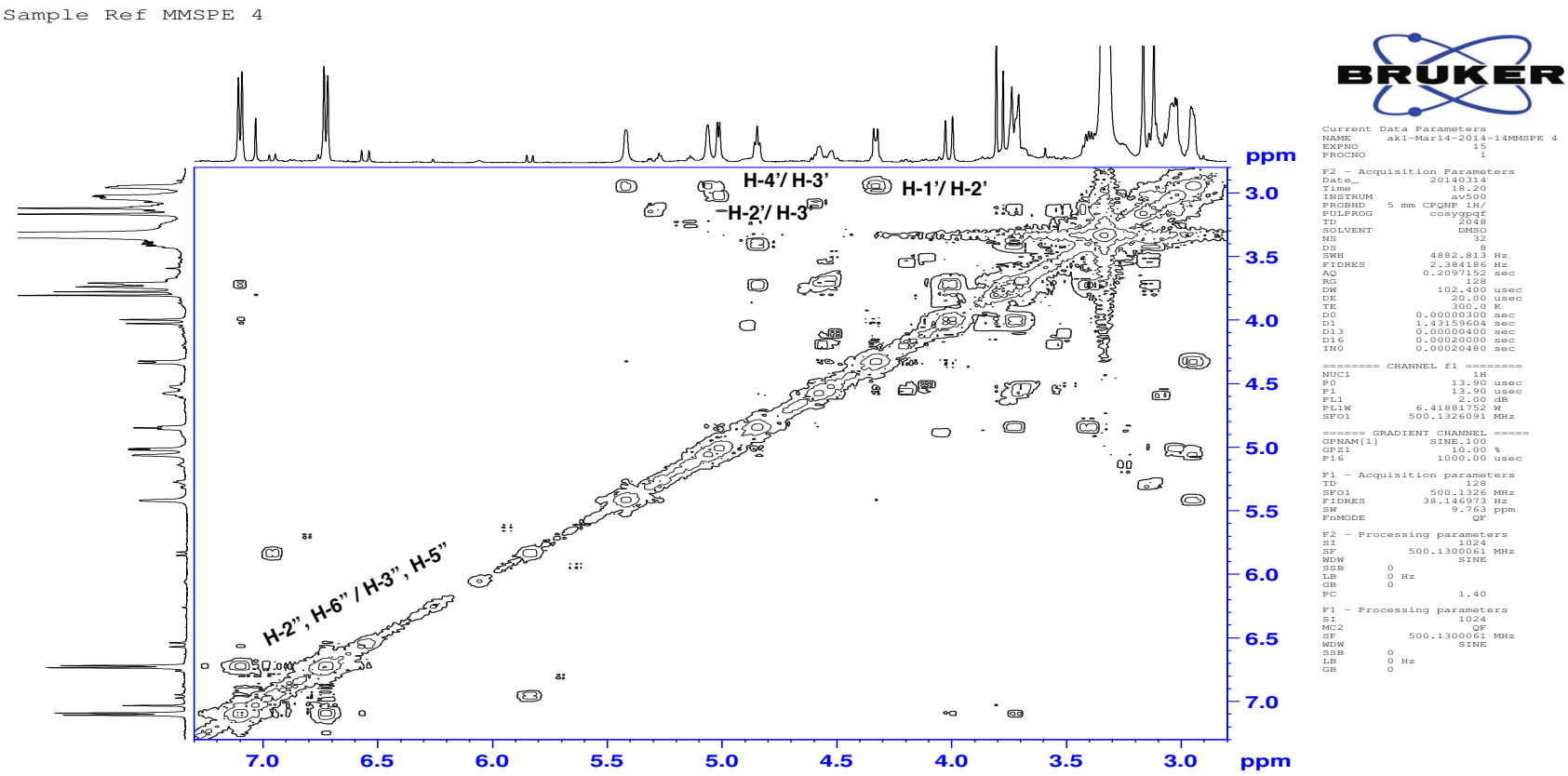

Figure 3.12 COSY NMR spectrum for **AK-2**

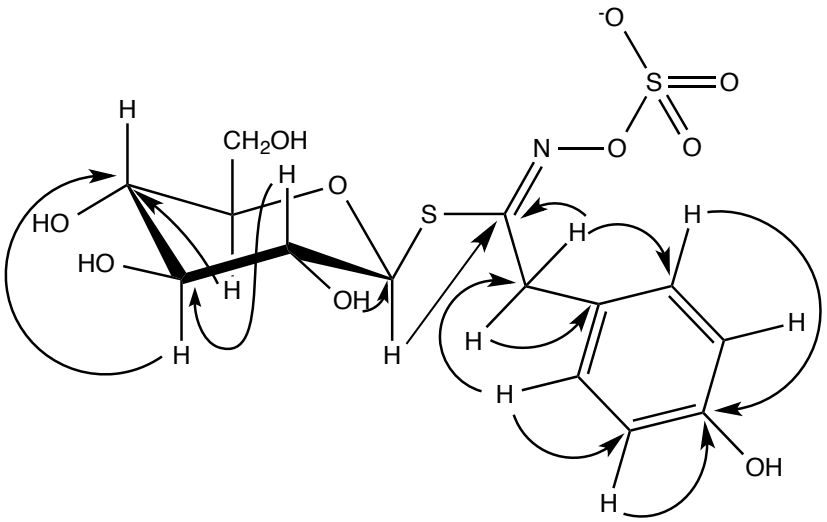

Figure 3.13 Selected HMBC correlations for **AK-2**

The methylene hydrogens (H_2-2) also showed a ^3J correlation to the aromatic carbons (C-2" and C-6", δ_C 129.0). The aromatic ring was revealed as an AA'BB' spin system in the ^{1}H NMR spectrum, two doublets (δ_H 7.09, H-2", -6" and δ_H 6.71, H-3", -5") integrating for two protons each, with a strong *ortho* coupling (J = 8.0 Hz) of the protons. Compound **AK-2** was therefore identified as (*E*)-(2-(4-hydroxyphenyl)-1-((3,4,5-trihydroxy-6-(hydroxymethyl) tetrahydro-2*H*-pyran-2-yl)thio)ethylidene) amino sulfate commonly known as glucosinalbin or 4-hydroxybenzyl glucosinolate. The ^{1}H and ^{13}C NMR data were comparable to published literature for the isolation of glucosinalbin from seeds of *Brassica juncea* (brown mustard) and *S.alba* (white mustard) (Fabre *et al.*, 1997; Toribio *et al.*, 2009).

Table 3.3 ^{1}H NMR (coupling constant, Hz) and ^{13}C NMR spectral data (ppm) and HMBC correlations of **AK-2**, recorded in DMSO-d_6

Position	^{1}H	^{13}C	^{2}J	^{3}J	^{13}C Fabre *et al.*, 1997 (CD_3OD, 100 MHz)
1	-	155.3			161.2
2	3.70, 3.99 s	37.0	C1, C1"	C2", C6"	38.9
1'	4.32	81.0		C1, C6'	82.6
2'	3.11, 5.00	81.3	C4'	C2'	74.1
3'	4.83, 5.41	69.1	C5'		71.1
4'	2.94, 5.06	78.0	C4'		79.3
5'	2.94	72.8	C6'		82.1
6'	3.70, 4.83	60.9			62.7
1"	-	126.5			127.8
2"	7.09 d (8.0)	129.0		C6"	130.3
3"	6.71 d (8.0)	115.3		C1", C5"	116.6
4"	9.33 br s	156.1			157.6
5"	6.71 d (8.0)	115.3	C4"		116.6
6"	7.09 d (8.0)	129.0	C5"	C2, C4"	130.3

Multiplicities of proton signals: s - singlet, d - doublet, br s – broad singlet

3.2.2 Isolation from *A. rusticana*

A kilogram of powdered A. rusticana was successively extracted with hexane, chloroform and methanol, and a yield of 0.23%, 0.61% and 0.78%, respectively, was obtained. The methanol extract (7.8 g) was subjected to silica gel VLC, which yielded 12 fractions (150 mL). An isocratic system of 70% acetonitrile in water was used as the mobile phase for the elution. Figure 3.14 shows the normal-phase analytical TLC of the VLC fractions. VLC fraction 5 (165. 1 mg) was isolated as a mixture of alkyl and aromatic glucosinolate, and attempts to separate these two compounds proved futile as they eluted as a single spot in all solvent systems employed. TLC and ^{1}H NMR analysis of the other VLC fractions revealed that fractions 6 and 7 were similar to fraction 5 with other minor compounds; the other fractions were primarily sugar so no further work was carried out on these fractions.

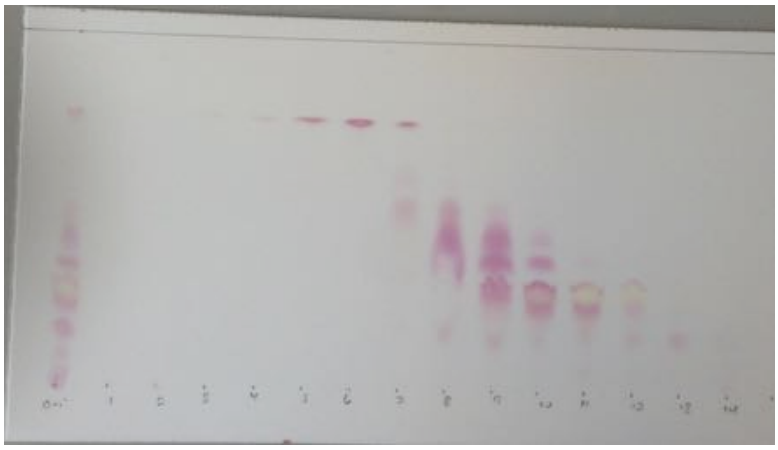

Figure 3.14 Analytical TLC of VLC fractions from *A. rusticana* methanol extract (Isocratic run of 70% acetonitrile in water, anisaldehyde reagent)

3.2.2.1 Characterisation of VLC fraction 5 (AK-3) as a mixture of allyl glucosinolate and phenylethyl glucosinolate

AK-3 was isolated as a brownish solid from the methanol extract of *A. rusticana*. The NMR and IR spectra data suggested a β-thioglucoside *N*–hydroxysulfate and two types of side chains: alkenyl and aromatic. The ESI-MS spectrum displayed $[M-H]^-$ ions at *m/z* 358.0 and 422.0 suggesting a molecular formula of $C_{10}H_{16}NO_9S_2^-$ and $C_{15}H_{20}NO_9S_2^-$ for the two types of glucosinolates (Figure 3.18). The side chain of the alkenyl glucosinolate was found to be a but-3-en-1-ylidene as revealed by the HMQC and HMBC NMR spectra, with proton resonances at δ_H 3.45, 3.56, 5.16, 5.29 and 5.99 ppm attributable to carbon resonances at δ_C 37.9, 118.4, and 134.6 ppm account for the all the positions on the alkenyl, whilst the aromatic glucosinolate had a phenylethyl side chain. The resonance of the phenyethyl side chain was observed in the down field region (δ_H 7.16 - 7.30 ppm) as a doublet and two-triplets which integrated for the five protons on the phenyl ring, a mono-substituted aromatic ring (Figure 3.19). The ethyl hydrogen H_2-3 (δ_H 3.05) showed a ^2J, ^3J and ^3J correlations to the phenyl carbons C-1" (δc 142.5), C-2", -6" (δc 129.6) and to the quaternary carbon of the sulphonated oxime C-1 (δ_C 161.1), respectively. A ^3J HMBC correlation revealed the

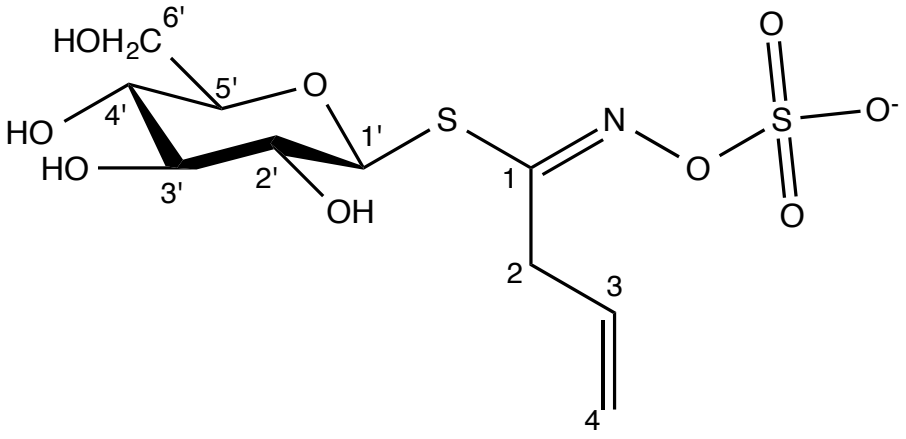

Figure 3.15 Structure for the alkenyl glucosinolate component of **AK-3** (**compound 1**)

thioglucosidic linkages for both compounds, for compound **1** hydrogen H-1' (δ_H 4.91) correlated to the quaternary carbon, C-1 (δ_C 160.4) and for compound **2** hydrogen H-1' (δ_H 4.82) correlated to the quaternary carbon, C-1 (δ_C 161.1). To confirm the presence of the two types of glucosinates, the ^{1}H NMR of **AK-3** was compared to pure glucosinolate standards, sinigrin and gluconasturtiin (Figure 3.17).

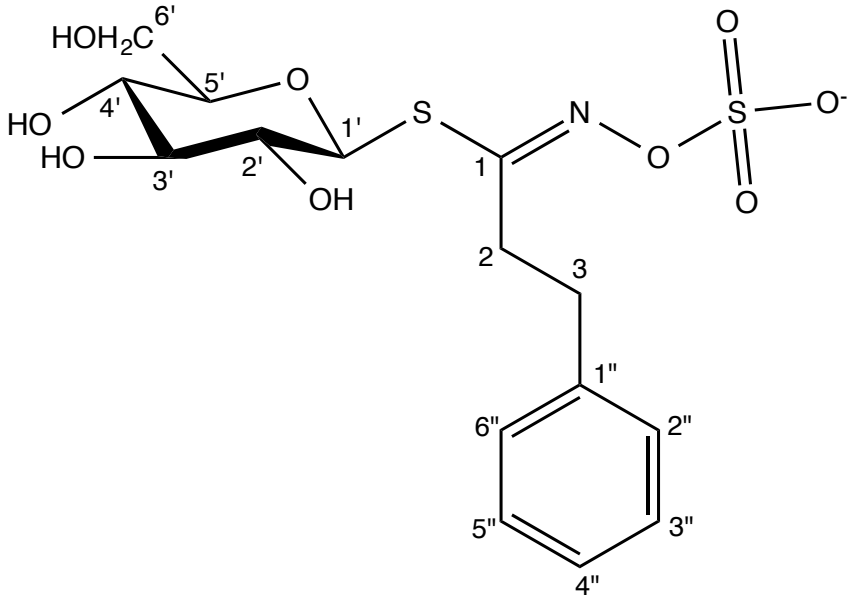

Figure 3.16 Structure for the aromatic glucosinolate component of **AK-3** (**compound 2**)

Compounds **1** and **2** of **AK-3** were structurally assigned by the HMBC correlations as shown in Figures 3.21 and 3.22, respectively and Tables 3.4 and 3.5 summarise the NMR data for both compounds. Compounds **1** and **2** were therefore identified as (*E*)-(1-((3,4,5-trihydroxy-6-(hydroxymethyl)tetrahydro-2H-pyran-2-yl)thio)but-3-en-1-ylidene)amino sulfate and (*E*)-(3-phenyl-1-((3,4,5-trihydroxy-6-(hydroxymethyl)tetrahydro-2H-pyran-2-yl)thio)propy- lidene) amino sulfate, respectively. Compounds **1** and **2** are also known as 2-propenyl glucosinolate and 2-phenylethyl glucosinolate, respectively. The ^{1}H and ^{13}C NMR data of compounds **1** and **2** were in good agreement with published literature for the isolation of 2-propenyl glucosinolate from *B. juncea* seeds and the isolation of 2-phenylethyl glucosinolate from *Barbarea verna* seeds (upland cress), respectively (Barillari *et al*., 2001; Wang *et al*., 2014). Additionally, these compounds have been reported for in *B. campestris*, *Raphanus sativum* L. niger (black radish), *Brassica rapa ruvo* (broccoletti seeds), *B. oleracea* and *Pringlea antiscorbutica* (Kerguelen cabbage*)* (Kim *et al*., 2004; Ediage *et al*., 2011; Toribio *et al*., 2011; Ares *et al*., 2014).

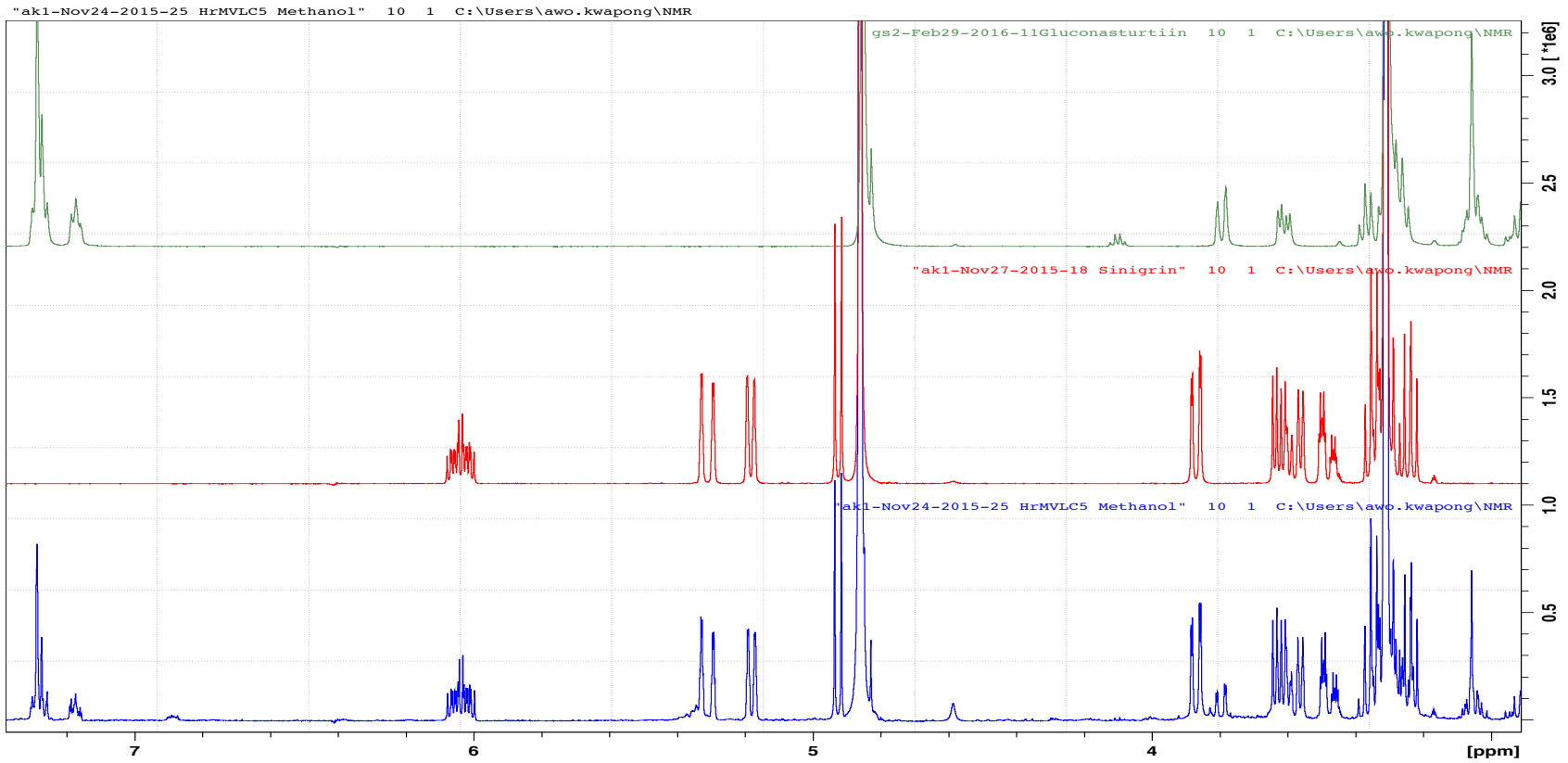

Figure 3.17 ^{1}H NMR spectral comparison of **AK-3** (blue spectrum) with gluconasturtiin (green spectrum) and sinigrin (red spectrum) standards, recorded in methanol-d_4, 500 MHz

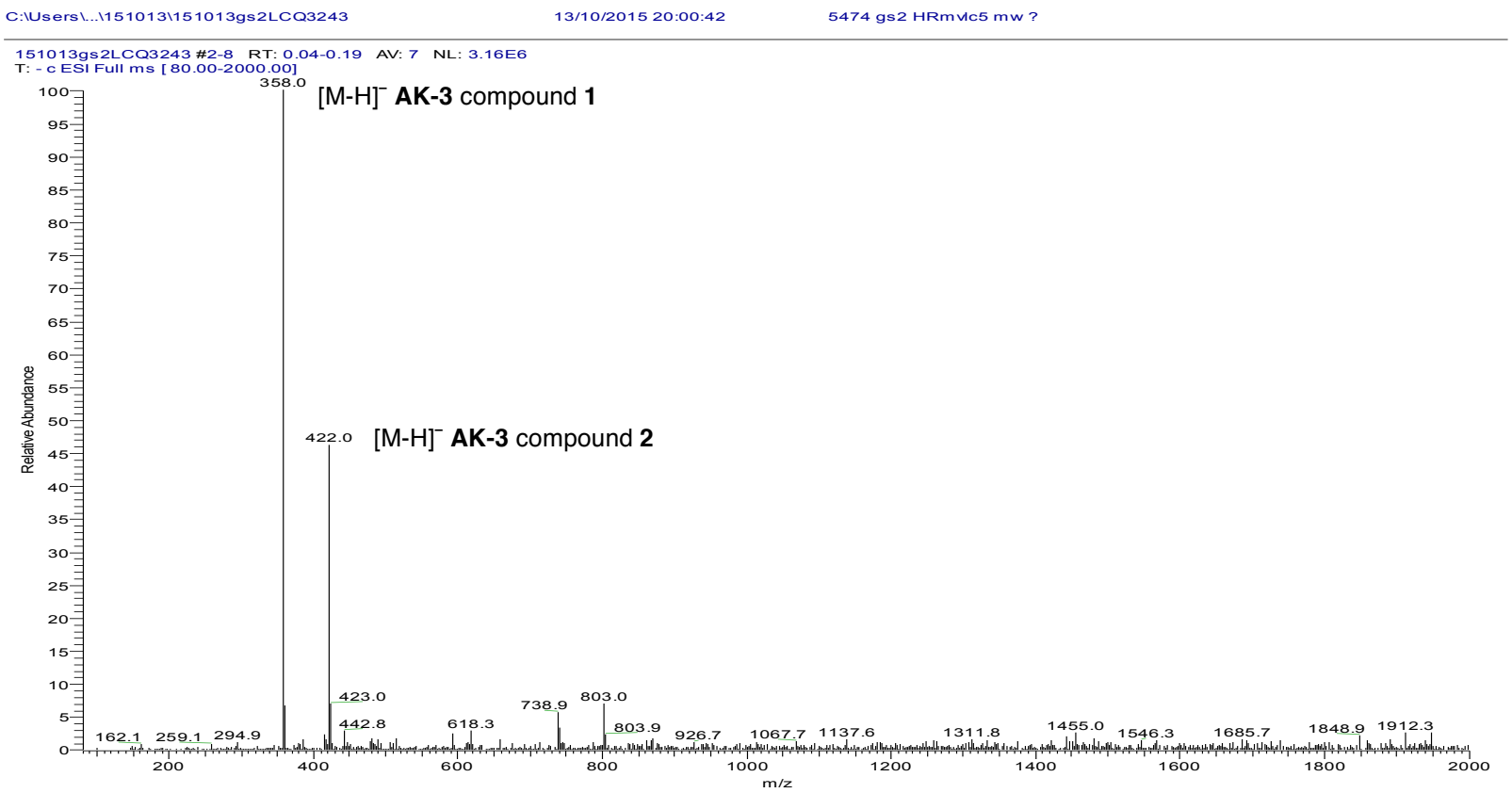

Figure 3.18 ESI-MS spectrum for the **AK-3** mixture in the negative ion mode

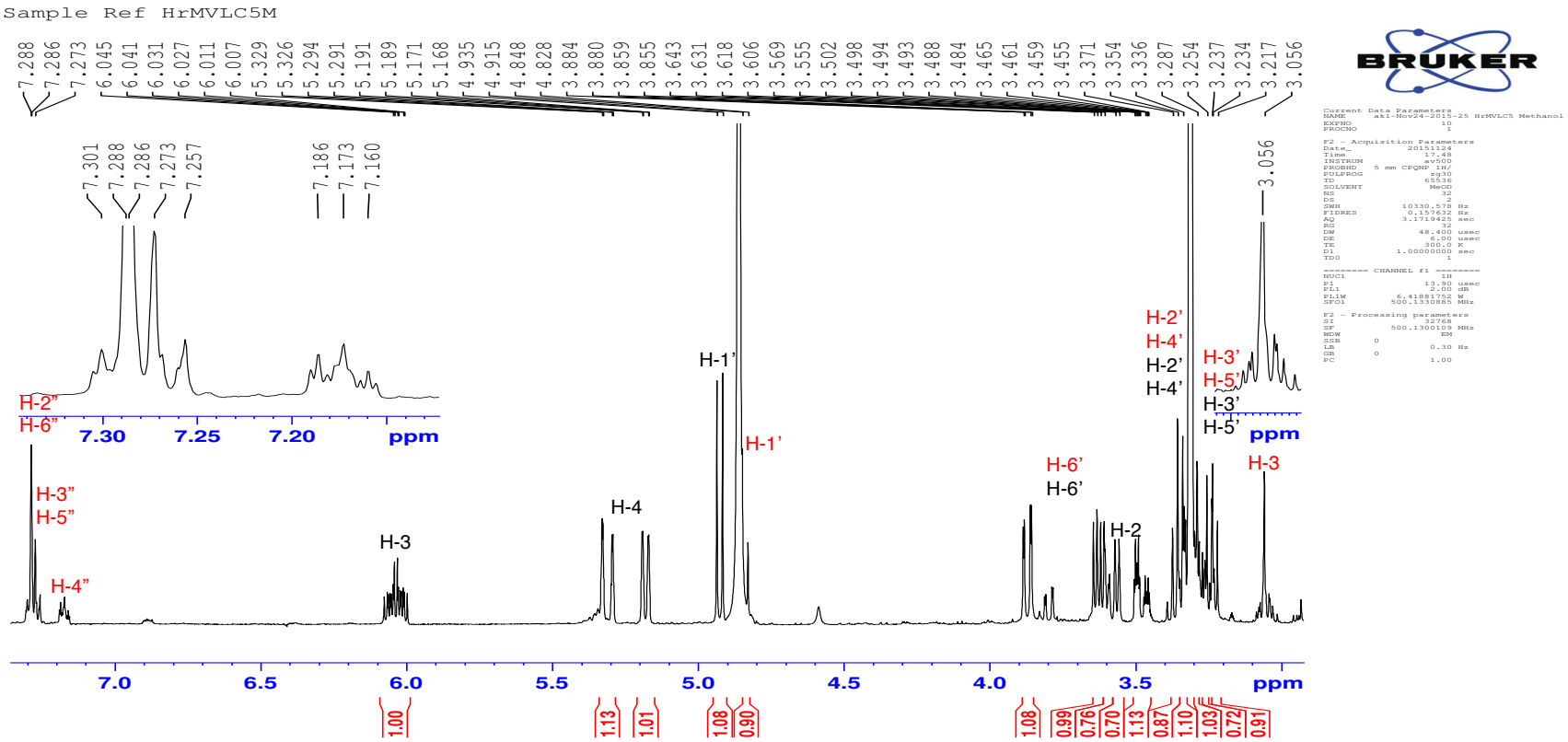

Figure 3.19 ¹H NMR spectrum for **AK-3** showing proton integration for compound **1** (labeled in black) and additional proton resonances for compound **2** (labeled in red) superimposed in the spectrum, recorded in CD_3OD, 500 MHz

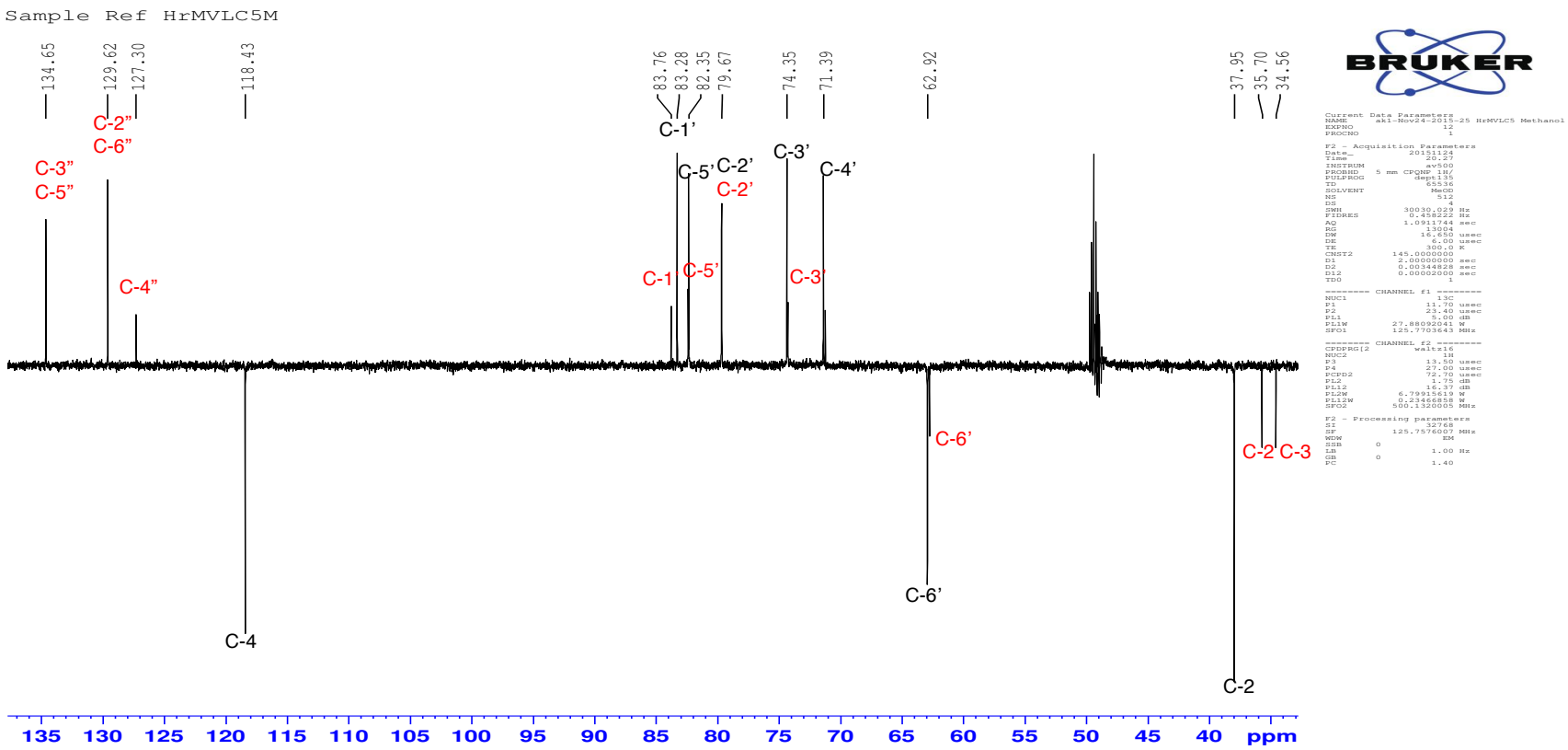

Figure 3.20 DEPT-135 NMR spectrum for **AK-3**, with carbon resonances for compound **1** labeled in black and that of compound **2** in red

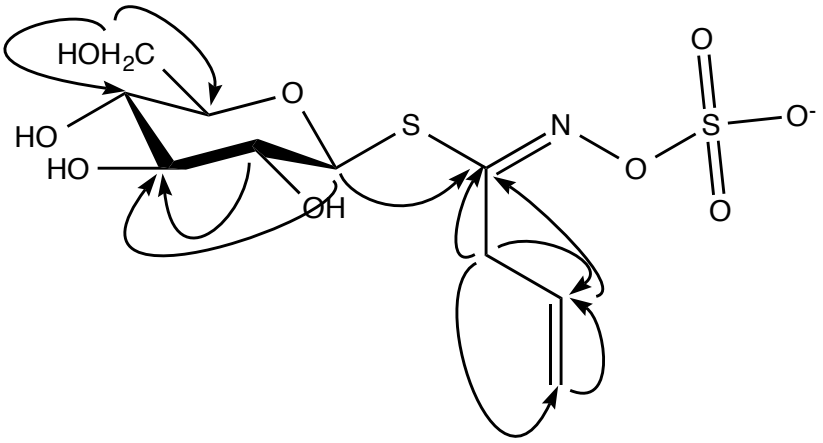

Figure 3.21 Selected HMBC correlations (solid arrows) for compound **1** of **AK-3**

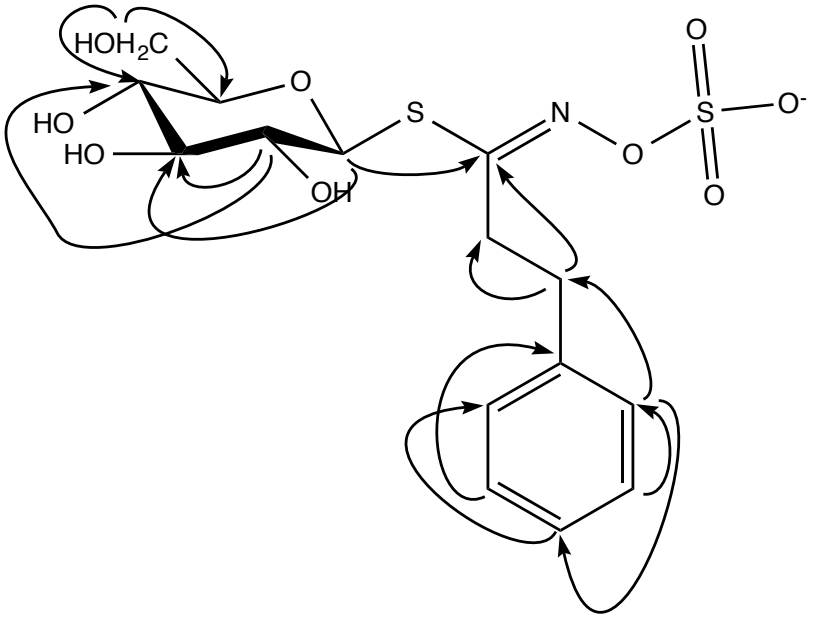

Figure 3.22 Selected HMBC (solid arrows) correlations for compound **2** of **AK-3**

Table 3.4 ^{1}H and ^{13}C NMR spectral data (ppm) and HMBC correlations of **AK-3** compounds **1**, recorded in methanol-d_4

Position	^{1}H	^{13}C	^{2}J	^{3}J	^{13}C Wang *et al.*, 2014 (D_2O, 125 MHz)
1	-	160.4			162.9
2	3.45 q, 3.56 dd	37.9	C1, C3	C4	36.1
3	5.99 m	134.6	C2	C1	132.0
4	5.16 dd, 5.29 dd	118.5	C3	C4	118.4
1’	4.91d	83.2		C1, C3’	81.5
2’	3.35 d	79.6	C3’	C4’	71.9
3’	3.21 d	74.3	C2’		77.0
4’	3.32 d	71.3			69.1
5’	3.25 d	82.3	C6’		80.0
6’	3.61 t, 3.85 dd	62.9	C6’	C4’	60.6

Multiplicities of proton signals: d - doublet, dd - doublet of doublets, t – triplet, m – multiplet, q - quintet

Table 3.5 ^{1}H and ^{13}C NMR spectral data (ppm) and HMBC correlations of **AK-3** compounds **2**, recorded in methanol-d_4

Position	^{1}H	^{13}C	^{2}J	^{3}J	^{13}C Barillari *et al.*, 2011 (D_2O, 125 MHz)
1	-	161.1			163.7
2	3.23 d	35.7			32.9
3	3.05 s	34.5	C2	C1, C2", C6"	34.2
1'	4.82 d	83.7		C1, C3'	82.0
2'	3.35 d	79.6	C3'	C4'	72.2
3'	3.21 d	74.3	C2'		77.4
4'	3.32 d	71.3			69.4
5'	3.25 d	82.3	C6'		80.4
6'	3.61 t, 3.85 dd	62.9	C5'	C4'	60.9
1"	-	142.5			140.9
2"	7.27 d	129.6		C3	129.1
3"	7.25 t	134.6	C2", C6"	C1"	129.1
4"	7.16 t	127.3		C2", C6"	127.0
5"	7.25 t	134.6		C1"	129.1
6"	7.27 d	129.6	C2"		129.1

Multiplicities of proton signals: s - singlet, d - doublet, dd - doublet of doublets, t - triplet

3.2.3 Biosynthesis of glucosinolates

Glucosinolates are nitrogen- and sulfur-rich secondary metabolites, which occur in all *Brassica* species and are known for their role in plant defense against pathogens, and their anti-carcinogenic activity (Mithen *et al.*, 2000; Sonderby *et al.*, 2010). They are characterized by the presence of a *β*-D-thioglucose group, with a sulphonated oxime group and different types of side-chain (Fenwick and Heaney, 1983). Like the isolated glucosinolates in sections 3.2.1.1, 3.2.1.2 and 3.2.2.1, the variable side-chain could be an aliphatic group (gluconapin and sinigrin), an aromatic group (glucosinalbin and glucosnasturtiin) or an indolyl group (glucobrassicin).

Glucosinolates are derived from amino acid through three independent biosynthetic pathways: this is the chain elongation of a precursor amino acid, formation of the core glucosinolate structure and modification of the elongated side chain of the amino acid (Sonderby *et al.*, 2010). Formation of the core glucosinolate commences with *N*-hydroxylation and decarboxylation of the precursor amino acid to an aldoxime (Mithen *et al.*, 2000; Fahey *et al.*, 2001). The aldoxime is then converted to a thiohydroxamic acid by the introduction of thioglucoside sulfur from a cysteine (Fahey *et al.*, 2001). A glycosyl unit from UDP-glucose is then transferred onto the thiohydroxamic acid to form a desulfoglucosinolate, which is later sulfated via 3'-phosphoadenosine 5'-phosphosulfate (PAPS), and a desulfoglucosinolate sulfotransferase to produce the glucosinolate (Mithen *et al.*, 2000; Fahey *et al.*, 2001). Figure 3.23 shows the biosynthesis of glucosinolates and this suggests a possible biosynthetic pathway for the formation of the isolated compounds, **AK-1**, **AK-2** and **AK-3**.

The structural diversity observed among the isolated glucosinolates is due to the different amino acid enlongation and modification processes undergone during their biosynthesis. Underhill and collegues explained the amino acid enlongation as being similar to the synthesis of leucine from valine and acetate, based on a biochemical study involving the

administration of ^{14}C-labeled precursors to plants, which was later supported by studies conducted by Chisholm and workers (Underhill *et al.*, 1962; Chisholm and Wetter, 1964). For modification of the aliphatic and alkylthioalkyl side chains, Mithen and co-workers suggested that Gsl-oxid, Gsl-alk and Gsl-oh loci are responsible for the oxidation of the methylthios, desaturation of the alkyl chains and hydroxylation of the alkenyls, respectively (Parkin *et al.*, 1992; Mithen *et al.*, 1995; Giamoustaris and Mithen, 1996; Mithen and Campos, 1996). It is also presumed that similar oxidation, desaturation and hydroxylation processes occur in aromatic and indole glucosinolates (Fahey *et al.*, 2001).

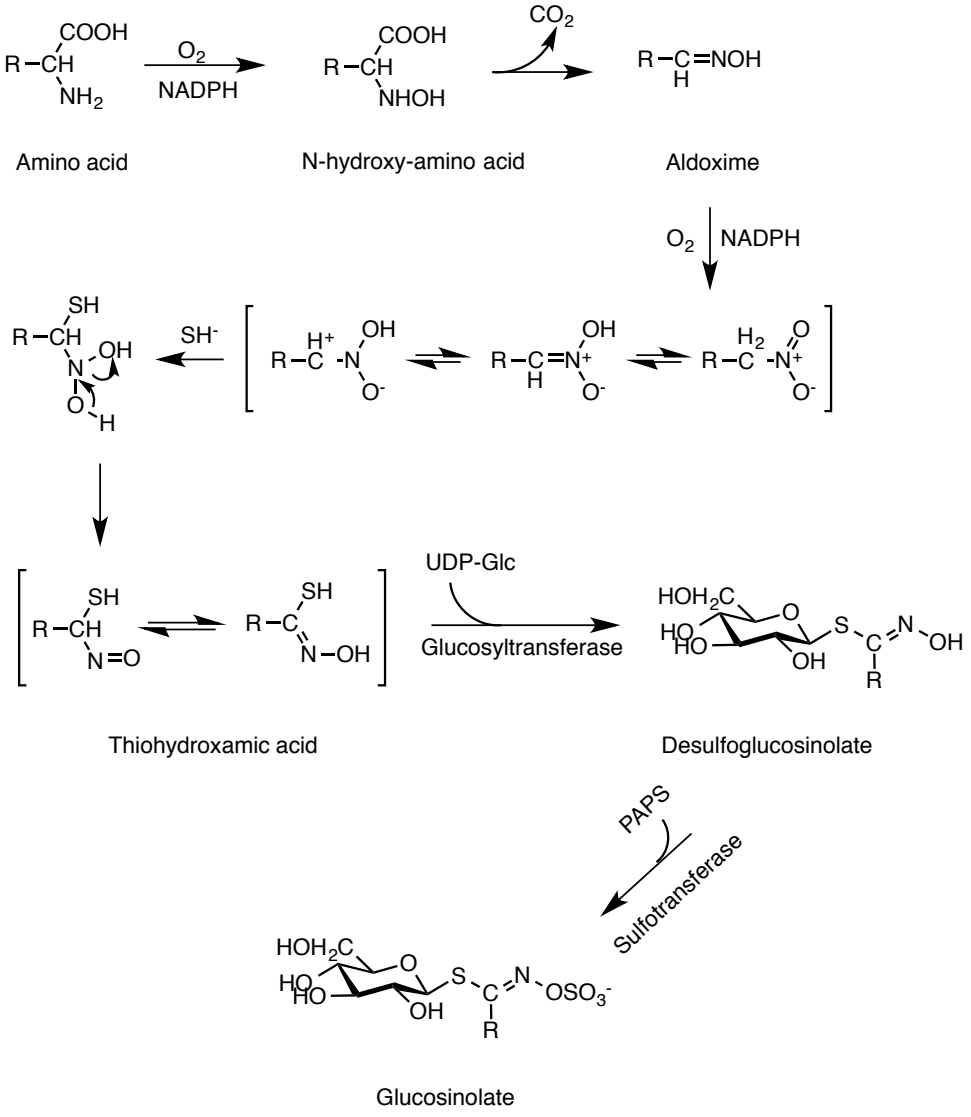

Figure 3.23 Biosynthetic pathway of glucosinolates

3.2.4 Isolation from *L. sativum*

Ground seeds (245 g) of *L. sativum* were initially extracted with petroleum ether in a Soxhlet and subsequently extracted with methanol. A yield of 20.4% and 18.2% was obtained for the petroleum ether and methanol extracts, respectively. The methanol extract (40 g) was subjected to the acid-base extraction (alkaloid extraction), which gave a yield of 1.1 g. The alkaloidal extract (0.8 g) was then subjected to gravity column chromatography (silica gel 60, 70-230 mesh, column size: 50 x 4 cm) and eluted with $CHCl_3$-EtOH-EtOAc-Me_2CO- conc. NH_3 (6:4:2:2:1, v/v). 210 fractions (Fr) were collected and combined in seventeen different pools. Pool D (Fr 10-12, 12.7 mg) and Pool E (Fr 14-15, 30 mg) were further purified by preparative TLC on silica gel, $CHCl_3$-MeOH-NH_3, 90:9:1 and 80:19:1, v/v, respectively. Both pools (D and E) yielded two dimeric imidazole alkaloids each, which gave a positive Dragendorff reaction. **AK-4** (4.5 mg) and **AK-6** (3.6 mg) were isolated from pool D and **AK-5** (10.3 mg) and **AK-7** (1.7 mg) from pool E. Figures 3.24 and 3.25 show the normal-phase analytical TLC of the column chromatography pool of fractions and the isolated dimeric imidazole alkaloids from pools E and D.

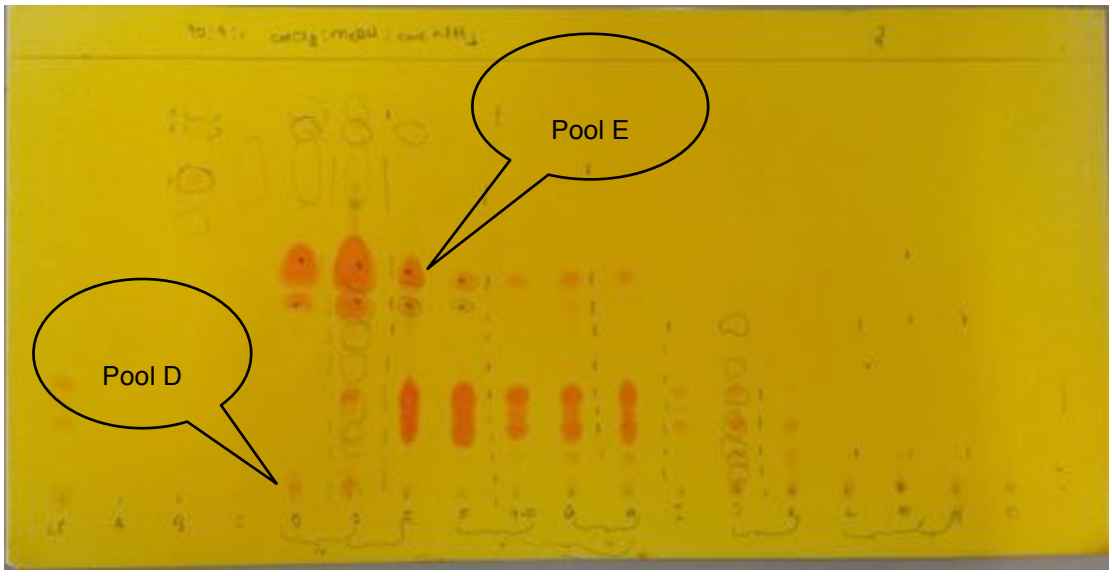

Figure 3.24 Analytical TLC of the column chromatography pool of fractions from *L. sativum* alkaloidal extract (detecting reagent Dragendorff's reagent)

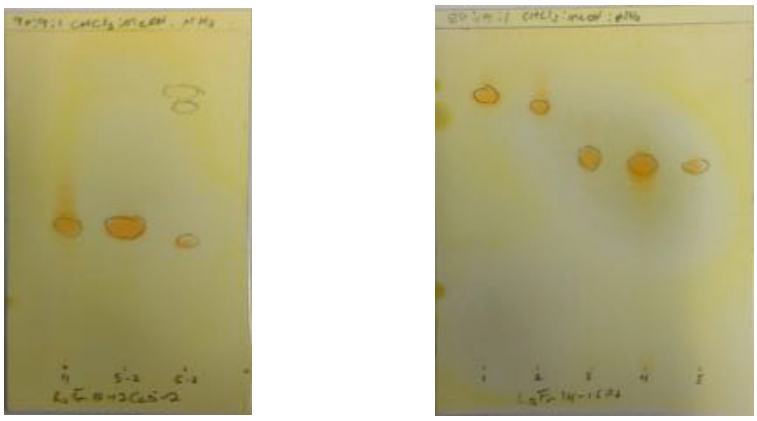

Figure 3.25 Analytical TLC of the isolated imidazole alkaloids from pools D and E

3.2.4.1 Characterisation of the isolated imidazole alkaloids

The ^{1}H NMR and COSY spectra data showed two aromatic spin systems for the isolated compounds (Table 3.6), a di-substituted and tri-substituted aromatic ring, respectively. The structures for the isolated compounds are shown in Figures 3.26 and 3.27.

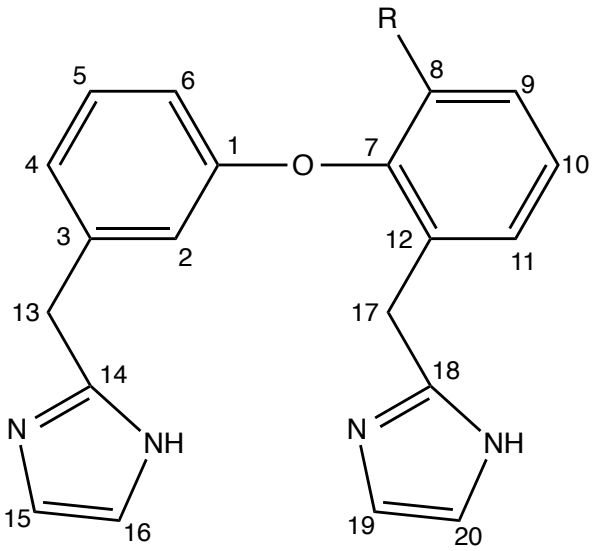

AK-4: R = OCH_3

AK-5: R = OH

Figure 3.26 Structure for **AK-4** and **AK-5**

Compound **AK-4** was isolated as a pale yellow solid. The ESI-MS gave an *m/z* at 361.3 $[M+H]^+$, which suggested that its molecular formula was $C_{21}H_{20}N_4O_2$. The R*f* value was 0.42 in a solvent system of $CHCl_3$: CH_3OH: conc NH_3 (90:9:1, v/v). Its ^1H and COSY NMR spectra revealed a di-substituted aromatic ring which was identified by proton resonances at δ_H 6.62 (s, *J* = 2.0 Hz, H-2), 6.81 (dd, *J* = 9.5, 0.5 Hz, H-4), 7.10 (t, *J* = 8.0, 8.0 Hz, H-5), 6.54 (dd, *J* = 8.0, 2.0 Hz, H-6) which coupled to each other and the meta-coupling of H-2 by H-6 ($^4J_{HH}$ = 2.0 Hz) (Figure 3.29). Coupling of proton signal at δ_H 6.98 (dd, *J* = 8.0, 1.5 Hz, H-9) to δ_H 7.14 (t, *J* = 8.0, 8.0 Hz, H-10) and δ_H 6.75 (dd, *J* = 8.0, 1.5 Hz, H-11) in the COSY spectrum (Figure 3.31) also indicated the presence of a further aromatic spin system, the tri-substituted aromatic ring. Both spin systems were confirmed by the HMQC and HMBC correlations (Table 3.7 and Figure 3.32). The methoxyl group (δ_c 56.3 and δ_H 3.65 (3H)) was assigned a position meta- to the imidazolylmethyl moiety and this was confirmed by a $^3J_{H\text{-}C}$ correlation to the aromatic quaternary carbon, C-8 (δ_C 154.0) (Figure 3.30). The proton signals at δ_H 6.83 (2H, s, H-15 and H-16) and δ_H 6.91 (2H, s, H-19 and H-20) and carbon signals at δ_C 122.8 (2C, C-15 and C-16), 147 (1C, C-14), 123.1(2C, C-19 and C-20) and 148.2 (1C, C-18) accounted for the two-imidazole rings. The signals at δ_H 3.96 (2H, s, H_2-13), δ_c 35.1 (1C, C-13) and δ_H 3.92 (2H, s, H_2-17), δ_c 29.7 (1C, C-17) were identified as the two methylenes, which connects the imidazole rings to the aromatic rings. The IR spectrum showed the presence of secondary amines at 2919.76 cm^{-1}. The combined NMR, IR and ESI-MS spectra data led to the assignment of the full structure of **AK-4**, which was comparable to with published literature for the isolation of dimeric imidazole alkaloids from *L. sativum* (Maier *et al.*, 1998). Compound **AK-4** was therefore identified as 2-(3-(2-((1*H*-imidazol-2-yl)methyl)-6-methoxyphenoxy) benzyl)-1*H*-imidazole.

Compound **AK-5** was also a pale yellow solid with an accurate mass measurement of an $[M+H]^+$ ion at *m/z* 347.1498, which suggested that its molecular formula was $C_{20}H_{18}N_4O_2$. Its R*f* value was 0.61 in a solvent system of $CHCl_3$: CH_3OH: conc NH_3 (80:19:1, v/v). Compound **AK-5** was similar to compound **AK-4**; it only varied by the absence of the methoxyl group and the presence of an aromatic hydroxyl group. Inspection of the HMBC spectrum allowed

the full assignment of all resonances (Table 3.8). Compound **AK-5** was therefore identified a 3-((1H-imidazol-2-yl)methyl)-2-(3-((1H-imidazol-2-yl)methyl) phenoxy)phenol commonly known as Lepidine B and the spectra data were comparable to published literature (Maier *et al.*, 1998).

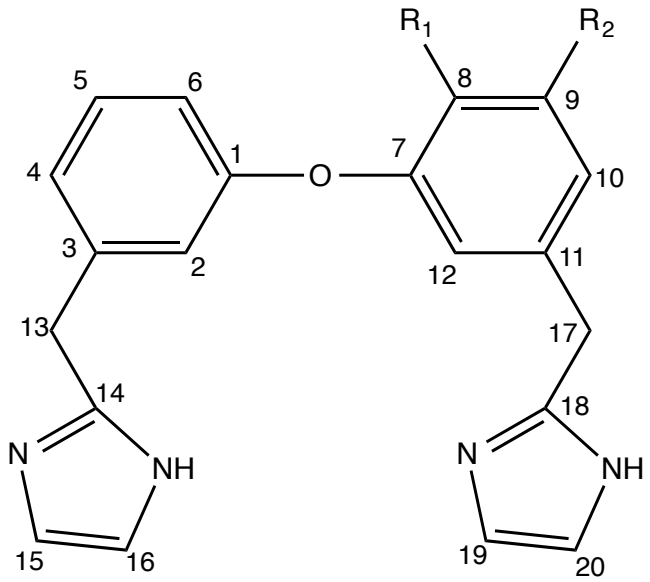

AK-6: R_1 = H, R_2 = OCH_3

AK-7: R_1 = OH, R_2 = H

Figure 3.27 Structure of **AK-6** and **AK-7**

Compound **AK-6** was a pale yellow solid. The accurate mass measurement gave an *m/z* at 361.1659 $[M+H]^+$, which suggested that the molecular formula was $C_{21}H_{20}N_4O_2$. The R*f* value was 0.39 in a solvent system of $CHCl_3$-MeOH-NH_3 (90:9:1, v/v). Compound **AK-6** was similar to compound **AK-4**; the only difference was the positioning of the methoxyl and imidazolyl methyl group on the tri-substituted aromatic ring (Figure 3.27). The difference between the two compounds was revealed by the splitting pattern of the aromatic protons on the tri-substituted aromatic ring of **AK-6** (δ_H 7.01 (2H, s, H-8 and H-10) and δ_H 6.85 (H, s, H-12)) and their barely resolved meta-couplings observed in the ^{1}H NMR spectrum, which was confirmed by H-8 and H-10 coupling to H-12 in the COSY spectrum. The positioning of these

aromatic hydrogens was also confirmed by HMBC correlations; a ^{4}J correlation of H-8 to quaternary aromatic carbon C-11 (δ_c 132.5), ^{2}J correlation of H-10 to C-11 and a ^{4}J correlation of H-12 to a quaternary aromatic carbon C-9 (δ_c 151.9) (Table 3.8). In addition, the NOESY spectrum revealed a cross peak between the methoxyl hydrogens (3H, s, δ_H 3.70) and the aromatic hydrogens (2H, s, δ_H 7.01, H-8 and H-10), which confirmed this structural arrangement. This compound was therefore assigned as 2-(3-(3-((1*H*-imidazol-2-yl)methyl)-5methoxy phenoxy)benzyl)-1*H*-imidazole. To our knowledge there has been no report of this compound though it is similar to the dimeric imidazole alkaloids isolated from *L. sativum* seeds by Maier and co-workers (1998).

Compound **AK-7** was also a pale yellow solid. The ESI-MS gave an $[M+H]^+$ ion at *m/z* 347.1 which indicated that its molecular formula was $C_{20}H_{18}N_4O_2$. Its R*f* value was 0.59 in a solvent system of $CHCl_3$: CH_3OH: conc NH_3 (80:19:1, v/v). This compound was similar to **AK-5**; the only difference was the positioning of the substituent imidazolyl methyl group on the ABC aromatic ring. The difference between the two compounds was revealed by the splitting pattern of the aromatic protons (δ_H 6.80 (d, H-9), δ_H 6.66 (dd, H-10) and δ_H 6.79 (s, H-12)), the *ortho* coupling (*J* = 8 Hz) of H-10 to H-9 and the meta-coupling (*J* = 1.5 Hz) of H-10 to H-12. Inspection of the HMQC and HMBC correlations allowed unambiguous assignment of all resonances. **AK-7** was therefore identified as 4-((1H-imidazol-2-yl)methyl)-2-(3-((1H-imidazol-2-yl)methyl)phenoxy) phenol commonly known as Lepidine E and the spectra data were in good agreement to the published literature (Maier *et al.*, 1998).

The NMR spectra data of the isolated imidazole alkaloids are shown in Tables 3.6-3.8 and the ^{1}H, COSY, ^{13}C, DEPT, HMQC and HMBC NMR spectra of **AK-5**, **AK-6** and **AK-7** are presented in the appendix section. The main differences in these compounds were due to the positioning of the substituent groups (hydroxyl, methoxyl and imidazolyl methyl moiety) on the ABC aromatic ring and this was evident in the splitting pattern of the aromatic protons (Figure 3.28).

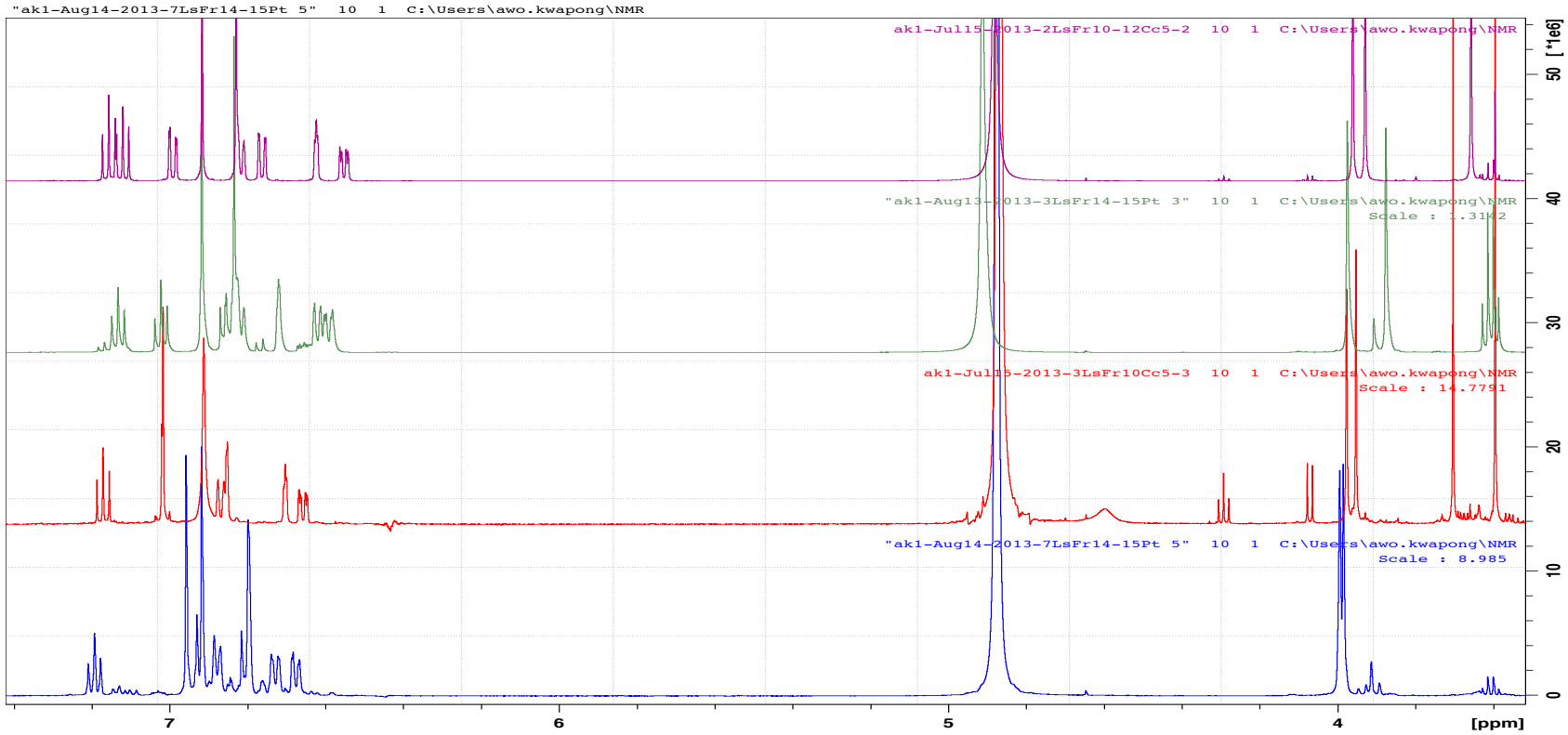

Figure 3.28 ^{1}H NMR spectrum of the isolated imidazole alkaloids, recorded in CD_3OD, 500 MHz. Key: LsFr10-12Cc5-2 – **AK-4**, LSFR14-15Pt 3 – **AK-5**, LsFr10Cc5-3 – **AK-6** and LsFr14-15Pt 5 – **AK-7**

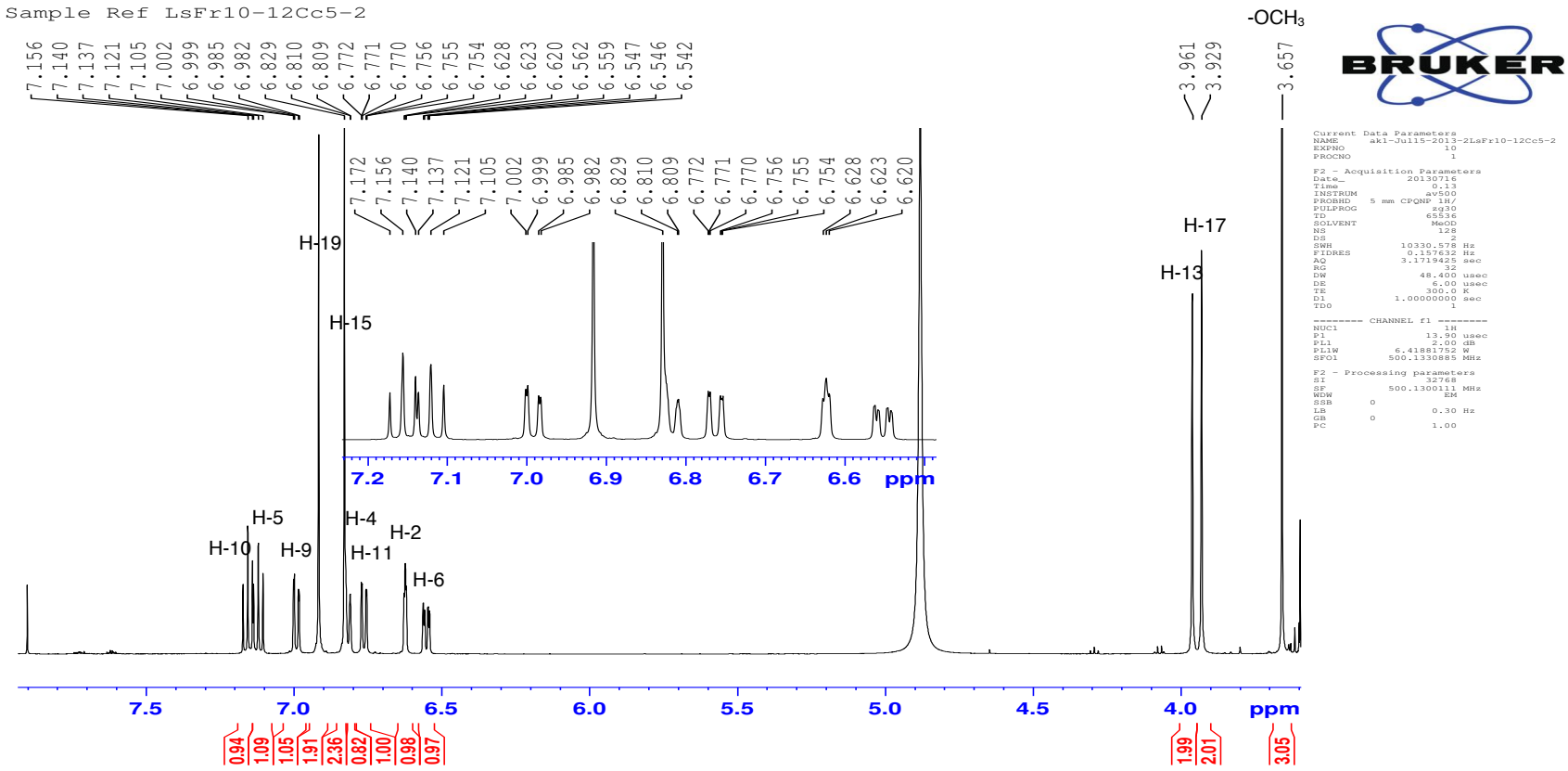

Figure 3.29 ^{1}H NMR spectrum for **AK-4**, recorded in CD_3OD, 500 MHz

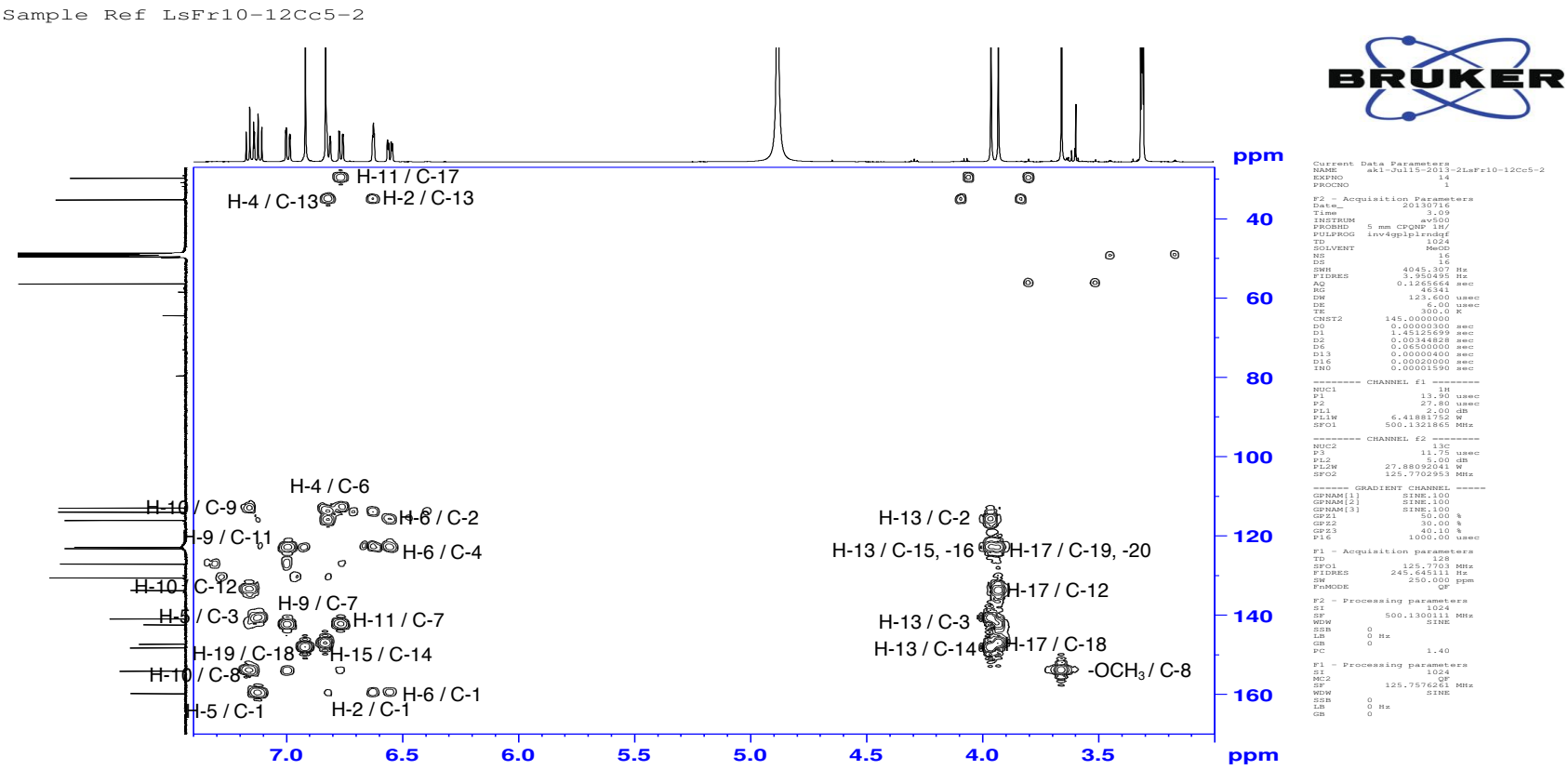

Figure 3.30 HMBC spectrum for **AK-4**

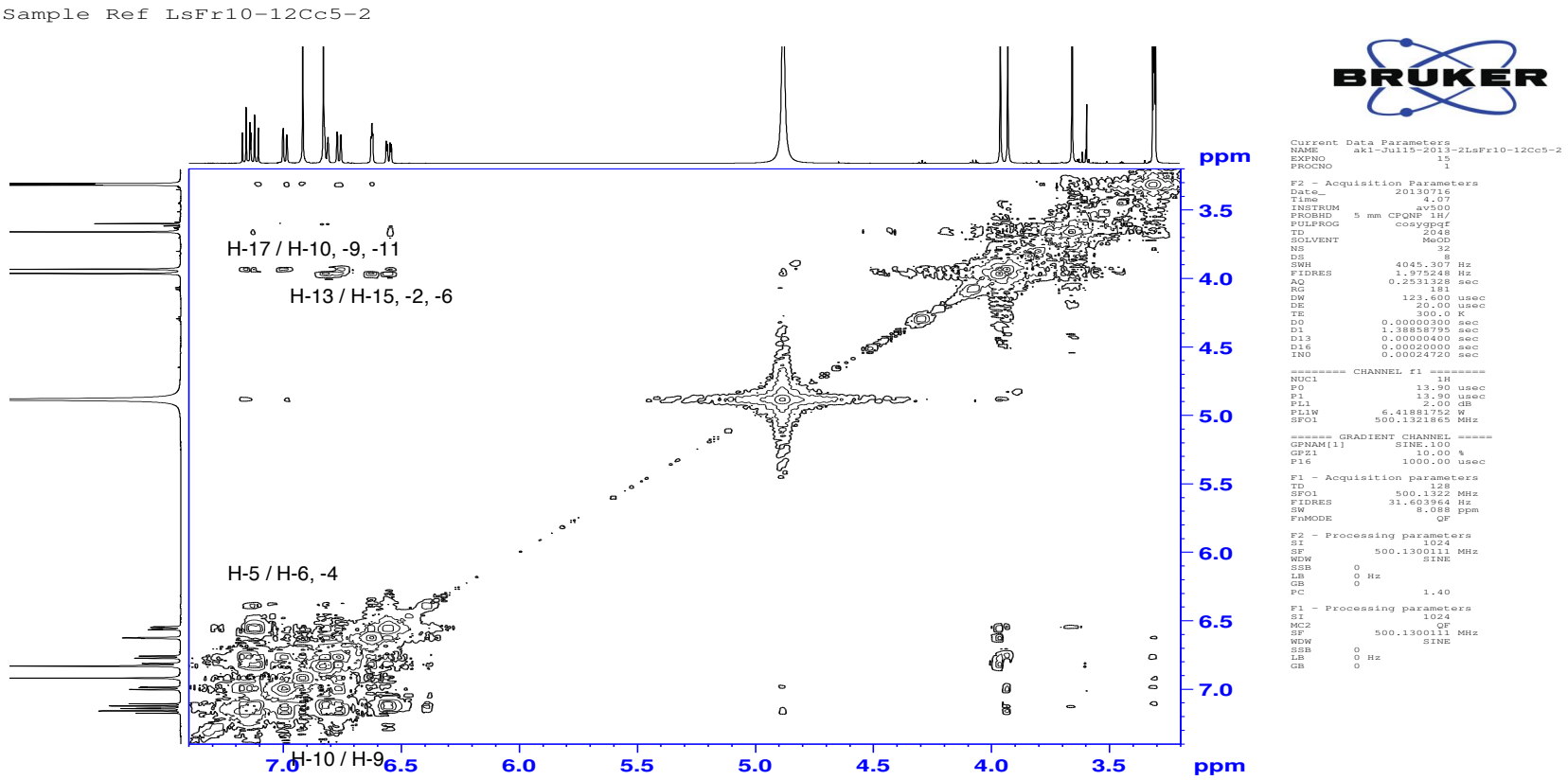

Figure 3.31 COSY NMR spectrum for **AK-4**

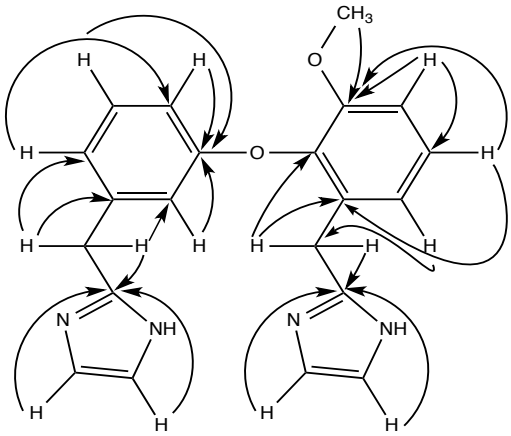

Figure 3.32 HMBC correlations for **AK-4**

Table 3.6 ^{1}H NMR spectral data (ppm) and coupling constants (Hz) of the isolated dimeric imidazole alkaloids, recorded in methanol-d_4

Position	AK-4	AK-6	AK-5	AK-7
1	-	-	-	-
2	6.62 (2.0) s	6.70 (2.0, 1.5) s	6.72 s	6.79 s
3	-	-	-	-
4	6.81 (9.5, 0.5) dd	6.86 (8.0, 2.0) dd	6.81 (8.0) d	6.86 (8.5) d
5	7.10 t	7.15 t	7.11 t	7.17 t
6	6.54 (8.0, 2.0) dd	6.64 (8.0, 2.0) dd	6.58 (8, 2.5) dd	6.72 (8.5, 1.0) dd
7	-	-	-	-
8	-	7.01 s	-	-
9	6.98 (8.0, 1.5) dd	-	6.85 (7.5) d	6.80 d
10	7.14 t	7.01 (1.5) s	7.00 t	6.66 (8.0, 1.5) dd
11	6.75 (8.0, 1.5) dd	-	6.61 (7.5) d	-
12	-	6.85 (1.5) s	-	6.79 (1.5) s
13 (2H)	3.96 s	3.95, 3.97 s	3.87 s	3.98 (5.0) d
14	-	-	-	-
15	6.83 s	6.91 s	6.91 s	6.91 s
16	6.83 s	6.91 s	6.83 s	6.91 s
17 (2H)	3.92 s	3.95, 3.97 s	3.97 s	3.98 (5) d
18	-	-	-	-
19	6.91 s	6.91 s	6.91 s	6.95 s
20	6.91 s	6.91 s	6.83 s	6.95 s
O-CH_3	3.65 s	3.70 s	-	-
OH	-	-		6.93 s

Multiplicities of proton signals: s - singlet, d - doublet, dd - doublet of doublets, t – triplet

Table 3.7 ^{13}C NMR spectral data (ppm) of the isolated dimeric imidazole alkaloids, recorded in methanol-d_4

Position	AK-4	AK-6	AK-5	AK-7
1	159.7	159.9	159.5	159.9
2	116.0	117.6	116.4	118.4
3	140.9	141.0	140.9	141.0
4	122.8	123.3	130.8	123.5
5	130.5	130.6	130.6	130.7
6	113.9	115.6	114.0	116.1
7	142.4	145.6	141.3	150.4
8	154.0	114.5	151.6	143.5
9	112.9	151.9	117.0	118.2
10	127.0	126.4	127.1	121.2
11	123.1	132.5	122.1	136.4
12	133.7	123.0	133.7	122.4
13	35.1	34.3	29.8	35.1
14	147.3	148.1	148.1	148.1
15	122.8	123.3	122.9	118.4
16	122.8	123.3	122.6	118.4
17	29.7	35.1	35.2	34.7
18	148.2	148.4	147.3	148.4
19	123.1	123.0	122.9	122.4
20	123.1	123.0	122.6	122.4
O-CH_3	56.3	56.5		

Table 3.8 HMBC correlations (^2J, ^3J and ^4J) of the isolated dimeric imidazole alkaloids, recorded in methanol-d_4

Position	AK-4	AK-6	AK-5	AK-7
1				
2	C1, C6		C1, C13, C6	
3				
4	C2, C6, C13	C5	C13, C6	C13, C6, C2
5	C1, C3	C1, C3	C3, C1	C3, C1
6	C1, C2		C1, C2	
7				
8		C11		
9	C8, C10, C7		C11, C7	C10
10	C9, C8, C12	C11	C9, C12, C8	C9, C17, C8
11	C7, C9, C17		C9, C7	
12		C9		C11, C7
13	C3, C14, C2, C4	C2, C3, C4, C14	C3, C14, C2, C15, C4,	C3, C14 C2, C4
14				
15	C14	C14	C16, C14	C14
16	C14	C14		C14
17	C12, C18, C7, C11	C10, C12, C18, C11	C18, C11, C19, C7,	C11
18				
19	C18	C18	C20	C18
20	C18	C18	C18	C18
O-CH_3	C8	C9		
OH			C8	C12

3.2.5 Isolation from *Z. officinale*

Powdered *Z. officinale* rhizome (55 g) was successively extracted with hexane, chloroform and methanol, a yield of 2.91%, 1.09% and 5.64%, respectively was obtained. The hexane and methanol extracts were subjected to normal phase- and reverse phase SPE, respectively. Two gingerol compounds were isolated from this process, **AK-8** and **AK-9**. **AK-**

8 was eluted from the hexane extract with hexane and ethyl acetate (7:3, v/v) and **AK-9** was eluted from the methanol extract with methanol and water (4:6, v/v).

3.2.5.1 Characterisation of the isolated gingerol compounds

The ^{1}H NMR and COSY spectra of both compounds (**AK-8** and **AK-9**) revealed an aromatic ring; this was a 4-hydroxy-3-methoxyphenyl moiety substituted at the quaternary aromatic carbon C-1' by a 5-hydroxy-alkane-3-one which was characteristic of gingerol compounds. The structures of the isolated gingerol compounds are shown in Figure 3.33.

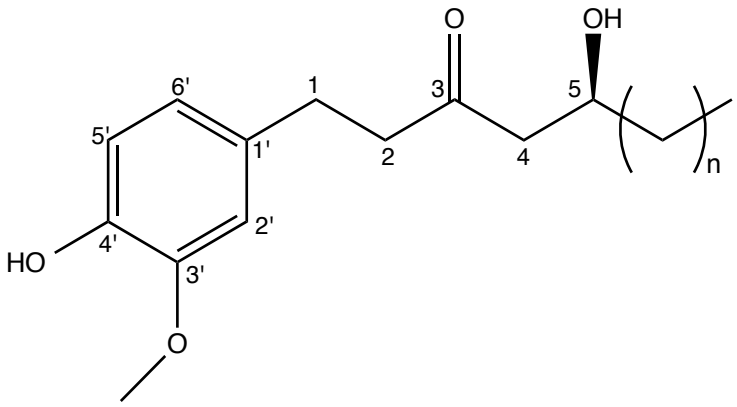

AK-8: n = 6

AK-9: n = 4

Figure 3.33 Structures for the isolated gingerol compounds

AK-8 was isolated as yellow oil. The ESI-MS gave an $[M+Na]^{+}$ ion at *m/z* 345.3, which indicated that its molecular formula was $C_{19}H_{30}O_4$. The ^{1}H NMR spectrum (Figure 3.34) accounted for all the 30 hydrogens, the splitting pattern and the coupling groups were consistent with published literature of [8]-gingerol (Shoji *et al*., 1982, Kim *et al*., 2008). A methoxyl group (δ_H 3.86), a hydroxyl group (δ_H 5.57) and three aromatic hydrogens; δ_H 6.67 (s, H-2'), 6.80 (d, *J* = 7.5 Hz, H-5') and 6.64 (d, *J* = 7.5 Hz, H-5) accounted for all positions on the 4-hydroxy-3-methoxyphenyl moiety. The proton signals at δ_H 1.25 (12H, m, H-6 to -

11), 2.45 and 2.54 (2H, d, H-4), 2.71 (2H, t, H-2), 2.81 (2H, t, H-1), 3.99 (1H, m, H-5), 2.98 (OH, br s, H-5) and a terminal methyl group (δ_H 0.83, H-12) accounted for the hydrogens on the 5-hydroxy-1-dodecan-3-one chain (Figure 3.34). In the ^{13}C NMR, 19 carbon signals were observed: 6 aromatic carbons, a methoxyl carbon (δ_C 56.0), 11 aliphatic carbons and a carbonyl carbon (δ_C 211.6, C-3). The methoxyl hydrogens showed a ^2J correlation to the aromatic quaternary carbon (δ_C 146.6, C-3'), which confirmed the direct attachment of the methoxyl group to the carbon. The hydroxyl hydrogen (δ_H 5.57) showed a ^2J correlation to the aromatic quaternary carbon C-4' (δ_C 144.1), which it was directly attached to and a ^3J correlation to the aromatic carbon C-5' (δ_C 114.5). This therefore confirmed the *ortho* position of the methoxyl group to the hydroxyl group on the 4-hydroxy-3-methoxyphenyl aromatic ring. The linkage of the 4-hydroxy-3-methoxyphenyl moiety to the 5-hydroxy-1-dodecan-3-one chain was confirmed by a ^2J and ^3J correlations of H-1 (δ_H 2.81) and H-2 (δH 2.71) to the aromatic carbons C-1' (δ_C 132.8), C-2' (δ_C 111.1) and C-6' (δ_C 120.8) (Figure 3.35 and Table 3.9, supporting information). The positions of the carbonyl carbon (δ_C 211.6, C-3) and hydroxyl group (2.98 br s) on the 5-hydroxy-1-dodecan-3-one chain was confirmed by a 2J correlations of H-2, H-4 and ^3J correlation of H-1 to the carbonyl carbon (δ_C 211.6, C-3) and a ^4J correlation of the hydroxyl hydrogen to C-7 (δ_C 29.7) (Figure 3.35). **AK-8** was therefore identified as 5-hydroxy-1-(4-hydroxy-3-methoxyphenyl) dodecan-3-one, commonly known as [8]-gingerol had previously been isolated from this plant (Shoji *et al.*, 1982).

AK-9 was isolated as a dark brown solid from the methanol extract of *Z. officinale.* The accurate mass measurement gave an $[M-H]^-$ ion at *m/z* 293.1753 which indicated that its molecular formula was $C_{17}H_{26}O_4$. The NMR spectrum for **AK-9** was very similar to that of **AK-8**, suggesting that it had the similar chemical structure. The difference between the two compounds was the lack of two methylene signals in the ^{1}H and ^{13}C NMR spectra of **AK-9** (Figures 3.36 and 3.37). Based on this evidence and analyses of the HMQC, HMBC and COSY correlations (Table 3.10 and Figure 3.38) and literature comparison, the structure of **AK-9** was readily determined to be 5-hydroxy-1-(4-hydroxy-3-methoxyphenyl) decan-3-one commonly known as [6]-gingerol (Shoji *et al.*, 1982; Kim *et al.*, 2008).

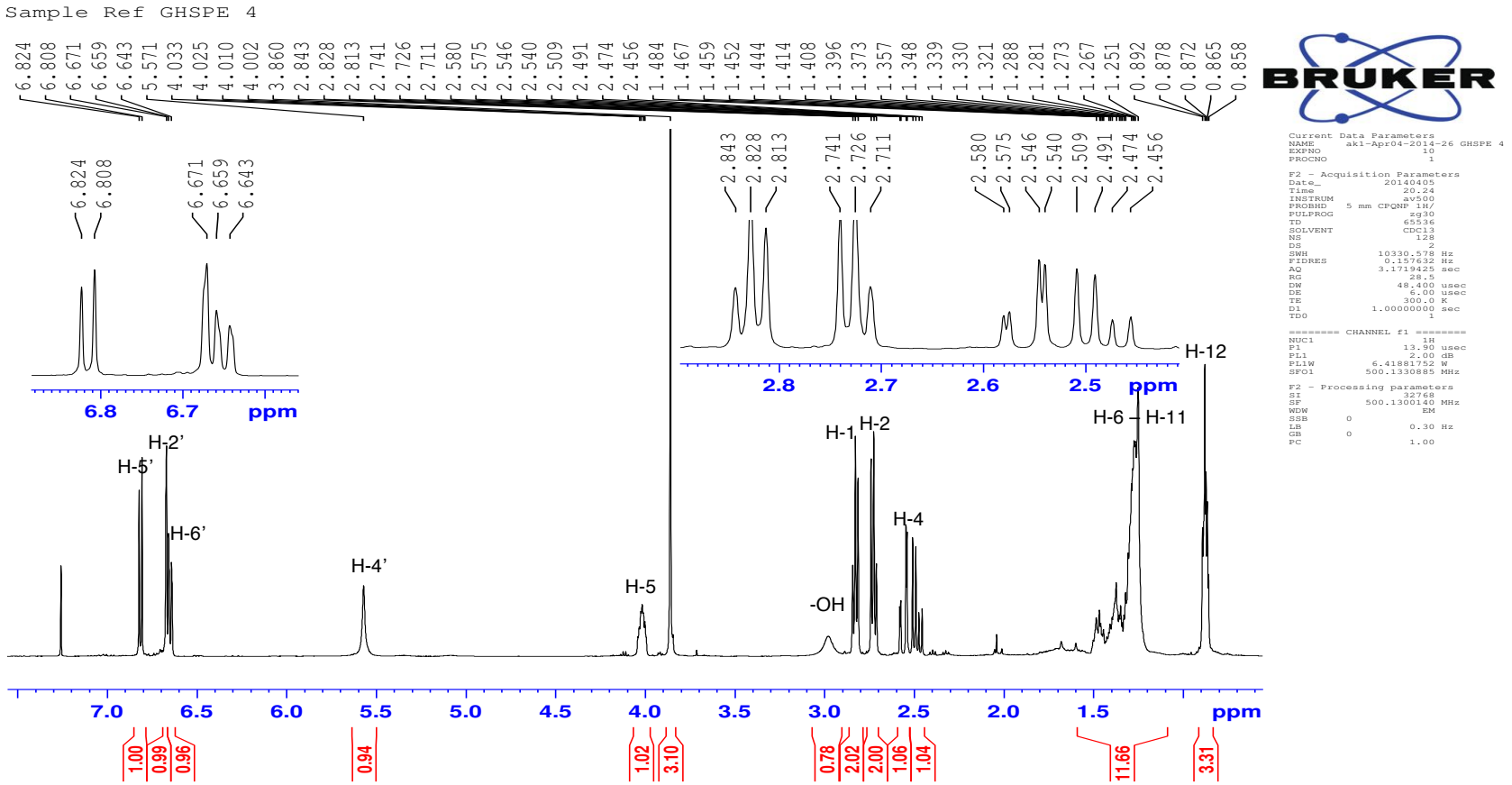

Figure 3.34 ^{1}H NMR spectrum for **AK-8**, recorded in $CDCl_3$, 500 MHz

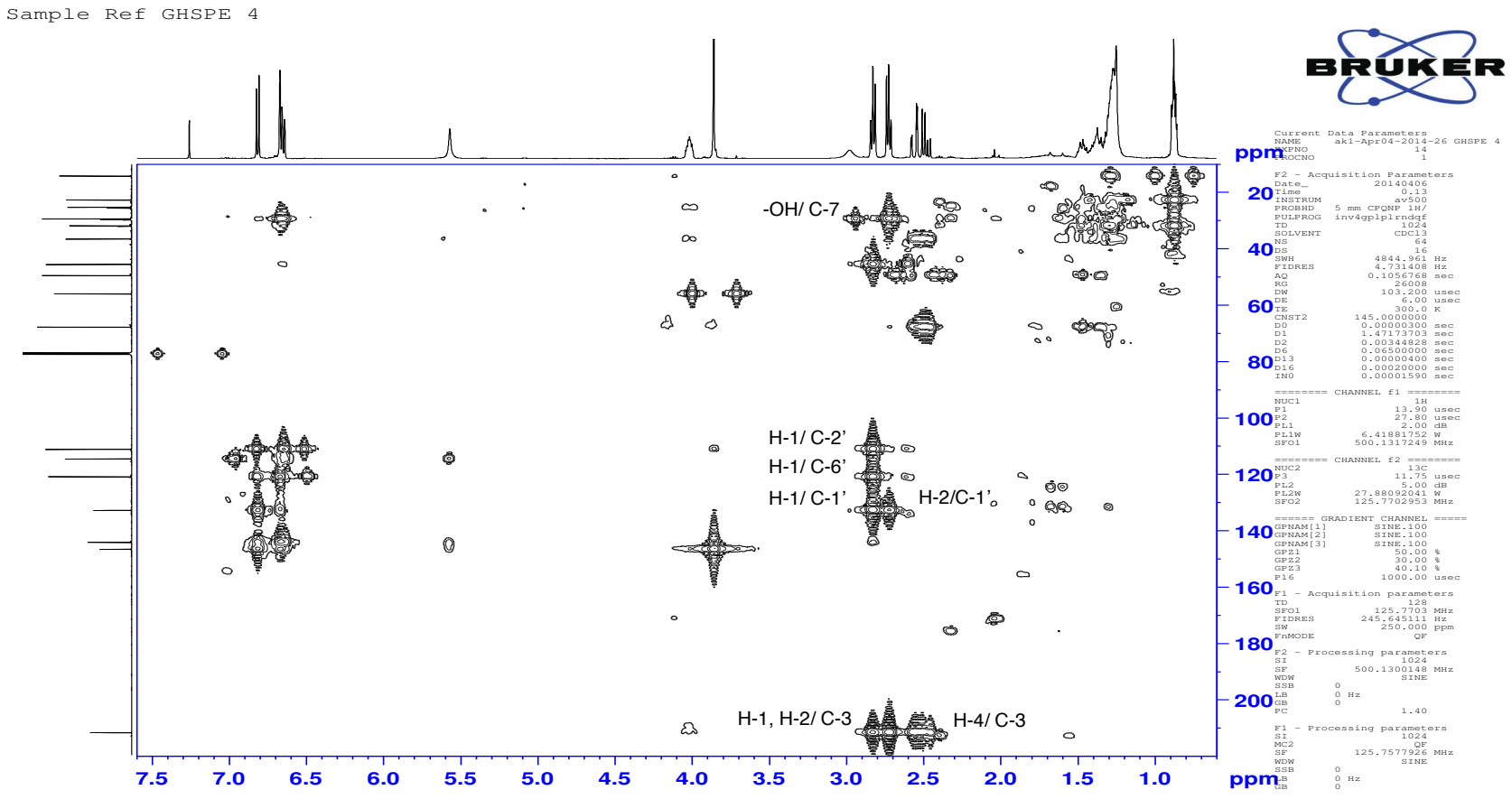

Figure 3.35 HMBC spectrum for **AK-8**

Table 3.9 ^{1}H (coupling constants, Hz) and ^{13}C NMR spectral data (ppm) and HMBC correlations of **AK-8**, recorded in chloroform-*d*

Position	^{1}H	^{13}C	^{2}J	^{3}J	^{4}J	^{13}C Shoji *et al.*, 1982 ($CDCl_3$, 100 MHz)
1	2.81(2H) t	29.4	C2, C1'	C3, C2', C6'		29.2
2	2.71(2H) t	45.6	C1, C3	C1'		45.4
3 (C=O)		211.6				211.4
4	2.45 d, 2.54 d (17.5)	49.5	C3, C5	C2, C6		49.4
5	3.99 m	67.8				67.8
6	1.25 (2H) m	36.5	C5			36.6
7	1.25 (2H) m	29.7		C5		29.2
8	1.25 (2H) m	25.2	C7	C10		22.6
9	1.25 (2H) m	25.6	C8, C10	C7, C11		25.5
10	1.25 (2H) m	22.7	C11	C8, C12		22.6
11	1.25 (2H) m	31.8	C10, C12			31.8
12	0.83 (3H) t	14.1	C11	C10		14.0
OH	2.98 br s	67.8			C7	67.8
1'		132.8				132.7
2'	6.67 s	111.1	C1', C3'	C1, C4', C6'		111.3
3'		146.6				146.8
4' (OH)	5.57 br s	144.1	C4'	C5'		144.2
5'	6.80 d (7.5)	114.5	C6'	C1'		114.7
6'	6.64 dd (7.5)	120.8		C2'		120.8
O-CH_3	3.86 s	56.0		C3'		55.8

Multiplicities of proton signals: s - singlet, d - doublet, dd - doublet of doublet, t - triplet, br s - broad singlet, and m - multiplet

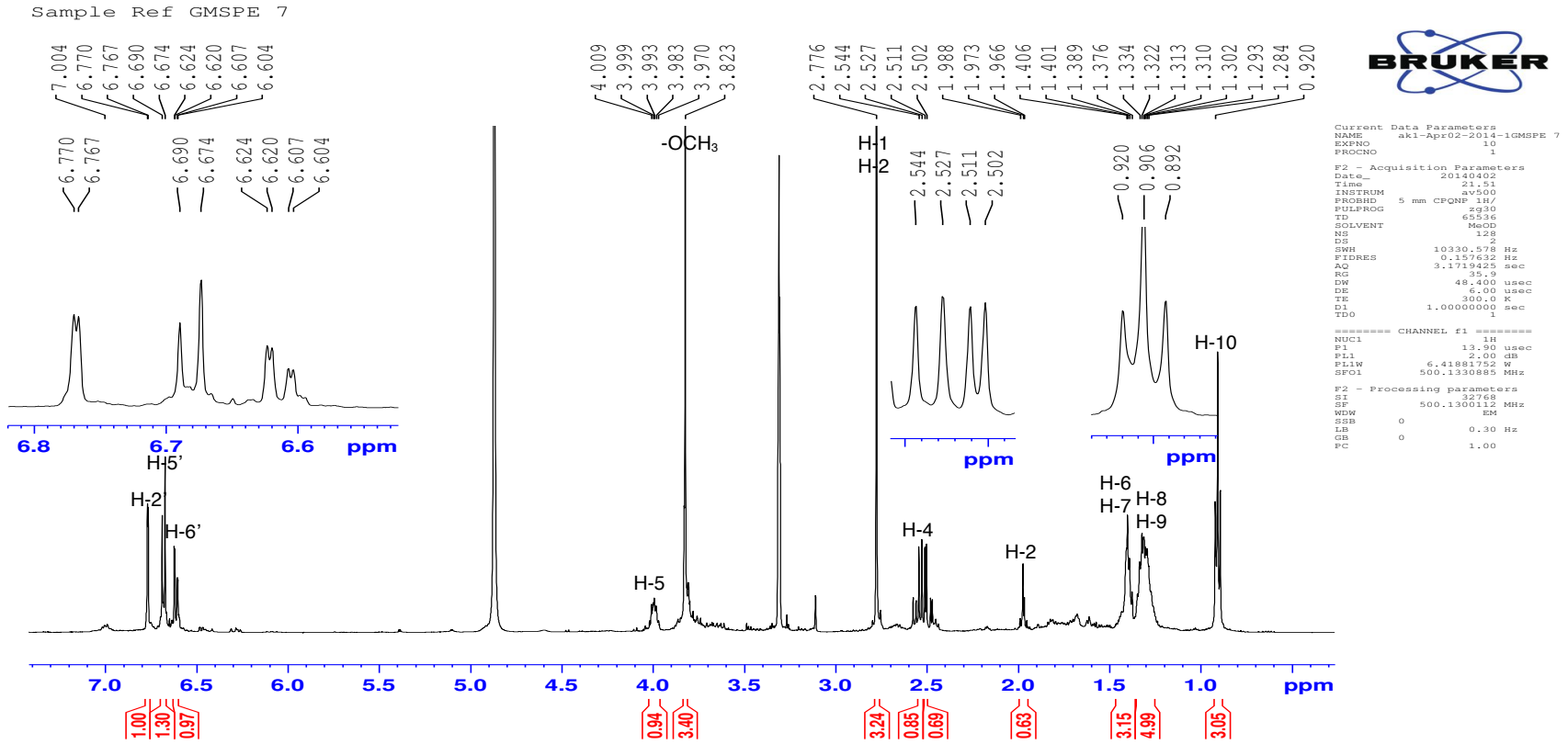

Figure 3.36 ^{1}H NMR spectrum for **AK-9**, recorded in CD_3OD, 500 MHz

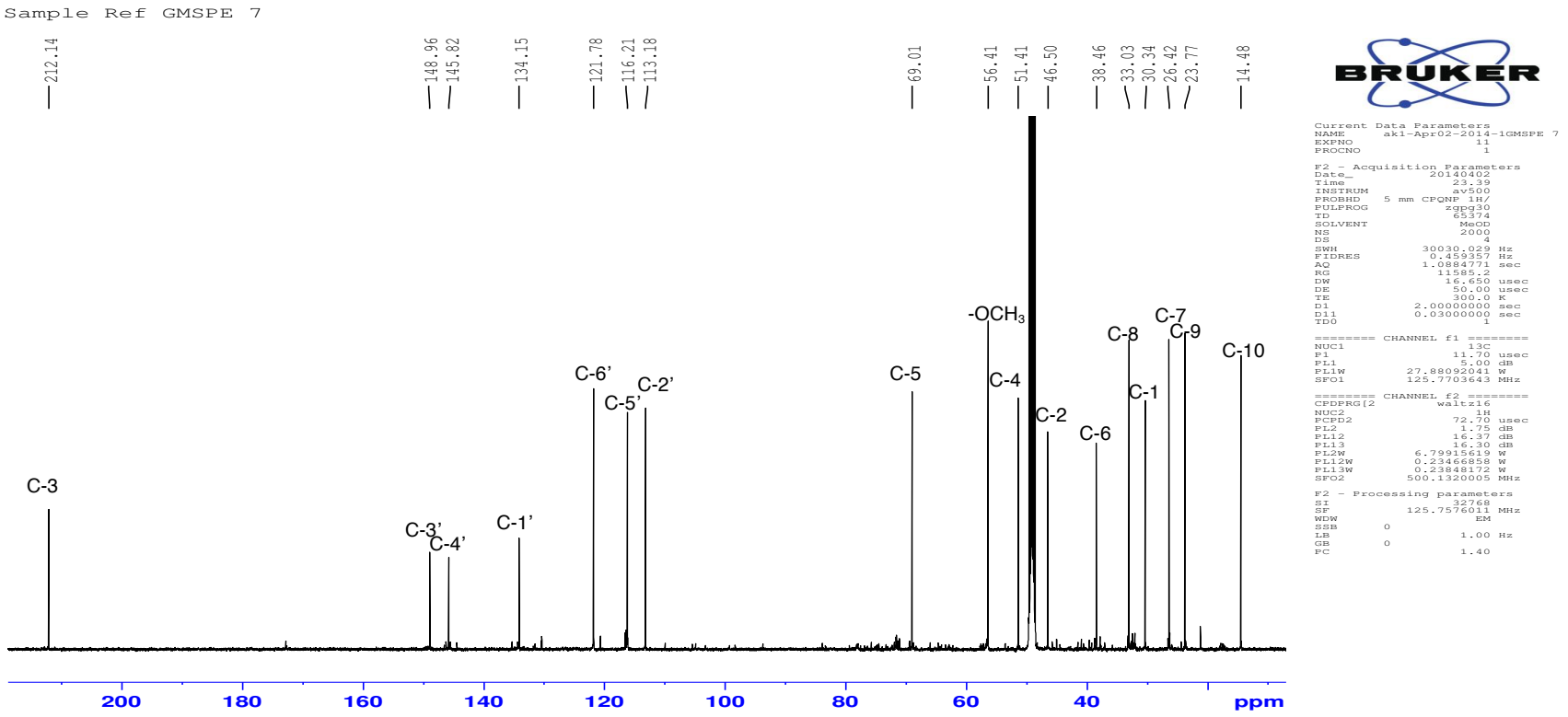

Figure 3.37 ^{13}C NMR spectrum for **AK-9**, recorded in CD_3OD, 500 MHz

Table 3.10 ^{1}H (coupling constants, Hz) and ^{13}C NMR spectral data (ppm) and HMBC correlations of **AK-9**, recorded in methanol-d_4

Position	^{1}H	^{13}C	^{2}J	^{3}J	^{13}C Kim *et al.*, 1982 (CD_3OD, 100 MHz)
1	2.77 (2H) s	30.3	C2, C1'	C2', C6', C3	30.6
2	2.77 s, 1.96 s	46.5	C1		46.7
3 (C=O)		212.1			212.1
4	2.50 d (4.5), 2.52 d (8.5)	51.4	C3, C5	C6	51.6
5	3.97m	69.0			69.2
6	1.37 (2H) m	38.4			38.7
7	1.37 m, 1.29 m	26.4		C9	26.6
8	1.29 (2H) m	33.0		C6	33.2
9	1.29 (2H) m	23.7	C10, C8		24.0
10	0.89 (3H) t	14.4	C9	C8	14.7
OH		69.0			
1'		134.1			134.2
2'	6.77 s (1.5)	113.1		C1, C6', C4'	113.3
3'		148.9			149.0
4' (OH)		145.8			145.9
5'	6.67 d (8)	116.2	C4'	C1', C3'	116.3
6'	6.60 dd (8.5, 1.5)	121.7		C1, C2', C4'	121.9
O-CH_3	3.82 s	56.4		C3'	56.6

Multiplicities of proton signals: s - singlet, d - doublet, dd - doublet of doublet, t – triplet and m – multiplet

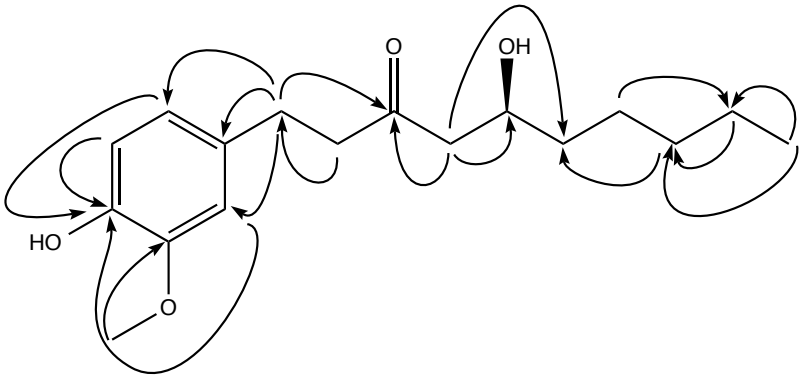

Figure 3.38 Selected HMBC correlations for **AK-9**

3.2.6 Isolation from *B. officinalis*

Powdered *B. officinalis* herb (200 g) was successively extracted with hexane, chloroform and methanol; this gave a yield of 0.4%, 1.6% and 5.2%, respectively. The methanol extract was subjected to reverse phase SPE and acid-base extraction (alkaloidal extraction). 10.26 g of the methanol extract gave an alkaloidal yield of 1.86%, from which a flavone (**AK-10**, 2.98 mg) was isolated as a solid residue by filtering and washing off the supernatant alkaloidal extract with ethyl acetate.

3.2.6.1 Characterisation of AK-10 as Acacetin-7-*O*-rutinoside (Linarin)

AK-10 was isolated as an amorphous white solid. The accurate mass measurement gave an $[M+H]^+$ ion at *m/z* 593.1870, which indicated that its molecular formula was $C_{28}H_{32}O_{14}$. The resonance pattern of the protons in the ^1H NMR spectrum and COSY couplings were indicative of a flavone with a rutinose substituent.

The NMR spectra revealed the presence of two phenyl rings (A and B) linked by a heterocyclic ring (C) (Figure 3.39), the core structure of a flavone. The heterocyclic ring linkage to aromatic ring B was revealed by a ^3J correlation of the heterocyclic hydrogen (H-3, s, δ_H 6.96) to the aromatic quaternary carbon (C-1', δ_C 122.6), which was *para* to the methoxyl group (δ_C 55.5, δ_H 3.86) on the aromatic ring B (Figure 3.41). The position of the

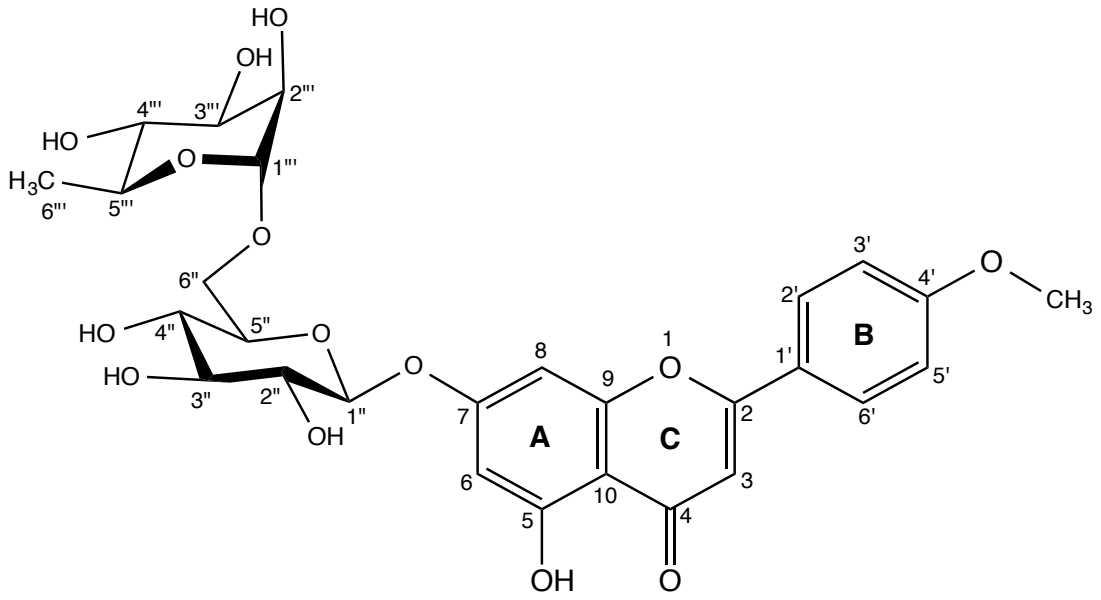

Figure 3.39 Structure for **AK-10**

methoxyl group on ring B was confirmed by a ^{3}J correlation of the methoxyl hydrogens (δ_H 3.86) to the aromatic quaternary carbon (C-4', δ_C 162.4). The *para* positioning of the methoxyl group and heterocyclic ring C linkage (Figure 3.43) supported the AA'BB' aromatic spin system of ring B, observed in the ^{1}H NMR spectrum (Figure 3.40) as two doublets (δ_H 7.14, H-2', -6' and δ_H 8.05, H-3', -5') integrating for two protons each, with a strong *ortho* coupling (J = 8.8 Hz) of the protons. The HMBC correlations of H-3 to the carbonyl carbon (C-4, δ_C 182.0) and to quaternary aromatic carbon (C-10, δ_C 105.4) confirmed their positions and the direct attachment of the heterocyclic ring C to the aromatic ring A.

The COSY NMR spectrum revealed the *meta* coupling of the two remaining aromatic hydrogens (H-6, δ_H 6.45 and H-8, δ_H 6.79). Their positions on the aromatic ring A was confirmed by HMQC and ^{2}J correlations of H-6 to an aromatic quaternary carbon (C-5, δ_C 161.1) bearing a hydroxyl group (δ_H 12.91) and H-8 to an aromatic quaternary carbon (C-9, δ_C 156.1) (Figure 3.41). The glycosidic linkage of the flavone to the rutinose moiety was revealed by a ^{3}J correlation of H-1" (δ_H 5.05) to the aromatic quaternary carbon (C-7, δ_c

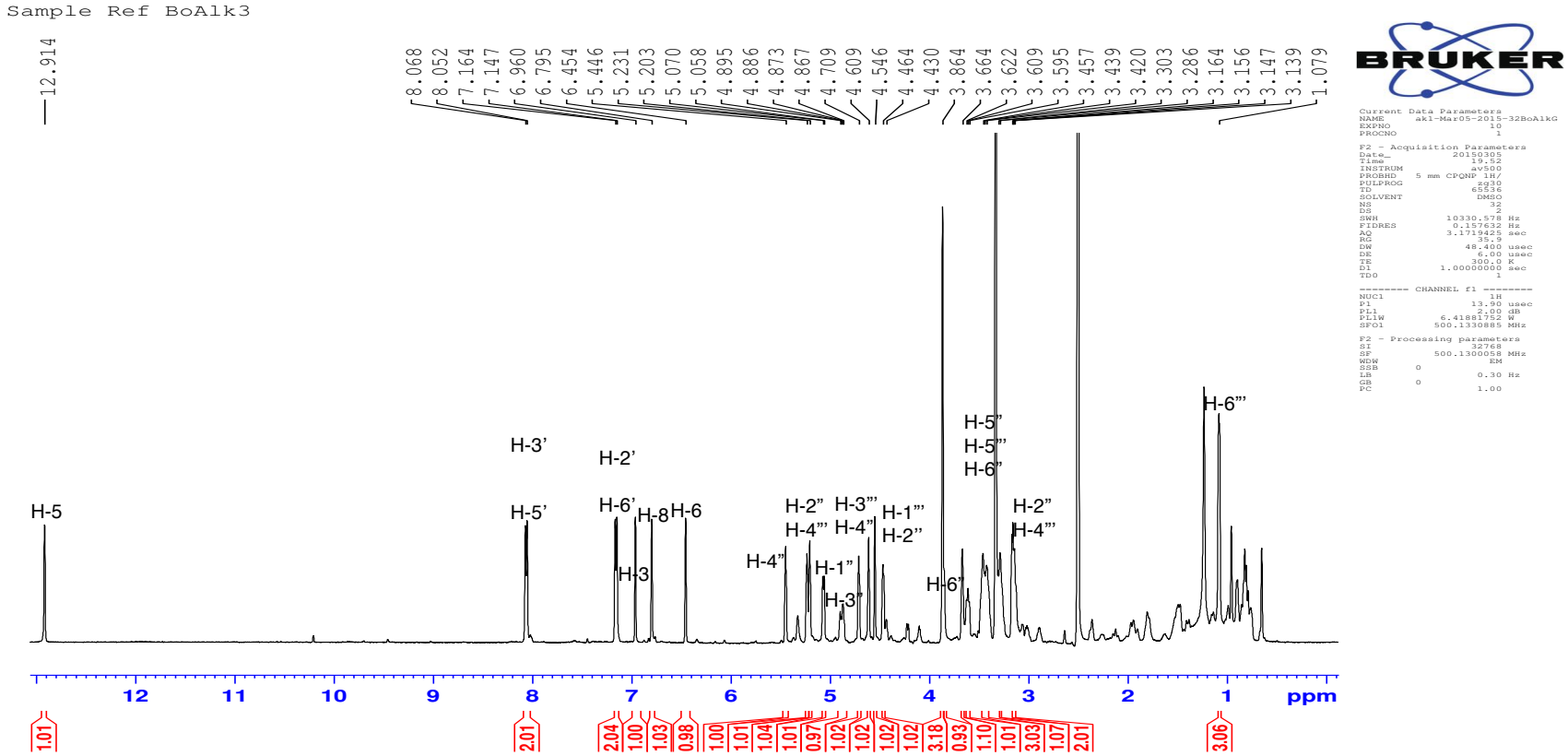

Figure 3.40 ^{1}H NMR spectrum for **AK-10**, recorded in DMSO, 500 MHz

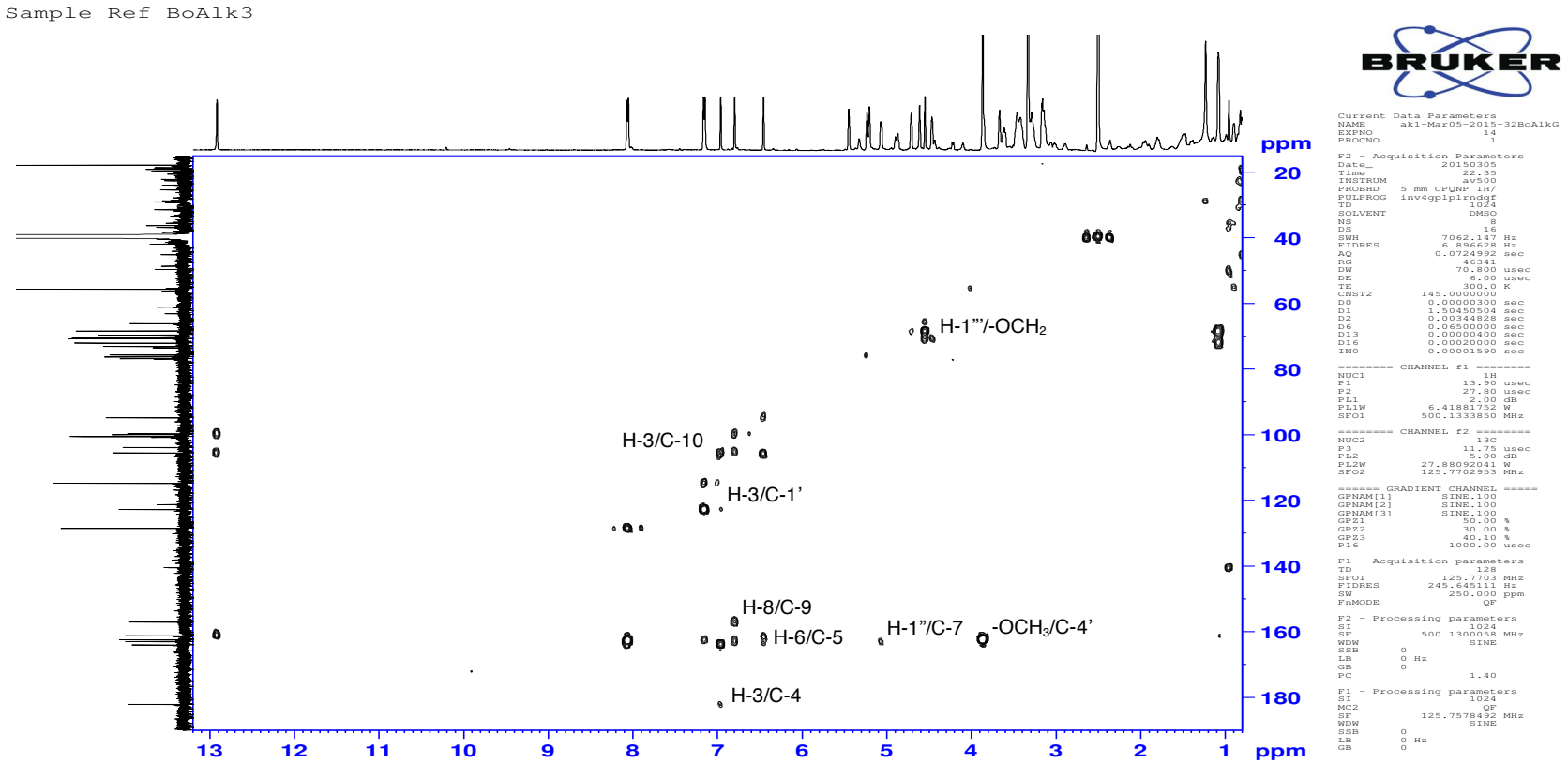

Current Data Parameters
NAME ak1-Mar05-2015-32BoAlkG
EXPNO 14
PROCNO 1

F2 - Acquisition Parameters
Date_ 20150305
Time 22.35
INSTRUM av500
PROBHD 5 mm CPQNP 1H/
PULPROG inv4gp1plrndqf
TD 1024
SOLVENT DMSO
NS 8
DS 16
SWH 7062.147 Hz
FIDRES 6.896628 Hz
AQ 0.0724992 sec
RG 4641
DW 70.800 usec
DE 6.00 usec
TE 300.0 K
CNST2 145.0000000
D0 0.00000300 sec
D1 1.50450504 sec
D2 0.00344828 sec
D6 0.06500000 sec
D13 0.00000400 sec
D16 0.00020000 sec
IN0 0.00001590 sec

======== CHANNEL f1 ========
NUC1 1H
P1 13.90 usec
P2 27.80 usec
PL1 2.00 dB
PL1W 6.41881752 W
SFO1 500.1333850 MHz

======== CHANNEL f2 ========
NUC2 13C
P3 11.75 usec
PL2 5.00 dB
PL2W 27.88092041 W
SFO2 125.7702953 MHz

====== GRADIENT CHANNEL =====
GPNAM[1] SINE.100
GPNAM[2] SINE.100
GPNAM[3] SINE.100
GPZ1 50.00 %
GPZ2 30.00 %
GPZ3 40.10 %
P16 1000.00 usec

F1 - Acquisition parameters
TD 128
SFO1 125.7703 MHz
FIDRES 245.645111 Hz
SW 250.000 ppm
FnMODE QF

F2 - Processing parameters
SI 1024
SF 500.1300058 MHz
WDW SINE
SSB 0
LB 0 Hz
GB 0
PC 1.40

F1 - Processing parameters
SI 1024
MC2 QF
SF 125.7578492 MHz
WDW SINE
SSB 0
LB 0 Hz
GB 0

Figure 3.41 HMBC NMR spectrum for **AK-10**

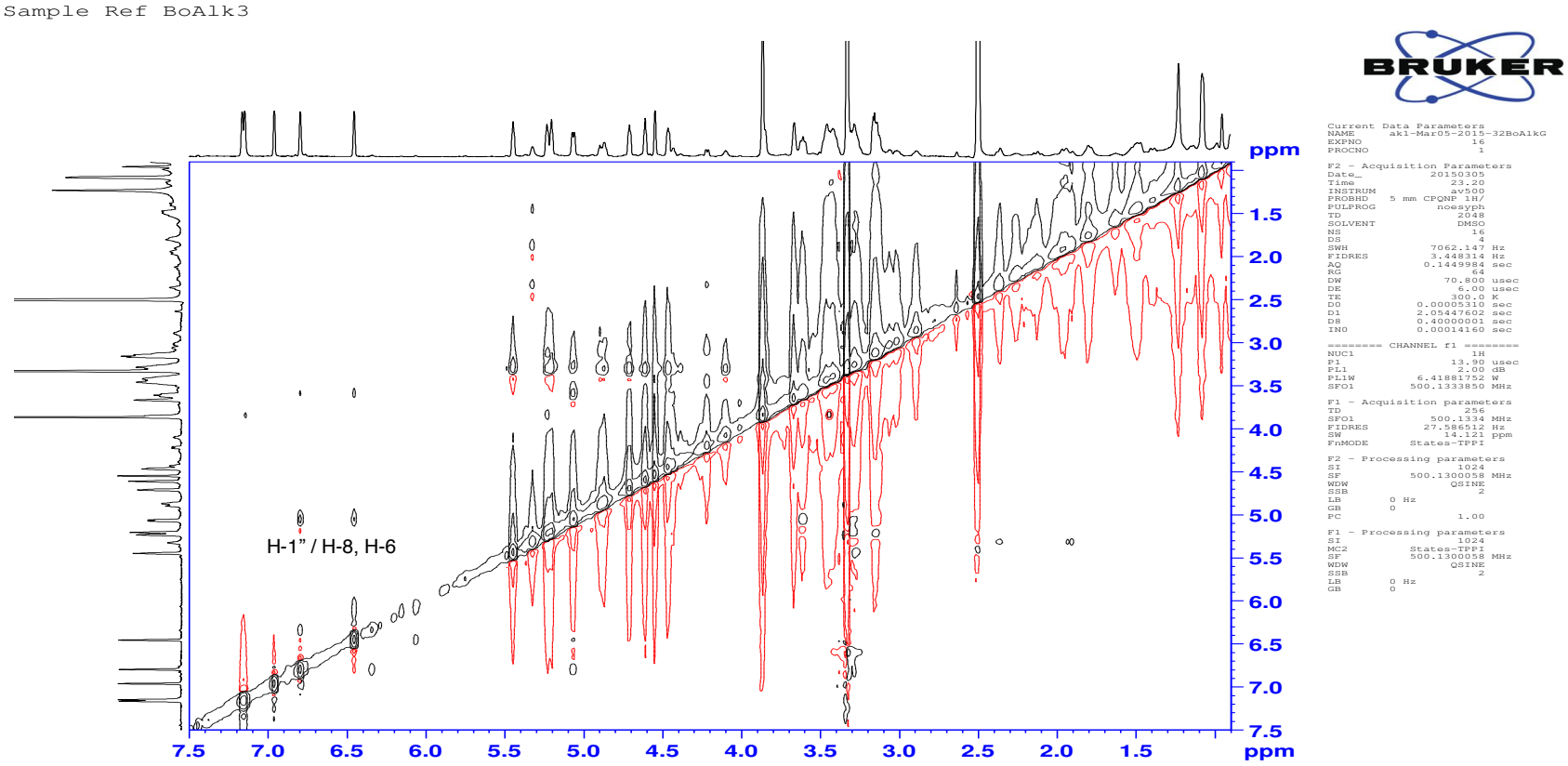

Figure 3.42 NOESY NMR spectrum for **AK-10**

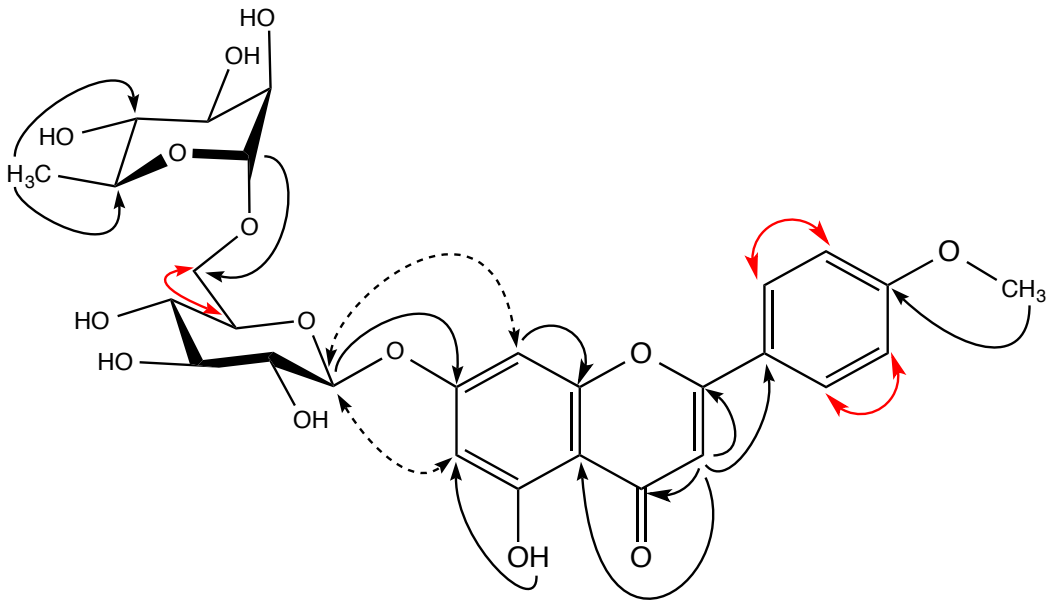

Figure 3.43 Selected HMBC (solid black arrow), COSY (solid red arrow) and NOESY (dotted black arrow) correlations for **AK-10**

162.9) and this was confirmed by the NOESY correlations between H-1" and the two aromatic hydrogens of ring A (H-6 and H-8) (Figure 3.42). The glycosidic bond in the rutinose moiety was revealed by a ^{3}J correlation of H-1"' (δ_H 4.54) of the rhamnose and oxymethylene carbon (C-6", δ_C 66.0) of glucose monomer. Full assignment of the all ^{1}H and ^{13}C resonances was achieved by analyses of the 2-dimensional NMR spectra (Table 3.11). **AK-10** was assigned as 5-hydroxy-2-(4-methoxyphenyl)-7-((3,4,5-trihydroxy-6-(((3,4,5-trihydroxy-6-methyltetrahydro-2H-pyran-2-yl)oxy)methyl)tetrahydro-2H-pyran-2-yl)oxy)-4H-chromen-4-one commonly known as linarin or acacetin-7-*O*-rutinoside. This compound had previously been isolated from *Cirsium coloradense, Valeriana wallichii*, and *Artemisia alba* (Gardne, 1973; Chari *et al.*, 1977; Saleh *et al.*, 1985). Additionally, it was isolated from, *Valeriana officinalis* and *Buddleja lindleyana* (Fernández *et al.*, 2004; Han and Chen, 2014). This is however, the first report of acacetin-7-*O*-rutinoside in *B. officinalis*. The ^{1}H and ^{13}C NMR data were in agreement with published literature for the isolation of acacetin-7-*O*-rutinoside from *Cirsium japonicum* (Park *et al.*, 1995).

Table 3.11 ^{1}H (coupling constants, Hz) and ^{13}C NMR spectral data (ppm) and HMBC correlations of **AK-10**, recorded in DMSO-d_6

Position	^{1}H	^{13}C	^{2}J	^{3}J	^{13}C Park *et al.*, 1995 (DMSO, 100 MHz)
2	-	163.9			163.9
3	6.96 s	103.8	C2, C4	C10, C1'	103.8
4	-	182.0			182.1
5 (OH)	12.91	161.1	C5	C6, C10	161.2
6	6.45 s	99.6	C5	C8, C10	100.5
7	-	162.9			157.0
8	6.79 s	94.7	C7, C9	C6, C10	94.8
9	-	156.1			163.0
10	-	105.4			105.5
1'	-	122.6			122.7
2'	7.14 d (8.8)	114.7	C1'	C4', C6'	128.4
3'	8.05 d (8.8)	128.4	C4'	C5'	114.7
4'	-	162.4			162.4
5'	8.05 d (8.8)	128.4	C4'	C3'	114.7
6'	7.14 d (8.8)	114.7	C1'	C2', C4'	128.4
-OCH_3	3.86	55.5		C4'	55.6
1"	5.05 d (7.2)	99.9		C7	100.0
2"	3.13, 5.20	76.7			73.1
3"	3.20, 4.83	76.2			76.3
4"	4.46, 5.40	73.0	C5"		69.8
5"	3.41	70.7			75.9
6" (-OCH_2)	3.41, 3.85	66.0			66.1
1"'	4.54	100.5	C2"'	C5"', C6"	100.4
2"'	3.66, 4.60	70.3			70.8
3"'	3.60, 4.70	75.6			70.4
4"'	3.17, 5.23	72.0			72.1
5"'	3.42	68.3			68.3
6"' (-CH_3)	1.07	17.8	C5"'	C4"'	17.8

Multiplicities of proton signals: s - singlet, d - doublet

3.2.7 Isolation from *U. tomentosa*

Powdered *U. tomentosa* vine cuttings (500 g) were successively extracted with hexane, chloroform and methanol; this gave a yield of 1.0%, 0.6% and 28.1%, respectively. The methanol extract was subjected to acid-base extraction, which gave a yield of 4.30 g. This extract was further worked on to isolate four alkaloids; **AK-11**, **AK-12**, **AK-13** and **AK-14**. The isolation scheme for the alkaloids is described in Figure 3.44 below.

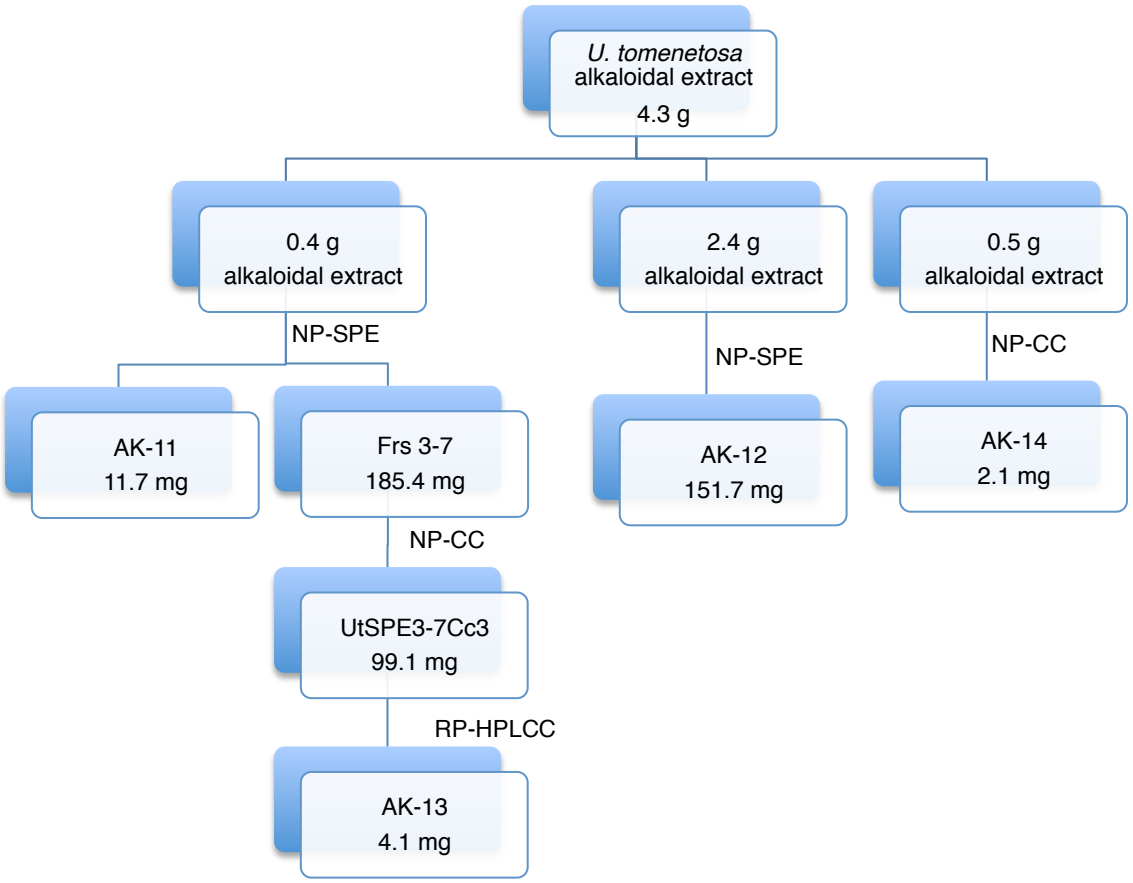

NP-SPE – normal-phase solid phase extraction, NP-CC – normal-phase gravity column chromatography and RP-HPLCC – reverse-phase high performance liquid chromatography

Figure 3.44 Isolation scheme for *U. tomentosa*

Compounds **AK-11**, **AK-12** and **AK-14** were eluted with ethyl acetate: hexane (7:3, v/v), ethyl acetate: methanol (9:1, v/v), and ethyl acetate, hexane and methanol (9:1:1, v/v), respectively. **AK-13** was isolated on preparative HPLC using a Phenomenex® Prodigy™ column ODS, 250 x 21.20 mm, 5 µm; 10 mL/min isocratic run, 60% acetonitrile in water, 254 nm. Figure 3.45 shows the HPLC chromatogram of the fraction (UtSPE3-7CC3) from which **AK-13** was isolated. Figures 3.46 and 3.47 show the normal-phase analytical TLC and ^{1}H NMR spectrum of the isolated oxindole compounds, respectively.

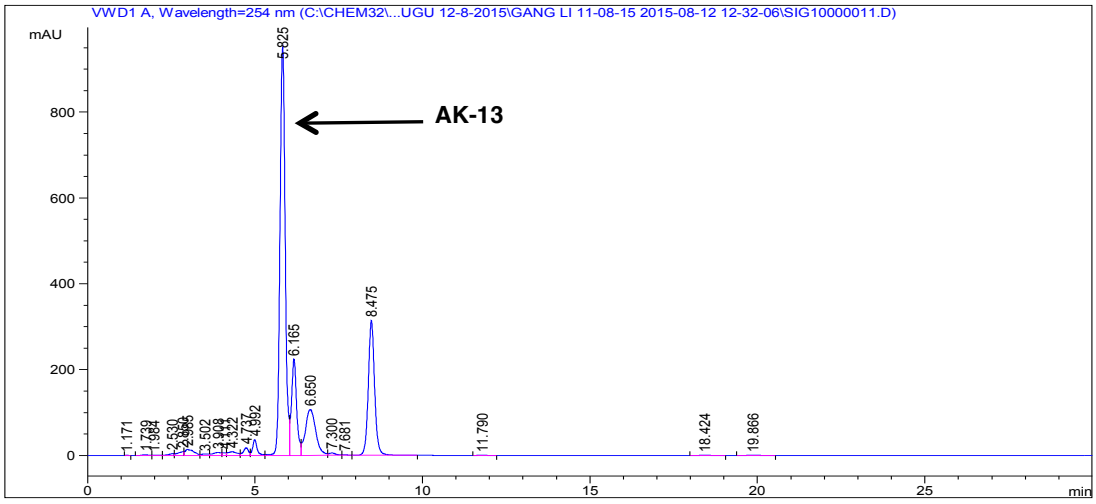

Figure 3.45 The analytical HPLC chromatogram of UtSPE3-7CC3 (Ascentis® column C18, 25 x 4.6 mm, 5 µm; 1 µL/min isocratic run, 60% acetonitrile in water, 254 nm)

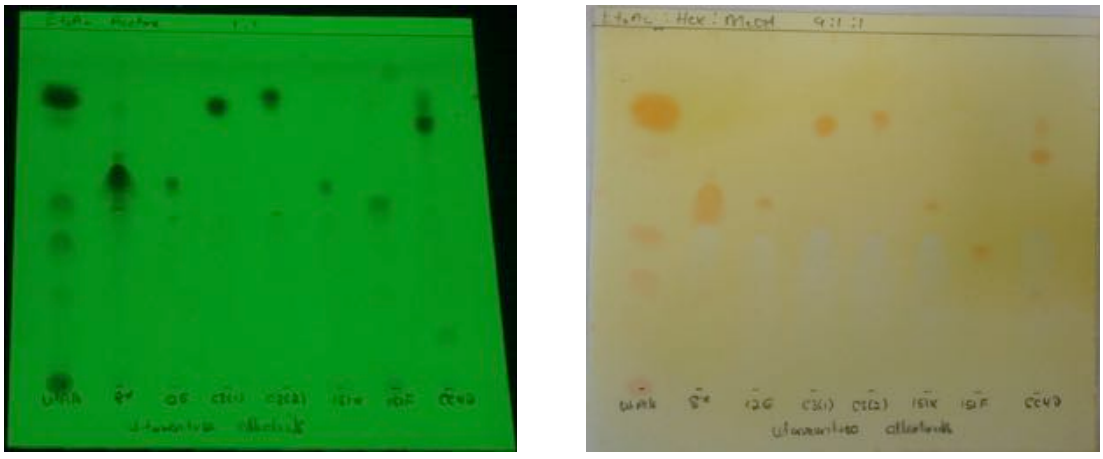

Figure 3.46 Analytical TLC plates for the isolated oxindole compounds; the left plate (ethyl acetate: acetone, 1:1, v/v, 254 nm) and the right plate (ethyl acetate: hexane: methanol, 9:1:1, v/v, Dragendorff's reagent), Key: 8*- **AK-11**, 12G - **AK-12**, C3(1) - **AK-13** and 151F - **AK-14**.

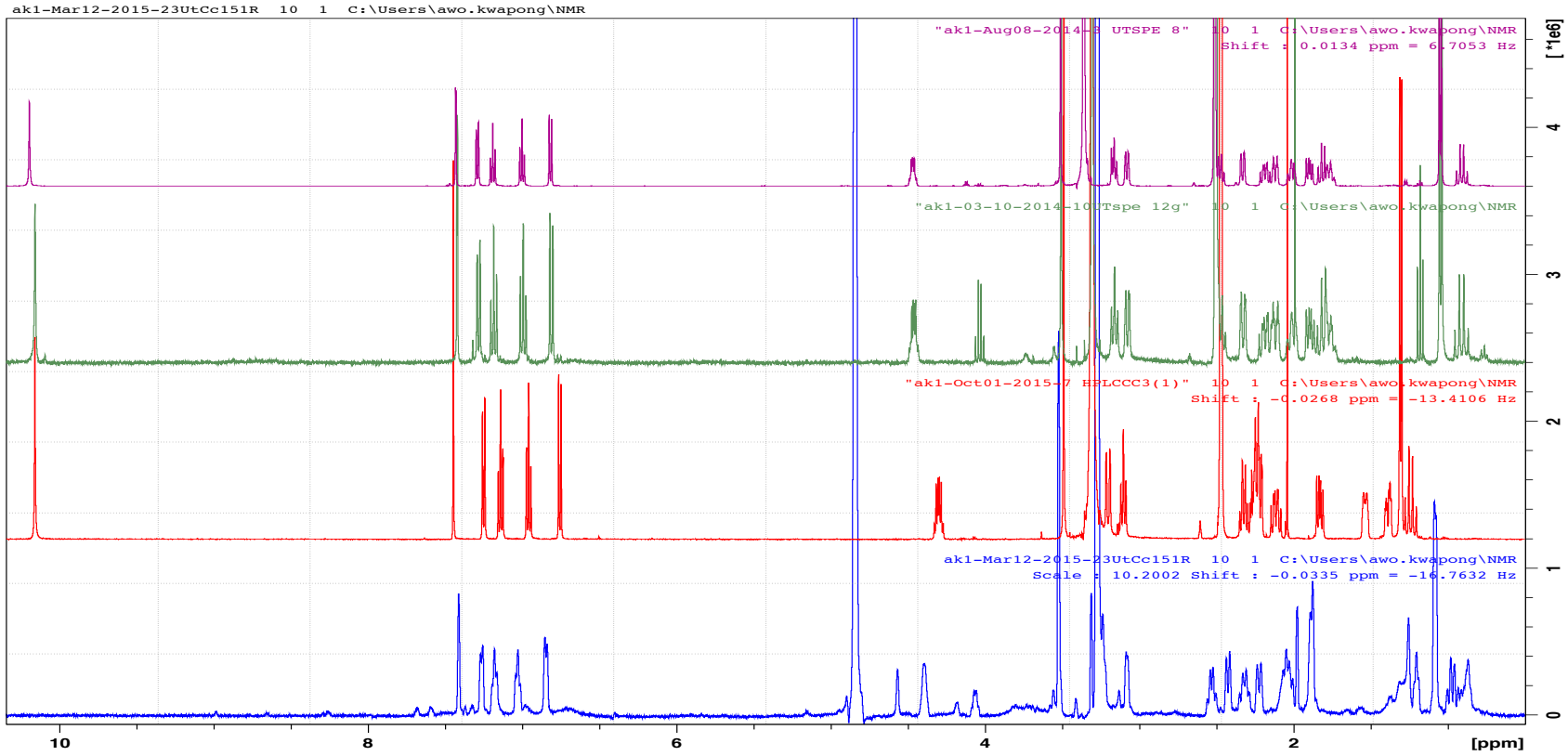

Figure 3.47 ^{1}H NMR spectrum for the isolated alkaloids (**AK-11** (purple spectrum), **AK-12** (green spectrum), **AK-13** (red spectrum) and **AK-14** (blue spectrum)), 500 MHz, **AK-11** to **-13** were recorded in DMSO and **AK-14** was recorded in CD_3OD

3.2.7.1 Characterisation of the isolated oxindole alkaloids

The NMR spectra and ESI-MS measurements for all four isolated compounds (**AK-11**, **AK-12**, **AK-13** and **AK-14**) were similar but the analytical TLC of the compounds showed different R*f* values; **AK-11** (0.56), **AK-12** (0.54), **AK-13** (0.75) and **AK-14** (0.39) in ethyl acetate: hexane: methanol, 9:1:1, v/v (Figures 3.46 and 3.47, supporting information). This indicated that they might be stereoisomers. A careful inspection of their NMR spectra revealed the presence of five rings and five chiral centers; C-3, C-7, C-15, C-20 and C-19 for all four compounds and Figure 3.48 shows core structure.

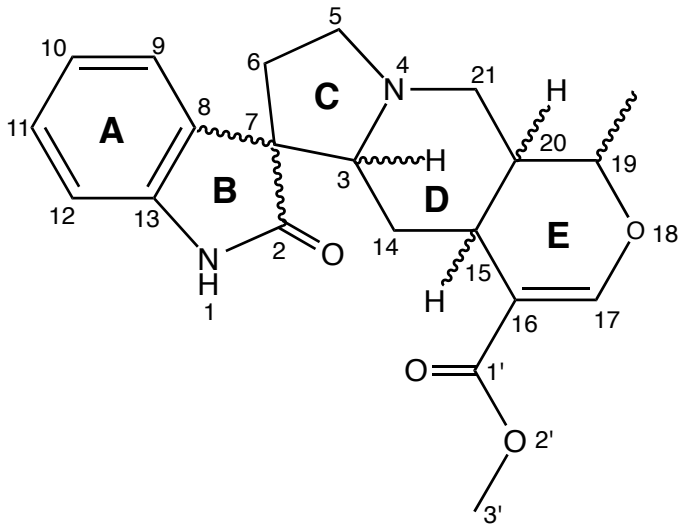

Figure 3.48 The core structure for the isolated oxindole alkaloids (**AK-11** to **-14**)

AK-11 was isolated as white needle-like crystals. The ESI-MS gave an $[M+H]^+$ ion at *m/z* 369.3, which indicated that its molecular formula was $C_{21}H_{24}N_2O_4$. The ^1H NMR spectrum revealed six proton signals in the low field region; five of them (δ_H 10.18 (s, H-1), δ_H 7.27 (d, *J* = 7.5 Hz, H-9), δ_H 6.97 (t, *J* = 7.5 Hz, H-10), δ_H 7.16 (t, *J* = 7.5 Hz, H-11), δ_H 6.79 (d, *J* = 8.0 Hz, H-12) accounted for all the positions on the oxindole nucleus (ring A and B) and the remaining one at δ_H 7.41 (s, *J* = 1.5Hz, H-17) was due to the olefinic hydrogen (ring E). H-9,

showed a ^{3}J correlation to the aromatic carbon C-11 (δ_C 127.2) and aromatic quaternary carbon C-13 (δ_C 141.9). H-10 *ortho* coupled to both H-9 and H-11 and showed a ^{3}J correlation to aromatic carbon C-12 (δ_C 108.8). H-11 *ortho* coupled to H-12, which in turn showed a $^{4}J_{HH}$ coupling to H-1. H-1 in turn showed a ^{2}J correlation to C-13. This then confirmed the structural assignment of the protons on the oxindole nucleus. The presence of a carbonyl group (C-2, δ_C 179.7) on ring B was revealed by the HMBC correlations of H-1, H_2-6 (2H, δ_H 1.86 and 2.15), H-3 (δ_H 2.30, dd, J = 9.0, 2.0 Hz) and H-14$_a$ (δ_H 2.09, d, J = 12.0, 3.0 Hz) to the carbonyl carbon (C-2). The IR absorption band at 1621.12 cm^{-1} confirmed the presence of the amide functional group in the structure. The HMBC correlations of the germinal protons; H-5$_a$ (δ_H 2.43, q, J = 9.0 Hz) to C-21 (δ_C 52.9), H-5$_b$ (δ_H 3.13, dd, J = 8.5, 1.5 Hz) to the spiro carbon C-7 (δ_C 54.8) and C-3 (δ_C 73.2), H-21$_a$ (δ_H 1.77, q, J = 10.5 Hz) to C-5 (δ_C 53.5), and C-20 (δ_C 40.3), H-21$_b$ (δ_H 3.05, dd, J = 7.5, 2.5 Hz) to C-15 (δ_C 29.7) and C-3 (δ_C 73.2), and the methine proton H-3 to C-8 (δ_C 133.8) and C-2 (δ_C 179.7), together with their chemical shifts indicated that the two methylenes and the methine were closely located near an electronegative atom, nitrogen at positions 3, 5 and 21. HMBC

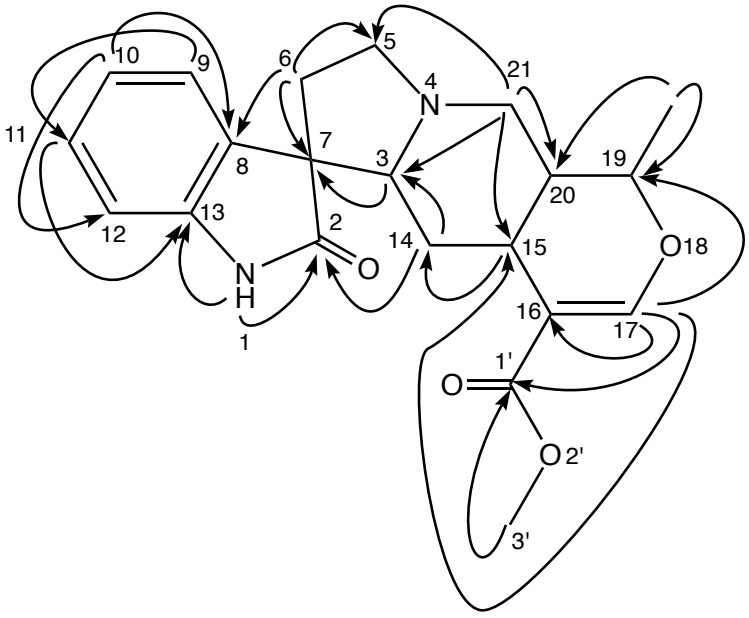

Figure 3.49 Selected HMBC correlations for **AK-11**

correlations of the methylene protons; H-6_a (δ_H 2.15, q, J = 8.5, 1.5 Hz) to C-7, H-6_b (δ_H 1.86, dd, J = 10.0, 7.5 Hz) to C-5 and C-8 and the coupling between H-6 and H-5, confirmed their position on the cyclic ring C. The ^3J correlation of methylene proton H-14_b (δ_H 0.86, q, J = 11.5 Hz) to C-3 and the coupling to H-15 (δ_H 1.98, t, J = 1.98 Hz), confirmed its position on the cyclic ring D. H-15 in turn coupled to H-20 (δ_H 1.71, q, J = 11.0 Hz), which suggested the methine carbon (C-20, δ_C 40.3) was the link between rings D and E. This was confirmed by the HMBC correlations of methylene hydrogen (H-21_a) and methyl hydrogens (δ_H 1.03, d, J = 7.0 Hz) to C-20, which bears H-20. The methyl hydrogens also showed a ^2J correlation to the oxygenated carbon (C-19, δ_C 73.3), to which this methyl group was directly attached (Figure 3.49). The olefinic hydrogen, H-17, showed HMBC correlations to the cyclic carbon C-15 (δ_C 29.7), cyclic quaternary carbon C-16 (δ_C 106.6), C-19 (δ_C 73.3) and carbonyl carbon C-1' (δ_C 166.1), this confirmed its placement on ring E. The methoxyl hydrogens (δ_H 3.50, H_3-3') showed a ^3J correlation to the carbonyl carbon, C-1' to which this methoxyl group was directly attached. The strong IR absorption bands at 1723.27 cm^{-1} (the ester carbonyl) and 1293.11 cm^{-1} (the cyclic ether) confirmed the presences of the functional group on the ring E. The NMR assignment of the other alkaloids (**AK-12**, **AK-13** and **AK-14**) was performed by essentially the same procedure. Full structural assignment of all ^1H and ^{13}C resonances was achieved by analyses of the 2- dimensional NMR spectra data as shown in Table 3.12.

A careful inspection of the ^1H and COSY NMR spectra of **AK-11** showed some key vicinal couplings ($^3J_{HH}$); an axial-axial coupling between H-15 (J = 9.0 Hz) and H-20 (J = 10.5, 2.5 Hz), a J_{ae} coupling between H-20 and the germinal proton H-21b (J = 2.5 Hz) and a J_{ae} coupling between H-3 (J = 2.5 Hz) and H-14a (J = 3.0 Hz). The NOESY spectrum revealed, cross peaks between H-15 and the methyl hydrogens (δ_H 1.03) and between H-20 and H-19. Based on the NOESY data, the coupling constants and by comparison with literature reports (Shamma *et al.*, 1967; Seki *et al.*, 1993; Muhammad *et al.*, 2001), **AK-11** was identified as isomitraphylline (Figure 3.50). The full NMR spectra of **AK-11** are shown in Figures 2.7 to 2.13 of the materials and methods chapter.

Table 3.12 ^{1}H (coupling constants, Hz) and ^{13}C NMR spectral data (ppm) and HMBC correlations of **AK-11**, recorded in DMSO-d_6

Position	^{1}H	^{13}C	^{2}J	^{3}J	^{4}J	^{13}C Seki *et al.*, 1993 ($CDCl_3$, 125 MHz)
1	10.18 s	-	C2, C13	C7, C8		-
2	-	179.7				180.7
3	2.30 dd (9.0, 2.5)	73.7	C7	C8		71.8
4	-	-				-
5a, b	2.43 q (9.0), 3.13 dd (8.5, 4.5)	53.5		C3, C7, C21		53.4
6a, b	2.15 q (8.5, 1.5) 1.86 dd (10.0, 7.5)	34.4	C5, C7	C2, C8		35.4
7	-	54.8				56.3
8	-	133.8				133.8
9	7.27 d (7.5)	123.1		C7, C11, C13		124.9
10	6.97 t (7.5)	121.6		C8, C12		122.4
11	7.16 t (7.5)	127.7		C9, C13		127.5
12	6.79 d (8.0)	108.8		C8, C10		109.3
13	-	141.9				139.9
14a, b	2.09 dd (12.0, 3.0), 0.86 q (11.5)	28.0	C3	C7	C2	29.1
15	1.98 t (9.0)	29.7				30.0
16	-	106.6				107.3
17	7.41 s (1.5)	153.6	C16	C1', C15, C19		153.8
18	-	-				-
19	4.43 m (3.9)	73.3				74.0
20	1.71 q (10.5, 2.5)	40.3				40.9
21a, b	1.77 q (10.5), 3.05 dd (7.5, 2.5)	52.9	C20	C3, C5, C15		54.3
1'	-	166.1				167.0
2'	-	-				-
3' (-OCH_3)	3.50 s	50.6		C1'		50.7
-CH_3	1.03 d (7.0)	14.7	C19	C20		14.8

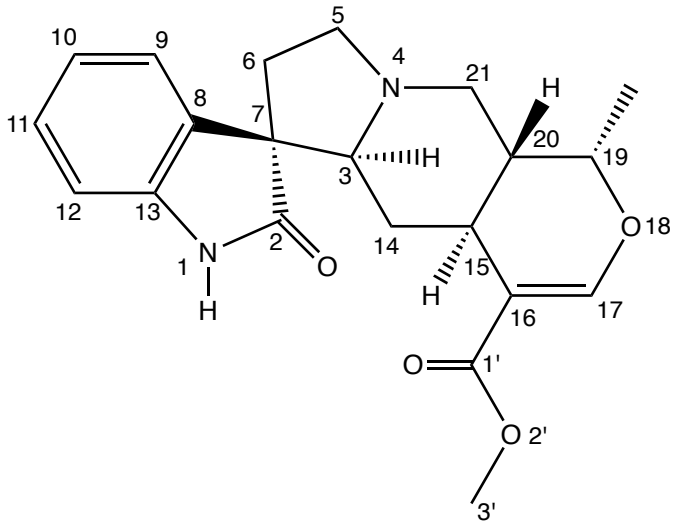

Isomitraphylline

Figure 3.50 Structure for **AK-11**

Inspection of the ^{1}H and COSY NMR spectra of **AK-12** showed some key vicinal couplings ($^{3}J_{HH}$); an axial-axial coupling between H-15 (J = 14.5, 10.0 Hz) and H-20 (J = 13.5, 4.5 Hz), J_{aa} couplings between the germinal proton H-14b (J = 14.0 Hz) and H-15, H-3 (J = 14.0, 2.5 Hz), J_{ae} coupling between H-3 and the germinal proton H-14a (J = 11.5, 3.5 Hz) and J_{ae} coupling between H-20 and H-19 (J = 4.0 Hz). The NOESY spectrum revealed, cross peaks between H-3 and H-15 and between H-21 and H-19. Based on the NOESY data, the coupling constants and by comparison with literature reports (Shamma *et al.*, 1967; Seki *et al.*, 1993; Muhammad *et al.*, 2001), **AK-12** was identified as mitraphylline (Figure 3.51).

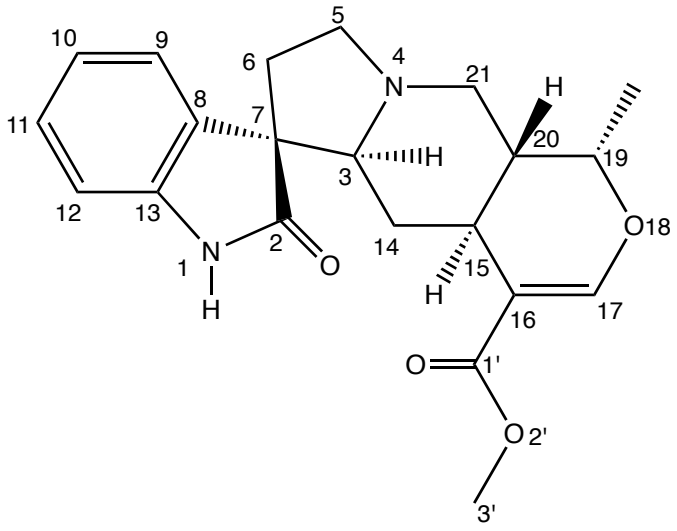

Mitraphylline

Figure 3.51 Structure for **AK-12**

Inspection of the ^{1}H and COSY NMR spectra of **AK-14** showed some key vicinal couplings ($^{3}J_{HH}$); an axial-equatorial coupling between H-15 (J = 6.5 Hz) and H-20 (J = 6.5 Hz), and a J_{aa} coupling between H-3 (J = 11.5 Hz) and the germinal proton H-14a (J = 11.5, Hz). The NOESY spectrum revealed, cross peaks between H-3 and H-14b and between H-15 and H-20. Based on the NOESY data, the coupling constants and by comparison with literature reports (Shamma *et al.*, 1967; Seki *et al.*, 1993; Muhammad *et al.*, 2001), **AK-14** was identified as speciophylline (Uncarine D, Figure 3.52).

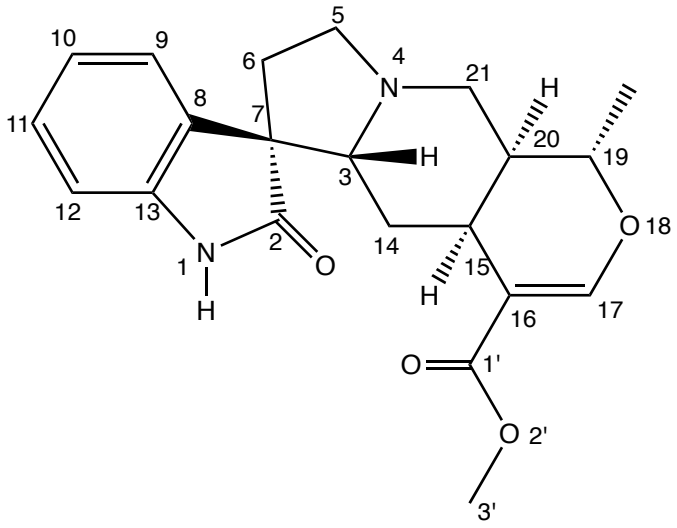

Speciophylline

Figure 3.52 Structure for **AK-14**

For **AK-13**, it was difficult to determine its stereochemistry using the NMR data obtained because of the severely overlapped proton signals at δ_H 2.23 (q, *J* = 12.0, 9.5 Hz). This signal integrated for 3 protons (H-3, H-15 and H-21a) and coupled to four protons at H-14a (*J* = 11.5 Hz), H-14b (*J* = 12.0 Hz), H-20 (*J* = 9.5, 4.5 Hz) and H-21b (*J* = 10.5, 1.0 Hz). The NOESY spectrum also revealed, a cross peak between the signal at δ_H 2.23 and H-9 (*J* = 7.0 Hz). This led to an inconclusive decision on the stereochemistry of **AK-13,** although we suspect it to be a formasonine (Uncarine B, Figure 3.53), based on the NOESY data, the coupling constants and by comparison with literature reports (Shamma *et al.*, 1967; Seki *et al.*, 1993; Muhammad *et al.*, 2001).

The ^{1}H and ^{13}C NMR data, and NOESY spectrum of the isolated oxindole alkaloids are shown in Section 3.2.8.5 and at the appendix section, respectively.

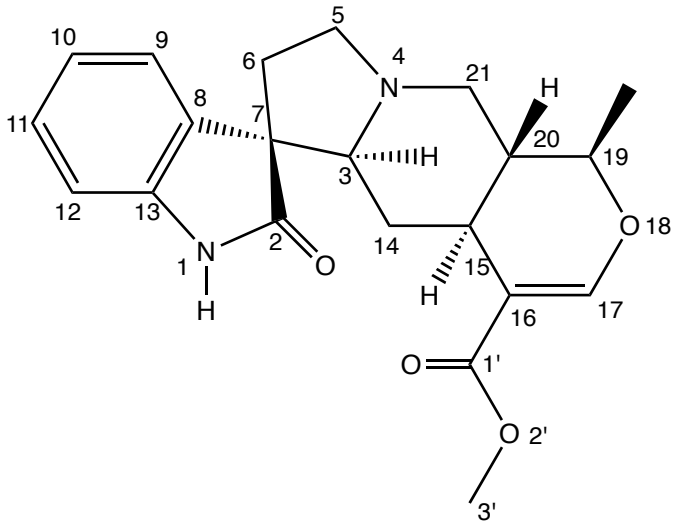

Formosanine

Figure 3.53 Tentative structure for **AK-13**

3.2.8 Isolation from *M. lowiana*

Powdered *M. lowiana* stem bark (592 g) was successively extracted with hexane, chloroform and methanol; this gave a yield of 0.7%, 1.1% and 2.2%, respectively. The hexane extract (**AK-17**) was extracted as a pure compound (an amide), which was identified by its ^{1}H NMR spectrum (Figure 3.62) and TLC run (R*f* value: 0.7, methanol: water (9:1, v/v). The methanol extract was subjected to reverse phase SPE, which yielded two compounds, **AK-15** (a flavone) and **AK-16** (an amide). **AK-15** (41.6 mg) was eluted with 60% methanol in water. **AK-16** (24.1mg) was eluted with methanol and water (9:1, v/v). A lignan compound, **AK-18** (15.3 mg) was isolated from the chloroform extract. It was obtained as a granular residue from the concentrated chloroform extract. The isolated granular residue was later washed in methanol to obtain the pure compound.

3.2.8.1 Characterisation of AK-15 as 4', 7-dihydroxy-5-methoxyflavone

AK-15 was isolated as a yellow solid. The accurate mass measurement gave an $[M-H]^-$ ion at *m/z* 283.0616 which indicated that its molecular formula was $C_{16}H_{12}O_5$. The ^1H NMR resonance pattern of this compound was indicative of a flavone (Brown, 1980).

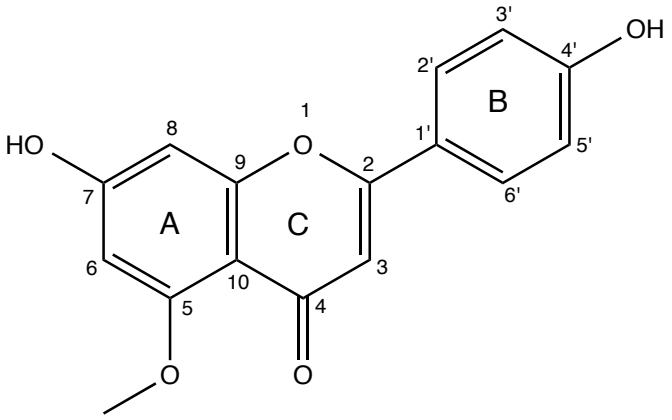

Figure 3.54 Structure for **AK-15**

The ^1H NMR spectrum revealed the presence of two aromatic singlets, δ_H 6.22 (*J* = 2.0 Hz, H-6) and δ_H 6.34 (*J* = 2.5 Hz H-8) on the aromatic ring A. The positioning of the methoxyl group (δ_C 55.8, δ_H 3.78) on this ring was confirmed by a ^3J correlation of the methoxyl hydrogens to the aromatic quaternary carbon (C-5, δ_C 163.0). This was also supported by the ^2J correlation of the aromatic singlet H-6 to C-5. The placement of the hydroxyl group on the aromatic ring A was revealed by the ^2J correlation of the hydroxyl hyrogen (δ_H 8.13) to the aromatic quaternary carbon (C-7, δ_C 163.9) and confirmed by the ^2J correlation of H-6 to C-7. The heterocyclic ring C was directly attached to the ring A at positions C-9 (δ_C 159.8) and C-10 (δ_C 106.3). This was confirmed by the ^2J correlation of H-8 to C-9 and the ^3J correlation of H-3 (δ_H 6.49) to C-10. H-3 also correlated to the carbonyl carbon (C-4, δ_C 159.8) and the aromatic quaternary carbon (C-2, δ_C 123.4), which confirmed the placement of these carbons (C-4 and C-2) on the heterocyclic ring C. The aromatic ring B was revealed as an AA'BB' spin system in the ^1H NMR spectrum, with two doublets (δ_H 7.36, H-2', -6' and

δ_H 6.83, H-3', -5') integrating for two protons each, with a strong *ortho* coupling (J = 8.5 Hz) of the protons. This spin system was well supported by the *para* positioning of the hydroxyl group (δ_H 8.06) to the C-1' (δ_C 124.8) - (C-2 δ_C 123.4) linkage on ring B, which was revealed by HMBC correlations as shown in Figure 3.55. Full assignment of the all ^{1}H and ^{13}C resonances was achieved by analyses of the 2-dimensional NMR spectra. The summary of this data is shown in Table 3.13 and the HMBC spectrum is shown in Figure 3.56. **AK-15** was therefore assigned as 7-hydroxy-2-(4-hydroxyphenyl)-5-methoxy-4H- chromen-4-one or 4',7-dihydroxy-5-methoxyflavone. This compound is also known as thevetiaflavone. The ^{1}H

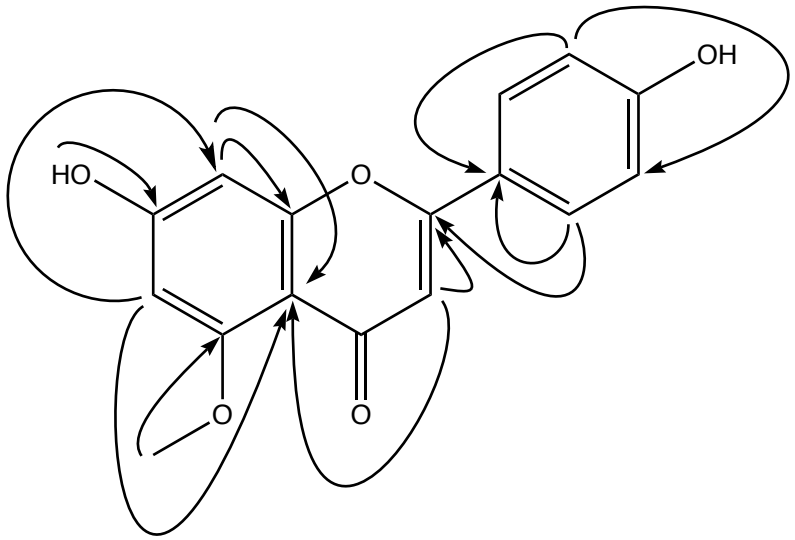

Figure 3.55 Selected HMBC correlations for **AK-15**

and ^{13}C NMR data of this compound are in good agreement with published literature (Aurnhammer *et al.*, 1971; Mbouangouerea *et al.*, 2007). This compound had previously been reported for in *Thevetia peruviana*, *Piptadenia africana*, *Capparis spinosa* and *Brucea javanica* (Aurnhammer *et al.*, 1971; Mbouangouerea *et al.*, 2007; Zhou *et al.*, 2010; Zhao *et al.*, 2011).

Table 3.13 ^{1}H (coupling constants, Hz) and ^{13}C NMR spectral data (ppm) and HMBC correlations of **AK-15**, recorded in methanol-d_4

Position	^{1}H	^{13}C	^{2}J	^{3}J	^{13}C Mbouangouerea *et al.*, 2007 ($CDCl_3$, 100 MHz)
2	-	162.6			163.8
3	6.49 s	103.2	C2	C10	115.8
4	-	166.0			182.4
5	-	163.0			163.0
6	6.22 s (2)	100.2	C5, C7	C8, C10	115.6
7	-	163.9			160.6
8	6.34 s (2.5)	94.8	C7, C9	C6, C10	115.8
9	-	159.8			164.5
10	-	106.3			128.1
-OCH_3	3.78 s	55.8		C5	53.2
-OH	8.13 s		C7		
1’	-	124.8			122.3
2’	7.36 d (8.5)	131.4	C1’	C2, C6’, C4’	99.1
3’	6.83 d (8.5)	116.3	C4’	C1’, C5’	103.2
4’	-	158.9			160.6
5’	6.83 d (8.5)	116.3	C4’	C1’, C3’	104.4
6’	7.36 d (8.5)	131.4	C1’	C2, C2’, C4’	99.1
-OH	8.06 s	-	C4’		

Multiplicities of proton signals: s – singlet and d - doublet

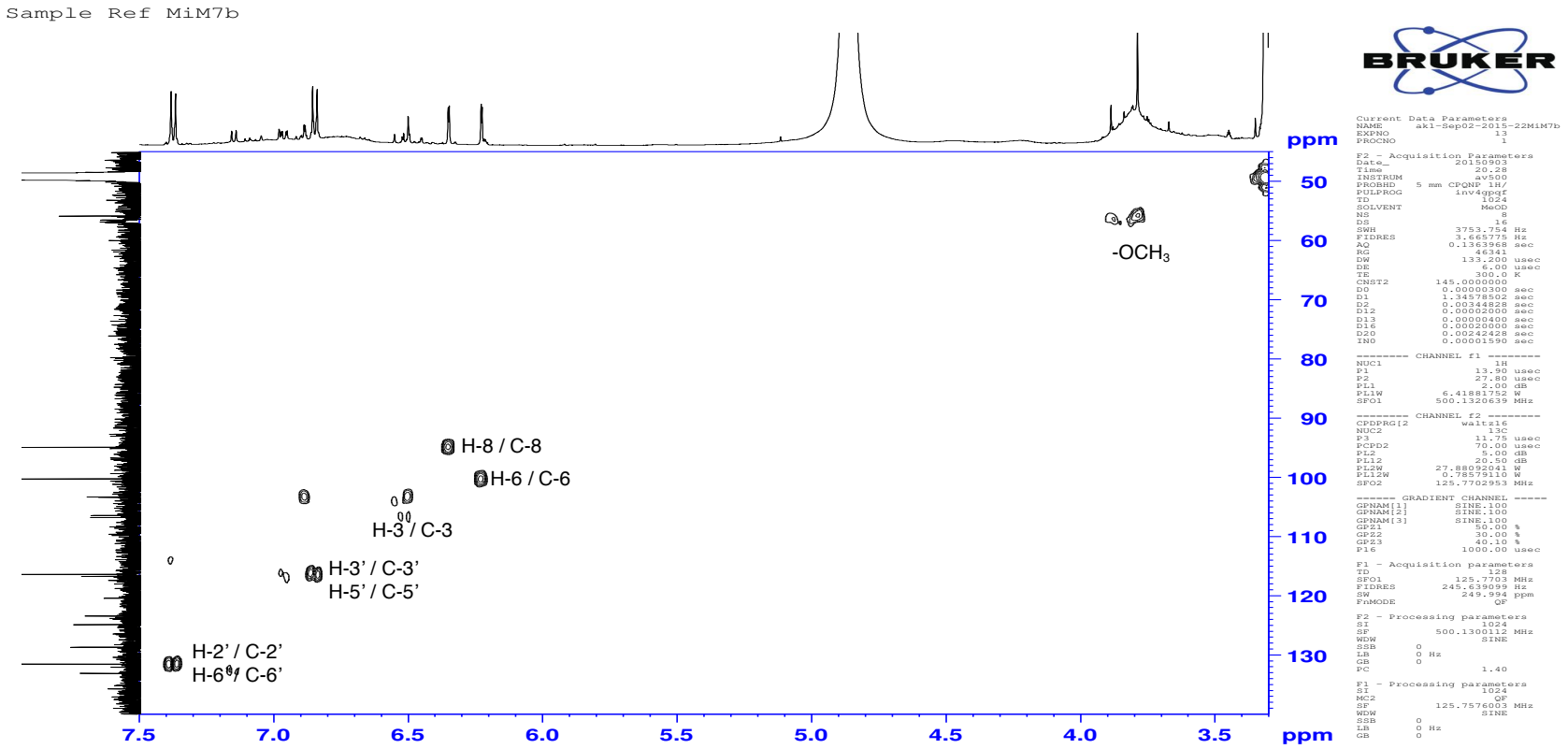

Figure 3.56 HMQC NMR spectrum for **AK-15**, recorded in CD_3OD, 500 MHz

3.2.8.2 Characterisation of AK-16 as 9-oxo-9-((3-phenylpropyl)amino)nonanoic acid

AK-16 was isolated as a brown solid. The HRTOFESIMS measurement gave an $[(M-H)-CO_2H]^-$ ion at *m/z* 261.185, which indicated that its molecular formula was $C_{18}H_{27}NO_3$.

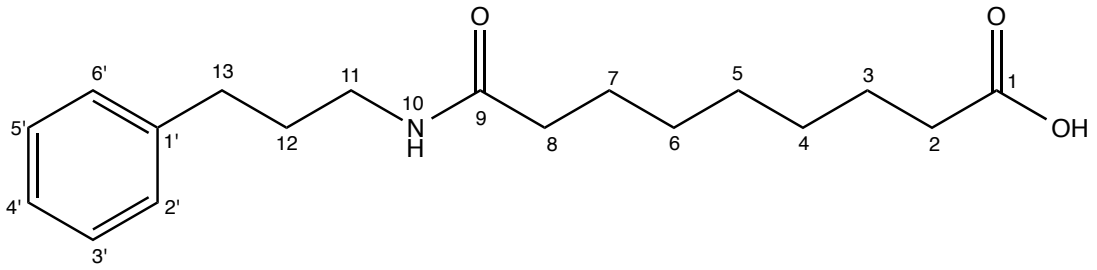

Figure 3.57 Structure for **AK-16**

The ^{1}H NMR spectrum revealed five aromatic hydrogens (δ_H 7.14 (d, H-2', -6'), δ_H 7.21 (t, H-3', -5') and δ_H 7.11(t, H-4')) and twenty methylene hydrogens (δ_H 1.29 (12H), δ_H 1.57 (4H), δ_H 2.25 (1H), δ_H 2.29 (1H) and δ_H 2.25 (2H)), which accounted for all the hydrogen positions on the 9-oxo-9-(propylamino)nonanoic acid chain. Its IR spectrum showed a strong absorption band at 1706.68 cm^{-1} and 3348.28 cm^{-1}, which confirmed the presence of the amide and the carboxylic acid functional groups, respectively. The aromatic ring of **AK-16** was assigned based on the HMBC correlations of the aromatic hydrogens to the aromatic carbons; H-2' to C-3' (δ_C 129.3), C-4' (δ_C 126.7), C-6' (δ_C 129.4), H-3' to C-1' (δ_C 144.0), C-5' (δ_C 129.3), H-4' to C-6', H-5' to C-6', C-1' and H-6' to C-5'. This structural assignment was well supported by the proton splitting pattern and integration observed in the ^{1}H NMR spectrum (Figure 3.58). The 9-oxo-9-(propylamino)nonanoic acid chain was assigned based on the HMQC and HMBC correlations as shown in Figure 3.60. The position of the amide carbonyl on the 9-oxo-9-(propylamino)nonanoic acid chain was revealed by a ^2J correlation of methylene hydrogen H-8 (δ_H 2.29) and a ^4J correlation of methylene hydrogens H-12 (δ_H 1.57) to its carbon C-9 (δ_C 176.2). H-12 also showed a ^3J correlation to the aromatic quaternary carbon C-1' (δ_C 144.0). This confirmed the placement of amide group, near the

phenyl moiety. The carboxylic group was positioned at the end of the chain, based on a ^{2}J correlation of the methylene hydrogen H-2 (δ_H 2.25) to carboxylic carbon C-1 (δ_C 177.8). H-2 also showed correlations to the carbons of the methylene envelope, which confirmed the placement of the carboxylic group. The phenyl moiety was linked onto the 9-oxo-9-(propylamino)nonanoic acid chain based on the HMBC correlations of the methylene hydrogens H-13 (δ_H 2.57) to the aromatic quaternary carbon C-1' and the aromatic carbons (C-2' and C-6'). Full structural assignment of all ^{1}H and ^{13}C resonances was achieved by analyses of the 2-dimensional NMR spectra data as shown in Table 3.14. **AK-16** was therefore assigned as 9-oxo-9-((3-phenylpropyl)amino)nonanoic acid. To our knowledge this is the first report of 9-oxo-9-((3-phenylpropyl)amino)nonanoic acid for *M. lowiana*.

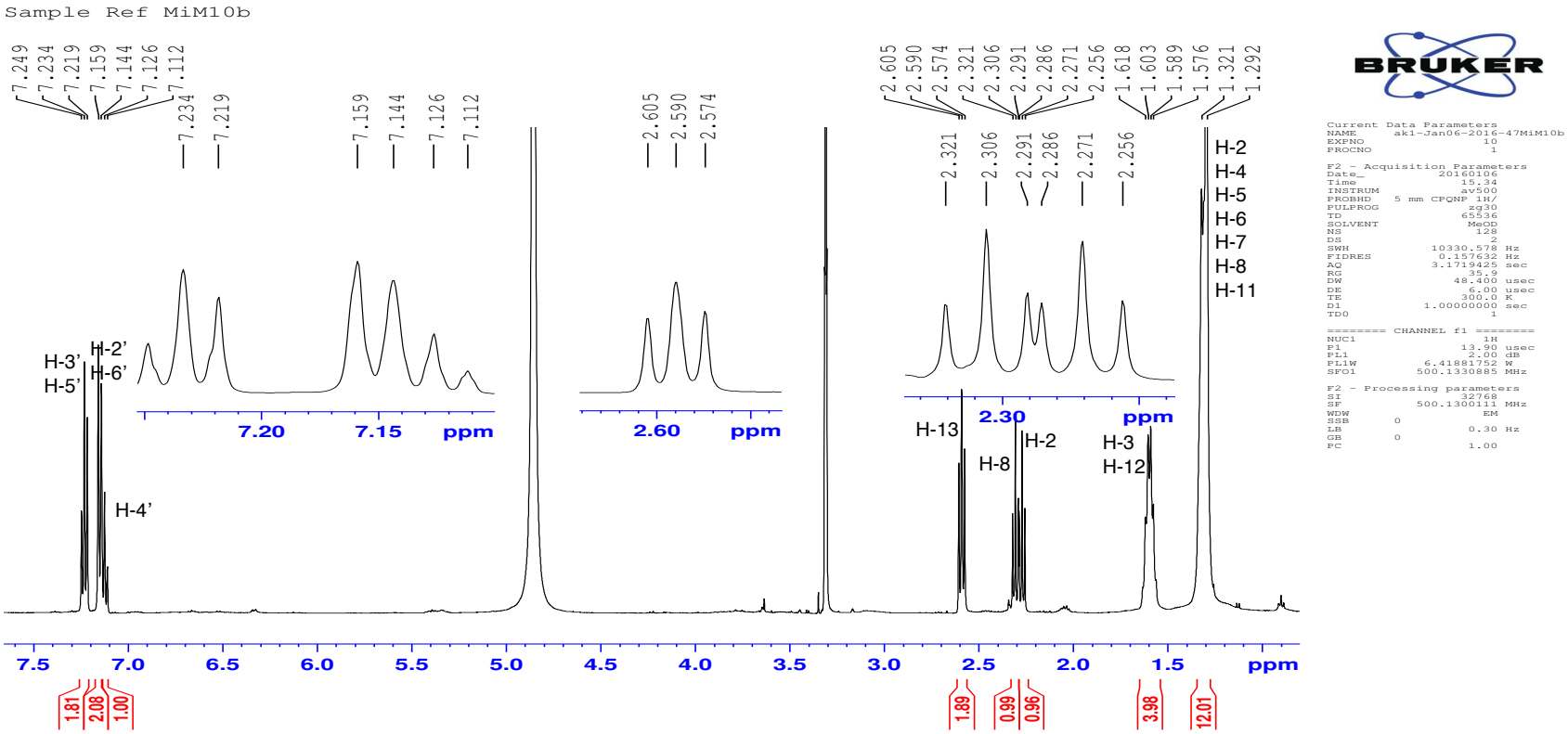

Figure 3.58 ^{1}H NMR spectrum for **AK-16**, recorded in CD_3OD, 500 MHz

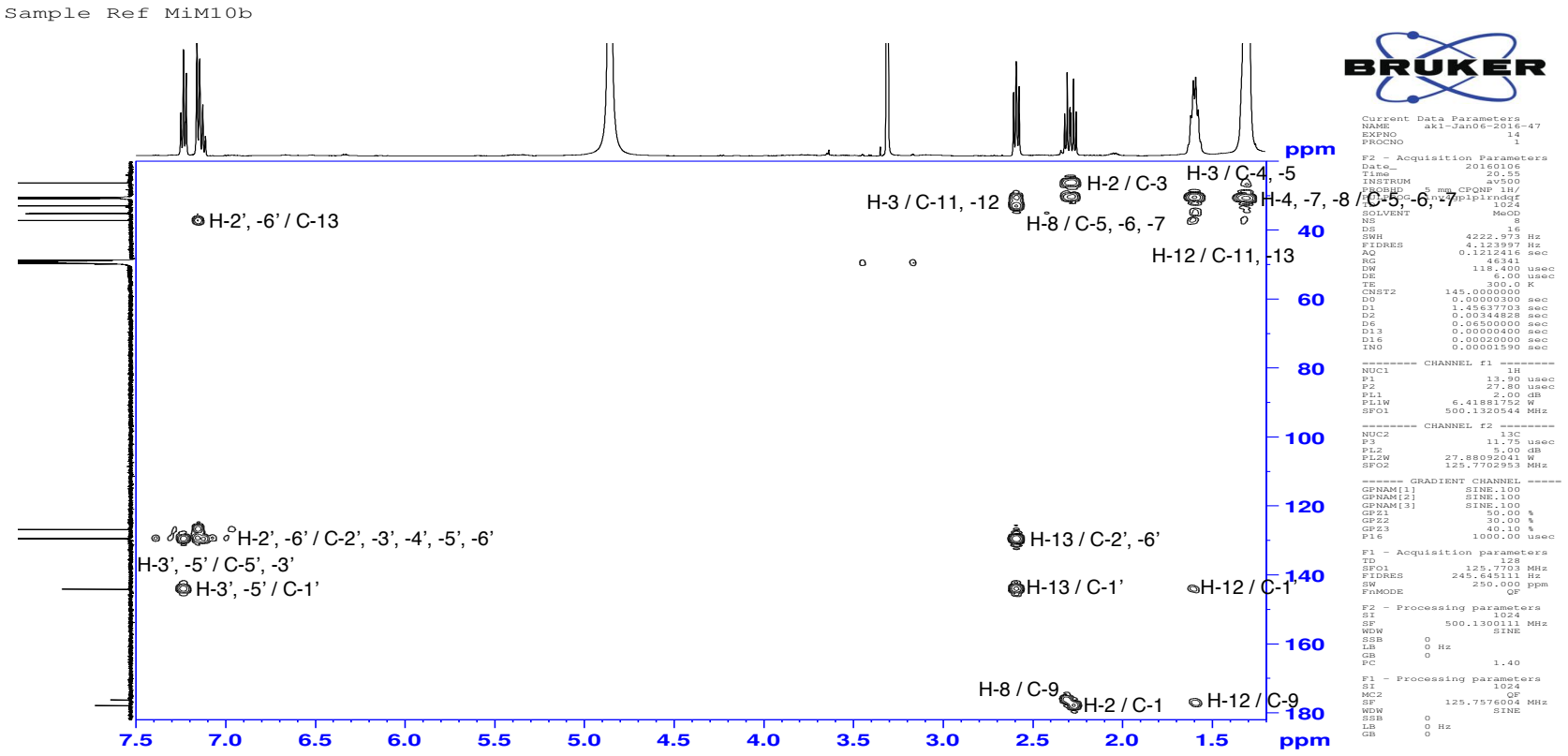

Figure 3.59 HMBC NMR spectrum for **AK-16**

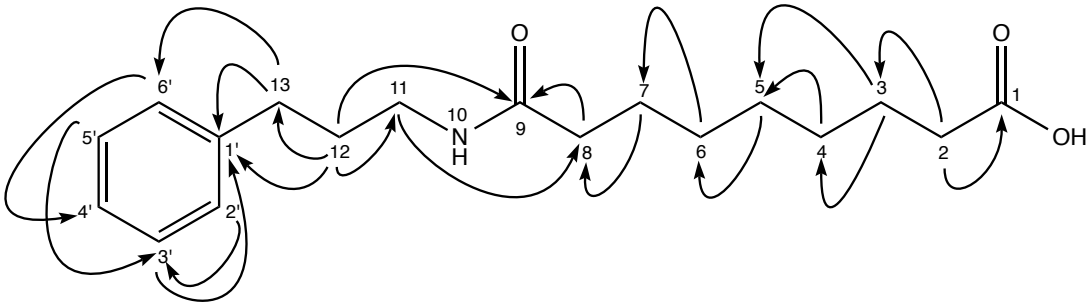

Figure 3.60 Selected HMBC correlations for **AK-16**

Table 3.14 ^{1}H (coupling constants, Hz) and ^{13}C NMR spectral data (ppm) and HMBC correlations of **AK-16**, recorded in methanol-d_4

Position	^{1}H	^{13}C	^{2}J	^{3}J	^{4}J
1 (COOH)	-	177.8			
2	2.25 t, 1.29	35.0	C1, C3		
3	1.57 q	26.1	C2, C4	C5	
4	1.29	30.4	C3, C5	C6	
5	1.29	30.6	C4, C6	C3	
6	1.29	30.7	C5, C7	C4	
7	1.29	30.2	C6, C8	C5	
8	2.29 t, 1.29	34.9	C9, C7		
9 (C=O)	-	176.2			
10 (N-H)	-	-			
11	1.29	30.6			C8
12	1.57 q	32.8	C11, C13	C1’	C9
13	2.57	37.0	C12, C1’	C2’, C6’, C11	
1’	-	144.0			
2’	7.14 d (7.5)	129.4	C3’	C4’, C6’, C13	
3’	7.21 t (7.5)	129.3	C2’	C1’, C5’	
4’	7.11 t (7.0)	126.7		C2’, C6’	
5’	7.21 t (7.5)	129.3	C6’	C1’, C3’	
6’	7.14 d (7.5)	129.4	C5’	C2’, C4’, C13	

Multiplicities of proton signals: d - doublet, t - triplet and q – quintet

3.2.8.3 Characterisation of AK-17 as 11-oxo-11-((3-phenylpropyl)amino)undecanoic acid

AK-17 was isolated as an olive green liquid. The HRTOFESIMS measurement gave an [(M-H)-CO_2H]$^-$ ion at *m/z* 287.2051, which indicated that its molecular formula was $C_{20}H_{31}NO_3$.

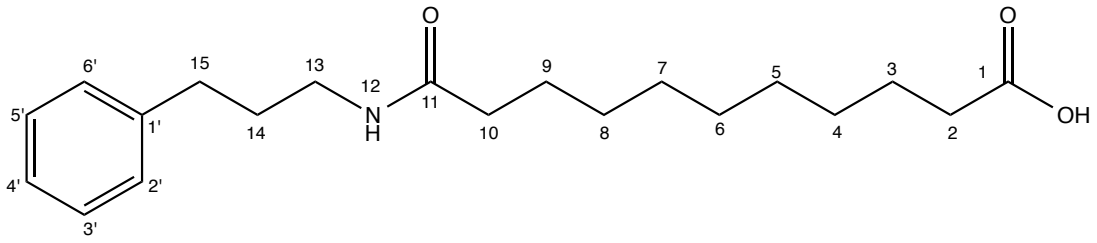

Figure 3.61 Structure for **AK-17**

The NMR spectrum for **AK-17** was similar to that of **AK-16**, suggesting that it has similar chemical structure. The difference between the two compounds was the presence of two extra methylenes (Figure 3.62). Based on this evidence and analyses of the HMQC, HMBC and COSY correlations (Figure 3.63 and Table 3.15, supporting information), the structure of **AK-17** was readily determined to be 11-oxo-11-((3-phenylpropyl)amino)undecanoic acid. To our knowledge this is the first report of 11-oxo-11-((3-phenylpropyl)amino)undecanoic acid for *M. lowiana*.

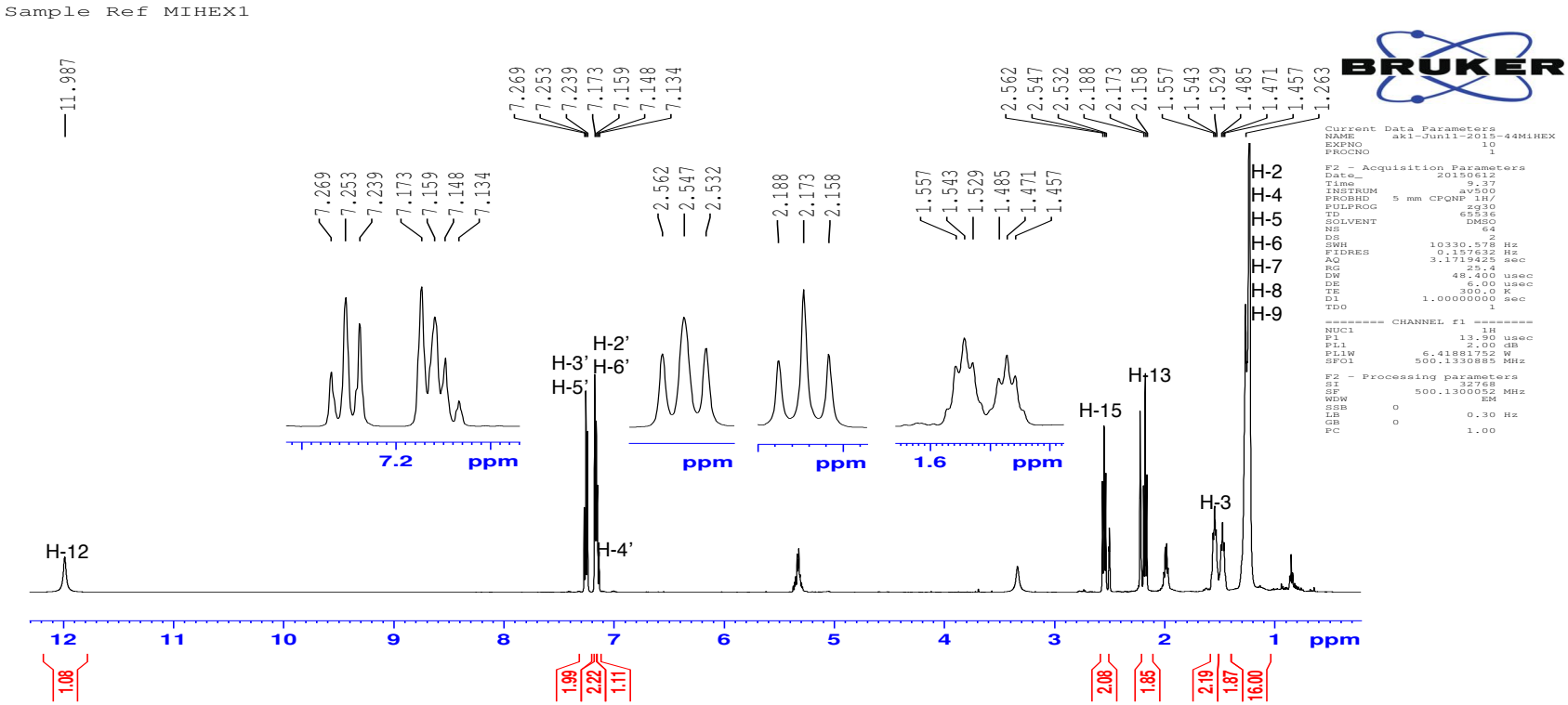

Figure 3.62 ^{1}H NMR spectrum for **AK-17**, recorded in DMSO, 500 MHz

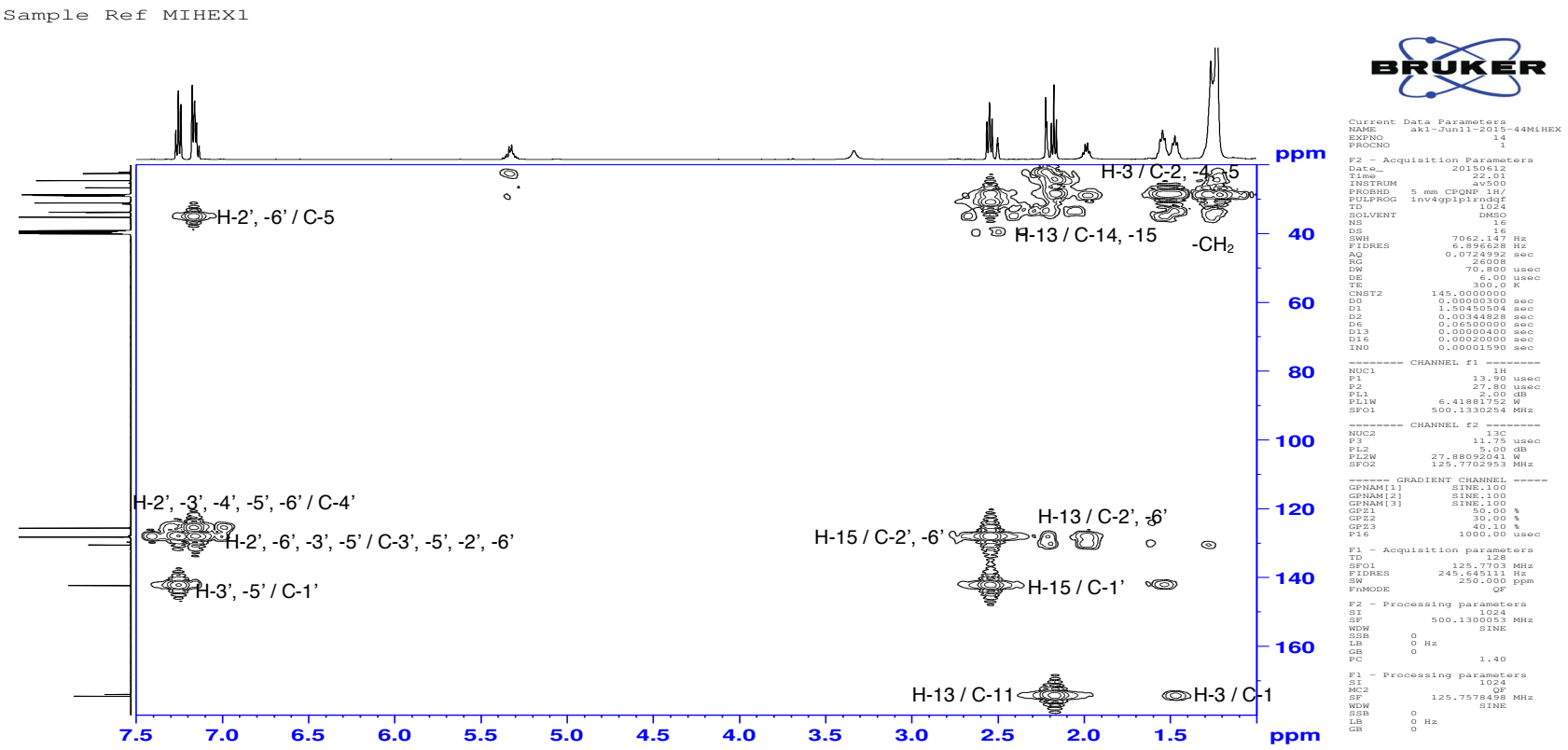

Figure 3.63 HMBC spectrum for **AK-17**

Table 3.15 ^{1}H (coupling constants, Hz) and ^{13}C NMR spectral data (ppm) and HMBC correlations of **AK-17**, recorded in DMSO-d_6

Position	^{1}H	^{13}C	^{2}J	^{3}J	^{4}J
1 (COOH)	-	174.4			
2	1.23	28.9	C3	C4	
3	1.45 dq (7.0)	24.4	C2, C4	C1	
4	1.23	28.6	C3, C5	C2	
5	1.23	28.7	C4, C6		
6	1.23	28.8	C5, C7		
7	1.23	28.8	C6, C8		
8	1.23	28.5	C7, C9		
9	1.23	28.9	C8, C10	C11	
10	1.23	28.8	C9, C11	C8	
11 (C=O)	-	173.9			
12 (N-H)	11.98	-			
13	2.15 t (7.5)	33.6		C11	C10
14	1.52 q (7.0)	31.0	C13	C1’	C11
15	2.53 t (7.5)	35.1	C1’, C14	C2’, C6’	
1’	-	142.2			
2’	7.15 d (7.0)	128.2	C3’	C4’	
3’	7.23 t (7.0)	128.1	C2’	C1’, C5’	
4’	7.13 t (7.0)	125.5			
5’	7.23 t (7.0)	128.1	C6’	C1’, C3’	
6’	7.15 d (7.0)	128.2	C5’	C4’, C15	

Multiplicities of proton signals: dq – doublet of quintet, t – triplet and q – quintet

3.2.8.4 Characterisation of AK-18 as 8-(4-hydroxy-3-methoxyphenyl)-3-methoxy-6,7-dimethyl-5,6,7,8-tetrahydronaphthalen-2-ol

AK-18 was isolated as pale yellow granules. The ESI-MS measurement gave an $[M-H]^-$ ion at *m/z* 327.1, which indicated that its molecular formula was $C_{20}H_{24}O_4$.

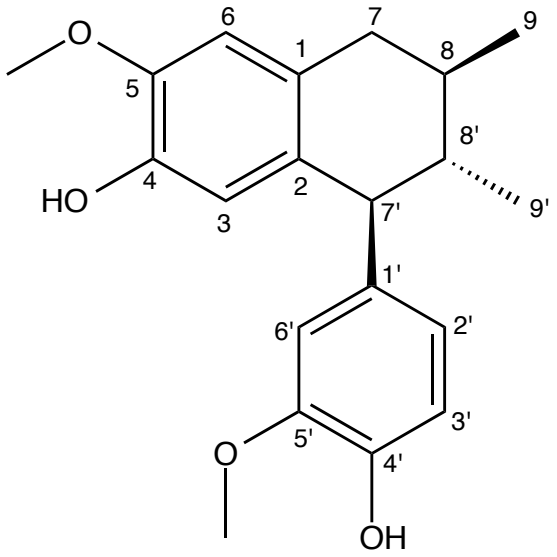

Figure 3.64 Structure for **AK-18**

The ^{1}H NMR spectrum (Figure 3.65) revealed a tri-substituted aromatic ring (δ_H 6.49 (dd, *J* = 8.0, 2.0 Hz, H-2'), δ_H 6.68 (d, *J* = 8.0 Hz, H-3') and δ_H 6.59 (s, *J* = 2.0 Hz, H-6')), a tetra-substituted aromatic ring (δ_H 6.01 (s, H-3) and δ_H 6.55 (s, H-6)), two methoxyl ((δc 55.4, δ_H 3.69) and (δc 55.6, δ_H 3.69)) and two hydroxyl groups (δ_H 8.41, δ_H 8.71). In addition, it revealed two methyl doublets (δ_H 1.01 (d, *J* = 6.0 Hz, H_3-9) and δ_H 0.77 (d, *J* = 6.0 Hz, H_3-9')), a methine doublet (δ_H 3.27, d, *J* = 10.0 Hz, H-7'), and a methine multiplet integrating for two protons (δ_H 1.46, H-8 and H-8'), as well as signals for the germinal protons of the methylene (δ_H 2.52, d, *J* = 11.0 Hz, H-7a and δ_H 2.64, dd, *J* = 16.5, 4.5 Hz, H-7b). These data suggested that **AK-18** was a 2,7'-cyclolignan derivative with two methoxyl and two hydroxyl groups. The 2,7'-cyclization and linkage to the aromatic rings was confirmed by the HMBC correlations of H_2-7 to C-1 and H-7' to C-1, C-2, C-1', C-2', C-6', C-8' and C-9', together with their chemical shifts (Figures 3.66, 3.68 and Table 3.16, supporting information). The methyl hydrogens placed on C-8 and C-8' of the phenyltetralin skeleton was revealed by the HMBC correlations of H_3-9 to C-7, C-8 and C-8', and H_3-9' to C-7', C-8' and C-8, which was confirmed by the COSY coupling between H_3-9 and H-8 and between

H_3-9' and H-8'. The HMBC correlations of the methoxyl hydrogens to C-5 (δ_C 145.5) and C-5' (δC 147.3), H-3 to C-1, C-5, C-7', H-6 to C-2, C-4, C-7, H-3' to C-1', C-4', C-5', H-6' to C-2', and C-6, together with their chemical shifts indicated that the two methoxyl and two hydroxyl groups were located at C-5, C-5', and, C-4 and C-4', respectively. In the NOESY spectrum, cross peaks between the methoxyl hydrogens and H-6, and between the methoxyl hydrogens and H-6', confirmed their placement on the aromatic rings (Figure 3.67). In addition, cross peaks between H-7 and H-6, H_3-9, between H-8' and H-6', H-2', between H-7' and H_3-9', and the hydroxyl hydrogens indicated that H-8' was trans-oriented to both H-7' and H-8 (Figure 3.67). Full structural assignment of all ^{1}H and ^{13}C resonances was achieved by analyses of the 2-dimensional NMR spectra data as shown in Table 3.16. **AK-18** was therefore assigned as 8-(4-hydroxy-3-methoxyphenyl)-3-methoxy-6,7-dimethyl-5,6,7,8-tetrahydronaphthalen-2-ol, which is commonly known as guaiacin. The ^{1}H and ^{13}C NMR data were in close agreement with published literature for guaiacin (Majumder *et al.*, 1972). Additionally, this compound has been reported for in *Myristica fragrans* and *Machilus wangchiana* (Yang *et al.*, 2008; Cheng *et al.*, 2009).

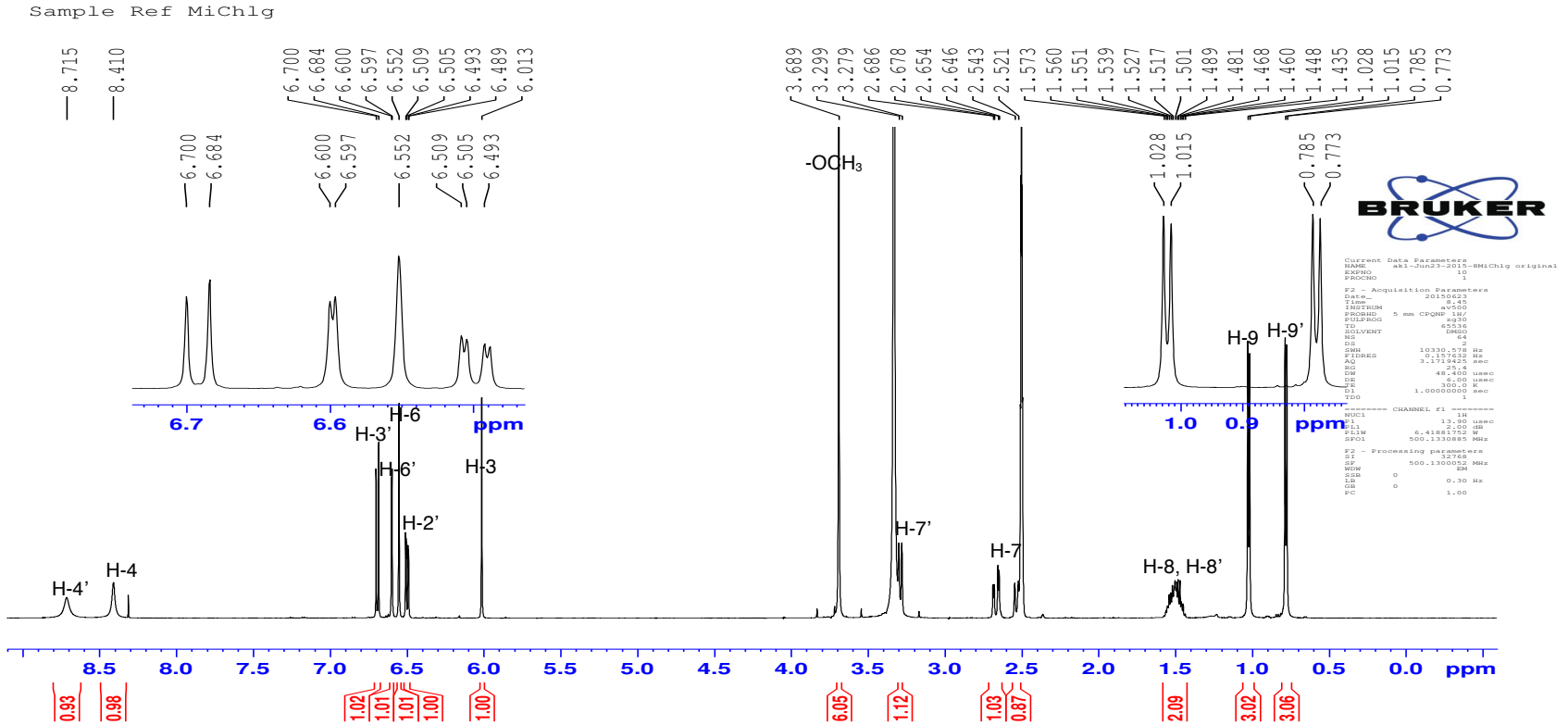

Figure 3.65 ^{1}H NMR spectrum for **AK-18**, recorded in DMSO, 500 MHz

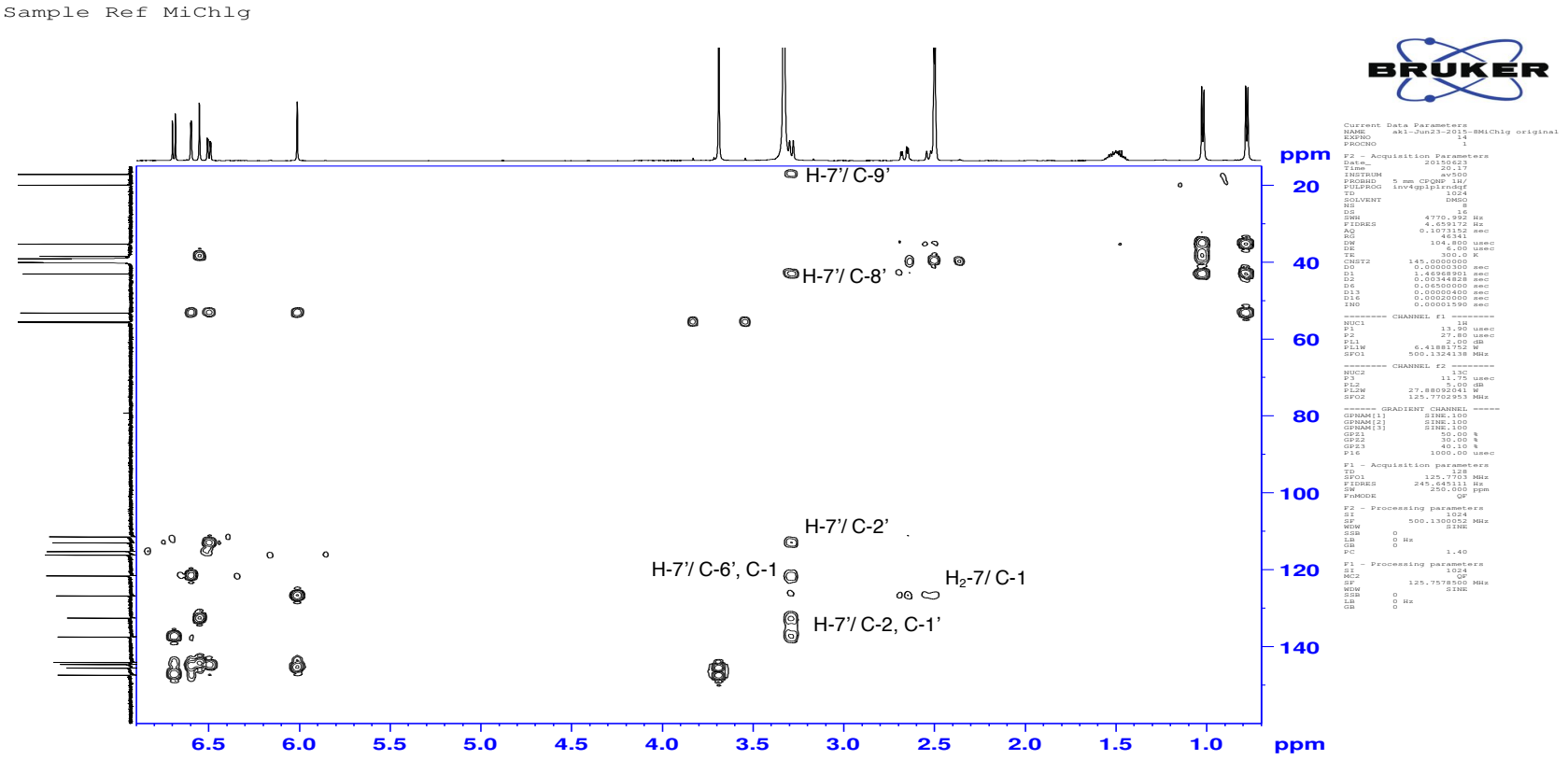

Figure 3.66 HMBC NMR spectrum for **AK-18**

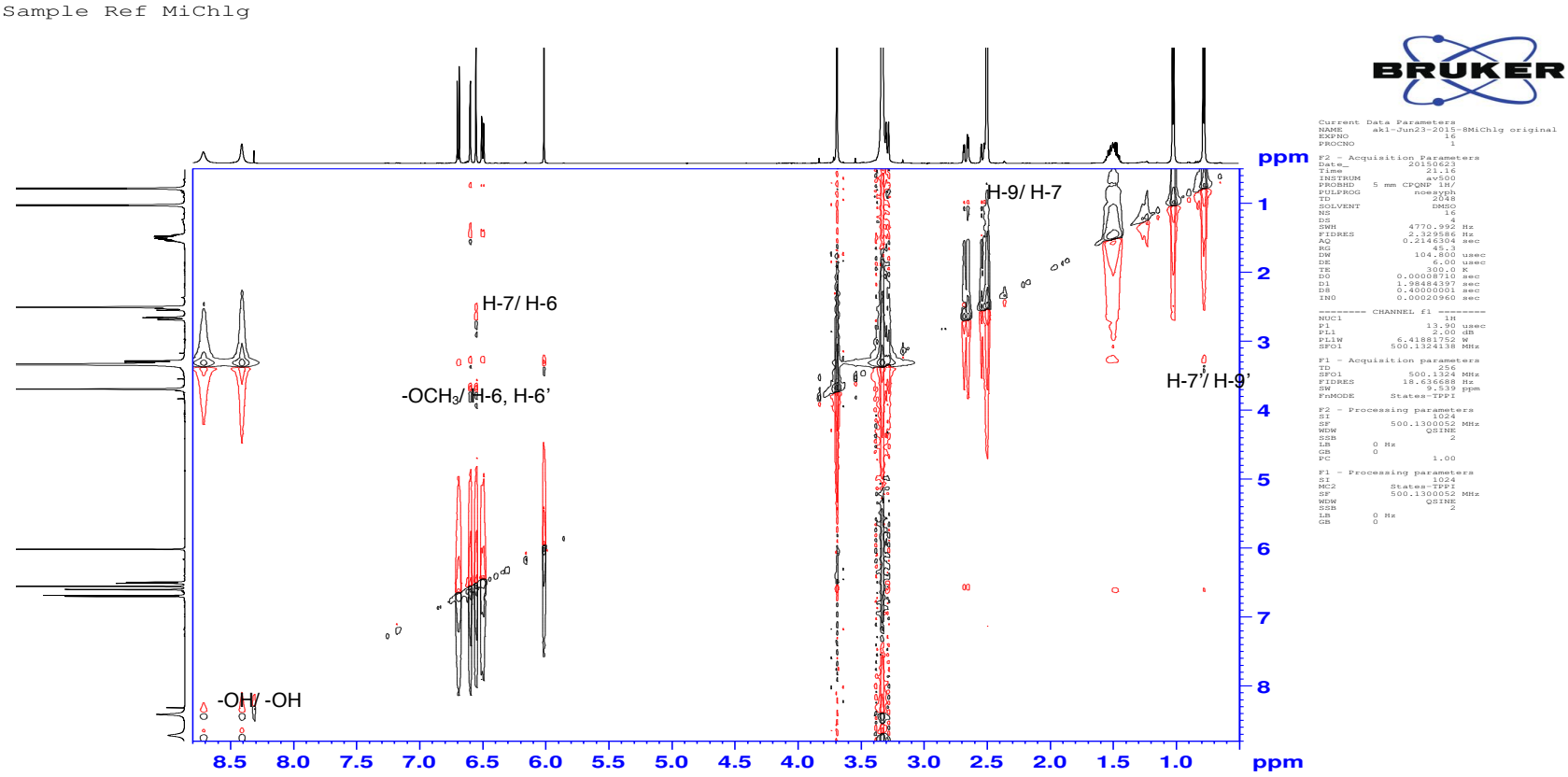

Figure 3.67 NOESY NMR spectrum for **AK-18**

Table 3.16 ^{1}H (coupling constants, Hz) and ^{13}C NMR spectral data (ppm) and HMBC correlations of **AK-18**, recorded in DMSO-d_6

Position	^{1}H	^{13}C	^{2}J	^{3}J	^{1}H Majumder *et al.*, 1972 ($CDCl_3$, 60 MHz)
1	-	126.7			
2	-	132.5			
3	6.01 s	116.1		C1, C5, C7’	6.50
4 (-OH)	8.41 br s	144.0			
5	-	145.5			
6	6.55 s	111.4		C2, C4, C7	6.68
7	2.52 d (11.0), 2.64 dd (16.0, 4.5)	38.3	C1		2.65 m
8	1.46 m	35.2			1.53 m
9 (-CH_3)	1.01 d (6.0)	19.8	C8	C7, C8’	1.05 d (6.0)
-OCH_3	3.69 s	55.4		C5	3.80 s
1’	-	137.4			
2’	6.49 dd (8.0, 2.0)	112.5	C3’	C4’, C6’, C7’	6.21
3’	6.68 d (8.0)	115.2	C4’	C1’, C5’	6.69
4’ (-OH)	8.71 br s	144.6			
5’	-	147.3			
6’	6.59 s (2.0)	112.9		C2’, C7’	6.61 s
7’	3.27 d (10.0)	53.1	C2, C1’, C8’	C1, C2’, C6’, C9’	2.65 m
8’	1.46 m	42.9			1.53 m
9’ (-CH_3)	0.77 d (6)	17.0	C8’	C7’, C8	0.84 d (6)
-OCH_3	3.69 s	55.6		C5’	3.80 s

Multiplicities of proton signals: br s - broad singlet, d - doublet, dd - double of doublet, s - singlet, and m - multiplet

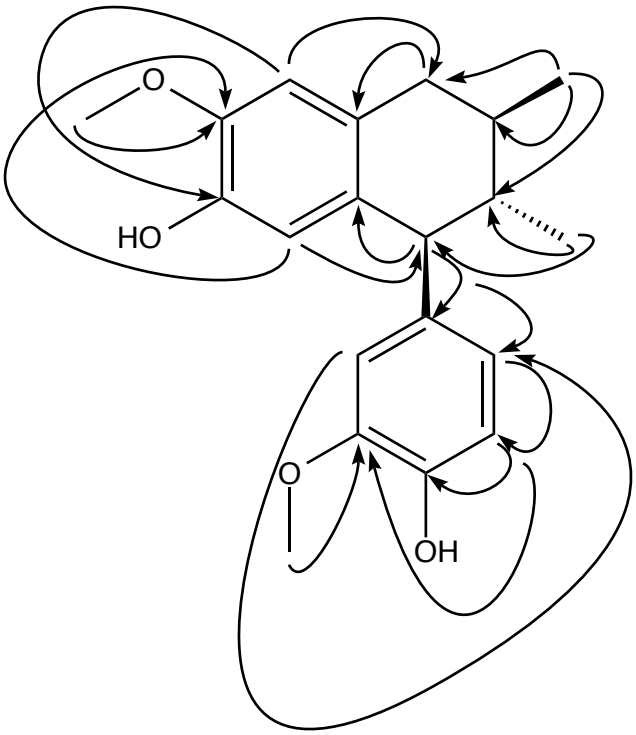

Figure 3.68 Selected HMBC correlations for **AK-18**

3.2.8.5 Physical Properties of isolated compounds

- *3-Butenyl glucosinolate (**AK-1**)*

  Amorphous greenish bluish solid; IR (film) V_{max}: 3396.42, 2924.76, 2074.86, 1641.19, 1576.40, 1238.76, 1112.10, 1058.20, 916.68, 877.15, 797.63, 642.89, 621.32 cm^{-1}; ^{1}H NMR (500 MHz, CD_3OD) and ^{13}C NMR (125 MHz, CD_3OD): see Table 3.2; HRTOFESIMS *m/z* 372.0406 $[M-H]^-$ (Calcd for $C_{11}H_{18}NO_9S_2^-$, 372.0423).

- *4-Hyroxylbenzyl glucosinolate (**AK-2**)*

  Straw coloured gummy liquid; IR (film) V_{max}: 3383.57, 3005.26, 2920.82, 1653.04, 1436.65, 1406.65, 1316.01, 1012.44, 951.11, 899.87, 703.08 cm^{-1}; ^{1}H NMR (500 MHz, DMSO) and ^{13}C NMR (125 MHz, DMSO): see Table 3.3; HRTOFESIMS *m/z*

424.0363 $[M-H]^-$ (Calcd for $C_{14}H_{18}NO_{10}S_2^-$, 424.0372).

- *2-Propenyl glucosinolate (**AK-3**, compound **1**)*

  Brownish solid. IR (film) V_{max}: 3376.02, 2925.35, 2859.50, 1642.95, 1575.29, 1411.14, 1235.05, 1057.99, 941.96, 876.48, 795.71, 701.20, 635.93 cm^{-1}; ^1H NMR (500 MHz, DMSO) and ^{13}C NMR (125 MHz, DMSO): see Table 3.4; ESI-MS *m/z* 358.0 $[M-H]^-$ (Calcd for $C_{10}H_{16}NO_9S_2^-$, 358.3663).

- *2-Phenylethyl glucosinolate (**AK-3**, compound **2**)*

  Brownish solid. IR (film) V_{max}: 3376.02, 2925.35, 2859.50, 1642.95, 1575.29, 1411.14, 1235.05, 1057.99, 941.96, 876.48, 795.71, 701.20, 635.93 cm^{-1}; ^1H NMR (500 MHz, DMSO) and ^{13}C NMR (500 MHz, DMSO): see Table 3.5; ESI-MS *m/z* 422.0 $[M-H]^-$ (Calcd for $C_{15}H_{20}NO_9S_2^-$, 422.4518).

- *2-(3-(2-((1H-imidazol-2-yl)methyl)-6-methoxyphenoxy)benzyl)-1H-imidazole (**AK-4**)*

  Pale yellow solid; λ_{max} (log ε) 225 (3.67), 278 (2.92) nm; IR (film) V_{max}: 2919.76, 1726.85, 1580.53, 1477.24, 1447.28, 1310.18, 1270.94, 1239.99, 1067.35, 988.93, 855.16, 736.56, 687.78 cm^{-1}; ^1H NMR (500 MHz, CD_3OD) and ^{13}C NMR (125 MHz, CD_3OD): see Tables 3.6-3.7; ESI-MS *m/z* 361.3 $[M+H]^+$ (Calcd for $C_{21}H_{20}N_4O_2$, 360.4103).

- *3-((1H-imidazol-2-yl)methyl)-2-(3-((1H-imidazol-2-yl)methyl)phenoxy)phenol (**AK-5**)*

  Pale yellow solid; λ_{max} (log ε) 226 (3.79), 272 (3.47) nm; IR (film) V_{max}: 2912.42, 1582.60, 1447.23, 1295.32,1239.29, 1191.03, 1140.03, 1098.60, 989.00, 956.15, 866.65, 737.08, 687.75 cm^{-1}; ^1H NMR (500 MHz, CD_3OD) and ^{13}C NMR (125 MHz, CD_3OD): see Tables 3.6-3.7; HRTOFESIMS *m/z* 347.1498 $[M+H]^+$ (Calcd for $C_{20}H_{18}N_4O_2$, 347.1508).

- *2-(3-(3-((1H-imidazol-2-yl)methyl)-5methoxy phenoxy)benzyl)-1H-imidazole (**AK-6**)*

  Pale yellow solid; λ_{max} (log ε) 218 (3.97), 228 (4.18) nm; IR (film) V_{max}: 2919.76, 1045.02, 971.15, 799.93, 610.64 cm^{-1}; ^{1}H NMR (500 MHz, CD_3OD) and ^{13}C NMR (125 MHz, CD_3OD): see Tables 3.6-3.7; HRTOFESIMS *m/z* 361.1659 $[M+H]^+$ (Calcd for $C_{21}H_{20}N_4O_2$, 361.1664).

- *4-((1H-imidazol-2-yl)methyl)-2-(3-((1H-imidazol-2-yl)methyl)phenoxy)phenol (**AK-7**)*

  Pale yellow solid; λ_{max} (log ε) 226 (3.82), 273 (3.17) nm; IR (film) V_{max}: 2916.54, 1729.41, 1584.85, 1558.69, 1505.37, 1486.34, 1446.99, 1429.11, 1240.52, 1099.19, 966.63, 863.04, 739.51, 688.47, 666.97 cm^{-1}; ^{1}H NMR (500 MHz, CD_3OD) and ^{13}C NMR (125 MHz, CD_3OD): see Tables 3.6-3.7; ESI-MS *m/z* 347.1 $[M+H]^+$ (Calcd for $C_{20}H_{18}N_4O_2$, 346.3836).

- *5-Hydroxy-1-(4-hydroxy-3-methoxyphenyl) dodecan-3-one (**AK-8**)*

  Yellow oil; λ_{max} (log ε) 232 (3.65), 281 (3.49) nm; IR (film) V_{max}: 3407.95, 2927.06, 2856.32, 1704.07, 1603.02, 1516.30, 1465.10, 1431.72, 1368.52, 1271.11, 1235.47, 1153.29, 1124.91, 1034.80, 813.37 cm^{-1}; ^{1}H (500 MHz, $CDCl_3$) and ^{13}C NMR (125 MHz, $CDCl_3$): see Table 3.9; ESI-MS *m/z* 345.3 $[M+Na]^+$ (Calcd for $C_{19}H_{30}O_4$, 322.4409).

- *5-Hydroxy-1-(4-hydroxy-3-methoxyphenyl) decan-3-one (**AK-9**)*

  Dark brown solid; λ_{max} (log ε) 232 (5.08), 280 (3.51) nm; IR (film) V_{max}: 3367.40, 2929.13, 2857.29, 1704.57, 1602.50, 1515.33, 1451.70, 1429.80, 1373.31, 1267.84, 1234.53, 1152.63, 1122.54, 1032.65, 815.16 cm^{-1}; ^{1}H NMR (500 MHz, CD_3OD) and ^{13}C NMR (125 MHz, CD_3OD): see Table 3.10; HRTOFESIMS *m/z* 293.1753 $[M-H]^-$ (Calcd for $C_{17}H_{26}O_4$, 293.1753).

- *Acacetin-7-O-rutinoside (**AK-10**)*

Needle-like crystals. IR (film) V_{max}: 3026.07, 2923.54, 2853.11, 1705.21, 1604.43, 1496.19, 1454.23, 1411.92, 1281.65, 1217.40, 1030.19, 934.23, 745.03, 722.36, 697.10 cm^{-1}; ^{1}H NMR (500 MHz, DMSO) and ^{13}C NMR (125 MHz, DMSO): see Table 3.11; HRTOFESIMS *m/z* 593.1870 $[M+H]^+$ (Calcd for $C_{28}H_{32}O_{14}$, 593.1870).

- *Isomitraphylline (**AK-11**)*

  White needle-like solid; λ_{max} (log ε) 243 (3.94), 281 (2.60) nm; IR (film) V_{max}: 3629.29, 3242.25, 2977.26, 2886.84, 1723.27, 1700.05, 1621.12, 1487.69, 1473.07, 1440.78, 1386.03, 1293.11, 1171.65, 1100.11, 1042.53, 920.27, 753.76, 603.93 cm^{-1}; ^{1}H NMR (500 MHz, DMSO) and ^{13}C NMR (125 MHz, DMSO): see Table 3.12; ESI-MS *m/z* 369.3 $[M+H]^+$ (Calcd for $C_{21}H_{24}N_2O_4$, 368.1736).

- *Mitraphylline (**AK-12**)*

  Granular white solid; IR (film) V_{max}: 3255.06, 2938.78, 2794.23, 1723.44, 1701.50, 1619.32, 1472.93, 1440.29, 1292.73, 1187.31, 1099.95, 753.93 cm^{-1}; ^{1}H NMR (500 MHz, DMSO) δ: 10.16 (1H, s, H-1), 2.31 (1H, d, *J* = 14.0, 2.5, H-3), 2.44 (1H, t, *J* = 9.5 Hz, H-5a), 3.14 (1H, t, *J* = 10.0 Hz, H-5b), 2.16 (1H, q, *J* = 12.5, 2.5 Hz, H-6a), 1.87 (1H, q, *J* = 8.5 Hz, H-6b), 7.27 (1H, d, *J* = 8.5 Hz, H-9), 6.97 (1H, t, *J* = 9.5, 1.0 Hz, H-10), 7.16 (1H, t, *J* = 9.5, 1.5 Hz, H-11), 6.80 (1H, d, *J* = 8.5 Hz, H-12), 2.10 (1H, d, *J* = 11.5, 3.5 Hz, H-14a), 0.87 (1H, q, *J* = 14.0 Hz, H-14b), 1.99 (1H, t, *J* = 14.5, 10.0 Hz, H-15), 7.42 (1H, s, *J* = 2.0, H-17), 4.43 (1H, m, *J* = 4.0 Hz, H-19), 1.73 (1H, d, *J* = 13.5, 4.5 Hz, H-20), 1.79 (1H, d, *J* = 12.5 Hz, H-21a), 3.06 (1H, d, *J* = 11.5, 2.5 Hz, H-21b), 3.51 (3H, s, H-3' (-OMe)), 1.05 (3H, d, *J* = 8.0 Hz, -Me); ^{13}C NMR (125 MHz, DMSO) δ: 179.5 (C-2), 73.5 (C-3), 53.3 (C-5), 34.2 (C-6), 54.3 (C-7), 133.6 (C-8), 123.9 (C-9), 121.4 (C-10), 127.0 (C-11), 108.6 (C-12), 141.7 (C-13), 27.8 (C-14), 29.5 (C-15), 106.3 (C-16), 153.4 (C-17), 73.1 (C-19), 40.1 (C-20), 52.7 (C-21), 165.6 (C-1'), 50.4 (C-3' (-OMe)), 14.3 ($-CH_3$); ESI-MS *m/z* 369.3 $[M+H]^+$ (Calcd for $C_{21}H_{24}N_2O_4$, 368.1736).

- *Formosanine (**AK-13**)*

  Amorphous white solid; IR (film) V_{max}: 2948.47, 2794.95, 1693.65, 1622.83, 1471.76, 1437.32, 1387.23, 1190.85, 1083.89, 740.72 cm^{-1}; ^{1}H NMR (500 MHz, DMSO) δ: 10.18 (1H, s, H-1), 2.23 (3H, q, *J* = 12.0, 9.5 Hz, H-3, H-15 and H-21a), 3.11 (1H, t, *J* = 8.0 Hz, H-5a), 2.34 (1H, q, *J* = 10.0 Hz, H-5b), 2.11 (1H, q, *J* = 5.5 Hz, H-6a), 1.85 (1H, q, *J* = 5.5 Hz, H-6b), 7.27 (1H, d, *J* = 7.0 Hz, H-9), 6.97 (1H, t, *J* = 7.5, 1.0 Hz, H-10), 7.15 (1H, t, *J* = 7.5, 1.0 Hz, H-11), 6.77 (1H, d, *J* = 8.0 Hz, H-12), 1.39 (1H, d, *J* = 11.5, 3.0 Hz, H-14a), 1.23 (1H, q, *J* = 12.0 Hz, H-14b), 7.47 (1H, s, H-17), 4.31 (1H, m, *J* = 6.5 Hz, H-19), 1.55 (1H, d, *J* = 9.5, 4.5 Hz, H-20), 3.21 (1H, d, *J* = 10.5, 1.0 Hz, H-21b), 3.52 (3H, s, H-3' (-OMe)), 1.23 (3H, d, *J* = 6.0 Hz, -Me); ^{13}C NMR (125 MHz, DMSO) δ: 179.9 (C-2), 73.6 (C-3), 54.3 (C-5), 34.0 (C-6), 55.3 (C-7), 133.6 (C-8), 123.1 (C-9), 121.7 (C-10), 127.7 (C-11), 108.9 (C-12), 141.8 (C-13), 29.4 (C-14), 30.3 (C-15), 109.3 (C-16), 154.6 (C-17), 72.0 (C-19), 37.0 (C-20), 52.6 (C-21), 166.6 (C-1'), 50.8 (C-3' (-OMe)), 18.3 ($-CH_3$); HRTOFESIMS *m/z* 369.1806 $[M+H]^+$ (Calcd for $C_{21}H_{24}N_2O_4$, 369.1814).

- *Speciophylline (**AK-14**)*

  Pale orange powder; IR (film) V_{max}: 3629.29, 3242.25, 2977.26, 2886.84, 1723.27, 1700.05, 1621.12, 1487.69, 1473.07, 1440.78, 1386.03, 1293.11, 1171.65, 1100.11, 1042.53, 920.27, 753.76, 603.93 cm^{-1}; ^{1}H NMR (500 MHz, CD_3OD) δ: 2.44 (1H, d, *J* = 11.5, H-3), 3.12 (1H, t, *J* = 1.0 Hz, H-5a), 2.53 (1H, q, *J* = 9.0 Hz, H-5b), 2.04 (2H, q, *J* = 9.5 Hz, H-6), 7.29 (1H, d, *J* = 7.0 Hz, H-9), 7.05 (1H, t, *J* = 7.0 Hz, H-10), 7.20 (1H, t, *J* = 8.0, H-11), 6.87 (1H, d, *J* = 7.0 Hz, H-12), 2.24 (1H, d, *J* = 11.5 Hz, H-14a), 0.96 (1H, q, *J* = 4.0 Hz, H-14b), 1.21 (1H, t, *J* = 5.0 Hz, H-15), 7.44 (1H, s, H-17), 4.43 (1H, m, H-19), 1.91 (1H, s, *J* = 6.5 Hz, H-20), 1.92 (1H, s, H-21a), 3.11 (1H, s, *J* = 4.5 Hz, H-21b), 3.55 (3H, s, H-3' (-OMe)), 1.11 (3H, d, *J* = 5.5 Hz, -Me); ^{13}C NMR (125 MHz, CD_3OD) δ: 179.5 (C-2), 75.5 (C-3), 55.0 (C-5), 35.5 (C-6), 57.2 (C-7), 134.6 (C-8), 124.2 (C-9), 123.7 (C-10), 129.3 (C-11), 110.6 (C-12), 144.5 (C-

13), 29.8 (C-14), 31.6 (C-15), 108.2 (C-16), 155.7 (C-17), 75.4 (C-19), 42.0 (C-20), 55.0 (C-21), 166.1 (C-1'), 51.4 (C-3' (-OMe)), 15.1(-CH_3); ESI-MS *m/z* 369.3 $[M+H]^+$ (Calcd for $C_{21}H_{24}N_2O_4$, 368.1736).

- *7-Hydroxy-2-(4-hydroxyphenyl)-5-methoxy-4H-chromen-4-one (**AK-15**)*

  Yellow solid; λ_{max} (log ε) 264 (4.29), 330 (4.34) nm; IR (film) V_{max}: 3254.4, 2937.93, 1707.11, 1610.79, 1510.57, 1451.77, 1368.94, 1254.57, 1021.36, 992.02, 823.84 cm^{-1}; ^1H NMR (500 MHz, CD_3OD) and ^{13}C NMR (125 MHz, CD_3OD): see Table 3.13; HRTOFESIMS *m/z* 283.0616 $[M-H]^-$ (Calcd for $C_{16}H_{12}O_5$, 283.0606).

- *9-oxo-9-((3-phenylpropyl)amino)nonanoic acid (**AK-16**)*

  Brown solid; λ_{max} (log ε) 206 (4.21), 267 (2.98) nm; IR (film) V_{max}: 3348.28, 2928.79, 2831.60, 1706.68, 1423.40, 1362.44, 1228.20, 1024.08, 697.89 cm^{-1}; ^1H NMR (500 MHz, CD_3OD) and ^{13}C NMR (125 MHz, CD_3OD): see Table 3.14; HRTOFESIMS *m/z* 261.1856 $[(M-H)-CO_2H]^-$ (Calcd for $C_{18}H_{27}NO_3$, 305.1991).

- *11-oxo-11-((3-phenylpropyl)amino)undecanoic acid (**AK-17**)*

  Olive green liquid; λ_{max} (log ε) 204 (4.22), 194 (3.21) nm; IR (film) V_{max}: 3365.70, 2924.43, 2853.62, 1708.64, 1454.02, 1216.63, 1024.43, 930.88, 749.38, 697.74 cm^{-1}; ^1H NMR (500 MHz, DMSO) and ^{13}C NMR (125 MHz, DMSO): see Table 3.15; HRTOFESIMS *m/z* 287.2051 $[(M-H)-CO_2H]^-$ (Calcd for $C_{20}H_{31}NO_3$, 333.4720).

- *8-(4-hydroxy-3-methoxyphenyl)-3-methoxy-6,7-dimethyl-5,6,7,8-tetrahydronaphthalen-2-ol (**AK-18**)*

  Pale yellow granules; λ_{max} (log ε) 240 (2.80), 285 (3.80) nm; IR (film) V_{max}: 3392.14, 2957.26, 2927.68, 2891.10, 2844.26, 1708.61, 1612.08, 1507.80, 1444.67, 1364.75, 1253.38,1106.34, 1027.12, 866.37, 799.05, 770.31, 622.91cm^{-1}; ^1H NMR (500 MHz, DMSO) and ^{13}C NMR (125 MHz, DMSO): see Table 3.16; ESI-MS *m/z* 327.1 $[M-H]^-$ (Calcd for $C_{20}H_{24}O_5$, 328.1675).

3.3 Biological evaluation

3.3.1 Antibacterial activity

The antibacterial activity of the crude extracts, isolated natural products and purchased natural products were assessed by the broth microdilution method as described by Andrews (2001), against *E. coli* NCTC 10418 and *S. aureus* strains. The observed activities are summarized in the Tables 3.17, 3.18 and 3.19. The structures of the purchased natural products are shown in Figures 3.73 and 3.74.

3.3.1.1 Crude extract

From Table 3.17, the hexane extracts showed the most potent antibacterial activity, demonstrated by the low MIC values, followed by the chloroform extracts. The methanol and alkaloidal extracts exhibited little or no activity within the assessed range of 1 to 512 µg/mL.

From the hexane extracts screened, *M. lowiana* (**AK-17**) was the most potent antibacterial agent with MIC values of 32, 64 and 32 µg/mL against *S. aureus* ATCC 25923, SA-1199B and XU212, respectively. This extract was obtained as almost pure compound, an 11-oxo-11-((3-phenylpropyl)amino) attached to an undecanoic acid (Figure 3.69) and the observed

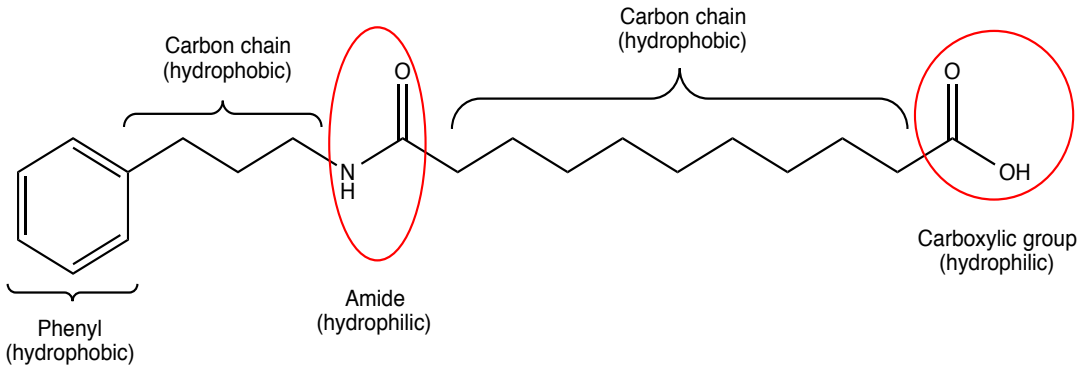

Figure 3.69 Amphipathic nature of *M. lowiana* hexane extract compound (**AK-17**)

Table 3.17 The MIC values of the crude extract against *S. aureus* strains

Extracts		MIC (µg/mL) for sample against indicated strain			
		ATCC 25923	**XU212**	**SA-1199B**	**RN4220**
S. alba	chloroform	> 512	> 512	> 512	> 512
	methanol	> 512	> 512	> 512	> 512
A. rusticana	hexane	128	128	64	n.t
	chloroform	256	512	512	n.t
	methanol	> 512	> 512	> 512	n.t
B. oleracea	hexane	128	256	128	n.t
	chloroform	512	> 512	64	n.t
	methanol	512	256	128	n.t
L. sativum	Petroleum ether	> 512	> 512	> 512	512
	methanol	> 512	> 512	> 512	512
	alkaloidal	512	512	> 512	> 512
Z. officinale	hexane	> 512	> 512	> 512	> 512
	chloroform	> 512	> 512	> 512	> 512
	methanol	> 512	> 512	> 512	> 512
M. lowiana	Hexane (**AK-17**)	32	64	32	n.t
	chloroform	64	64	64	n.t
	methanol	> 512	> 512	> 512	n.t
B. officinalis	hexane	128	128	128	128
	chloroform	256	256	256	256
	methanol	> 512	> 512	> 512	> 512
U. tomentosa	hexane	n.t	128	128	128
	chloroform	n.t	512	> 512	256
	methanol	n.t	256	128	128
	alkaloidal	n.t	512	512	256
Positive control	Tetracycline		128		
	Norfloxacin	2		32	
	Erythromycin				128

n.t - not tested

antibacterial activity may be due to its fatty acid chain. As research findings have shown a direct correlation between fatty acid chains of amide compounds and antibacterial activity

(Kabara *et al.*, 1972a).

Fatty acids have long been known for their antibacterial activity against important pathogenic microorganisms, including *S. aureus* (Mundt *et al.*, 2003; Wille and Kydonieus, 2003; Zhang *et al.*, 2012), *Streptococcus pyogenes* (Kabara *et al.*, 1972b; Choi *et al.*, 2013), *Helicobacter pylori* (Sun *et al.*, 2003), *Chlamydia trachomatis* (Bergsson *et al.*, 1998) and *Neisseria gonorrhoeae* (Bergsson *et al.*, 1999). However, their exact antibacterial mode of action is still not well understood. It has been suggested that their activity is through cellular membrane interaction via solubulisation, which is possible because of their amphipathic structure (hydrophilic and hydrophobic ends) (Galbraith and Milter, 1973; Shin *et al.*, 2007; Desbois and Smith, 2010). Other research suggests that their mechanism of action is through the inhibition of bacterial cellular energy production (Greenway and Dyke, 1979; Peters and Chin, 2003; Boyaval *et al.*, 1995), inhibition of bacterial enzyme activity (Zheng *et al.*, 2005; Won *et al.*, 2007; Hamel, 2009; Sado-Kamdem *et al.*, 2009), impairment of bacterial nutrient uptake (Galbraith and Milter, 1973; Shibasaki and Kato, 2010), generation of toxic peroxidation or auto-oxidation products (Knapp and Melly, 1986; Hazell and Graham, 1990; Adolph *et al.*, 2004; Schonfeld and Wojtczak, 2008) or through the induction of bacterial cell lysis (Chamberlain *et al.*, 1991; Shin *et al.*, 2007). It is therefore plausible that this compound may have achieved antibacterial activity through any of these mechanisms.

3.3.1.2 Isolated natural products

The isolated natural products showed a range of antibacterial activity against the test strains. The observed MIC values are outlined in Table 3.18. **AK-16**, another amide, was the most active against the *S. aureus* strains, followed by the phenylpropanoid derivatives (**AK-8** and **AK-9**). The other isolated natural products, the glucosinolates, alkaloids, flavones and aryltetralin lignan had little or no activity against the test strains.

Table 3.18 The MIC values of the isolated compounds against *S. aureus* and *E. coli*

Compounds		MIC (µg/mL) for sample against indicated strain			
Type of natural product	**Identification**	**ATCC 25923**	**XU212**	**SA-1199B**	***E.coli* NCTC 10418**
Glucosinolates	AK-1	> 512	> 512	> 512	> 512
	AK-2	512	> 512	> 512	> 512
	AK-3	512	> 512	> 512	> 512
Dimeric imidazole alkaloids	AK-4	512	> 512	> 512	> 512
	AK-6	512	> 512	> 512	> 512
	AK-5	512	> 512	> 512	> 512
	AK-7	512	> 512	> 512	> 512
Phenylpropanoid derivatives	AK-8	128	> 512	128	> 512
	AK-9	128	> 512	128	> 512
Flavone	AK-10	> 64	> 64	> 64	> 64
Oxindole alkaloids	AK-11	512	> 512	> 512	> 512
	AK-12	512	> 512	> 512	> 512
	AK-13	512	> 512	> 512	> 512
	AK-14	n.t	n.t	n.t	> 64
Flavone	AK-15	n.t	n.t	n.t	> 64
Amide	AK-16	32	64	32	> 512
Aryltetralin lignan	AK-18	512	512	512	> 512
Positive control	Tetracycline		128		
	Norfloxacin			32	
	Ciprofloxacin	< 0.0625			< 0.0625

n.t – not tested

The glucosinolates (**AK-1**, **AK-2** and **AK-3**) showed little or no antibacterial activity within the concentration range tested. This corresponds well with published literature that intact glucosinolate compounds have minimal or no antibacterial activity against pathogenic microorganisms, *S. aureus*, *Enterococcus faecalis*, *E. coli*, *A. baumanii*, *Klebsiella pneumoniae* and *Proteus mirabilis* (Shofran *et al.*, 1998; Ares *et al.*, 2014). These compounds are also known to be relatively non-reactive (Fahey *et al.*, 2001), this could probably explain their inactivity.

The alkaloids, both the imidazoles (**AK-4**, **AK-5**, **AK-6** and **AK-7**) and the oxindoles (**AK-11**, **AK-12**, **AK-13** and **AK-14**) showed little or no antibacterial activity within the concentration range tested. The inactivity of the isolated imidazoles corresponds well with published literature that imidazole-derived alkaloids have no antibacterial activity against *S. aureus* and *P. aeruginosa* (Rudolph *et al.*, 2013). Although the isolated imidazoles did not exhibit appreciable antibacterial activity, some synthesized 5-(nitro/bromo)-2-styryl benzimidazoles have shown good activity against *S. aureus*, *E. coli*, *K. pneumoniae*, *E. faecalis*, *C. albicans* and *Aspergillus fumigatus* with MIC values ranging from 1 to 62.5 µg/mL (Shingalapur *et al.*, 2009).

Extensive research on *U. tomentosa* has shown that its metabolites especially the oxindole alkaloids have cytotoxic (Muhammad *et al.*, 2001), anti-inflammatory (Aquino *et al.*, 1991; Rizzi *et al.*, 1993; Lemaire *et al.*, 1999), immunostimulant (Keplinger *et al.*, 1999) and CNS-related activities (Kang *et al.*, 2002). Garcia and colleagues reported the moderately poor inhibitory activity of isopteropodine against *S. aureus* (150 µg/mL) and *Bacillus subtilis* (250 µg/mL) (Garcıa *et al.*, 2014). This is contrary to what was observed in this study for the isolated oxindole alkaloids, which are stereoisomers of isopteropdine. The isolated oxindole alkaloids inhibited *S. aureus* ATCC 25923 at a slightly higher MIC value, 512 µg/mL but were inactive against the other strains. The difference in antibacterial activity of these oxindole alkaloids is not unusual, as stereoisomers sometimes do exhibit different biological activity (Hutt and O'Grady, 1996).

The gingerols (**AK-8** and **AK-9**) showed moderate activity against *S. aureus* ATCC 25923 and 1199B at 128 µg/mL but they were inactive against XU212 and *E. coli* NCTC 10418. This difference in antibacterial activity may be related to structural features of the gingerols, characteristics that may reduce or increase recognition and transport out of the cell. Although the gingerols were active against SA-1199B, their activity was less significant compared to norfloxacin (MIC = 32 µg/mL), a known NorA pump substrate (Kaatz *et al.*, 1993). A structure-activity relationship study on quinolones showed that the presence of

bulky substituent at C-7, and a bulky and hydrophobic substituent at C-8 of the quinolone molecule decreased their activity against efflux-mediated resistant mutants of *S. aureus* (Takenouchi *et al.*, 1996). This may explain the high MIC values of the gingerols, as they have a bulky hydrophobic side chain (5-hydroxy-alkan-3-one), (Figure 3.70).

Other gingerol compounds, 10-gingerol and 12-gingerol have also shown good inhibitory activity against oral pathogens, *Porphyromonas gingivalis*, *Porphyromonas endodotalis* and *Prevotella intermedia* with MIC values ranging from 6 to 30 µg/mL (Park *et al.*, 2008). There have also been reports of gingerols showing good activity against *Helicobacter pylori* (Mahady *et al.*, 2003; Zhang *et al.*, 2013), *Mycobacterium avium* and *Mycobacterium tuberculosis* (Hiserodt *et al.*, 1998).

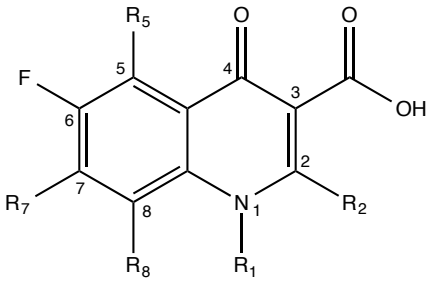

Quinolone molecule

Norfloxacin: $R_1 = CH_2CH_3$, $R_2 = H$, $R_5 = H$, R_7 = piperazin-1-yl, $R_8 = H$

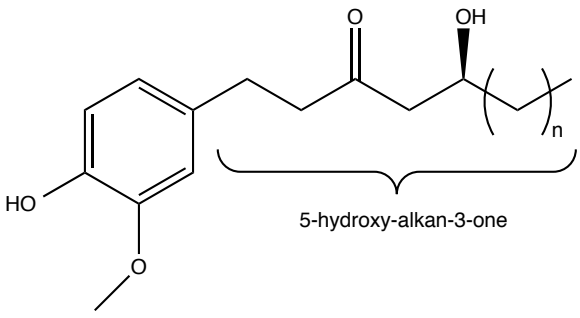

AK-8 (8-gingerol) n = 6

AK-9 (6-gingerol) n = 4

Figure 3.70 Structure of quinolone molecule and the isolated gingerols

The flavones (**AK-10** and **AK-15**) did not show antibacterial activity within the concentration range tested (MIC value: > 64 µg/mL) even though they belong to the flavone class of metabolites, which are well known for their broadly antibacterial activity (Gibbons, 2004). Their inactivity may be due to the lack of lipophilic groups in the chemical structure. As research findings have shown that flavonoids possessing lipophilic groups such as prenyl or geranyl groups display better antibacterial activity (Barron and Ibrahim, 1996; Avila *et al*., 2008). Structure-activity relationship studies on flavones have also shown that antibacterial activity is improved by the presence of certain substituent groups on the core molecule (Figure 3.71, structure of a flavone). The presences of an *O*-acyl (Babu *et al*., 2005) or *O*-alkylamino chain (Babu *et al*., 2006) on the ring A at position 7 or the presence of a lipophilic group at position 6 or 8 (Tsuchiya *et al*., 1996; Šmejkal *et al*., 2008) or a hydroxyl group at

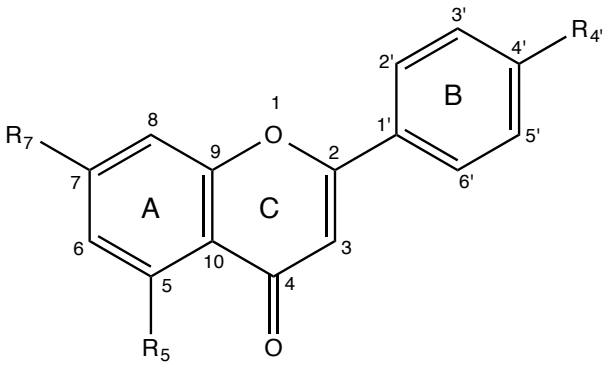

AK-10: R_5 = OH, R_7 = Rutinose, $R_{4'}$ = OCH_3

AK-15: R_5 = OCH_3, R_7 = OH, $R_{4'}$ = OH

Figure 3.71 The core structure of a flavone with the substituent groups for the isolated flavones (**AK-10** and **AK-15**) indicated beneath

position 5 (Šmejkal *et al*., 2008) has been shown to improve antibacterial activity. Although **AK-10** has a hydroxyl group at position 5 (Figure 3.71) there was no observed activity. Probably the methoxyl group on the ring B position 4' may have contributed to the lack of activity, as research findings from Alcaraz *et al*. and Šmejkal *et al*. have shown that methoxyl

group on ring B decreases antibacterial activity (Alcaraz *et al*., 2000; Šmejkal *et al*., 2008).

AK-16 exhibited good antibacterial activity against the Gram-positive bacteria but not the Gram-negative bacteria. Its activity was comparable to that of *M. lowiana* hexane extract (**AK-17**). This was expected as they belong to the same class of compounds, amides. They only varied in the length of the methylene chain but this did not have any obvious effect on their antibacterial activity.

AK-18 (guaiacin) showed little activity against the *S. aureus* strains with an MIC value of 512 µg/mL but was inactive against *E. coli* within the concentration range tested. This compound belongs to the lignan class of metabolites, which are well known for their enormous structural diversity and broad biological activities (MacRae and Towers, 1984; Saleem *et al*., 2005). Some lignans are known to have anticancer (particularly true of the podophyllotoxin group of lignans), anti-inflamatory, anti-oxidative, immunosuppressive and antimicrobial activities (MacRae and Towers, 1984; Saleem *et al*., 2005). Compounds which are closely related to.

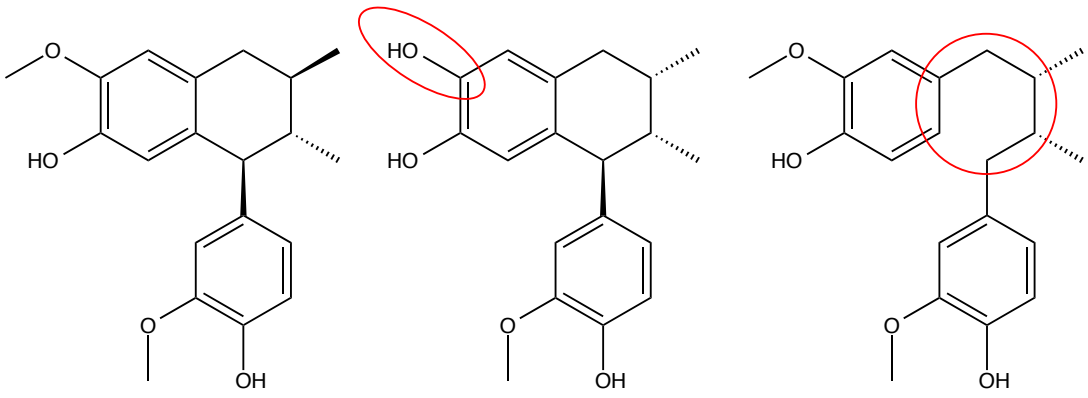

a) Guaiacin **b)** Nor-isoguaiacin **c)** Dihydroguaiaretic acid

Figure 3.72 Structures showing the resemblance among the compounds, the isolated guaiacin, nor-isoguaiacin and dihydroguaiaretic acid (the red rings indicate the structural differences in comparison to guaiacin)

the isolated guaiacin, such as nor-isoguaiacin (MIC = 100 µg/mL) and dihydroguaiaretic acid

(MIC = 10 µg/mL) had previously been reported to inhibit the growth of *Streptococcus* species, *S. aureus* and *B. subtilis* (Gisvold and Thaker, 1974). Their MIC values were lower and better than that of guaiacin, probably because of the minor structural differences (Figure 3.72, supporting information). This is a good indication that structural modification of this compound is likely to improve its antibacterial activity. Almost all of the isolated compounds were inactive against *E. coli* NCTC 1018 and at least one multidrug resistant *S. aureus* strain. This inactivity may be due to the unique outer membrane of *E. coli* and the active expression of efflux pumps of the strains (Nikaido, 1994; Nikaido, 1998).

3.3.1.3 Isothiocyanates and other selected natural products

Additional natural products, which were not isolated in this study, were purchased and screened for antibacterial activity. Almost all of the compounds purchased were obtained from the plants under study in this project with the exception of 4-methoxyphenyl isothiocyanate, which is a synthetic product. The compounds were selected based on good biological activity observed for an extract or a fraction or similar isolated compound in this study. The structures of the screened compounds and their MIC values are shown in Figures 3.73 to 3.74 and Table 3.19, respectively. All the compounds were purchased from Sigma-Aldrich.

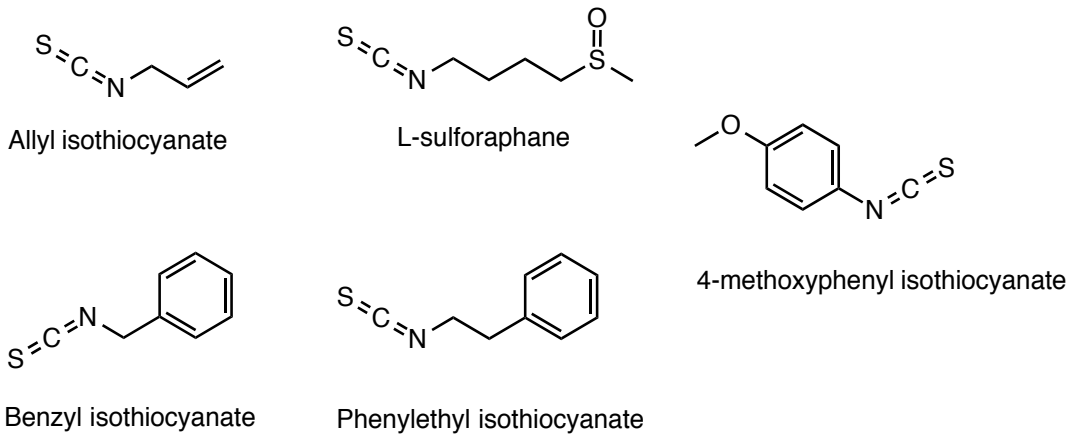

Figure 3.73 Chemical structures of selected isothiocyanates

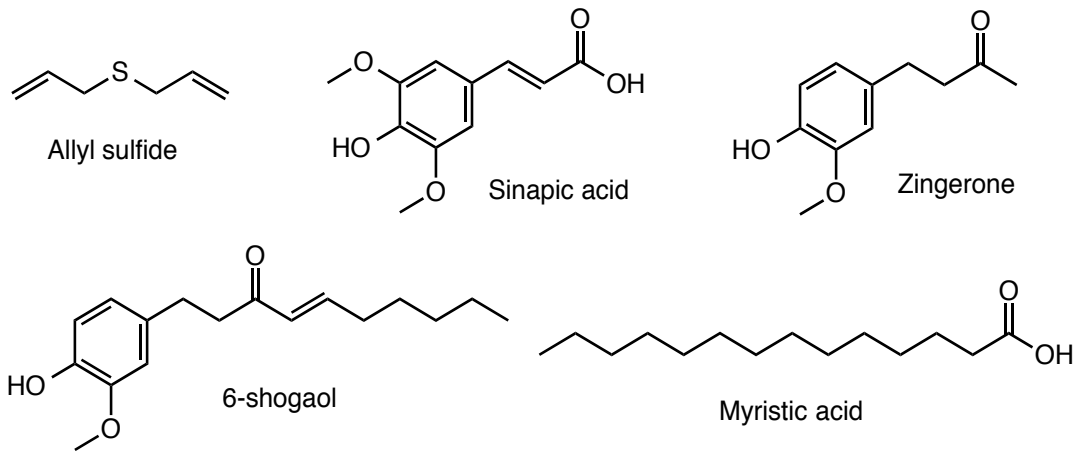

Figure 3.74 Chemical structures of the other selected compounds

Table 3.19 The MIC values of the selected isothiocyanates and other compounds against *S. aureus* and *E. coli*

Compounds		MIC (μg/mL) for sample against indicated strain			
		ATCC 25923	**XU212**	**SA-1199B**	***E.coli* NCTC 10418**
Allyl isothiocyanate		512	> 512	512	> 512
L-sulforaphane		64	32	32	64
Benzyl isothiocyanate		256	512	256	128
4-methoxyphenyl isothiocyanate		256	128	128	512
Phenylethyl isothiocyanate		16	32	32	256
Sinigrin		512	> 512	> 512	> 512
Allyl sulfide		512	> 512	> 512	> 512
Sinapic acid		> 512	> 512	> 512	> 512
6-shogaol		32	32	32	> 512
Zingerone		512	> 512	> 512	> 512
Myristic acid		128	16	64	128
Positive control	Tetracycline		128		
	Norfloxacin			32	
	Ciprofloxacin	< 0.0625			< 0.0625

The isothiocyanate compounds were the most active against the test strains with the

exception of allyl isothiocyanate. Myristic acid and 6-shogaol showed relatively good activity while the other compounds, sinigrin (Figure 3.15), allyl sulfide, sinapic acid and zingerone showed little or no activity against the test strains.

The isothiocyanates are products that are commonly found in the *Brassica* vegetables. They are hydrolysis product of glucosinolates, which are produced when damaged plant tissue releases myrosinase, a glycoprotein that cleaves the *β*-glucosyl moiety of a glucosinolate. This leaves the unstable aglycone, thiohydroxamate-*O*-sulfonate to rearrange itself to form an isothiocyanate or the other breakdown products; nitrile and thiocyanate (Figure 3.75) (Mithen *et al.*, 2000; Fahey *et al.*, 2001). The selected isothiocyanates, L-sulforaphane, allyl, benzyl and phenylethyl isothiocyanates are hydrolysis product of glucoraphanin, sinigrin, glucotropaeolin and gluconurstatiin, respectively (Aires *et al.*, 2009).

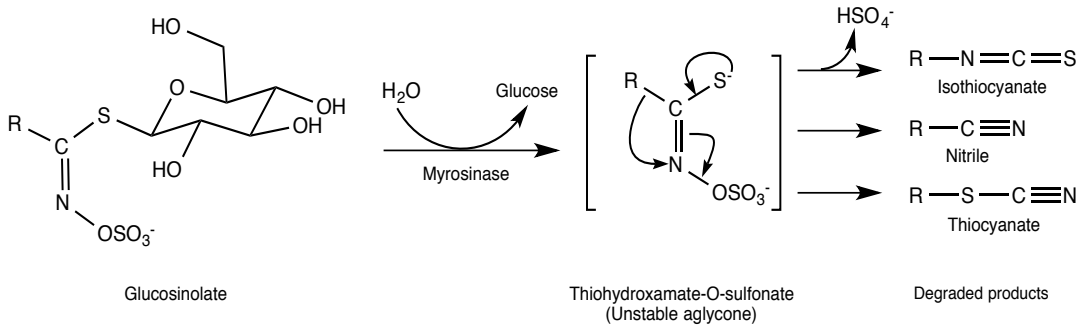

Figure 3.75 Generalised scheme for glucosinolate hydrolysis

The isothiocyanates exhibited potent but varied antibacterial activity against the test strains. In the case of the aliphatic isothiocyanates, L-sulforaphane (SFN) showed good activity against both Gram-positive and Gram-negative bacteria with MIC values ranging from 32 to 64 µg/mL while allyl isothiocyanate (AITC) had little (MIC = 512 µg/mL) or no activity against the test strains. The aromatic isothiocyanates, especially, phenylethyl isothiocyanate (PEITC) was the most potent with MIC values ranging from 16 to 256 µg/mL against the test strains while benzyl isothiocyanate (BITC) and 4-methoxyphenyl isothiocyanate were active in the range of 128 to 512 µg/mL. Previous studies on isothiocyanates reported a

higher activity for aromatic isothiocyanates when compare to the aliphatic ones (Kim and Lee, 2009; Jang *et al*., 2010), which was not observed in this study. Wilson and co-workers reported good antibacterial activity for PEITC and BITC but did not agree that the aromatic isothiocyanates had better antibacterial activity than the aliphatic ones (Wilson *et al*., 2013). As their extensive research work also showed varied antibacterial activity for both the aromatic and aliphatic isothiocyanates against *Bacillus cereus*, *B. subtilis*, *E. faecalis*, *Enterococcus faecium*, *Lactobacillus plantarum*, *Lactobacillus monocytogenes*, *S. aureus*, *Staphylococcus xylosus*, *K. pneumoniae*, *E. coli*, *P. aeruginosa*, *Salmonella enteritidis*, *Salmonella enterica* serovar *typhimurium* and *Serratia marcescens* (Wilson *et al*., 2013). They also suggested that structural features such as the sulfinyl group, the molecule size or the hydrocarbon chain may be responsible for the antibacterial activity but not necessarily the aromatic structure (Wilson *et al*., 2013). Other research has shown that isothiocyanates readily react with thiols, peptides, proteins and enzymes because of their strong electrophilic nature (Kolm *et al*., 1995; Jacob and Anwar, 2008; Cejpek *et al*., 2000). This would probably explain the observed antibacterial activity exhibited by the isothiocyanates. As such reactions *in vivo* result in modification of proteins or enzymes, which can significantly disturb the cell biochemical processes and survival (Jacob and Anwar, 2008; Dias *et al*., 2014).

Sinigrin (glucosinolate) a precursor of allyl isothiocyanate showed little or no activity against the test strains. The inactivity of sinigrin is consistent with published literature (Shofran *et al*., 1998). This also supports the observation that intact glucosinolate compounds have no or minimal antibacterial activity against pathogenic microorganisms (Shofran *et al*., 1998; Ares *et al*., 2014).

Allyl sulfide a product of *Allium* species and *A. rusticana* (Bernhard *et al*., 1964) showed minimal activity against *S. aureus* ATCC 25923 (MIC = 512 µg/mL) and a previous report showed good activity; Rattanachaikunsopon and Phumkhachorn reported an MIC value of 64 ± 1.4 µg/mL against *S. aureus* ATCC 25923 (Rattanachaikunsopon and Phumkhachorn, 2008). This wide variation in activity against *S. aureus* ATCC 25923 may be due to the

different inoculum size, the methods and the culture media used. The lack of activity against the SA-1199B (NorA) and XU212 (TetK) may be due to the active expression of the efflux pumps and intrinsic resistance caused by the lipopolysaccharide outer membrane of *E. coli*.

Sinapic acid is a product found in most plants including the *Brassica* vegetables (Nićiforović and Abramovič, 2014). It did not show activity against the test strains within the range assessed (1- 512 µg/mL) but may be active at higher concentrations. Findings from Tesaki and co-workers have shown that sinapic acid exhibits antibacterial activity at higher concentrations, *E. coli* (MIC = 493.3 µg/mL), *Salmonella enteritidis* (MIC = 448.4 µg/mL) and *S. aureus* (MIC = 403.5 µg/mL) (Tesaki *et al*., 1998). Engels and colleagues later confirmed this; their findings showed that sinapic acid inhibited *B. subtilis* (MIC = 300 µg/mL), *E. coli* (MIC = 700 µg/mL) and *S. aureus* (MIC = 300 µg/mL) (Engels *et al*., 2012).

Zingerone and 6-shogaol are natural products derived from *Z. officinale.* 6-shogaol showed good inhibitory activity against the *S. aureus* strains with an MIC value of 32 µg/mL. This was not the case for zingerone as it poorly inhibited the activity of *S. aureus* ATCC 25923 (MIC = 512 µg/mL). On comparing the antibacterial activity of the phenylpropanoid derivatives from ginger, 6-shogaol was the most potent probably because of its structure. The presence of a carbon-carbon double bond in the dec-4-en-3-one side chain of shogaol, improved its lipophilicity, and hence its membrane permeability. There is the need to investigate this hypothesis, though it has already been proven for fatty acids (Kabara *et al*., 1972b). Research findings have also shown that there is a direct correlation between carbon-carbon double bonds of unsaturated fatty acids and antibacterial efficacy (Feldlaufer *et al*., 1993; Desbois *et al*., 2008), this could possibly explain the better activity of shogaol.

From the antibacterial study of the test extracts and compounds, it is evident that the test samples were not as active as the antibiotics but with structural modification, the activity of promising ones (amides, L-sulforaphane, phenylethyl isothiocyanate, benzyl isothiocyanate, shogaol and myristic acid) can be improved.

3.3.2 Bacterial plasmid conjugation inhibition

The isolated and selected natural products were assessed for anti-conjugative activity by the plasmid conjugation inhibition assay as described by Rice and Bonomo (2005). The infective plasmids pKM101 (IncN), TP11 ($IncI_2$), pUB307 (IncP) and R7K (IncW) were used as representatives of a variety of plasmid transfer systems. All test compounds were screened at a sub-inhibitory concentration, a quarter of their MIC against *E. coli* NCTC 10418. Samples, which were inactive against *E. coli* NCTC 10418 were tested at 100 µg/mL, active samples were tested at SIC values indicated in the graphs; Figures 3.74-3.77. All samples tested at 100 µg/mL have not been indicated in the graphs; Figures 3.74-3.77. The observed activities are shown in the Figures 3.74-3.77. The total number of cells used for the plasmid assays are as follows: donors [pKM101 ($1.1 \times 10^{10} \pm 1.4 \times 10^{8}$ cfu/mL), TP114 ($3.0 \times 10^{10} \pm 2.8 \times 10^{9}$ cfu/mL), pUB307 ($3.1 \times 10^{10} \pm 4.9 \times 10^{9}$ cfu/mL) and R7K ($3.7 \times 10^{10} \pm 1.8 \times 10^{9}$ cfu/mL)] recipients [ER1793 ($1.9 \times 10^{10} \pm 5.3 \times 10^{9}$ cfu/mL) and JM109 ($3.1 \times 10^{10} \pm 5.0 \times 10^{8}$ cfu/mL)].

3.3.2.1 The effect of natural products on the conjugal transfer of plasmid pKM101 (IncN)

Twenty-nine natural products were assessed for anti-conjugative activity against IncN plasmid pKM101 (Figure 3.77). Out of this number only 3 actively inhibited the conjugal transfer of pKM101; these were phenylethyl isothiocyanate (PEITC), benzyl isothiocyanate (BITC) and allyl isothiocyanate (AITC) (Figure 3.76).

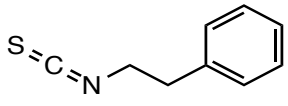

Phenylethyl isothiocyanate

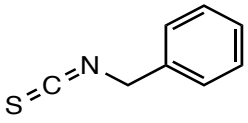

Benzyl isothiocyanate

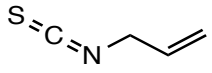

Allyl isothiocyanate

Figure 3.76 Structures of the compounds, which actively inhibited the conjugal transfer of IncN plasmid pKM101

PEITC completely prevented the conjugal transfer of pKM101 at a sub-inhibitory concentration of 64 µg/mL. A similar anti-conjugal activity was observed for BITC. At a concentration of 32 µg/mL, it significantly reduced the conjugal transfer of pKM101 to 0.3 ± 0.6%. The similar anti-conjugal activity of these compounds may be due to their similar structural features (Figure 3.76), an aromatic moiety attached to β-thioglucoside *N*–hydroxysulfate. AITC also showed a significantly reduction in the conjugal of pKM101. It reduced the conjugal transfer to 6.0 ± 1.0% at a concentration of 100 µg/mL.

Although PEITC showed good activity, a mixture containing its precursor, gluconasturtiin and sinigrin (**AK-3**) did not show any conjugal inhibition against pKM101. The transfer frequency exceeded 120%, which indicated that the mixture probably enhanced conjugation. The lack of conjugal inhibition by the gluconasturtiin-sinigrin mixture may be due to antagonism or concentration differences, as pure sinigrin showed moderate conjugal inhibition (21.5 ± 6.2% at 100 µg/mL).

Moderate activity was observed for 3-butenyl glucosinolate (**AK-1**), 4-hydroxylbenzyl glucosinolate (**AK-2**), 6-gingerol (**AK-9**), lepidine E (**AK-7**) and 2-(3-(2-((1*H*-imidazol-2-yl)methyl)-6-methoxyphenoxy)benzyl)-1*H*-imidazole (**AK-4**). Their conjugal frequencies ranged from 18.0 ± 2.0% to 31.0 ± 7.0%.

The other compounds including linoleic acid and novobiocin (Figure 3.78) exhibited poor or no inhibitory activity; their conjugation frequencies were greater than 50%. The inactivity of linoleic acid against the conjugal transfer of pKM101 is consistent with published literature, as it has been shown to be inactive against the IncN plasmid pKM101 (Fernandez-Lopez *et al.*, 2005).

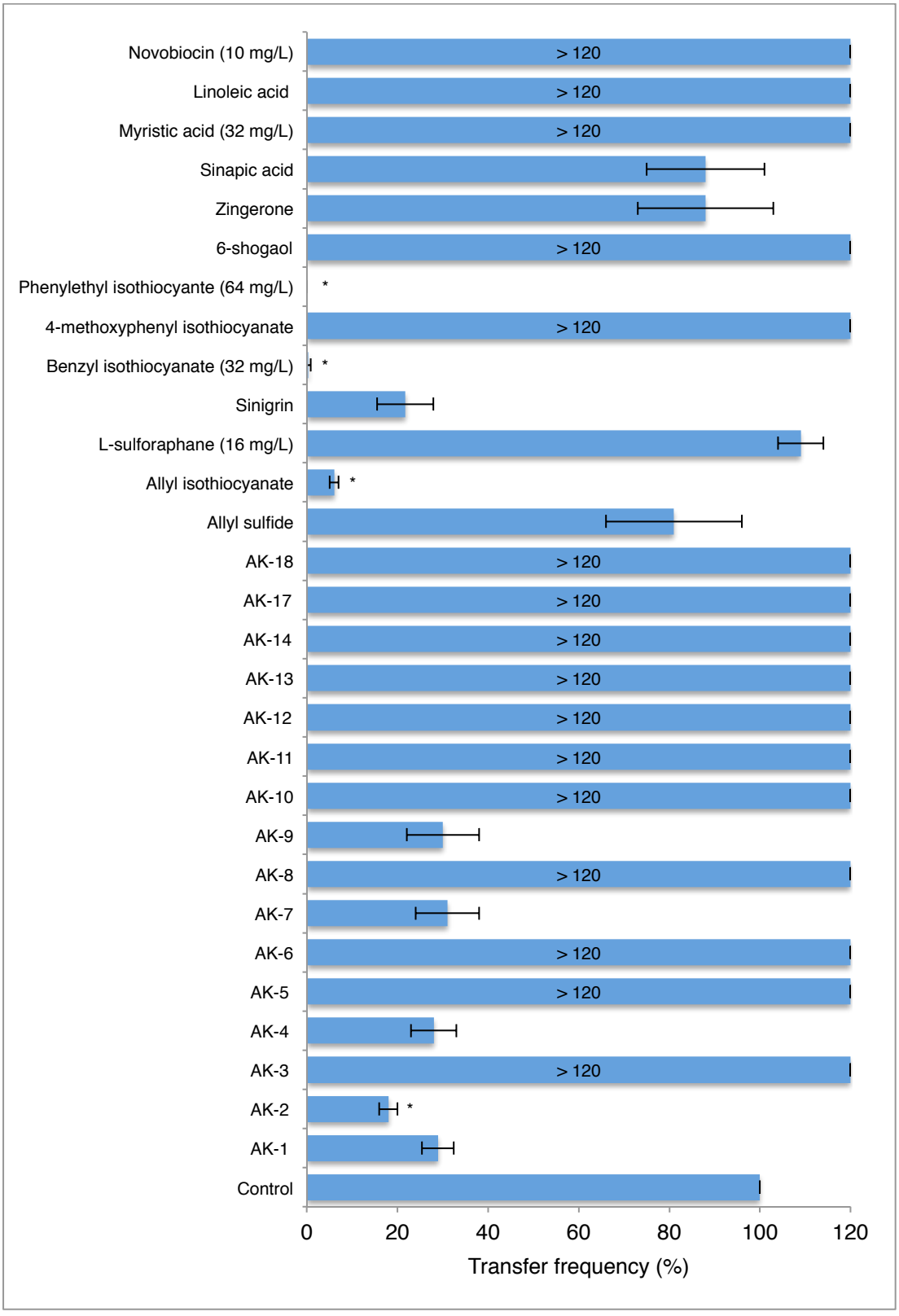

Each bar represents the mean transfer frequency ± SD of at least three independent experiments (*$p < 0.05$). Transfer frequency is expressed as a percentage relative to the control, which is without the test sample (100%).

Figure 3.77 The influence of the natural products on the conjugal transfer of IncN plasmid pKM101

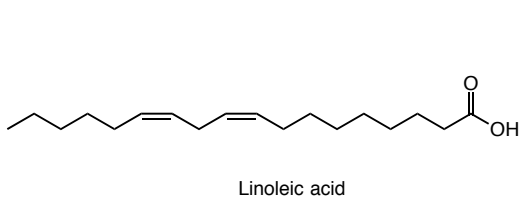

Linoleic acid

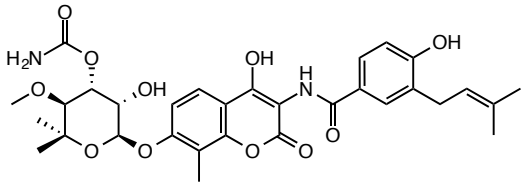

Novobiocin

Figure 3.78 Structures of linoleic acid and novobiocin

Novobiocin on the other hand, had previously been reported to have shown moderate anti-conjugative activity against pKM101 at a concentration of 10 µg/mL (Maree *et al*., 2014) but this was not observed in this study. Probably its activity is plasmid specific as a reduction in conjugal transfer was observed for plasmids TP114 and pUB307 (Figures 3.81 and 3.82). The observed activity of novobiocin against the plasmids TP114 and pUB307 may be due to its known inhibitory activity against the DNA gyrase B subunit (Maxwell, 1993; Maxwell, 1999; Hooper *et al*., 1984). Hooper and colleagues established the importance of a functioning DNA gyrase B subunit in bacterial conjugation (Hooper *et al*., 1989). They demonstrated this effect using coumermycin (Figure 3.79) a known DNA gyrase B subunit inhibitor against the transfer of plasmid R64drd-11 ($IncI_1$), which resulted in reduced plasmid conjugation (Hooper *et al*., 1989).

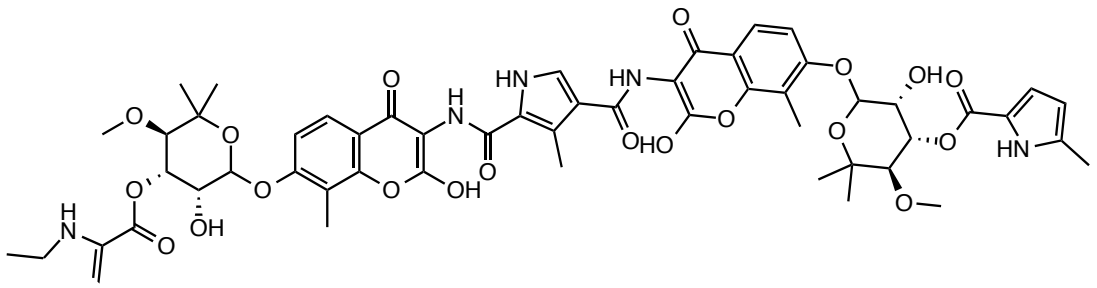

Figure 3.79 Structure of coumermycin

It is worth noting that these aminocoumarin compounds (coumermycin and novobiocin) may inhibit or reduce the conjugal transfer of some plasmids (Hooper *et al*., 1989), but they are

not true plasmid conjugal inhibitors (non-specific) as they do not target a conjugation-specific protein (Fernandez-Lopez *et al.*, 2005). They rather inhibit DNA gyrase, a general factor in DNA metabolism (Fernandez-Lopez *et al.*, 2005).

The challenge with any bacterial plasmid conjugation assay at present is that there are few known potent conjugal inhibitors, which are dehydrocrepenynic acid, linoleic acid, oleic acid (Fernandez-Lopez *et al.*, 2005), 2-hexadecynoic acid, 2-octadecynoic acid (Getino *et al.*, 2015) and, tanzawaic acid A and B (Getino *et al.*, 2016). In addition, these known conjugal inhibitors are plasmid incompatibility group-specific, which limits their use. So far there is no known true conjugal inhibitor (specific) for the plasmid incompatibility group N (IncN), P (IncP), and I_2 ($IncI_2$) hence the use of only a negative control for anti-conjugation screening. For IncW R7K plasmid, linoleic acid was used as the positive control. This is one plasmid incompatibility group (IncW), which is actively inhibited by all the known anti-conjugative agents.

3.3.2.2 The effect of natural products on the conjugal transfer of plasmid TP114 ($IncI_2$)

Of the 29 compounds assessed, BITC was the only compound, which actively inhibit the conjugal transfer of TP114 (Figure 3.81). At a concentration of 32 µg/mL, BITC significantly reduced the conjugal transfer frequency of TP114 to 10.00 ± 2.00%. The activity of PEITC (64 µg/mL) and AITC (100 µg/mL) were moderate, as they reduced the conjugal transfer of TP114 to 22.6 ± 4.0% and 29.0 ± 3.0%, respectively. Their activity was comparable to novobiocin (10 µg/mL), which reduced conjugation of TP114 to 26.6 ± 6.0%. Interestingly, the sinigrin-gluconasturtiin mixture (AK-3, 100 µg/mL), which was inactive against pKM101, showed moderate activity against TP114. It significantly reduced the conjugation of TP114 to 14.2 ± 1.7%, which was relatively better than novobiocin. The other compounds exhibited a varied activity from moderate to poor inhibition of conjugation.

3.3.2.3 The effect of natural products on the conjugal transfer of plasmid pUB307 (IncP)

4-Methoxyphenyl isothiocyanate and BITC (Figure 3.80) were the only active conjugal inhibitors against the conjugal transfer of plasmid pUB307. 4-Methoxyphenyl isothiocyanate (100 µg/mL) significantly reduced the conjugal transfer of plasmid pUB307 to 5.2 ± 2.8%. BITC (32 µg/mL) inhibited the conjugation of pUB307 to 7.0 ± 1.0%.

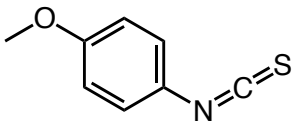

4-Methoxyphenyl isothiocyanate

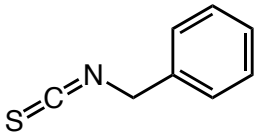

Benzyl isothiocyanate

Figure 3.80 Structures of the compounds, which actively inhibited the conjugal transfer of IncP plasmid pUB307

The inhibitory activity expressed by these two isothiocyanates (4-methoxyphenyl isothiocyanate and BITC) was relatively better than novobiocin, which is known to inhibit the conjugation of pUB307 (Maree *et al.*, 2014). Ten of the screened samples (**AK-1**, **AK-2**, **AK-10**, **AK-17**, **AK-18**, AITC, allyl sulfide, singrin, PEITC and sinapic acid) exhibited moderate activity, which was comparable to novobiocin. Their conjugal inhibition against plasmid pUB307 ranged from 15.2 ± 2.2% to 31.0 ± 6.0% (Figure 3.82). The other compounds exhibited poor or no inhibitory activity against the conjugal transfer of pUB307.

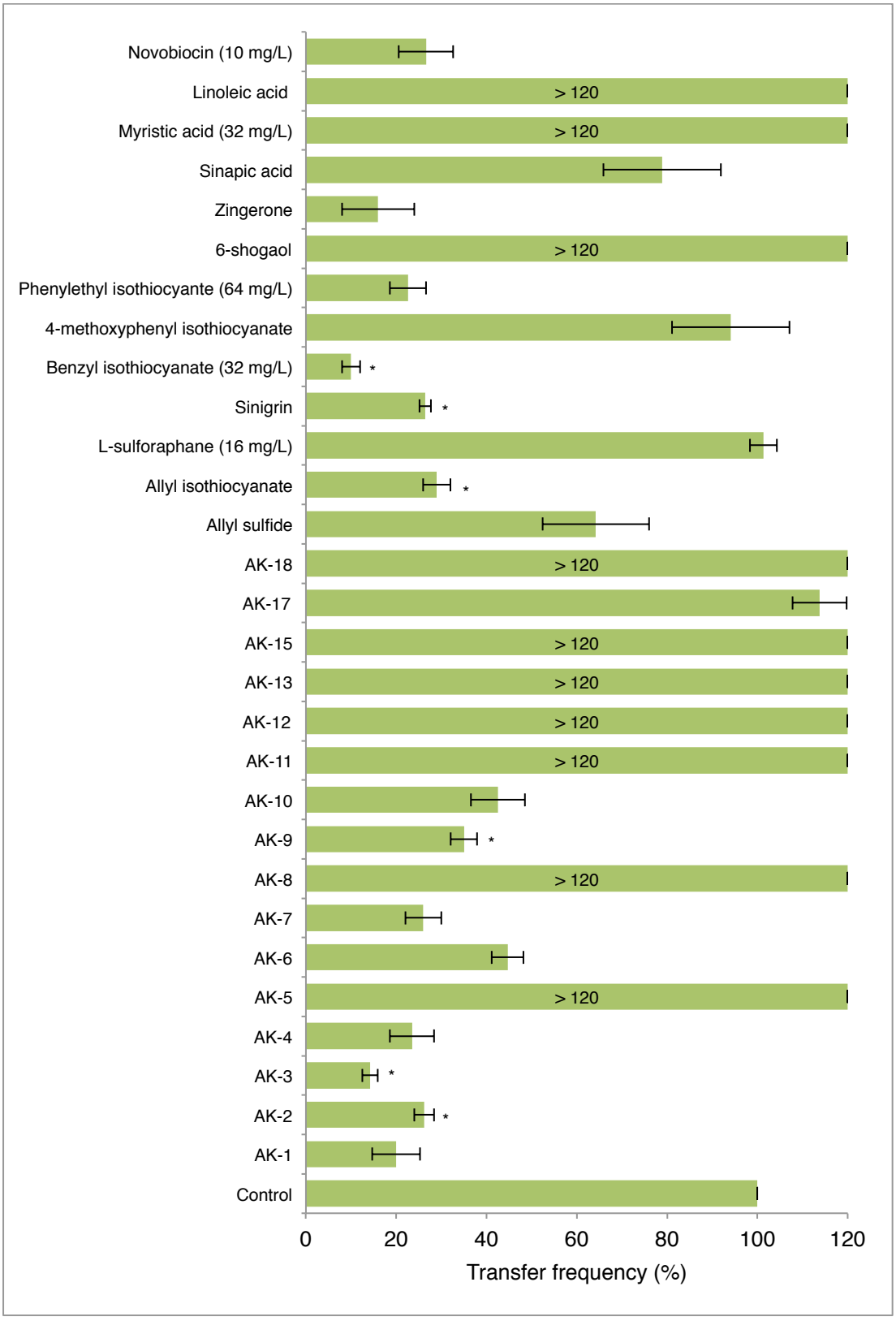

Each bar represents the mean transfer frequency ± SD of at least three independent experiments (*$p < 0.05$). Transfer frequency is expressed as a percentage relative to the control, which is without the test sample (100%).

Figure 3.81 The influence of the natural products on the conjugal transfer of IncI$_2$ plasmid TP114

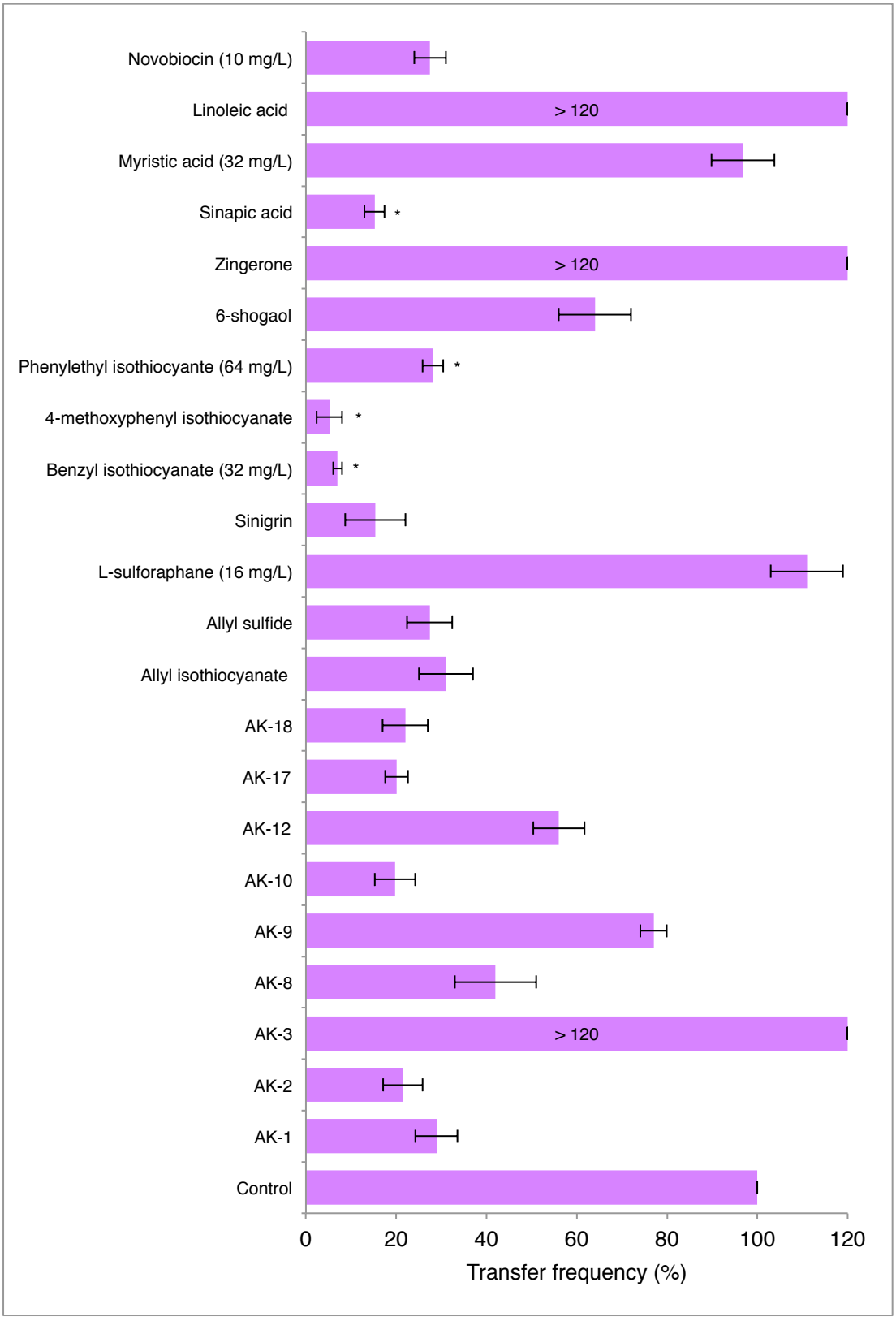

Each bar represents the mean transfer frequency ± SD of at least three independent experiments (*$p < 0.05$). Transfer frequency is expressed as a percentage relative to the control, which is without the test sample (100%).

Figure 3.82 The influence of the natural products on the conjugal transfer of IncP plasmid pUB307

3.3.2.4 The effect of natural products on the conjugal transfer of plasmid R7K (IncW)

None of the assessed compounds including the known moderate IncW plasmid inhibitor (linoleic acid) (Fernandez-Lopez *et al.*, 2005) were able to actively reduce the conjugal transfer of R7K to less than 10% (Figure 3.83). 11-oxo-11-((3-phenylpropyl)amino)undecanoic acid (**AK-17**) and L-sulforaphane (SFN) (Figure 3.84) were the only compounds that exhibited appreciable inhibitory activity comparable to the inhibitory

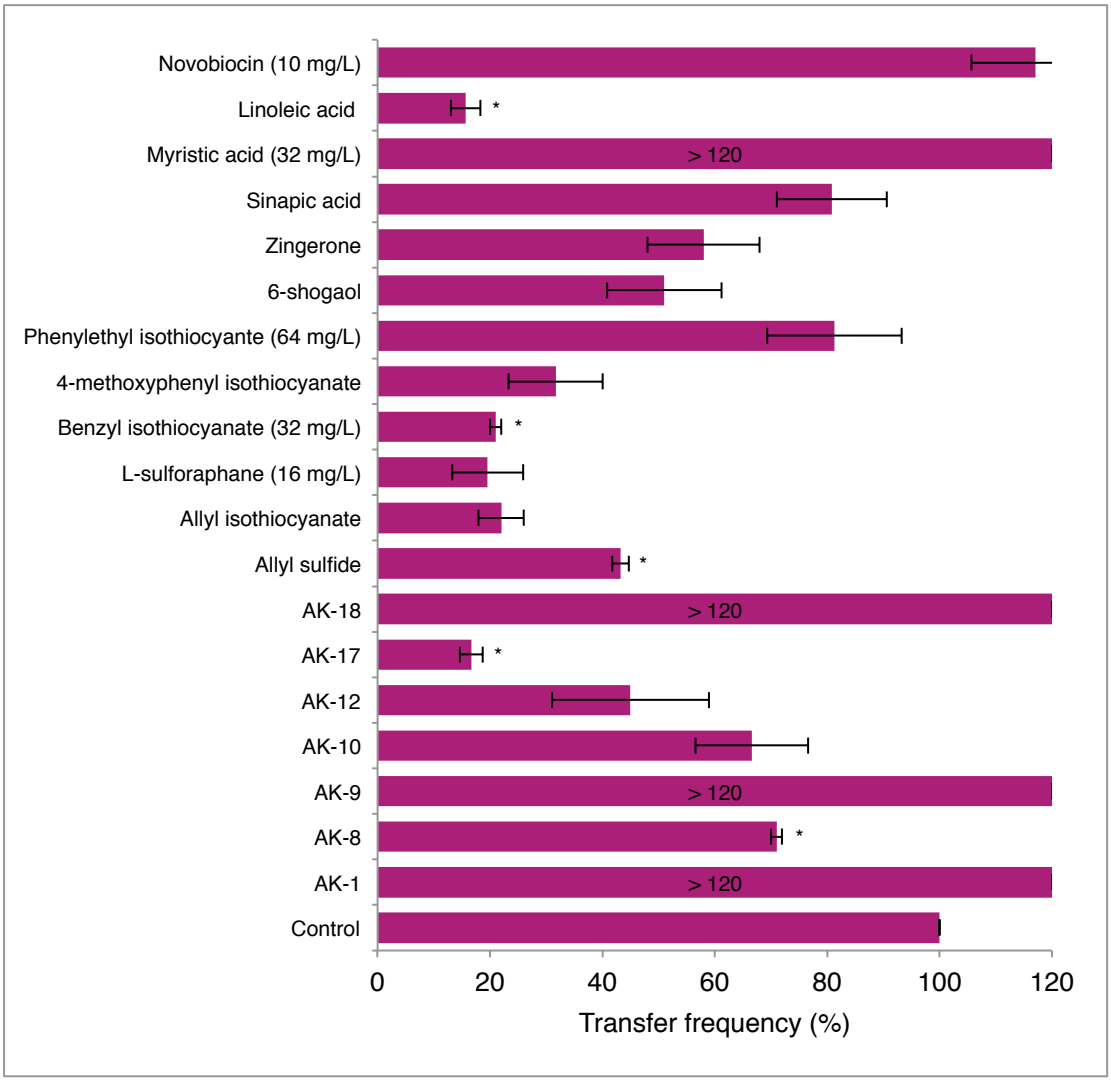

Each bar represents the mean transfer frequency ± SD of at least three independent experiments (*$p < 0.05$). Transfer frequency is expressed as a percentage relative to the control, which is without the test sample (100%).

Figure 3.83 The influence of the natural products on the conjugal transfer of IncW plasmid R7K

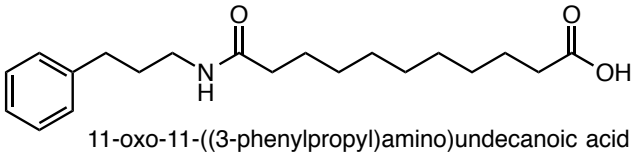

11-oxo-11-((3-phenylpropyl)amino)undecanoic acid

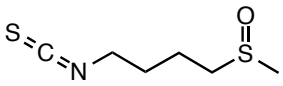

L-sulforaphane

Figure 3.84 Structures of the compounds, which showed appreciable inhibition against IncW plasmid R7K

activity of linoleic acid (15.7 ± 2.6%). **AK-17** and SFN reduced the conjugal transfer frequency of R7K to 16.7 ± 2.0% and 19.6 ± 6.3%, respectively. **AK-17** shares some structural features with linoleic acid, such as a long aliphatic chain and a carboxylic group, which has been shown to be essential for anti-conjugative activity (Getino *et al.*, 2015). In addition, it has an aromatic ring and this structural feature has been recently reported to contribute to the conjugal inhibitory activity of tanzawaic acid against IncW plasmids (Getino *et al.*, 2016). Given the structural similarities between **AK-17** and the two known IncW plasmid conjugation inhibitors, the similar structural features may probably explain for the observed anti-conjugative activity of **AK-17**. For SFN, we hypothesize that its oxygenated sulphur (S=O) and isothiocyanate (-N=C=S) moiety may be responsible for the observed anti-conjugative activity. As this compound does not have any of the structural features of previously reported IncW plasmid inhibitors (Getino *et al.*, 2015).

Overall, the isothiocyanate and glucosinolate compounds showed promising anti-conjugative activity against the test plasmids. BITC (32 µg/mL), PEITC (64 µg/mL) and AITC (100 µg/mL) showed consistent and significant active to moderate conjugal inhibitory activity against all the test plasmids (broad range inhibitory activity). 4-Methoxyphenyl isothiocyanate was active against the conjugal transfer of plasmid pUB307 and R7K. It reduced the conjugal transfer of pUB307 and R7K to 5.2 ± 2.8 and 31.7± 8.4%, respectively. Although 4-methoxyphenyl isothiocyanate has a similar chemical structure as BITC and PEITC, it did not show inhibitory activity against pKM101 and TP114. This may be due to the presence of a methoxyl group and the absence of a methylene unit in its chemical structure (Figure 3.80). Hence it may be active at a different target on the conjugation machineries, which

may be plasmid incompatibility group specific. This is possible, as the literature has shown component variation in the conjugation machineries, the mobilizable (MOB) and mating pair formation (Mpf) systems (Alvarez-Martinez and Christie, 2009; Smillie *et al.*, 2010; Getino *et al.*, 2015).

L-Sulforaphane was the only isothiocyanate compound, which showed specificity. It moderately inhibited the conjugal transfer of the IncW plasmid R7K to 19.6 ± 6.3% at a concentration of 16 µg/mL.

The glucosinolates (sinigrin, gluconapin (**AK-1**), and glucosinalbin (**AK-3**)) showed consistent and moderate conjugal inhibitory activity against plasmids pKM101, TP114 and pUB307. These results suggested that the isothiocyanates have better anti-conjugative activity than their precursors, the glucosinolates. To our knowledge this is the first report of anti-conjugative activity for these glucosinolate and isothiocyanate compounds. However, there are other reports of the biological activities for these compounds; such as their cancer chemo-protective activity (Wattenberg, 1977; Wattenberg, 1981; Chung *et al.*, 1985; Musk and Johnson, 1993; Hecht *et al.*, 1996; Chung *et al.*, 1996), antimicrobial activity (Kim and Lee, 2009; Jang *et al.*, 2010; Wilson *et al.*, 2013; Borges *et al.*, 2015), nematocidal activity (Lazzeri *et al.*, 1993; Mayton *et al.*, 1996) and their activity as allelochemicals (Brown and Morra, 1995; Charron and Sams, 1999; Smith, 2000).

A general observation with this broth conjugation assay was that the results were generally reproducible but the errors in determination of the conjugation frequency were mostly wide (> 20%). These wide deviations may be due to the fact that conjugal inhibition takes place in an extremely narrow range of concentration for some of these compounds. A similar observation has been made by Sarah Soares, a PhD student who is working on improving this system of screening. She is setting up a luminescence-based high-throughput conjugation assay in combination with a secondary assay that would rule out factors such as growth inhibition and plasmid loss.

3.3.2.5 The influence of concentration on the inhibitory effect of BITC on plasmid transfer

BITC (32 µg/mL), which showed good anti-conjugative activity, was further evaluated at sub-inhibitory concentrations (0.125 to 64 µg/mL) against the conjugal transfer of plasmids pKM101, TP114 and pUB307. The observed activities are shown in Figure 3.85.

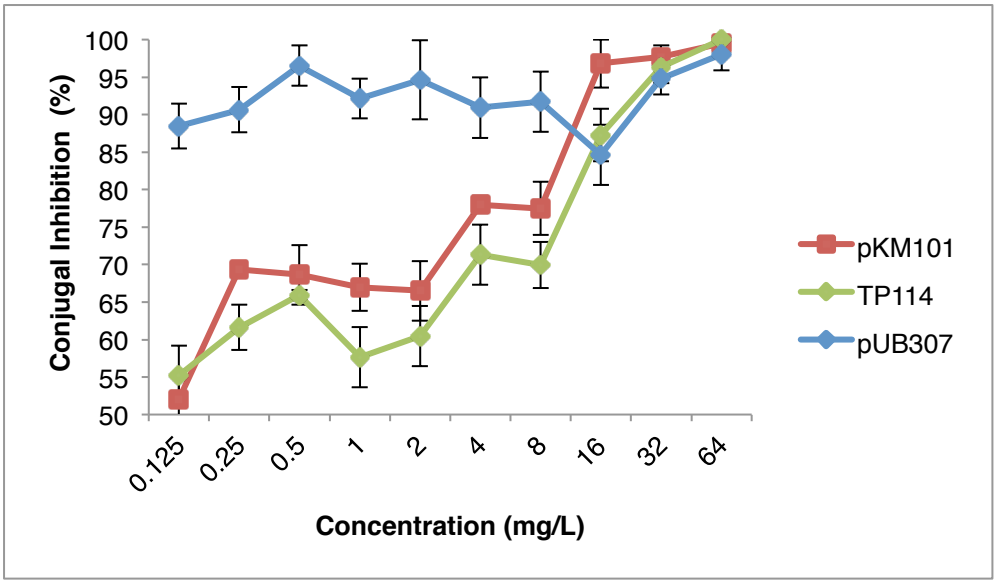

The values represent the mean conjugal inhibition frequency (%) ± SD of at least three independent experiments

Figure 3.85 The effect of varying concentrations of BITC on the conjugal transfer of plasmids pKM101 (IncN), TP114 ($IncI_2$) and pUB207 (IncP)

At a low concentration of 0.125 µg/mL, BITC moderately inhibited the conjugal transfer of all test plasmids by > 50%. A gradual increase in conjugation inhibition of plasmids pKM101 and TP114 was observed with an increase in concentration from 0.125 to 64 µg/mL (Figure 3.85). For plasmid pUB307, increase in concentration of BITC did not significantly change inhibitory activity, as BITC's conjugal inhibition ranged between 88.5 ± 3.0% and 98.0 ± 2.2% for concentrations 0.125 and 64 µg/mL, respectively. The IC_{50} of BITC was found to be 2.19, 1.24 and 0.34 µg/mL against pKM101, TP114 and pUB307 respectively. Their *p*-value was obtained to be 0.73, which indicated that the IC_{50}s were not significantly different .The anti-conjugative activity of BITC was found to be concentration dependent for plasmids pKM101

and TP114.

3.3.2.6 The influence of concentration on the inhibitory effect of 4-methoxyphenyl isothiocyanate on plasmid transfer of pUB307

4-methoxyphenyl isothiocyanate (100 µg/mL), which showed good anti-conjugative activity against the conjugal transfer of pUB307, was further evaluated at sub-inhibitory concentrations (1 to 128 µg/mL). The observed activities are shown in Figure 3.86.

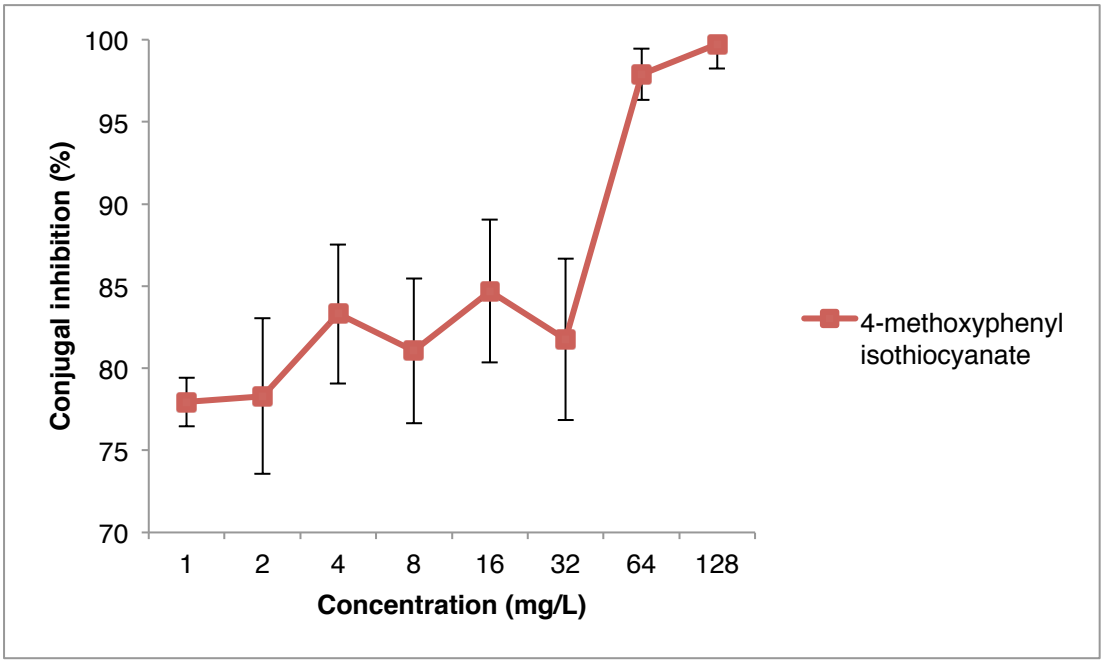

The values represent the mean conjugal inhibition frequency (%) ± SD of at least three independent experiments

Figure 3.86 The effect of varying concentrations of 4-methoxyphenyl isothiocyanate on the conjugal transfer of IncP plasmid pUB207

At a concentration of 1 µg/mL, 4-methoxyphenyl isothiocyanate moderately inhibited the conjugal transfer of plasmid pUB307 by 78.0 ± 1.5%. This inhibition frequency was steadily maintained to concentration 32 µg/mL, after which there was a sharp increase in conjugal inhibition of pUB307. Complete conjugal inhibition was observed at a concentration of 128 µg/mL, this suggests that the anti-conjugative activity of 4-methoxyphenyl isothiocyanate is concentration dependent.

3.3.2.7 The influence of concentration on the inhibitory effect of AK-17 on plasmid transfer of R7K (IncW)

AK-17 (11-oxo-11-((3-phenylpropyl)amino)undecanoic acid, 100 µg/mL), which showed good anti-conjugative activity against the conjugal transfer of R7K, was further evaluated at sub-inhibitory concentrations (16 to 256 µg/mL).

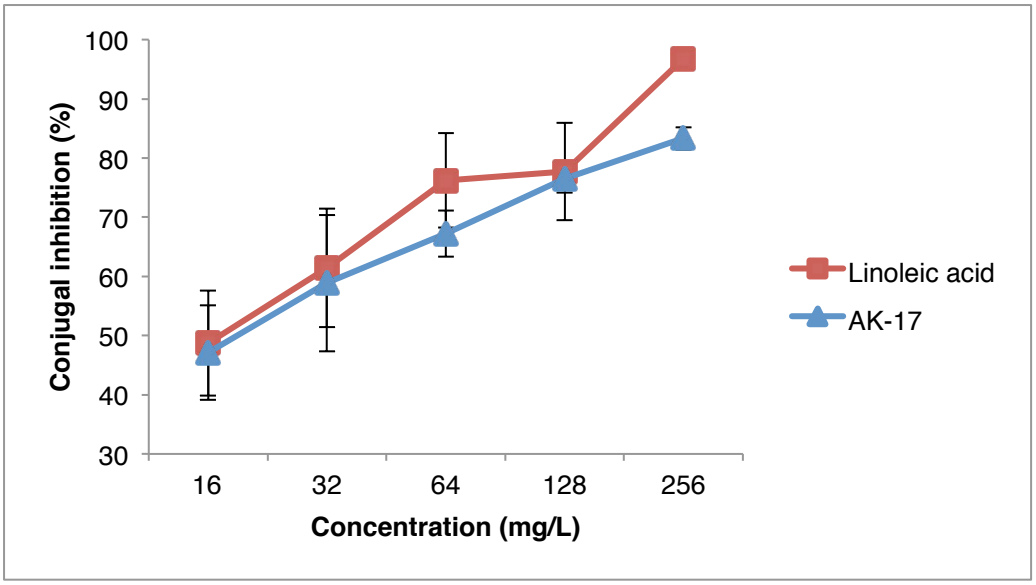

The values represent the mean conjugal inhibition frequency (%) ± SD of at least three independent experiments

Figure 3.87 The effect of varying concentrations of **AK-17** on the conjugal transfer of IncW plasmid R7K

AK-17 showed a gradual increase in conjugal inhibition of plasmid R7K with increase in concentration from 16 to 256 µg/mL (Figure 3.87). Its anti-conjugative activity was comparable to that of linoleic acid, although the activity of the linoleic acid seemed slightly better. The IC_{50} of linoleic acid and **AK-17** was found to be 60.5 and 77.8 µg/mL against the conjugal transfer of IncW plasmid R7K. Statistically the activity of both compounds were found to be the same as their *p*-value (0.68) indicated that their IC_{50s} were not significantly different.

3.3.3 Bacterial plasmid elimination studies

The compounds, which showed potent inhibition (transfer frequency < 20%) against the transfer of one or more plasmids, were further assessed for plasmid elimination activity. This was to help us determine whether plasmid loss contributed to their anti-conjugative activity. The inoculum sizes used for the plasmid elimination assay were pKM101 ($1.2 \times 10^{10} \pm 1.5 \times 10^{9}$ cfu/mL), TP114 ($1.1 \times 10^{10} \pm 3.4 \times 10^{9}$ cfu/mL), pUB307 ($1.6 \times 10^{10} \pm 5.3 \times 10^{9}$ cfu/mL) and R7K ($4.7 \times 10^{10} \pm 1.4 \times 10^{9}$ cfu/mL). The results of the plasmid elimination assay are summarized in Table 3.20.

Table 3.20 Plasmid elimination activity of selected compounds

Compound (µg/mL)	Plasmid elimination (%)[a]			
	pKM101 (IncN)	TP114 ($IncI_2$)	pUB307 (IncP)	R7K (IncW)
AK-1 (100)	0	0	0	0
AK-2 (100)	0	0	0	n.t
AK-17 (100)	0	0	0	0
Allyl isothiocyanate (100)	19.7 ± 6.6	6.6 ± 1.0	0	47.4 ± 7.2
L-sulforaphane (16)	0	66.0 ± 2.0	56.2 ± 2.9	12.4 ± 2.4
Sinigrin (100)	0	0	0	n.t
Benzyl isothiocyanate (32)	0	26.5 ± 8.0	0	0
4-methoxyphenyl isothiocyanate (100)	0	0	0	6.2 ± 1.2
Phenylethyl isothiocyanate (64)	0	78.0 ± 8.0	64.8 ± 15.4	3.0 ± 0.6
Control: Promethazine (16)	68.6 ± 15.0	37.2 ± 5.0	91.2 ± 6.7	8.3 ± 2.1

[a] The results are expressed as the number of colonies cured/number of colonies examined (percent eliminated) at one-quarter of their MICs. The results represent the mean ± SD of at least three independent experiments. n.t – not tested.

The glucosinolates (**AK-1**, **AK-2** and sinigrin) and the amide (**AK-17**) did not show plasmid eliminating activity against the test plasmids. The aliphatic isothiocyanates (AITC and SFN) on the other hand showed broad range of anti-plasmid activity. They were active against at least three of the test plasmids with SFN (16 µg/mL) exhibiting the most efficient elimination (> 50% elimination) against plasmids TP114 and pUB304 (Table 3.20). The aromatic isothiocyanates showed varied plasmid eliminating activity. BITC (32 µg/mL) showed moderate anti-plasmid activity against plasmid TP114 only, with a plasmid elimination of 26.5 ± 8.0% while 4-methoxyphenyl isothiocyanate (100 µg/mL) was active against plasmid R7K only, with a marginal plasmid elimination of 6.2 ± 1.2%. PEITC on the other hand showed plasmid elimination activity against TP114, pUB307 and R7K. At a concentration of 64 µg/mL, PEITC caused a 78.0 ± 8.0% and 64.6 ± 15.4% plasmid elimination of pUB307 and TP114, respectively. This was the highest anti-plasmid activity observed for the test compounds. PEITC's anti-plasmid activity against TP114 was also relatively higher than that of promethazine (16 µg/mL), a known anti-plasmid agent (Splenger *et al.*, 2006; Schelz *et al.*, 2006). The varied anti-plasmid activity of the isothiocyanates may be due to the different molecular mechanism of action exhibited by the isothiocyanates. From the results, it is plausible that compounds that exhibited moderate to high anti-plasmid activity (≥ 20% plasmid loss) against the test plasmids may have contributed to the observed reduction in conjugation of these plasmids, especially for PEITC and AITC (Figures 3.77, 3.81, 3.82 and 3.84). It is also worth noting that some of the test compounds such as SFN, showed moderate plasmid elimination of TP114 (66.0 ± 2.0% plasmid loss) and pUB307 (56.5 ± 2.9% plasmid loss) but this did not result in significant reduction in bacterial plasmid conjugation. SFN had no inhibitory effect on the bacterial plasmid conjugation of both plasmids; the conjugation transfer frequency was 101.3 ± 3.00% and 111.0 ± 8.0% for TP114 and pUB307, respectively (Figures 3.81 - 3.82). These findings suggested that plasmid elimination may contribute to reduction in conjugation for some compounds but may not necessarily be solely responsible for their anti-conjugative activity.

3.3.4 Antibiotic potentiation activity

Some of the compounds were further assessed for antibiotic potentiation activity by the broth microdilution method described by Smith *et al* (2005). The compounds were assessed at sub-inhibitory concentrations in combination with the relevant antibiotic against *S. aureus* strains over expressing MDR efflux pumps (SA-1199B which over-expresses the NorA pump and XU212 which over-expresses the TetK pump). The observed activities are summarized in the Table 3.21.

Table 3.21 Antibiotic potentiation activity of selected compounds

Test samples (µg/mL)	**MIC (µg/mL) for sample with indicated antibiotic for strain (fold reduction)**	
	SA-1199B (NorA) **Norfloxacin at 32 µg/mL**	**XU212 (TetK)** **Tetracycline at 128 µg/mL**
AK-1 (128)	> 32 (0)	> 128 (0)
AK-8 (32)	8 (4)	32 (4)
AK-12 (128)	16 (2)	128 (0)
AK-17 (16)	8(4)	64 (2)
AK-18 (128)	16 (2)	128 (0)
Shogaol (8)	8 (4)	64 (2)
Zingerone (128)	16 (2)	64 (2)
Allyl isothiocyanate (100)	16 (2)	64 (2)
Benzyl isothiocyanate (32)	< 0.0625 (> 512)	0.25 (512)
Reserpine (20)	8 (4)	64 (2)

BITC was the most active compound in the antibiotic potentiation assay (Table 3.21). At a concentration of 32 µg/mL, it reduced the MIC of norfloxacin from 32 to less than 0.0625 µg/mL against SA-1199B and the MIC of tetracycline from 128 to 0.25 µg/mL against XU212. Its antibiotic potentiation activity was better than reserpine (20 µg/mL), a known multidrug efflux pump inhibitor (Markham and Neyfakh, 1996; Gibbons and Udo, 2000). **AK-**

8 (32 µg/mL) exhibited a slightly better activity in comparison to reserpine. It caused a four-fold reduction in the MIC of tetracycline against XU212 but its activity against SA-1199B was same as reserpine's activity. **AK-17** (16 µg/mL) and shogaol (8 µg/mL) displayed a similar antibiotic potentiation activity to the control reserpine against the effluxing strains. They caused a four-fold reduction in the MIC of norfloxacin against SA-1199B and a two-fold reduction in the MIC of tetracycline against XU212. Zingerone and AITC displayed similar activities, a two-fold reduction in MICs of norfloxacin and tetracycline against the test strains. **AK-1** was the only compound, which did not show antibiotic activity potentiation against any of the test strains. It rather caused an increase in the MIC values. This increase in MIC value may be indicative of some interaction between **AK-1** and the antibiotics, possibly causing pronounced extrusion of the antibiotics. The other test compounds showed either a two-fold reduction or maintained the MIC of the antibiotics against the test strains.

The exact mechanism of antibiotic potentiation activity for these compounds against the MDR effluxing strains has not been identified. However, literature reports have shown that such compounds may achieve activity through; direct blockage of the efflux pumps thereby decreasing antibiotic extrusion (Poole, 2007; Shukla *et al*., 2007), formation of substrate complexes that allows entry in to the cell and/or prevent extrusion from the cell (Zloh *et al*., 2004), competitive or noncompetitive binding such that there is reduced extrusion of antibiotics (Ohene-Agyei *et al*., 2014) or disruption of the efflux pump's energy source (Schindler, 2013). Any one or a combination of these suggested mechanisms might have contributed to the observed antibiotic potentiation activities of the test compounds.

3.3.5 Antifungal activity studies

The alkaloidal extract of *L. sativum* and a few of the compounds were assessed for antifungal activity by the broth microdilution method according to the guidelines of EUCAST (Rodríguez-Tudela *et al*., 2003), against *C. albicans* ATCC 66027 and *C. tropicalis* ATCC 750. The observed activities are summarized in the Tables 3.22.

Table 3.22 Antifungal activity of selected compounds

Test sample		MIC (µg/mL)	
		***C. albicans* ATCC 66027**	***C. tropicalis* ATCC 750**
L. sativum alkaloidal extract		> 512	> 512
AK-17		512	32
AK-18		> 512	512
Control	Itraconazole	0.125	0.125
	Amphotericin B	0.25	0.25

AK-17 was the only test compound that showed antifungal activity, demonstrated by the low MIC value (32 µg/mL) against *C. tropicalis* ATCC 750. It had no antifungal activity against *C. albicans* ATCC 66027 like the other test compounds. The antifungal activity of **AK-17** against *C. tropicalis* ATCC 750 was lower compared to the control antifungals, itraconazole (0.125 µg/mL) and amphotericin B (0.25 µg/mL). One would expect that the *L. sativum* alkaloidal extract, from which the dimeric imidazoles were isolated, would have antifungal activity as azoles are well known for antifungal activity (Majoros and Kardos, 2008). However, this was not observed for the *L. sativum* alkaloidal extract, as their MICs against the test strains were greater than 512 µg/mL. The dimeric imidazoles isolates were not tested because of lack of sufficient quantities.

3.3.6 Cytotoxicity studies of benzyl isothiocyanate and allyl isothiocyanate

The toxicity levels of two of the identified anti-conjugative agents (BITC and AITC) were assessed against human dermal fibroblast, adult (HDFa; C-013-5C) cells. The Sulforhodamine B assay as previously described by Skehan *et al*. (1990) was used for the screening. The observed activities are shown in the Figure 3.88.

The IC_{50} of BITC and AITC against the HDFa cells were 30.3 µg/mL (203 µM) and 63.9 µg/mL (645 µM), respectively. A comparison of the cytotoxic value of BITC with its anti-conjugative concentration against the test plasmids revealed that its cytotoxic-IC_{50} level was above the concentration needed to cause 50% reduction in plasmid conjugal transfer (Figure

3.85; pKM101 (IC_{50} = 14.7 µM), TP114 (IC_{50} = 8.3 µM) and pUB307 (IC_{50} = 2.3 µM)). These data suggest that BITC showed anti-conjugative activity at non-toxic

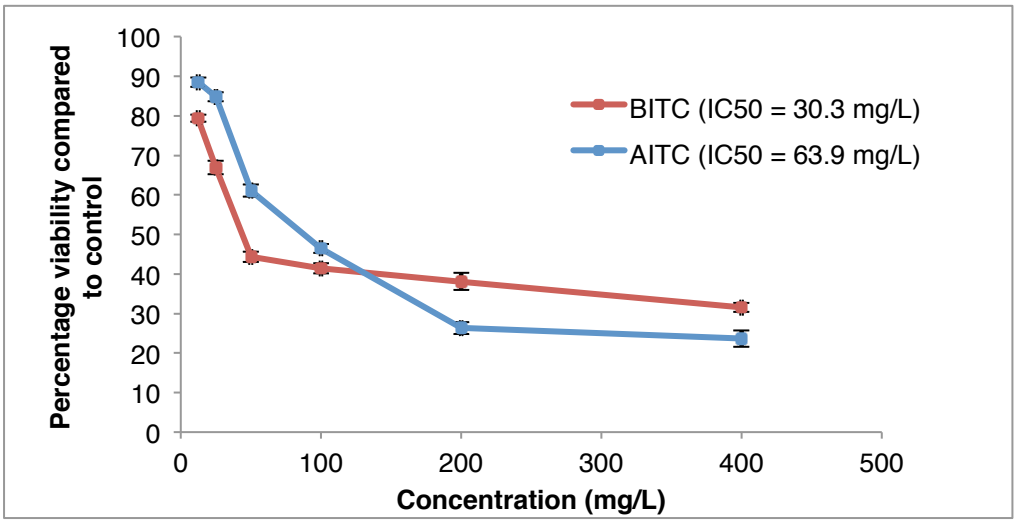

The values represent the mean cell viability (%) ± SD of at least three independent experiments

Figure 3.88 Cytotoxicity study using HDFa cells

concentrations. The same cannot be said about AITC as its cytotoxic-IC_{50} was below the 100 µg/mL, needed to cause about 69.0±6.0% to 94.0±1.0% reduction in conjugal transfer of the test plasmids (Figures 3.77 and 3.81-3.83). Although a dose response study was not conducted on AITC because it showed moderate anti-conjugative activity, the obtained data shows that its cytotoxic-IC_{50} is likely to be closer to the concentration needed to cause 50% reduction in plasmid transfer.

A comparison of the cytotoxic-IC_{50} of BITC (203 µM) with previously identified conjugal inhibitors showed some variations. BITC was less toxic than tanzawaic acid A (IC_{50} = 190 µM), tanzawaic acid B (IC_{50} = 180 µM), 2-hexadecynoic acid (IC_{50} = 100 µM) and 2-octadecynoic acid (IC_{50} = 90 µM) against the human foreskin fibroblasts ATCC (SCRC-1041) but was more toxic than oleic acid (IC_{50} = 350 µM) and linoleic acids (IC_{50} = 300 µM) (Getino *et al.*, 2016). Although they all exhibited some level of toxicity against the human cell lines, at their anti-conjugative IC_{50} they were non-toxic.

Chapter 4 Conclusions

4.1 Conclusions and future work

In this era where antimicrobial resistance is increasing and the world is running out of effective antimicrobials, identifying a potent compound, which inhibits the mechanism of dissemination of MDR genes and/ or a resistance mechanism, would be a better alternative to targeting bacterial growth processes. This alternative approach is necessary as the existing antibiotics, which target bacterial growth processes are unable to effectively inhibit the multidrug-resistant bacteria (Smith and Romesberg, 2007). Conjugation, a mechanism for the transfer MDR genes and multidrug-efflux pumps, proteinaceous transporters whose substance extrusion function confers multidrug-resistance in bacteria were targeted in this study.

Extracts of different polarity from eight selected medicinal plants (*Sinapis alba*, *Amoracia rusticana*, *Brassica oleracea*, *Lepidium sativum*, *Zingiber officinale*, *Myristica Iowiana*, *Borago officinalis* and *Uncaria tomentosa*) were screened against *Escherichia coli* conjugation pairs and *Staphylococcus aureus* strains expressing distinct efflux-related multidrug-resistance pumps for anti-conjugal and antibiotic potentiation activity, respectively. Of these, only extracts from *S. alba*, *L. sativum*, *Z. officinale*, *M. Iowiana* and *B. officinalis* showed promising anti-conjugal activity by reducing bacterial plasmid conjugation to less than 15% (Table 3.1). Further phytochemical work on the extracts led to the isolation of 19 compounds (Section 3.2.8.5), of which three were novel compounds, 2-(3-(3-((1*H*-imidazol-2-yl)methyl)-5methoxyphenoxy)benzyl)-1*H*-imidazole (AK-6), 9-oxo-9-((3-phenylpropyl) amino)nonanoic acid (AK-16) and 11-oxo-11-((3-phenylpropyl)amino)undecanoic acid (AK-17).

Biological evaluation of the isolated compounds and selected natural products led to the identification of 6 potent anti-conjugals; these were benzyl isothiocyanate (BITC),

phenylethyl isothiocyanate (PEITC), 4-methoxylphenyl isothiocyanate, allyl isothiocyanate, 11-oxo-11-((3-phenylpropyl)amino)undecanoic acid (AK-17) and sulforaphane. Of these, BITC and AK-17 were the most potent. BITC, an aromatic isothiocyanate from the *Brassica* vegetables showed a significantly broad-range anti-conjugal activity against all the tested plasmids. At a sub-inhibitory concentration of 32 µg/mL, it reduced the conjugal transfer of pKM101 (IncN), TP114 ($IncI_2$), pUB307 (IncP) and R7K (IncW) to 0.3 ± 0.6%, 10.0 ± 2.0%, 7.0 ± 1.0% and 21.0 ± 1.0%, respectively. It also exhibited moderate plasmid eliminating activity against plasmid TP114 only. Findings from this study suggest that the molecular structure such as that of BITC and PEITC (an aromatic ring linked to an isothiocyanate moiety by a methylene) promoted broad-range anti-conjugal activity. It was observed that, the absence of the methylene and substitution of a methoxyl group on the aromatic ring of a similar BITC structure resulted in a narrow-range of activity for 4-methoxylphenyl isothiocyanate. This finding would be useful for structural modification of the aromatic isothiocyanates for improved anti-conjugal activity and specificity.

AK-17, a new amide isolated from *M. lowiana* showed specificity in its conjugal inhibitory activity. It was active against the plasmid R7K, only. At a sub-inhibitory concentration of 100 µg/mL, it actively reduced the conjugal transfer of R7K to 16.7 ± 2.0%. Its anti-conjugal activity was comparable to the known IncW conjugation inhibitor, linoleic acid. AK-17 had no plasmid eliminating activity against the tested plasmids. Unpublished data from our laboratory showed that, AK-17 was non-toxic at its anti-conjugal concentration. This makes this compound a good candidate for further studies such as identification of its mechanism of action and for synthesis of analogues for improved activity. We propose the use of a binding assay and spectroscopy to study the affinity between these compounds and the plasmid DNA. Radiolabeled conjugation assay and genetic analysis could also be used to identify the target site and mechanism of action of the compound.

BITC, AK-17 and 5-hydroxy-1-(4-hydroxy-3-methoxyphenyl) dodecan-3-one (AK-8) were identified to have antibiotic potentiation activity at sub-inhibitory concentrations. They

significantly augmented the antibiotic activity of norfloxacin and tetracycline against MDR effluxing strains, SA-1199B (NorA) and XU212 (TetK), respectively. However, the exact mechanism of antibiotic potentiation was not identified in this study. We therefore recommend that further studies be carried out on these compounds and their analogues using methods such as intracellular accumulation assay to monitor direct inhibition of the substrate transport (Lomovskaya *et al.*, 2001), binding assay to study the affinity between these compounds and the efflux pumps (Su and Yu, 2007; Nakashima *et al.*, 2013) or computational methods to explore the molecular interactions and conformational changes between the compounds and the efflux pump (Trott and Olson, 2010; Durrant and McCammon, 2011).

In conclusion, promising natural product conjugal inhibitors and antibiotic potentiation agents were identified in this study. The work presented also shows that inhibition of bacterial conjugation and potentiation of antibiotic activity against MDR effluxing strains are rational approaches that should be considered in the search for new drugs to combat the spread of MDR genes and MDR bacteria.

Presentations

- UCL School of Pharmacy Research Day, 18th September 2015. Oral presentation: Natural product inhibitors of bacterial type IV secretion systems and efflux pumps.
- 12th ULLA Summer School (European University Consortium for Pharmaceutical Sciences) July 5-9, 2015, Paris, France. Poster presentation: Natural product inhibitors of conjugal transfer of plasmid mediated antibiotic resistance in *E. coli*.
- 54th Annual Interscience Conference on Antimicrobial Agents and Chemotherapy (ICAAC), September 5-9, 2014, Washington DC, USA. Poster presentation: Natural product inhibitors of conjugal transfer of plasmid mediated antibiotic resistance in *E. coli*.
- 54th Annual Interscience Conference on Antimicrobial Agents and Chemotherapy

(ICAAC), September 5-9, 2014, Washington DC, USA. Poster presentation: Screening for natural product inhibitors of multidrug-efflux pumps in *S. aureus.*

- UCL School of Pharmacy Research Day, 18th September 2015. Poster presentation: Screening for natural product inhibitors of plasmid transfer and multidrug-efflux.

The following manuscripts are under preparation from the work reported in this thesis:

- A new imidazole alkaloid from *Lepidium sativum*
- Bioactive amides from *Myristica lowiana*

References

ADOLPH, S., BACH, S., BLONDEL, M., CUEFF, A., MOREAU, M., POHNERT, G., POULET, S. A., WICHARD, T. & ZUCCARO, A. 2004. Cytotoxicity of diatom-derived oxylipins in organisms belonging to different phyla. *Journal of Experimental Biology,* 207**,** 2935-2946.

AGERSO, Y. & GUARDABASSI, L. 2005. Identification of Tet 39, a novel class of tetracycline resistance determinant in *Acinetobacter* spp. of environmental and clinical origin. *Journal of Antimicrobial Chemotherapy,* 55**,** 566-569.

AGUILAR, J. L., ROJAS, P., MARCELO, A., PLAZA, A., BAUER, R., REININGER, E., KLAAS, C. A. & MERFORT, I. 2002. Anti-inflammatory activity of two different extracts of *Uncaria tomentosa* (Rubiaceae). *Journal of Ethnopharmacology* 81**,** 271-276.

AHN, E. & OH, J. S. 2012. Inhibitory effect of galanolactone isolated from *Zingiber officinale* Roscoe extract on adipogenesis in 3T3-L1 cells. *Journal of the Korean Society for Applied Biological Chemistry,* 55**,** 63-68.

AHN, S. I., LEE, J. K. & YOUN, H. S. 2009. Inhibition of homodimerization of toll-like receptor 4 by 6-shogaol. *Molecules and Cells,* 27**,** 211-215.

AIRES, A., MOTA, V. R., SAAVEDRA, M. J., ROSA, E. A. & BENNETT, R. N. 2009. The antimicrobial effects of glucosinolates and their respective enzymatic hydrolysis products on bacteria isolated from the human intestinal tract. *Journal of Applied Microbiology,* 106**,** 2086-2095.

ALCARAZ, L. E., BLANCO, S. E., PUIG, O. N., TOMAS, F. & FERRETTI, F. H. 2000. Antibacterial activity of flavonoids against methicillin-resistant *Staphylococcus aureus* strains. *Journal of Theoretical Biology,* 205**,** 231-240.

ALEKSHUN, M. N. & LEVY, S. B. 2007. Molecular mechanisms of antibacterial multidrug resistance. *Cell,* 128**,** 1037-1050.

ALVAREZ-MARTINEZ, C. E. & CHRISTIE, P. J. 2009. Biological diversity of prokaryotic type IV secretion systems. *Microbiology and Molecular Biology Reviews,* 73**,** 775-808.

AMABILE-CUEVAS, C. F. 2013. Antibiotic resistance: from Darwin to Lederberg to Keynes. *Microbial Drug Resistance,* 19**,** 73-87.

ANDREWS, J. M. 2001. Determination of minimum inhibitory concentrations. *Journal of Antimicrobial Chemotherapy,* 48**,** 5-16.

APPELQVIST, L. D., KORNFELD, A. K. & WENNERHOLM, J. E. 1981. Sterols and steryl esters in some *Brassica* and *Sinapis* seeds. *Phytochemistry,* 20**,** 207-210.

AQUINO, R., DE FEO, V., DE SIMONE, F., PIZZA, C. & CIRIO, G. 1991. Plant metabolites. new compounds and anti- inflammatory activity of *Uncaria tomentosa*. *Journal of*

Natural Produts 54**,** 453-459.

AQUINO, R., DE SIMONE, F., VINCIERI, F. F. & PIZZA, C. 1990. New polyhydroxylated triterpenes from *Uncaria tomentosa*. *Journal of Natural Products,* 53**,** 559-564.

ARAYA, J. J., ZHANG, H., PRISINZANO, T. E., MITSCHER, L. A. & TIMMERMANN, B. N. 2011. Identification of unprecedented purine-containing compounds, the zingerines, from ginger rhizomes (*Zingiber officinale* Roscoe) using a phase-trafficking approach. *Phytochemistry,* 72**,** 935-941.

ARES, A. M., NOZAL, M. J., BERNAL, J. L. & BERNAL, J. 2014. Optimized extraction, separation and quantification of twelve intact glucosinolates in broccoli leaves. *Food Chemistry,* 152**,** 66-74.

ARUTYUNOV, D. & FROST, L. S. 2013. F conjugation: back to the beginning. *Plasmid,* 70**,** 18-32.

AURNHAMMER, G., WAGNER, H., HORHAMRNER, L. & FARKAS, L. 1971. Notiz iiber die synthese des thevetiaflavons, eines apigenin-5-methylathers aus *Thevetia peruviana*. *European Journal of Inorganic Chemistry,* 104**,** 1703-1705.

AVILA, H. P., SMANIA EDE, F., MONACHE, F. D. & SMANIA, A., JR. 2008. Structure-activity relationship of antibacterial chalcones. *Bioorganic & Medicinal Chemistry,* 16**,** 9790-9794.

BABU, K. S., BABU, T. H., SRINIVAS, P. V., KISHORE, K. H., MURTHY, U. S. & RAO, J. M. 2006. Synthesis and biological evaluation of novel C (7) modified chrysin analogues as antibacterial agents. *Bioorganic & Medicinal Chemistry Letters,* 16**,** 221-224.

BABU, K. S., BABU, T. H., SRINIVAS, P. V., SASTRY, B. S., KISHORE, K. H., MURTY, U. S. & RAO, J. M. 2005. Synthesis and in vitro study of novel 7-*O*-acyl derivatives of Oroxylin A as antibacterial agents. *Bioorganic & Medicinal Chemistry Letters,* 15**,** 3953-3956.

BALIGA, M. S., HANIADKA, R., PEREIRA, M. M., D'SOUZA, J. J., PALLATY, P. L., BHAT, H. P. & POPURI, S. 2011. Update on the chemopreventive effects of ginger and its phytochemicals. *Critical Reviews in Food Science and Nutrition,* 51**,** 499-523.

BALKE, D. T. & DIOSADY, L. L. 2000. Rapid aqueous extraction of mucilage from whole white mustard seed. *Food Research International* 33**,** 347-356.

BARILLARI, J., GUEYRARD, D., ROLLIN, P. & IORI, R. 2001. *Barbarea verna* as a source of 2-phenylethyl glucosinolate, precursor of cancer chemopreventive phenylethyl isothiocyanate. *Fitoterapia,* 72**,** 760-764.

BARON, C. & COOMBES, B. 2007. Targeting bacterial secretion systems: benefits of disarmament in the microcosm. *Infectious Disorders-Drug Targets (Formerly Current Drug Targets-Infectious Disorders),* 7**,** 19-27.

BARRON, D. & IBRAHIM, R. K. 1996. Isoprenylated flavonoids - A survey. *Phytochemistry* 43**,** 921-982.

BENNETT, P. M. 2008. Plasmid encoded antibiotic resistance: acquisition and transfer of antibiotic resistance genes in bacteria. *British Journal Pharmacology,* 153 Suppl 1**,** S347-S57.

BENNETT, P. M., GRINSTED, J. & RICHMOND, M. H. 1977. Transposition of TnA does not generate deletions. *Molecular and General Genetics MGG,* 154**,** 205-211.

BERGSSON, G., ARNFINNSSON, J., S., K., STEINGRIMSSON, O. & THORMAR, H. 1998. *In vitro* Inactivation of *Chlamydia trachomatis* by fatty acids and monoglycerides. *Antimicrobial Agents and Chemotherapy,* 42**,** 2290-2294.

BERGSSON, G., STEINGRIMSSON, O. & THORMAR, H. 1999. *In vitro* susceptibilities of *Neisseria gonorrhoeae* to fatty acids and monoglycerides. *Antimicrobial Agents and Chemotherapy,* 43**,** 2790-2792.

BERNHARD, R. A., SAGHIR, A. R., JACOBSEN, J. V. & MANN, L. K. 1964. Isolation and identification of allyl monosulfide and ally alcohol from *Allium*. *Archives of Biochemistry and Biophysics,* 107**,** 137-140.

BORGES, A., ABREU, A. C., FERREIRA, C., SAAVEDRA, M. J., SIMOES, L. C. & SIMOES, M. 2015. Antibacterial activity and mode of action of selected glucosinolate hydrolysis products against bacterial pathogens. *Journal of Food Science and Technology,* 52**,** 4737-4748.

BOSWELL, J. T. & SOWERBY, J. 1863. *English botany: or coloured figures of British plants.,* Piccadilly, London, Robert Hardwicke.

BOUCHER, H. W., TALBOT, G. H., BRADLEY, J. S., EDWARDS, J. E., GILBERT, D., RICE, L. B., SCHELD, M., SPELLBERG, B. & BARTLETT, J. 2009. Bad bugs, no drugs: no ESKAPE! An update from the Infectious Diseases Society of America. *Clinical Infectious Diseases,* 48**,** 1-12.

BOYAVAL, P., CORRE, C., DUPUIS, C. & ROUSSEL, E. 1995. Effects of free fatty acids on propionic acid bacteria. *Le Lait,* 75**,** 17-29.

BRADFORD, P. A. 2001. Extended-spectrum beta-lactamases in the 21st century: characterization, epidemiology, and detection of this important resistance threat. *Clinical Microbiology Reviews,* 14**,** 933-51, table of contents.

BROWN, J. P. 1980. A review of the genetic effects of naturally occurring flavonoids, anthraquinones and related compounds. *Mutation Research,* 75**,** 243-277.

BROWN, P. D. & MORRA, M. J. 1995. Glucosinolate-containing plant tissues as bioherbicides. *Journal of Agricultural and Food Chemistry,* 43**,** 3070-3074.

BUCAR, F., WUBE, A. & SCHMID, M. 2013. Natural product isolation-how to get from biological material to pure compounds. *Natural Product Reports,* 30**,** 525-545.

BUCK, P. A. 1956. Origin and taxonomy of broccoli. *Economic Botany,* 10**,** 250-253.

CAO, G. Y., XU, W., YANG, X. W., GONZALEZ, F. J. & LI, F. 2015. New neolignans from the seeds of *Myristica fragrans* that inhibit nitric oxide production. *Food Chemistry,* 173**,** 231-237.

CARATTOLI, A. 2009. Resistance plasmid families in Enterobacteriaceae. *Antimicrobical Agents and Chemotherapy,* 53**,** 2227-2238.

CDC 2013. Centers for Disease Control and Prevention. Antibiotic resistance threats In the United States, 2013.

CEJPEK, K., VALUŠEK, J. & VELÍŠEK, J. 2000. Reactions of allyl isothiocyanate with alanine, glycine, and several peptides in model systems. *Journal of Agricultural and Food Chemistry,* 48**,** 3560-3565.

CHAMBERLAIN, N. R., MEHRTENS, B. G., XIONG, Z., KAPRAL, F. A., BOARDMAN, J. L. & REARICK, J. I. 1991. Correlation of carotenoid production, decreased membrane fluidity, and resistance to oleic acid killing in *Staphylococcus aureus* 18Z. *Infection And Immunity,* 59**,** 4332-4337.

CHARI, V. M., JORDAN, M., WAGNER, H. & THIES, P. W. 1977. A 13C-NMR study of the structure of acyl-linarin *Valeriana wallichii*. *Phytochemistry,* 16**,** 1110-1112.

CHARPENTIER, N., BOSTYN, S. & COIC , J. P. 1998. Isolation of a rich glucosinolate fraction by liquid chromatography from an aqueous extract obtained by leaching dehulled rapeseed meal (*Brassica napus* L.). *Industrial Crops and Products* 8**,** 151 - 158.

CHARRON, C. G. & SAMS, C. E. 1999. Inhibition of *Pythium ultimum* and *Rhizoctonia solani* by shredded leaves of *Brassica* species. *Journal of the American Society of Horticultural Science,* 124**,** 462-467.

CHENG, W., ZHU, C., XU, W., FAN, X., YANG, Y., LI, Y., CHEN, X., WANG, W. & SHI, J. 2009. Chemical constituents of the bark of *Machilus wangchiana* and their biological activities. *Journal of Natural Products* 72**,** 2145–2152

CHEVALLIER, A. 2001. *Encyclopedia of medicinal plants,* London, United Kingdom, Dorling Kindersley Ltd.

CHISHOLM, M. D. & WETTER, L. R. 1964. Biosynthesis of mustard oil glucosides: iv. the administration of methionine-C14 and related compounds to horseradish. *Canadian Journal of Biochemistry,* 42**,** 1033-1040.

CHOI, J. S., PARK, N. H., HWANG, S. Y., SOHN, J. H., KWAK, I., CHO, K. K. & CHOI, I. S. 2013. The antibacterial activity of various saturated and unsaturated fatty acids against several oral pathogens. *Journal of Environmental Biology,* 34**,** 673-676.

CHUNG, F. L., KELLOFF, G., STEELE, V., PITTMAN, B., ZANG, E., JIAO, D., RIGOTTY, J., CHOI, C. I. & RIVENSON, A. 1996. Chemopreventive efficacy of arylalkyl isothiocyanates and *N*-acetylcysteine for lung tumorigenesis in Fischer rats. *Cancer Research* 56**,** 772-778.

CHUNG, F. L., WANG, M. & HECHT, S. S. 1985. Effects of dietary indoles and isothiocyanates on *N*-nitrosodimethylamine and 4-(methylnitrosamine)-1-(3-pyridyl)-1-butanone alpha- hydroxylation and DNA methylation in rat liver. *Cancer Research,* 45**,** 539-543.

COETZEE, J. N., DATTA, N. & HEDGES, R. W. 1972. R factors from *Proteus rettgeri*. *Microbiology,* 72**,** 543-552.

COUTURIER, M., EBEX, F., BERGQUIST, P. L. & MAAS, W. K. 1988. Identification and classification of bacterial plasmids. *Microbiological Reviews,* 52**,** 375-395.

COX, J. R. & SERPERSU, E. H. 1997. Biologically important conformations of aminoglycoside antibiotics bound to an aminoglycoside 3'-phosphotransferase as determined by transferred nuclear overhauser effect spectroscopy. *Biochemistry,* 36**,** 2353-2359.

DATTA, N. & HEDGES, R. W. 1971. Compatibility groups among fi– R factors. *Nature,* 234**,** 222-223.

DE WILDE, W. 2000. *Flora Malesiana. Myristicaceae,* The Netherlands, Nationaal Nederland, Universiteit Leiden branch.

DELCOUR, A. H. 2009. Outer membrane permeability and antibiotic resistance. *Biochim Biophys Acta,* 1794**,** 808-16.

DESBOIS, A. P., LEBL, T., YAN, L. & SMITH, V. J. 2008. Isolation and structural characterisation of two antibacterial free fatty acids from the marine diatom, *Phaeodactylum tricornutum*. *Applied Microbiology and Biotechnology,* 81**,** 755-764.

DESBOIS, A. P. & SMITH, V. J. 2010. Antibacterial free fatty acids: activities, mechanisms of action and biotechnological potential. *Applied Microbiology and Biotechnology,* 85**,** 1629-1642.

DIAS, C., AIRES, A. & SAAVEDRA, M. J. 2014. Antimicrobial activity of isothiocyanates from cruciferous plants against methicillin-resistant *Staphylococcus aureus* (MRSA). *Applied Microbiology and Biotechnology,* 15**,** 19552-19561.

DIMROTH, P. 1997. Primary sodium ion translocating enzymes. *Biochimica et Biophysica Acta***,** 11-51.

DIVAKARAN, V. & BABU, K. N. 2016. Mustard. In: Encyclopedia of Food and Health. 4**,** 10-19.

DODSON, C. D. & STERMITZ, F. R. 1986. Pyrrolizidine alkaloids from borage (*Borago officinalis*) seeds and flowers. *Journal of Natural Products,* 49**,** 727-728.

DOUCET-POPULAIRE, F., TRIEU-CUOT, P., ANDREMONT, A. & COURVALIN, P. 1992. Conjugal transfer of plasmid DNA from *Enterococcus faecalis* to *Escherichia coli* in digestive tracts of gnotobiotic mice. *Antimicrobial Agents and Chemotherapy,* 36**,** 502-504.

DU, Q., ZHANG, L., CUI, H., WANG, K., XIU, L. & SHENG, L. 2008. Isolation of glucosinolates from broccoli seeds by use of high-speed countercurrent chromatography. *Acta Chromatographica,* 20**,** 489-496.

DUGAN, J., ROCKEY, D. D., JONES, L. & ANDERSEN, A. A. 2004. Tetracycline resistance in *Chlamydia suis* mediated by genomic islands inserted into the chlamydial inv-like gene. *Antimicrobial agents and chemotherapy,* 48**,** 3989-3995.

DURKEET, A. B. & HARBORNE, J. B. 1973. Flavonol glycosides in *Brassica* and *Sinapis*. *Phytochemistry,* 12**,** 1085-1089.

DURRANT, J. D. & MCCAMMON, J. A. 2011. Molecular dynamics simulations and drug discovery. *BMC Biology,* 9**,** 71.

EDDOUKS, M., MAGHRANI, M., ZEGGWAGH, N. A. & MICHEL, J. B. 2005. Study of the hypoglycaemic activity of *Lepidium sativum* L. aqueous extract in normal and diabetic rats. *Journal of Ethnopharmacology,* 97**,** 391-395.

EDIAGE, E. N., DI MAVUNGU, J. D., SCIPPO, M. L., SCHNEIDER, Y. J., LARONDELLE, Y., CALLEBAUT, A., ROBBENS, J., VAN PETEGHEM, C. & DE SAEGER, S. 2011. Screening, identification and quantification of glucosinolates in black radish (*Raphanus sativus* L. *niger*) based dietary supplements using liquid chromatography coupled with a photodiode array and liquid chromatography-mass spectrometry. *Journal of Chromatography A,* 1218**,** 4395-43405.

EKUNDAYO, O., LAAKSO, I. & HILTUNEN, R. 1988. Composition of ginger (*Zingiber officinale* Roscoe) volatile oils from Nigeria. *Flavour and Fragrance Journal,* 3**,** 85-90.

ENDO, K., KANNO, E. & OSHIMA, Y. 1990. Structures of antifungal diarylheptenones, gingerenones A, B, C and isogingerenone B, isolated from the rhizomes of *Zingiber officinale*. *Phytochemistry,* 29**,** 797-799.

ENGELS, C., SCHIEBER, A. & GÄNZLE, M. G. 2012. Sinapic acid derivatives in defatted oriental mustard (*Brassica juncea* L.) seed meal extracts using UHPLC-DAD-ESI-MS n and identification of compounds with antibacterial activity. *European Food Research and Technology,* 234**,** 535-542.

ENGLER, M. M. & ENGLER, M. B. 1998. Dietary borage oil alters plasma, hepatic and vascular tissue fatty acid composition in spontaneously hypertensive rats. *Prostaglandins, Leukotrienes and Essential Fatty Acids,* 59**,** 11-15.

FABRE, N., BON, M., MOULIS, C., FOURASTE, I. & STANISLA, E. 1997. Three glucosinolates from seeds of *Brassica juncea. Phytochemistry,* 45**,** 525-527.

FAHEY, J. W., ZALCMANN, A. T. & TALALAY, P. 2001. The chemical diversity and distribution of glucosinolates and isothiocyanates among plants. *Phytochemistry* 56**,** 5-51.

FAHEY, J. W., ZHANG, Y. & TALALAY, P. 1997. Broccoli sprouts: An exceptionally rich source of inducers of enzymes that protect against chemical carcinogens.

Proceedings of the National Academy of Sciences 94**,** 10367-10372.

FELDLAUFER, M. F., KNOX, D. A., LUSBY, W. R. & SHIMANUKI, H. 1993. Antimicrobial activity of fatty acids against *Bacillus* larvae, the causative agent of American foulbrood disease *Apidologie,* 24**,** 95-99.

FENWICK , G. R. & HEANEY, R. K. 1983. Glucosinolates and their breakdown products in cruciferous crops, foods and feeding stuffs. *Food Chemistry* 11**,** 249-271.

FERNÁNDEZ, S., WASOWSKI, C., PALADINI, A. C. & MARDER, M. 2004. Sedative and sleep-enhancing properties of linarin, a flavonoid-isolated from *Valeriana officinalis*. *Pharmacology Biochemistry and Behavior,* 77**,** 399-404.

FERNANDEZ-LOPEZ, R., MACHON, C., LONGSHAW, C. M., MARTIN, S., MOLIN, S., ZECHNER, E. L., ESPINOSA, M., LANKA, E. & DE LA CRUZ, F. 2005. Unsaturated fatty acids are inhibitors of bacterial conjugation. *Microbiology,* 151**,** 3517-3526.

FOSTER, S. & HOBBS, C. 2002. *A field guide to Western medicinal plants and herbs,* Boston, MA, United States, Houghton Mifflin

FRANCIS, K. S., SURESH, E. & NAIR, M. S. 2014. Chemical constituents from *Myristica fragrans* fruit. *Natural Product Research,* 28**,** 1664-1668.

FRANZ, C., BAUER, R., CARLE, R., TEDESCO, D., TUBARO, A. & ZITTERL-EGLSEER, K. 2007. Study on the assessment of plants/herbs, plant/herb extracts and their naturally or synthetically produced components as 'additives' for use in animal production. *European Food Safety Authority Journal***,** 1-297.

FRONZES, R., SCHÄFER, E., WANG, L., SAIBIL, H. R., ORLOVA, E. V. & WAKSMAN, G. 2009. Structure of a type IV secretion system core complex. *Science,* 323**,** 266-268.

FROST, L. S., LEPLAE, R., SUMMERS, A. O. & TOUSSAINT, A. 2005. Mobile genetic elements: the agents of open source evolution. *Nature Reviews Microbiology,* 3**,** 722-732.

FURUYA, E. Y. & LOWY, F. D. 2006. Antimicrobial-resistant bacteria in the community setting. *Nature Reviews Microbiology,* 4**,** 36-45.

GALBRAITH, H. & MILTER, T. B. 1973. Effect of long chain fatty acids on bacterial respiration and amino acid uptake. *Journal of Applied Bacteriology,* 36**,** 659-675.

GALIMAND, M., GUIYOULE, A., GERBAUD, G., RASOAMANANA, B., CHANTEAU, S., CARNIEL, E. & COURVALIN, P. 1997. Multidrug resistance in *Yersinia pestis* mediated by a transferable plasmid. *New England Journal of Medicine,* 337**,** 677-681.

GANESAN, A. 2004. Natural products as a hunting ground for combinatorial chemistry. *Current Opinion in Biotechnology,* 15**,** 584-590.

GARCIA, R., CAYUNAOA, C., BOCICA, R., BACKHOUSEA, N., DELPORTEA, C.,

ZALDIVARB, M. & ERAZO, S. 2014. Antimicrobial activity of isopteropodine. *Zeitschrift für Naturforschung C,* 60**,** 385-388.

GARDNE, R. C. 1973. Acacetin-7-*O*-rutinoside and pectolinarin from *Cirsium coloradense*. *Phytochemistry,* 12**,** 223.

GELBRAND, H., MILLER-PETRIE, M., PANT, S., GANDRA, S., LEVINSON, J., BARTER, D., WHITE, A., LAXMINARAYAN, R., GANGULY, N. K. & KARIUKI, S. 2015. The State of the World's Antibiotics 2015. *Wound Healing Southern Africa,* 8**,** 30-34.

GERRITS, M. M., DE ZOETE, M. R., ARENTS, N. L. A., KUIPERS, E. J. & KUSTERS, J. G. 2002. 16S rRNA Mutation-Mediated Tetracycline Resistance in *Helicobacter pylori*. *Antimicrobial Agents and Chemotherapy,* 46**,** 2996-3000.

GETINO, M., FERNANDEZ-LOPEZ, R., PALENCIA-GANDARA, C., CAMPOS-GOMEZ, J., SANCHEZ-LOPEZ, J. M., MARTINEZ, M., FERNANDEZ, A. & DE LA CRUZ, F. 2016. Tanzawaic acids, a chemically novel Set of bacterial conjugation inhibitors. *PLoS One,* 11**,** 1-13.

GETINO, M., SANABRIA-RIOS, D. J., FERNANDEZ-LOPEZ, R., CAMPOS-GOMEZ, J., SANCHEZ-LOPEZ, J. M., FERNANDEZ, A., CARBALLEIRA, N. M. & DE LA CRUZ, F. 2015. Synthetic fatty acids prevent plasmid-mediated horizontal gene transfer. *MBio,* 6**,** 1-8.

GHANTE, M. H., BADOLE, S. L. & BODHANKAR, S. L. 2011. *Health benefits of garden cress (Lepidium sativum Linn.) seed extracts. In: nuts and seeds in health and disease prevention*, Elsevier Inc.

GIAMOUSTARIS, A. & MITHEN, R. 1996. Genetics of aliphatic glucosinolates. IV. Side-chain modification in *Brassica oleracea*. *Theoretical and Applied Genetics,* 93**,** 1006-1010.

GIBBONS, S. 2004. Anti-staphylococcal plant natural products. *Natural Product Reports,* 21**,** 263-277.

GIBBONS, S. 2008. Phytochemicals for bacterial resistance - strengths, weaknesses and opportunities. *Planta Medica* 74**,** 594-602.

GIBBONS, S. 2012. *An introduction to planar chromatography*

and its application to natural products Isolation. In natural products isolation, New York, USA, Humana Press.

GIBBONS, S., OLUWATUYI, M. & KAATZ, G. W. 2003. A novel inhibitor of multidrug efflux pumps in *Staphylococcus aureus*. *Journal of Antimicrobial Chemotherapy,* 51**,** 13-17.

GIBBONS, S. & UDO, E. E. 2000. The effect of reserpine, a modulator of multidrug efflux pumps, on the *in vitro* activity of tetracycline against clinical isolates of Methicillin Resistant *Staphylococcus aureus* (MRSA) possessing the tet(K) determinant. *Phytotherapy Research,* 14**,** 139 - 140.

GIEDRAITIENĖ, A., VITKAUSKIENĖ, A., NAGINIENĖ, R. & PAVILONIS, A. 2011. Antibiotic resistance mechanisms of clinically important bacteria. *Medicina (kaunas),* 47**,** 137-146.

GISVOLD, O. & THAKER, E. 1974. Lignans from *Larrea divaricata*. *Journal of Pharmaceutical Sciences,* 63**,** 1905-1907.

GOKAVI, S. S., MALLESHI, N. G. & GUO, M. 2004. Chemical composition of garden cress (*Lepidium sativum*) seeds and its fractions and use of bran as a functional ingredient. *Plant Foods for Human Nutrition,* 59**,** 105-111.

GONCALVES, C., DINIS, T. & BATISTA, M. T. 2005. Antioxidant properties of proanthocyanidins of *Uncaria tomentosa* bark decoction: a mechanism for anti-inflammatory activity. *Phytochemistry,* 66**,** 89-98.

GREENWAY, D. L. A. & DYKE, K. G. H. 1979. Mechanism of the inhibitory action of linoleic acid on the growth of *Staphylococcus aureus*. *Journal of General Microbiology,* 115**,** 233-245.

GRINDLEY, N. D. F., HUMPHREYS, G. O. & ANDERSON, E. S. 1973. Molecular studies of R factor compatibility groups. *Journal of bacteriology,* 115**,** 387-398.

GU, J., WAKIZONO, Y., DOHI, A., NONAKA, M., SUGANO, M. & YAMADA, K. 1998. Effect of dietary fats and sesamin on the lipid metabolism and immune function of Sprague Dawley rats. *Bioscience, Biotechnology, and Biochemistry,* 62**,** 1917-1924.

GUARRERA, P. M. 2005. Traditional phytotherapy in Central Italy (Marche, Abruzzo, and Latium). *Fitoterapia,* 76**,** 1-25.

HAMEL, F. G. 2009. Preliminary report: inhibition of cellular proteasome activity by free fatty acids. *Metabolism,* 58**,** 1047-1049.

HAN, B.-X. & CHEN, J. 2014. Acacetin-7-rutinoside from *Buddleja lindleyana*, a new molluscicidal agent against *Oncomelania hupensis*. *Zeitschrift für Naturforschung C,* 69.

HANCOCK, R. E. W. 1997. The bacterial outer membrane as a drug barrier. *Trends in microbiology,* 5**,** 37-42.

HARBIGE, L. S., LAYWARD, L., MORRIS-DOWNES, M. M., DUMONDE, D. C. & AMOR, S. 2000. The protective effects of omega-6 fatty acids in experimental autoimmune encephalomyelitis (EAE) in relation to transforming growth factor-beta 1 (TGF- 1) up-regulation and increased prostaglandin E2 (PGE2) production. *Clinical and Experimental Immunology* 122**,** 445-452.

HARVEY, A. L., EDRADA-EBEL, R. & QUINN, R. J. 2015. The re-emergence of natural products for drug discovery in the genomics era. *Nature Reviews Drug Discovery,* 14**,** 111-129.

HARVEY, D. J. 1981. Gas chromatographic and mass spectrometric studies of ginger constituents identification of gingerdiones and new hexahydrocurcumin

analogues. *Journal of Chromarography,* 212**,** 75-84.

HAZELL, S. & GRAHAM, D. Y. 1990. Unsaturated fatty acids and viability of *Helicobacter* (Campylobacter) *pylori*. *Journal Of Clinical Microbiology,* 28**,** 1060-1061.

HECHT, S. S., TRUSHIN, N., RIGOTTY, J., CARMELLA, S. G., BORUKHOVA, A., AKERKAR, S. & RIVENSON, A. 1996. Complete inhibition of 4-(methylnitrosamino)-1-(3-pyridly)-1-butanone-induced rat lung tumorigenesis and favorable modification of biomarker by phenethyl isothiocyanate. *Cancer Epidemiology, Biomarkers and Prevention,* 5**,** 645-652.

HEINEMANN, J. A. & SPRAGUE JR, G. F. 1989. Bacterial conjugative plasmids mobilize DNA transfer between bacteria and yeast. *Nature,* 340**,** 205-209.

HEITZMAN, M. E., NETO, C. C., WINIARZ, E., VAISBERG, A. J. & HAMMOND, G. B. 2005. Ethnobotany, phytochemistry and pharmacology of *Uncaria* (Rubiaceae). *Phytochemistry,* 66**,** 5-29.

HERRMANN, M., JOPPE, H. & SCHMAUS, G. 2002. Thesinine-4'-O-B-D-glucoside the first glycosylated plant pyrrolizidine alkaloid from *Borago officinalis*. *Phytochemistry* 60**,** 399-402.

HIRAI, K., IRIKURA, T., IYOBE, S. & MITSUHASHI, S. 1984. Inhibition of conjugal transfer of R plasmids by norfloxacin in *Pseudomonas aeruginosa*. *Chemotherapy,* 32**,** 471-476.

HISERODT, R., FRANZBLAU, S. & ROSEN, R. 1998. Isolation of 6-, 8-, and 10-gingerol from ginger rhizome by HPLC and preliminary evaluation of Inhibition of *Mycobacterium avium* and *Mycobacterium tuberculosis*. *Journal of Agricultural and Food Chemistry,* 46**,** 2504-2508.

HOOPER, D. C. 2000. Mechanisms of action and resistance of older and newer fluoroquinolones. *Clinical Infectious Diseases* 31**,** S24-S38.

HOOPER, D. C., WOLFSON, J. S., MCHUGH, G. L., SWARTZ, M. D., TUNG, C. & SWARTZ, M. N. 1984. Elimination of plasmid pMG110 from *Escherichia coli* by novobiocin and other inhibitors of DNA gyrase. *Antimicrobial Agents and Chemotherapy,* 25**,** 586-590.

HOOPER, D. C., WOLFSON, J. S., TUNG, C., SOUZA, K. S. & SWARTZ, M. N. 1989. Effects of Inhibition of the B Subunit of DNA Gyrase on Conjugation in *Escherichia coli*. *Journal of Bacteriology,* 171**,** 2235-2237.

HUANG, Q., IWAMOTO, M., AOKI, S., TANAKA, N., TAJIMA, K., YAMAHARA, J., TAKAISHI, Y., YOSHIDA, M., TOMIMATSU, T. & TAMAI, Y. 1991. Anti-5-hydroxytryptamine3 effect of galanolactone, diterpenoid isolated from ginger. *Chemical and Pharmaceutical Bulletin,* 39**,** 397-399.

HUTT, A. J. & O'GRADY, J. 1996. Drug chirality: a consideration of the significance of stereochemistry of antimicrobial agents. *Journal of Antimicrobial Chemotherapy,* 37**,** 7-32.

INGRAM, L. C., RICHMOND, M. H. & SYKES, R. B. 1973. Molecular characterization of the R factors implicated in the carbenicillin resistance of a sequence of *Pseudomonas aeruginosa* strains isolated from burns. *Antimicrobial Agents and Chemotherapy,* 3**,** 279-288.

JACOB, C. & ANWAR, A. 2008. The chemistry behind redox regulation with a focus on sulphur redox systems. *Physiologia Plantarum,* 133**,** 469-480.

JACOBY, G. A. & MUNOZ-PRICE, L. S. 2005. The new β-lactamases. *New England Journal of Medicine,* 352**,** 380-391.

JANG, M., HONG, E. & KIM, G. H. 2010. Evaluation of antibacterial activity of 3-butenyl, 4-pentenyl, 2-phenylethyl, and benzyl isothiocyanate in *Brassica* vegetables. *Journal of Food Science,* 75**,** M412-M416.

JIANG, H., TIMMERMANN, B. N. & GANG, D. R. 2007. Characterization and identification of diarylheptanoids in ginger (*Zingiber officinale* Rosc.) using high-performance liquid chromatography/electrospray ionization mass spectrometry. *Rapid Commun Mass Spectrom,* 21**,** 509-518.

JUMA, A. B. H. B. A. 2007. The effects of *Lepidium sativum* seeds on fracture-induced healing in rabbits. *Medscape General Medicine,* 9**,** 23.

KAATZ, G. W., SEO, M. S. & RUBLE, C. A. 1993. Efflux-mediated fluoroquinolone resistance in *Staphylococcus aureus*. *Antimicrobial Agents and Chemotherapy,* 37**,** 1086 - 1094.

KABARA, J. J., CONLEY, A. J. & TRUANT, J. P. 1972a. Relationship of chemical structure and antimicrobial activity of alkyl amides and amines. *Antimicrobial Agents and Chemotherapy,* 2**,** 492-498.

KABARA, J. J., SWIECZKOWSKI, D. M., CONLEY, A. J. & TRUANT, J. 1972b. Fatty acids and derivatives as antimicrobial agents. *Antimicrobial Agents and Chemotherapy,* 2**,** 23-28.

KANG, T. H., MATSUMOTO, K., TOHDA, M., MURAKAMI, Y., TAKAYAMA, H., KITAJIMA, M., AIMI, N. & WATANABE, H. 2002. Pteropodine and isopteropodine positively modulate the function of rat muscarinic M1 and 5-HT2 receptors expressed in *Xenopus oocyte*. *European Journal of Pharmacology,* 444.

KEPLINGER, K., LAUS, G., WURM, M., P. DIERICH, M. P. & TEPPNER, H. 1999. *Uncaria tomentosa* (Wild.) DC. - Ethnomedicinal use and new pharmacological, toxicological and botanical results. *Journal of Ethnopharmacology* 64**,** 23-34.

KIKUZAKI, H., KOBAYASHI, M. & NAKATANI, N. 1991. Diarylheptanoids from rhizomes of *Zingiber officinale*. *Phytochemistry,* 30**,** 3647-3651.

KIKUZAKI, H., TSAI, S. & NAKATANI, N. 1992. Gingerdiol related compounds from the rhizomes of *Zingiber officinale*. *Phytochemistry,* 31**,** 1783-1786.

KIM, J. S., LEE, S. I., PARK, H. W., YANG, J. H., SHIN, T. Y., KIM, Y. C., BAEK, N. I., KIM,

S. H., CHOI, S. U., KWON, B. M., LEEM, K. H., JUNG, M. Y. & KIM, D. K. 2008. Cytotoxic components from the dried rhizomes of *Zingiber officinale* Roscoe. *Archives of Pharmacal Research,* 31**,** 415-418.

KIM, M. G. & LEE, H. S. 2009. Growth-inhibiting activities of phenethyl isothiocyanate and its derivatives against intestinal bacteria. *Journal of Food Science,* 74**,** M467-M471.

KIM, Y. K., ISHII, G. & KIM, G. H. 2004. Isolation and identification of glucosinolates in edible parts of chinese cabbages (*Brassica campestris* L. *ssp. Peckinensis*). *Food Science Technology Research,* 10**,** 469 - 473.

KINASHI, H., MURAYAMA, M., MATSUSHITA, H. & NIMI, O. 1993. Structural analysis of the giant linear plasmid SCP1 in various *Streptomyces coelicolor* strains. *Microbiology,* 139**,** 1261-1269.

KITAJIMA, M., HASHIMOTO, K., YOKOYA, M., TAKAYAMA, H., SANDOVAL, M. & AIMI, N. 2003. Two new nor-triterpene glycosides from Peruvian *Uncaria tomentosa*. *Journal of Natural Products***,** 66.

KNAPP, H. R. & MELLY, M. A. 1986. Bactericidal effects of polyunsaturated fatty acids. *The Journal of Infectious Diseases,* 154**,** 84-94.

KODERA, Y., MATUURA, H., YOSHIDA, S., SUMIDA, T., ITAKURA, Y., FUWA, T. & NISHINO, H. 1989. Allixin, a stress compound from garlic. *Chemical and Pharmaceutical Bulletin,* 37**,** 1656-1658.

KOLM, R. H., DANIELSON, U. H., ZHANG, Y., TALALAY, P. & MANNERVIK, B. 1995. Isothiocyanates as substrates for human glutathione transferases: structure-activity studies. *Biochemical Journal,* 311**,** 453-459.

LANGER, P. J., SHANABRUCH, W. G. & WALKER, G. C. 1981. Functional organization of plasmid pKM101. *Journal of bacteriology,* 145**,** 1310-1316.

LAUS, G. & KEPLINGER, D. 1994. Separation of stereoisomeric oxindole alkaloids from *Uncaria tomentosa* by high performance liquid chromatography. *Journal of Chromatography A,* 662**,** 243-249.

LAZZERI, L., TACCONI, R. & PALMIERI, S. 1993. In vitro activity of some glucosinolates and their reaction products toward a population of the nematode *Heterodera schachtii*. *Journal of Agricultural and Food Chemistry,* 41**,** 825-829.

LEMAIRE, I., ASSINEWE, V., CANO, P., AWANG, D. V. C. & ARNASON, J. T. 1999. Stimulation of interleukin-1 and -6 production in alveolar macrophages by the neotropical liana, *Uncaria tomentosa*. *Journal of Ethnopharmacology* 64**,** 109-115.

LEVY, S. B. 2002. Factors impacting on the problem of antibiotic resistance. *Journal of Antimicrobial Chemotherapy,* 49**,** 25-30.

LEVY, S. B. & MARSHALL, B. 2004. Antibacterial resistance worldwide: causes, challenges and responses. *Nature Medicine,* 10**,** S122-S129.

LI, X. Z. & NIKAIDO, H. 2004. Efflux-Mediated Drug Resistance in Bacteria. *Drugs* 64**,** 159 - 204.

LIM, T. K. 2016. *Edible medicinal and non-medicinal plants,* Switzerland, Springer.

LOMOVSKAYA, O., WARREN, M. S., LEE, A., GALAZZO, J., FRONKO, R., LEE, M., BLAIS, J., CHO, D., CHAMBERLAND, S., RENAU, T., LEGER, R., HECKER, S., WATKINS, W., HOSHINO, K., ISHIDA, H. & LEE, V. J. 2001. Identification and characterization of inhibitors of multidrug resistance efflux pumps in *Pseudomonas aeruginosa*: novel agents for combination therapy. *Antimicrobial Agents and Chemotherapy,* 45**,** 105-116.

LU, J., GUAN, S., SHEN, X., QIAN, W., HUANG, G., DENG, X. & XIE, G. 2011. Immunosuppressive activity of 8-gingerol on immune responses in mice. *Molecules,* 16**,** 2636-2645.

LUJAN, S. A., GUOGAS, L. M., RAGONESE, H., MATSON, S. W. & REDINBO, M. R. 2007. Disrupting antibiotic resistance propagation by inhibiting the conjugative DNA relaxase. *Proceedings of the National Academy of Sciences,* 104**,** 12282-12287.

LV, H. & SHE, G. 2012. Naturally occurring diarylheptanoids - A supplementary version *Records of Natural Products* 6**,** 321-333.

MACRAE, W. D. & TOWERS, G. H. N. 1984. Biological activities of lignans. *Phytochemistry,* 23**,** 1207-1220.

MAGHRANI, M., ZEGGWAGH, N. A., MICHEL, J. B. & EDDOUKS, M. 2005. Antihypertensive effect of *Lepidium sativum* L. in spontaneously hypertensive rats. *Journal of Ethnopharmacology,* 100**,** 193-197.

MAGIORAKOS, A. P., SRINIVASAN, A., CAREY, R. B., CARMELI, Y., FALAGAS, M. E., GISKE, C. G., HARBARTH, S., HINDLER, J. F., KAHLMETER, G. & OLSSON‐LILJEQUIST, B. 2012. Multidrug‐resistant, extensively drug‐resistant and pandrug‐resistant bacteria: an international expert proposal for interim standard definitions for acquired resistance. *Clinical Microbiology and Infection,* 18**,** 268-281.

MAHADY, G. B., PENDLAND, S. L., YUN, G. S., LU, Z. Z. & STOIA, A. 2003. Ginger (*Zingiber officinale* Roscoe) and the gingerols Inhibit the growth of Cag A+ strains of *Heliobacter pylori*. *Anticancer Research,* 23**,** 3699-3702.

MAIER, U. H., GUNDLACH, H. & ZENK, M. H. 1998. Seven imidazole alkaloids from *Lepidium sativum*. *Phytochemistry,* 49**,** 1791-1795.

MAJOROS, L. & KARDOS, G. 2008. Fungicidal activity of azole antifungal agents. *Anti-Infective Agents in Medicinal Chemistry (Formerly Current Medicinal Chemistry-Anti-Infective Agents),* 7**,** 118-125.

MAJUMDER, P. L., CHATTERJEE, A. & SENGUPTA, G. C. 1972. Lignans from *Machilus edulis*. *Phytochemistry,* 11**,** 811-814.

MALDONADO-BONILLA, L. D., BETANCOURT-JIMÉNEZ, M. & LOZOYA-

GLORIA, E. 2008. Local and systemic gene expression of sesquiterpene phytoalexin biosynthetic enzymes in plant leaves. *European Journal of Plant Pathology,* 121**,** 439-449.

MALI, R. G., MAHAJAN, S. G. & MEHTA, A. A. 2007. *Lepidium sativum* (Garden cress): a review of contemporary literature and medicinal properties. *Oriental Pharmacy and Experimental Medicine,* 7**,** 331-335.

MAREE, J. E., KHONDKAR, P., KWAPONG, A. A., OYEDEMI, B. M., ALJARBA, T. M., STAPLETON, P., VILJOEN, A. M. & GIBBONS, S. 2014. Bioactive acetophenones from *Plectranthus venteri*. *Phytochemistry Letters,* 10**,** cxli-cxliv.

MARKHAM, P. N. & NEYFAKH, A. A. 1996. Inhibition of the multidrug transporter NorA prevents emergence of norfloxacin resistance in *Staphylococcus aureus*. *Antimicrobial Agents and Chemotherapy,* 40**,** 2673-2674.

MARON, D. M. & AMES, B. N. 1983. Revised methods for the Salmonella mutagenicity test. *Mutation Research/Environmental Mutagenesis and Related Subjects,* 113**,** 173-215.

MASUDA, N., SAKAGAWA, E., OHYA, S., GOTOH, N., TSUJIMOTO, H. & NISHINO, T. 2000. Contribution of the MexX-MexY-OprM efflux system to intrinsic resistance in *Pseudomonas aeruginosa*. *Antimicrobial Agents and Chemotherapy,* 44**,** 2242-2246.

MAXWELL, A. 1993. The interaction between coumarin drugs and DNA gyrase. *Molecular Microbiology* 9**,** 681-686.

MAXWELL, A. 1999. DNA gyrase as a drug target *Biochemical Society Transactions* 27**,** 48-53.

MAYNARD, C., BEKAL, S., SANSCHAGRIN, F., LEVESQUE, R. C., BROUSSEAU, R., MASSON, L., LARIVIÈRE, S. & HAREL, J. 2004. Heterogeneity among virulence and antimicrobial resistance gene profiles of extraintestinal *Escherichia coli* isolates of animal and human origin. *Journal of Clinical Microbiology,* 42**,** 5444-5452.

MAYTON, H. S., OLIVIER, C., VAUGHN, S. F. & LORIA, R. 1996. Correlation of fungicidal activity of *Brassica* species with allyl isothiocyanate production in macerated leaf tissue. *Phytopathology* 86**,** 267-271.

MAZODIER, P. & DAVIES, J. 1991. Gene transfer between distantly related bacteria. *Annual Review of Genetics,* 25**,** 147-171.

MB-MED.IT 2013. *Uncaria tomentosa*. http://www.mb-med.it/it/prodotto/uncaria-tomentosa/. [Accessed 24 March 2016].

MBOUANGOUEREA, R. N., TANEA, P., NGAMGAA, D., DJEMGOUA, P., CHOUDHARYB, M. I. & NGADJUIC., B. T. 2007. Piptaderol from *Piptadenia africana*. *African Journal of Traditional, Complementary and Alternative Medicines,* 4**,** 294-298.

MCCONNELL, M. M., WILLSHAW, G. A., SMITH, H. R., SCOTLAND, S. M. & ROWE, B. 1979. Transposition of ampicillin resistance to an enterotoxin plasmid in an

Escherichia coli strain of human origin. *Journal of Bacteriology,* 139**,** 346-355.

MCGEE, H. 2004. *A survey of tropical spices*, Hodder and Stoughton.

MCMANUS, M. C. 1997. Mechanisms of bacterial resistance to antimicrobial agents. *American Journal of Health-System Pharmacists,* 54**,** 1420-1433.

MCMURRY, L., PETRUCCI, R. E. & LEVY, S. B. 1980. Active efflux of tetracycline encoded by four genetically different tetracycline resistance determinants in *Escherichia coli*. *Proceedings of the National Academy of Sciences,* 77**,** 3974-3977.

MICHEL-BRIAND, Y. & LAPORTF, J. M. 1985. Inhibition of conjugal transfer of R plasmids by nitrofurans. *Microbiology,* 131**,** 2281-2284.

MINGEOT-LECLERCQ, M., GLUPCZYNSKI, Y. & TULKENS, P. M. 1999. Aminoglycosides: activity and resistance. *Antimicrobial Agents and Chemotherapy,* 43**,** 727-737.

MITHEN, R. & CAMPOS, H. 1996. Genetic variation of aliphatic glucosinolates in *Arabidopsis thaliana* and prospects for map based gene cloning. *Entomologia Experimentalis et Applicata,* 80**,** 202-205.

MITHEN, R., CLARKE, J., LISTER, C. & DEAN, C. 1995. Genetics of aliphatic glucosinolates. III. Side chain structure of aliphatic glucosinolates in *Arabidopsis thaliana*. *Heredity,* 74**,** 210-215.

MITHEN, R. F., DEKKER, M., VERKERK, R., RABOT, S. & JOHNSON, I. T. 2000. The nutritional significance, biosynthesis and bioavailability of glucosinolates in human foods. *Journal of the Science of Food and Agriculture,* 80**,** 967 - 984.

MORENO, D. A., CARVAJAL, M., LOPEZ-BERENGUER, C. & GARCIA-VIGUERA, C. 2006. Chemical and biological characterisation of nutraceutical compounds of broccoli. *Journal of Pharmaceutical and Biomedical Analysis,* 41**,** 1508-1522.

MUHAMMAD, I., DUNBAR, D. C., KHAN, R. A., GANZERA, M. & KHAN, I. A. 2001. Investigation of Uña De Gato I. 7-Deoxyloganic acid and 15N NMR spectroscopic studies on pentacyclic oxindole alkaloids from *Uncaria tomentosa*. *Phytochemistry,* 57**,** 781-785.

MUNDT, S., KREITLOW, S. & JANSEN, R. 2003. Fatty acids with antibacterial activity from the cyanobacterium *Oscillatoria redekei* HUB 051. *Journal of Applied Phycology* 15**,** 263-267.

MUSK, S. R. & JOHNSON, I. T. 1993. Allyl isothiocyanate is selectively toxic to transformed cells of the human colorectal tumour line HT29. *Carcinogenesis,* 14**,** 2079-2083.

NAKAMURA, S., INOUE, S., SHIMIZU, M., IYOBE, S. & MITSUHASHI, S. 1976. Inhibition of conjugal transfer of R plasmids by pipemidic acid and related compounds. *AntimicrobialAgents and Chemotherapy,* 10**,** 779-785.

NAKASHIMA, R., SAKURAI, K., YAMASAKI, S., HAYASHI, K., NAGATA, C., HOSHINO, K.,

ONODERA, Y., NISHINO, K. & YAMAGUCHI, A. 2013. Structural basis for the inhibition of bacterial multidrug exporters. *Nature,* 500**,** 102-106.

NASH, R. P., MCNAMARA, D. E., BALLENTINE, W. K., 3RD, MATSON, S. W. & REDINBO, M. R. 2012. Investigating the impact of bisphosphonates and structurally related compounds on bacteria containing conjugative plasmids. *Biochemical and Biophysical Research Communications,* 424**,** 697-703.

NATARAJAN, C. P., PADMABAI, R., KRISHNAMURTHY, M. N., RAGHAVAN, B., SANKARACHARYA, N. B., KUPPUSWAMY, S., GOVINDRAJAN, V. S. & LEWIS, Y. S. 1972. Chemical composition of ginger varieties and dehydration studies on ginger. *Journal of Food Science and Technology,* 9**,** 120-124.

NEHDI, I. A., SBIHI, H., TAN, C. P. & AL-RESAYES, S. I. 2012. Garden cress (*Lepidium sativum* Linn.) seed oil as a potential feedstock for biodiesel production. *Bioresource Technology,* 126**,** 193-197.

NEU, H. C. 1992. The crisis in antibiotic resistance. *Science,* 257**,** 1064-1073.

NEWMAN, D. J. & CRAGG, G. M. 2016. Natural Products as sources of new drugs from 1981 to 2014. *Journal of Natural Products,* 79**,** 629-661.

NIĆIFOROVIĆ, N. & ABRAMOVIČ, H. 2014. Sinapic acid and its derivatives: natural sources and bioactivity. *Comprehensive Reviews in Food Science and Food Safety,* 13**,** 34-51.

NIKAIDO, H. 1985. Role of permeability barriers in resistance to β-lactam antibiotics. *Pharmacology & therapeutics,* 27**,** 197-231.

NIKAIDO, H. 1994. Prevention of drug access to bacterial targets: Permeability barriers and active efflux *Science,* 264**,** 382-388.

NIKAIDO, H. 1998. Antibiotic resistance caused by Gram-negative multidrug efflux pumps. *Clinical Infectious Diseases,* 27**,** S32 - S41.

NIKAIDO, H. 2009. Multidrug resistance in bacteria. *Annual Review of Biochemtry,* 78**,** 119-146.

O'NEILL, J. 2014. Review on antimicrobial resistance: Antimicrobial resistance: Tackling a crisis for the health and wealth of nations. *London: Wellcome Trust***,** 1-18.

OHENE-AGYEI, T., MOWLA, R., RAHMAN, T. & VENTER, H. 2014. Phytochemicals increase the antibacterial activity of antibiotics by acting on a drug efflux pump. *Microbiologyopen,* 3**,** 885-96.

PARK, J. C., LEE, J. H. & CHOI, J. S. 1995. A flavone diglycoside from *Cirsium japonicum* var. ussuriense. *Phytochemistry,* 39**,** 261-262.

PARK, M., BAE, J. & LEE, D. S. 2008. Antibacterial activity of [10]-gingerol and [12]-gingerol isolated from ginger rhizome against periodontal bacteria. *Phytotherapy Research,*

22**,** 1446-9.

PARKIN, I., MAGRATH, R., KEITH, D., SHARPE, A., MITHEN, R. & LYDIATE, D. 1992. Genetics of aliphatic glucosinolates. I. Hydroxylation of alkenylglucosinolates in *Brasica napus. Heredity,* 72**,** 594-598.

PAULSEN, I. T. B., M. H.; SKURRAY, R. A. 2006. Proton-dependent multidrug efflux systems. *Microbiological Reviews,* 60**,** 575-608.

PÉREZ-BALIBREA, S., MORENO, D. A. & GARCÍA-VIGUERA, C. 2008. Influence of light on health-promoting phytochemicals of broccoli sprouts. *Journal of the Science of Food and Agriculture,* 88**,** 904-910.

PERTZ, H. H., LEHMANN, J., ROTH-EHRANG, R. & ELZ, S. 2011. Effects of ginger constituents on the gastrointestinal tract: role of cholinergic M3 and serotonergic 5-HT3 and 5-HT4 receptors. *Planta Medica,* 77**,** 973-978.

PETERS, JEANNE S. & CHIN, C.-K. 2003. Inhibition of photosynthetic electron transport by palmitoleic acid is partially correlated to loss of thylakoid membrane proteins. *Plant Physiology and Biochemistry,* 41**,** 117-124.

PIDDOCK, L. J. 2006. Clinically relevant chromosomally encoded multidrug resistance efflux pumps in bacteria. *Clinical Microbiology Reviews,* 19**,** 382-402.

PIFFARETTI, J. C., ARINI, A. & FREY, J. 1988. pUB307 mobilizes resistance plasmids from *Escherichia coli* into *Neisseria gonorrhoeae*. *Molecular and General Genetics,* 212**,** 215-218.

PLANTVILLAGE.ORG 2014. *Armoracia rusticana*. http://www.plantvillage.org/en/topics/horseradish [Accessed 24 March 2016].

PLANTVILLAGE.ORG 2015a. *Brassica oleracea*. https://www.plantvillage.org/en/topics/broccoli. [Accessed 24 March 2016].

PLANTVILLAGE.ORG 2015b. *Lepidium sativum*. http://www.plantvillage.org/en/topics/cress. [Accessed 24 March 2016].

POOLE, K. 2004. Efflux-mediated multiresistance in Gram-negative bacteria. *Clinical Microbiology Infectious Diseases* 10**,** 12 - 26.

POOLE, K. 2005. Efflux-mediated antimicrobial resistance. *Journal of Antimicrobial Chemotherapy,* 56**,** 20-51.

POOLE, K. 2007. Efflux pumps as antimicrobial resistance mechanisms. *Annals of Medicine,* 39**,** 162-176.

RADWAN, H. M., EL-MISSIRY, M. M., AL-SAID, W. M., ISMAIL, A. S., SHAFEEK, K. A. A. & SEIF-EL-NASR, M. M. 2007. Investigation of the glucosinolates of *Lepidium sativum* growing in Egypt and their biological activity. *Research Journal of Medicine and Medical Sciences,* 2**,** 127-132.

RATTANACHAIKUNSOPON, P. & PHUMKHACHORN, P. 2008. Diallyl sulfide content and antimicrobial activity against food-borne pathogenic bacteria of chives (*Allium schoenoprasum*). *Bioscience, Biotechnology, and Biochemistry,* 72**,** 2987-2991.

REYNOLDS, E. & COVE, J. H. 2005. Enhanced resistance to erythromycin is conferred by the enterococcal msrC determinant in *Staphylococcus aureus*. *Journal of Antimicrobial and Chemotherapy,* 55**,** 260-264.

RICE, L. B. & BONOMO, R. A. 2005. *Genetic and biochemical mechanisms of bacterial resistance to antimicrobial agents. In: Antibiotics in laboratory medicine,* USA, Lippincott Williams & Wilkins.

RIZZI, R., RE, F., BIANCHI, A., DE FEO, V., DE SIMONE, F., BIANCHI, L. & STIVALA, L. A. 1993. Mutagenic and antimutagenic activities of *Uncaria tomentosa* and its extracts. *Journal of Ethnopharmacology* 38**,** 63-77.

RODRIGUEZ-MARTINEZ, J. M., PASCUAL, A., GARCIA, I. & MARTINEZ-MARTINEZ, L. 2003. Detection of the plasmid-mediated quinolone resistance determinant qnr among clinical isolates of *Klebsiella pneumoniae* producing AmpC-type beta-lactamase. *Journal of Antimicrobial Chemotherapy,* 52**,** 703-706.

RODRÍGUEZ-TUDELA, J. L., BARCHIESI, F., BILLE, J., CHRYSSANTHOU, E., CUENCA-ESTRELLA, M., DENNING, D., DONNELLY, J. P., DUPONT, B., FEGELER, W., MOORE, C., RICHARDSON, M. & VERWEIJ, P. E. 2003. Method for the determination of minimum inhibitory concentration (MIC) by broth dilution of fermentative yeasts. *Clinical Microbiology and Infection,* 9**,** i-viii.

ROSS, J. I., EADY, E. A., COVE, J. H. & CUNLIFFE, W. J. 1998. 16S rRNA mutation associated with tetracycline resistance in a gram-positive bacterium. *Antimicrobial Agents and Chemotherapy,* 42**,** 1702-1705.

RUDOLPH, K. E., LIBERIO, M. S., DAVIS, R. A. & CARROLL, A. R. 2013. Pteridine-, thymidine-, choline- and imidazole-derived alkaloids from the Australian ascidian, *Leptoclinides durus*. *Organic & Biomolecular Chemistry,* 11**,** 261-270.

SADO-KAMDEM, S. L., VANNINI, L. & GUERZONI, M. E. 2009. Effect of alpha-linolenic, capric and lauric acid on the fatty acid biosynthesis in *Staphylococcus aureus*. *International Journal of Food Microbiology,* 129**,** 288-294.

SALEEM, M., KIM, H. J., ALI, M. S. & LEE, Y. S. 2005. An update on bioactive plant lignans. *Natural Product Reports,* 22**,** 696-716.

SALEH, N. A. M., EL-NEWUMY, S. I., ABDALLA, M. F., ABOU-ZAID, M. M., DELLAMONICA, G. & CHOPIN, J. 1985. Flavonoid glycosides of *Artemisia alba* and *A. herba-alba*. *Phytochemistry,* 24**,** 201-203.

SARAWILCOX. 2006. Cationic peptides: A new hope. *The Science Creative Quartely* [Online].

SCHELZ, Z., MOLNAR, J. & HOHMANN, J. 2006. Antimicrobial and antiplasmid activities of essential oils. *Fitoterapia,* 77**,** 279-85.

SCHINDLER, B. D. J., P.; KAATZ, G. W. 2013. Inhibition of drug efflux pumps in *Staphylococcus aureus*: current status of potentiating existing antibiotics. *Future Micriobiology,* 8**,** 491-507.

SCHONFELD, P. & WOJTCZAK, L. 2008. Fatty acids as modulators of the cellular production of reactive oxygen species. *Free Radical Biology and Medicine,* 45**,** 231-241.

SEKI, H., TAKAYAMA, H., AIMI, N., SAKAI, S. & PONGLUX, D. 1993. A nuclear magnetic resonance study on the eleven steroisomers of heteroyohimbine-type oxindole alkaloids. *Chemical and Pharmaceutical Bulletin,* 41**,** 2077-2086.

SEMWAL, R. B., SEMWAL, D. K., COMBRINCK, S. & VILJOEN, A. M. 2015. Gingerols and shogaols: Important nutraceutical principles from ginger. *Phytochemistry* 117.

SHAFRAN, S. D. 1990. The basis of antibiotic resistance in bacteria. *The Journal of Otolaryngology,* 19**,** 158-168.

SHAMMA, M., SHINE, R. J., KOMPIS, I., STICZAY, T., MORSINGH, F., POISSON, J. & POUSSET, J. L. 1967. The stereochemistry of the pentacyclic oxindole alkaloids. *Journal of the American Chemical Society,* 89**,** 1739-1740.

SHARMA, S. & AGARWAL, N. 2011. Nourishing and healing prowess of garden cress (*Lepidium sativum* Lin.) A review. *Indian Journal of Natural Products and Resources* 2**,** 292-297.

SHARMA, S. K. & MOHAN, A. 2006. Multidrug-resistant tuberculosis: a menace that threatens to destabilize tuberculosis control. *Chest Journal,* 130**,** 261-272.

SHIBASAKI, I. & KATO, N. 2010. In combined effects on antibacterial activity of fatty acids and their esters against gram-negative bacteria. *The pharmacological effects of lipids (Kabara ed JJ)***,** 15-24.

SHIN, S. Y., BAJPAI, V. K., KIM, H. R. & KANG, S. C. 2007. Antibacterial activity of eicosapentaenoic acid (EPA) against foodborne and food spoilage microorganisms. *LWT - Food Science and Technology,* 40**,** 1515-1519.

SHINGALAPUR, R. V., HOSAMANI, K. M. & KERI, R. S. 2009. Synthesis and evaluation of *in vitro* anti-microbial and anti-tubercular activity of 2-styryl benzimidazoles. *European Journal of Medicinal Chemistry* 44**,** 4244-4248.

SHOFRAN, B. G., PURRINGTON, S. T., BREIDT, F. & FLEMING, H. P. 1998. Antimicrobial properties of sinigrin and its hydrolysis products. *Journal of Food Science,* 63.

SHOJI, N., IWASA, A., TAKEMOTO, T., ISHIDA, Y. & OHIZUMI, Y. 1982. Cardiotonic principles of ginger (*Zingiber officinale* Roscoe). *Journal of Pharmaceutical Sciences,* 71**,** 1174 -1175.

SHUKLA, S., WU, C. P., NANDIGAMA, K. & AMBUDKAR, S. V. 2007. The naphthoquinones, vitamin K3 and its structural analog plumbagin, are substrates of the multidrug resistance-linked ABC drug transporter ABCG2. *Molecular Cancer*

Therapeutics 6**,** 3279-3286.

SKEHAN, P., STORENG, R., SCUDIERO, D., MONKS, A., MCMAHON, J., VISTICA, D., WARREN, J. T., BOKESCH, H., KENNEY, S. & BOYD, M. R. 1990. New colorimetric cytotoxicity assay for anticancer-drug screening. *Journal of the National Cancer Institute,* 82**,** 1107-1112.

ŠMEJKAL, K., CHUDÍK, S., KLOUCEK, P., MAREK, R., CVACKA, J., URBANOVÁ, M., JULÍNEK, O. E., KOKOŠKA, L., ŠLAPETOVÁ, T. & HOLUBOVÁ, P. 2008. Antibacterial C-geranyl flavonoids from *Paulownia tomentosa* fruits. *Journal of Natural Products,* 71**,** 706-709.

SMILLIE, C., GARCILLAN-BARCIA, M. P., FRANCIA, M. V., ROCHA, E. P. & DE LA CRUZ, F. 2010. Mobility of plasmids. *Microbiology and Molecular Biology Reviews,* 74**,** 434-452.

SMITH, E., WILLIAMSON, E., ZLOH, M. & GIBBONS, S. 2005. Isopimaric acid from *Pinus nigra* shows activity against multidrug-resistant and EMRSA strains of *Staphylococcus aureus*. *Phytotherapy Research,* 19**,** 538-542.

SMITH, E. C., WILLIAMSON, E. M., WAREHAM, N., KAATZ, G. W. & GIBBONS, S. 2007. Antibacterials and modulators of bacterial resistance from the immature cones of *Chamaecyparis lawsoniana*. *Phytochemistry,* 68**,** 210-217.

SMITH, L. W. & CULVENOR, C. C. J. 1981. Plant sources of hepatotoxic pyrrolizidine alkaloids. *Journal of Natural Products,* 44**,** 129-152.

SMITH, P. A. & ROMESBERG, F. E. 2007. Combating bacteria and drug resistance by inhibiting mechanisms of persistence and adaptation. *Nature Chemical Biology,* 3**,** 549-556.

SMITH, V. L. 2000. Reduction in snap bean emergence by seed treat- ment with dried Canola residue. *HortScience* 35**,** 92-94.

SOLEDADE, M., PEDRAS, C. & SMITH, K. C. 1997. Sinalexin, a phytoalexin from white mustard elicited by destruxin B and *Alternaria brassicae*. *Phytochemistry,* 46**,** 833-837.

SONDERBY, I. E., GEU-FLORES, F. & HALKIER, B. A. 2010. Biosynthesis of glucosinolates gene discovery and beyond. *Trends in Plant Science,* 15**,** 283-290.

SPELLBERG, B., GUIDOS, R., GILBERT, D., BRADLEY, J., BOUCHER, H. W., SCHELD, W. M., BARTLETT, J. G., EDWARDS, J., JR. & INFECTIOUS DISEASES SOCIETY OF, A. 2008. The epidemic of antibiotic-resistant infections: a call to action for the medical community from the Infectious Diseases Society of America. *Clinical Infectious Diseases,* 46**,** 155-164.

SPLENGER, G., MOLNAR, A., SCHELZ, Z., AMARAL, L., SHARPLES, D. & MOLNAR, J. 2006. The mechanism of plasmid curing in bacteria. *Current Drug Targets,* 7**,** 1389-4501.

SPRATT, B. G. 1994. Resistance to antibiotics mediated by target alterations. *Science,* 264**,** 388-393.

STEPHENS, J. M. 2015. Broccoli-*Brassica oleracea* L. (Italica group) *Series of the Horticultural Sciences Department, Electronic Data Information Source of UF/IFAS Extension*.

SU, C. C. & YU, E. W. 2007. Corrigendum to "Ligand-transporter interaction in the AcrB multidrug efflux pump determined by fluorescence polarization assay" [FEBS Lett. 581 (2007) 4972-4976]. *FEBS Letters,* 581**,** 5548-5548.

SUMMERS, D. 2009. *The biology of plasmids*, John Wiley & Sons.

SUN, C. Q., O'CONNOR, C. J. & ROBERTON, A. M. 2003. Antibacterial actions of fatty acids and monoglycerides against *Helicobacter pylori*. *FEMS Immunology & Medical Microbiology,* 36**,** 9-17.

TAKENOUCHI, T., TABATA, F., IWATA, Y., HANZAWA, H., SUGAWARA, M. & SATOSHI OHYA, S. 1996. Hydrophilicity of quinolones Is not an exclusive factor for decreased activity in efflux-mediated resistant mutants of *Staphylococcus aureus*. *Antimicrobial Agents and Chemotherapy,* 40**,** 1835-1842.

TENOVER, F. C. 2006. Mechanisms of antimicrobial resistance in bacteria. *American Journal of Infection Control,* 34**,** S3-10; discussion S64-73.

TESAKI, S., TANABE, S., ONO, H., FUKUSHI, E., KAWABATA, J. & WATANABE, M. 1998. 4-Hydroxy-3-nitrophenylacetic and sinapic acids as antibacterial compounds from mustard seeds. *Bioscience, Biotechnology, and Biochemistry,* 65**,** 998-1000.

THOMAS, C. M. & SUMMERS, D. 2008. Bacterial plasmids. In: Encyclopedia of Life Sciences (ELS). John Wiley & Sons, Ltd: Chichester.

TOLMASKY, M. E. 2000. Bacterial resistance to aminoglycosides and beta-lactams: the Tn1331 transposon paradigm. *Frontiers in Bioscience,* 5**,** d20-d29.

TOLMASKY, M. E., ROBERTS, M., WOLOJ, M. & CROSA, J. H. 1986. Molecular cloning of amikacin resistance determinants from a *Klebsiella pneumoniae* plasmid. *Antimicrobial Agents and Chemotherapy,* 30**,** 315-320.

TORIBIO, A., BOUDESOCQUE, L., RICHARD, B., NUZILLARD, J. M. & RENAULT, J. H. 2011. Preparative isolation of glucosinolates from various edible plants by strong ion-exchange centrifugal partition chromatography. *Separation and Purification Technology,* 83**,** 15-22.

TORIBIO, A., NUZILLARD, J. M., PINEL, B., BOUDESOCQUE, L., LAFOSSE, M., DE LA POYPE, F. & RENAULT, J. H. 2009. Pilot-scale ion-exchange centrifugal partition chromatography: purification of sinalbin from white mustard seeds. *Journal of Separation Science,* 32**,** 1801-1807.

TRAKA, M. H., MELCHINI, A. & MITHEN, R. F. 2014. Sulforaphane and prostate cancer interception. *Drug Discovery Today,* 19**,** 1488-1492.

TROTT, O. & OLSON, A. J. 2010. AutoDock Vina: improving the speed and accuracy of docking with a new scoring function, efficient optimization, and multithreading. *Journal of Computational Chemistry,* 31**,** 455-461.

TRUONG-BOLDUC, Q. C., DUNMAN, P. M., STRAHILEVITZ, J., PROJAN, S. J. & HOOPER, D. C. 2005. MgrA is a multiple regulator of two new efflux pumps in *Staphylococcus aureus*. *Journal of Bacteriology,* 187**,** 2395-2405.

TSUCHIYA, H., SATOB, M., MIYAZAKIA, T., FUJIWARAC, S., TANIGAKID, S., OHYAMAE, M. & IINUMA, M. 1996. Comparative study on the antibacterial activity of phytochemical flavanones against methicillin-resistant *Staphylococcus aureus*. *Journal of Ethnopharmacology,* 50**,** 27-34.

TUOMANEN, E. & TOMASZ, A. 1990. Mechanism of phenotypic tolerance of nongrowing pneumococci to beta-lactam antibiotics. *Scandinavian Journal of Infectious Diseases. Supplementum,* 74**,** 102-112.

UEKI, S., MIYOSHI, M., SHIDO, O., HASEGAWA, J. & WATANABE, T. 2008. Systemic administration of [6]-gingerol, a pungent constituent of ginger, induces hypothermia in rats via an inhibitory effect on metabolic rate. *European Journal of Pharmacology,* 584**,** 87-92.

UNDERHILL, E. W., CHISHOLM, M. D. & WETTER, L. R. 1962. Biosynthesis of mustard oil glucosides: i. administration of C14-labelled compounds to horseradish, nasturtium, and watercress. *Canadian Journal of Biochemistry and Physiology,* 40**,** 1505-1514.

VACILLOTTO, G., FAVRETTO, D., SERAGLIA, R., PAGIOTTI, R., TRALDI, P. & MATTOLI, L. 2013. A rapid and highly specific method to evaluate the presence of pyrrolizidine alkaloids in *Borago officinalis* seed oil. *Journal of Mass Spectrometry,* 48**,** 1078-1082.

VALDERRAMA, J. C. M. 2000. Review: Distribution of flavonoids in the Myristicaceae. *Phytochemistry* 55**,** 505-511.

VAN WYK, B. & WINK, M. 2004. *Medicinal plants of the world : an illustrated scientific guide to important medicinal plants and their uses,* Oregon, Oregon : Timber Press.

VAN-BEEK, T. A., POSTHUMUS, M. A., LELYVELD, G. P., PHIET, H. V. & YEN, B. T. 1987. Investigation of the essential oil of Vietnamese ginger. *Phytochemistry,* 26**,** 3005-3010.

VIVEIROS, M., LEANDRO, C. & AMARAL, L. 2003. Mycobacterial efflux pumps and chemotherapeutic implications. *International Journal of Antimicrobial Agents,* 22**,** 274-278.

WANG, M., SAHM, D. F., JACOBY, G. A. & HOOPER, D. C. 2004. Emerging plasmid-mediated quinolone resistance associated with the qnr gene in *Klebsiella pneumoniae* clinical isolates in the United States. *Antimicrobial Agents and Chemotherapy,* 48**,** 1295-1299.

WANG, M., TRAN, J. H., JACOBY, G. A., ZHANG, Y., WANG, F. & HOOPER, D. C. 2003.

Plasmid-mediated quinolone resistance in clinical isolates of *Escherichia coli* from Shanghai, China. *Antimicrobial Agents and Chemotherapy,* 47**,** 2242-2248.

WANG, T., LIANG, H. & YUAN, Q. 2014. Separation and purification of sinigrin and gluconapin from defatted Indian mustard seed meals by macroporous anion exchange resin and medium pressure liquid chromatography. *Separation Science and Technology,* 49**,** 1838-1847.

WATERS, V. L. 1999. Conjugative transfer in the dissemination of beta-lactam and aminoglycoside resistance. *Frontier in Bioscience,* 4**,** D433-D456.

WATTENBERG, L. W. 1977. Inhibition of carcinogenic effects of polycyclic hydrocarbons by benzyl isothiocyanate and related compounds. *Journal of the National Cancer Institute,* 58**,** 395-398.

WATTENBERG, L. W. 1981. Inhibition of carcinogen-induced neoplasia by sodium cyanate, tert-butylisocyanate and benzyl isothiocyanate administered subsequent to carcinogen exposure. *Cancer Research,* 41**,** 2991-2994.

WEIGEL, L. M., CLEWELL, D. B., GILL, S. R., CLARK, N. C., MCDOUGAL, L. K., FLANNAGAN, S. E., KOLONAY, J. F., SHETTY, J., KILLGORE, G. E. & TENOVER, F. C. 2003. Genetic analysis of a high-level vancomycin-resistant isolate of *Staphylococcus aureus*. *Science,* 302**,** 1569-1571.

WEIGEL, L. M., DONLAN, R. M., SHIN, D. H., JENSEN, B., CLARK, N. C., MCDOUGAL, L. K., ZHU, W., MUSSER, K. A., THOMPSON, J., KOHLERSCHMIDT, D., DUMAS, N., LIMBERGER, R. J. & PATEL, J. B. 2007. High-level vancomycin-resistant *Staphylococcus aureus* isolates associated with a polymicrobial biofilm. *Antimicrobial Agents and Chemotherapy,* 51**,** 231-238.

WEIL, M. J., ZHANG, Y. & NAIR, M. G. 2005. Tumor cell proliferation and cyclooxygenase inhibitory constituents in Horseradish (*Armoracia rusticana*) and Wasabi (*Wasabia japonica*). *Journal of Agricultural and Food Chemistry,* 53**,** 1440-1444.

WHO 2011. Emergence of multi-drug resistant Neisseria gonorrhoeae: Threat of global rise in untreatable sexually transmitted infections. *World Health Organization*

WILLE, J. J. & KYDONIEUS, A. 2003. Palmitoleic acid isomer (C16:1-6) in human skin sebum is effective against Gram-positive bacteria. *Skin Pharmacology and Applied Skin Physiology,* 16**,** 176-187.

WILLIAMS, J. J. & HERGENROTHER, P. J. 2008. Exposing plasmids as the Achilles' heel of drug-resistant bacteria. *Current Opinion in Chemical Biology,* 12**,** 389-399.

WILSON, A. E., BERGAENTZLÉ, M., BINDLER, F., MARCHIONI, E., LINTZ, A. & ENNAHAR, S. 2013. In vitro efficacies of various isothiocyanates from cruciferous vegetables as antimicrobial agents against foodborne pathogens and spoilage bacteria. *Food Control,* 30**,** 318-324.

WIRTH, C. & WAGNER, H. 1997. Pharmacologically active procyanidines from the bark of *Uncaria tomentosa*. *Phytomedicine,* 4**,** 265-266.

WON, S. R., HONG, M. J., KIM, Y. M., LI, C. Y., KIM, J. W. & RHEE, H. I. 2007. Oleic acid: an efficient inhibitor of glucosyltransferase. *FEBS Letters,* 581**,** 4999-5002.

WONG, C. P., HSU, A., BUCHANAN, A., PALOMERA-SANCHEZ, Z., BEAVER, L. M., HOUSEMAN, E. A., WILLIAMS, D. E., DASHWOOD, R. H. & HO, E. 2014. Effects of sulforaphane and 3,3'-diindolylmethane on genome-wide promoter methylation in normal prostate epithelial cells and prostate cancer cells. *PLoS One,* 9**,** 1-14.

YAMAHARA, J., MATSUDA, H., YAMAGUCHI, S., SHIMODA, H., MURAKAMI, N. & YOSHIKAWA, M. 1995. Pharmacological study on ginger processing. I. Antiallergic activity and cardiotonic action of gingerols and shogaols. *Natural Medicines,* 49**,** 76-83.

YANG, X., HUANG, X. & AHMAT, M. 2008. New neolignan from seed of *Myristica fragrans*. *China Journal of Chinese Materia Medica,* 33**,** 397-402.

YOUNG, H. Y., LUO, Y. L., CHENG, H. Y., HSIEH, W. C., LIAO, J. C. & PENG, W. H. 2005. Analgesic and anti-inflammatory activities of [6]-gingerol. *Journal of Ethnopharmacology,* 96**,** 207-210.

ZHANG, H., ZHANG, L., PENG, L. J., DONG, X. W., WU, D., WU, V. C. & FENG, F. Q. 2012. Quantitative structure-activity relationships of antimicrobial fatty acids and derivatives against *Staphylococcus aureus*. *Journal of Zhejiang University Science B,* 13**,** 83-93.

ZHANG, Y., ZHENG, Y., HU, S. & LIU, H. 2013. Anti-*Helicobacter pylori* effect of 6-gingerol in vitro. *Modern Food Science and Technology,* 29**,** 1259-1261.

ZHAO, M., LAU, S. T., ZHANG, X. Q., YE, W. C., LEUNG, P. S., CHE, C. T. & LIN, Z. X. 2011. Bruceines K and L from the ripe fruits of *Brucea javanica*. *Helvetica Chimica Acta,* 94**,** 2099-2105.

ZHENG, C. J., YOO, J. S., LEE, T. G., CHO, H. Y., KIM, Y. H. & KIM, W. G. 2005. Fatty acid synthesis is a target for antibacterial activity of unsaturated fatty acids. *FEBS Letters,* 579**,** 5157-5162.

ZHOU, H., JIAN, R., KANG, J., HUANG, X., LI, Y., ZHUANG, C., YANG, F., ZHANG, L., FAN, X., WU, T. & WU, X. 2010. Anti-inflammatory effects of caper (*Capparis spinosa* L.) fruit aqueous extract and the isolation of main phytochemicals. *Journal of Agricultural and Food Chemistry,* 58**,** 12717-21.

ZLOH, M., KAATZ, G. W. & GIBBONS, S. 2004. Inhibitors of multidrug resistance (MDR) have affinity for MDR substrates. *Bioorganic & Medicinal Chemistry Letters,* 14**,** 881-885.

Appendices

Appendix A: NMR and HRTOFESIMS spectra for AK-5

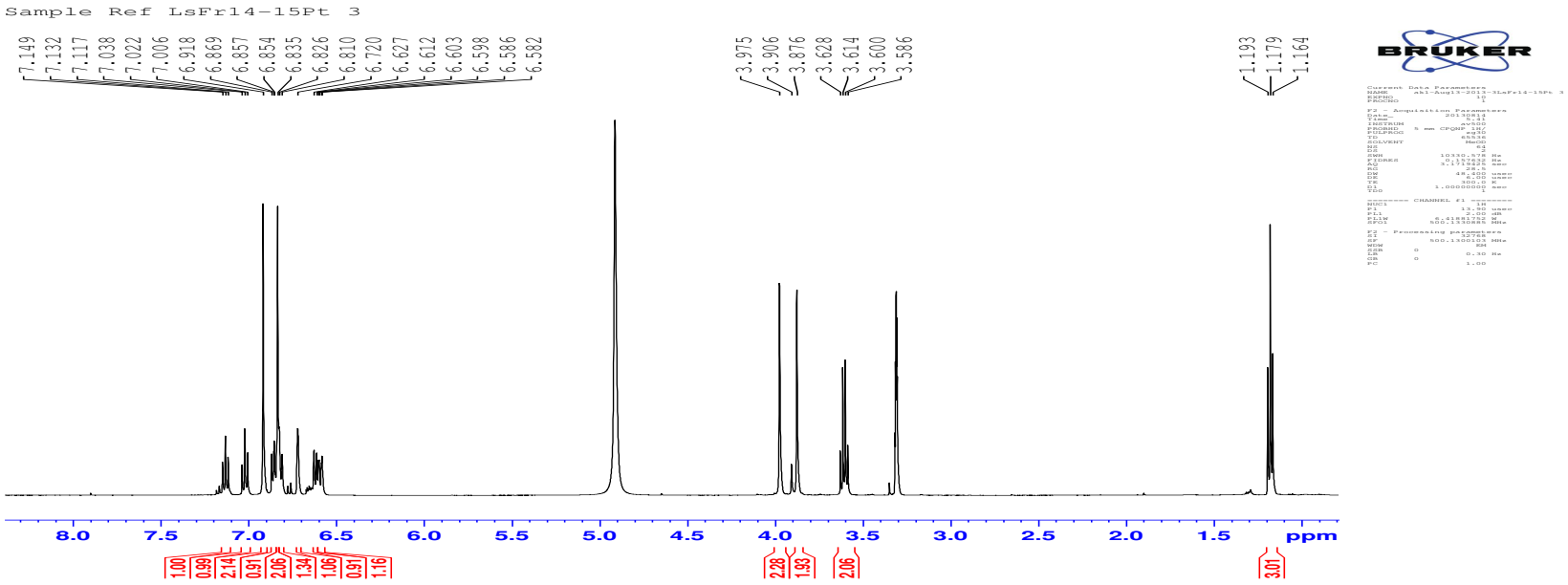

Figure A.1 ^{1}H NMR spectrum for **AK-5**, recorded in CD_3OD, 500 MHz

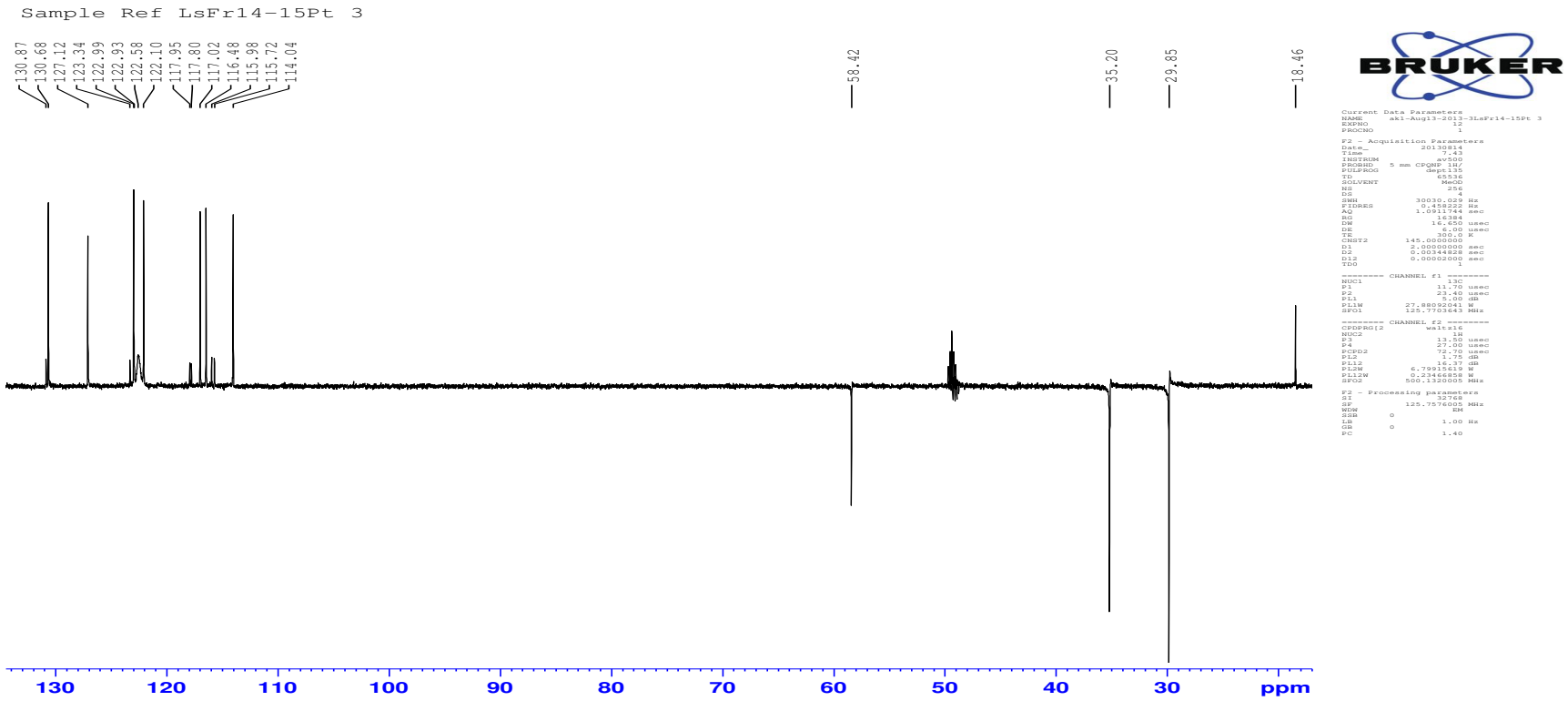

Figure A.2 DEPT-135 spectrum for **AK-5**

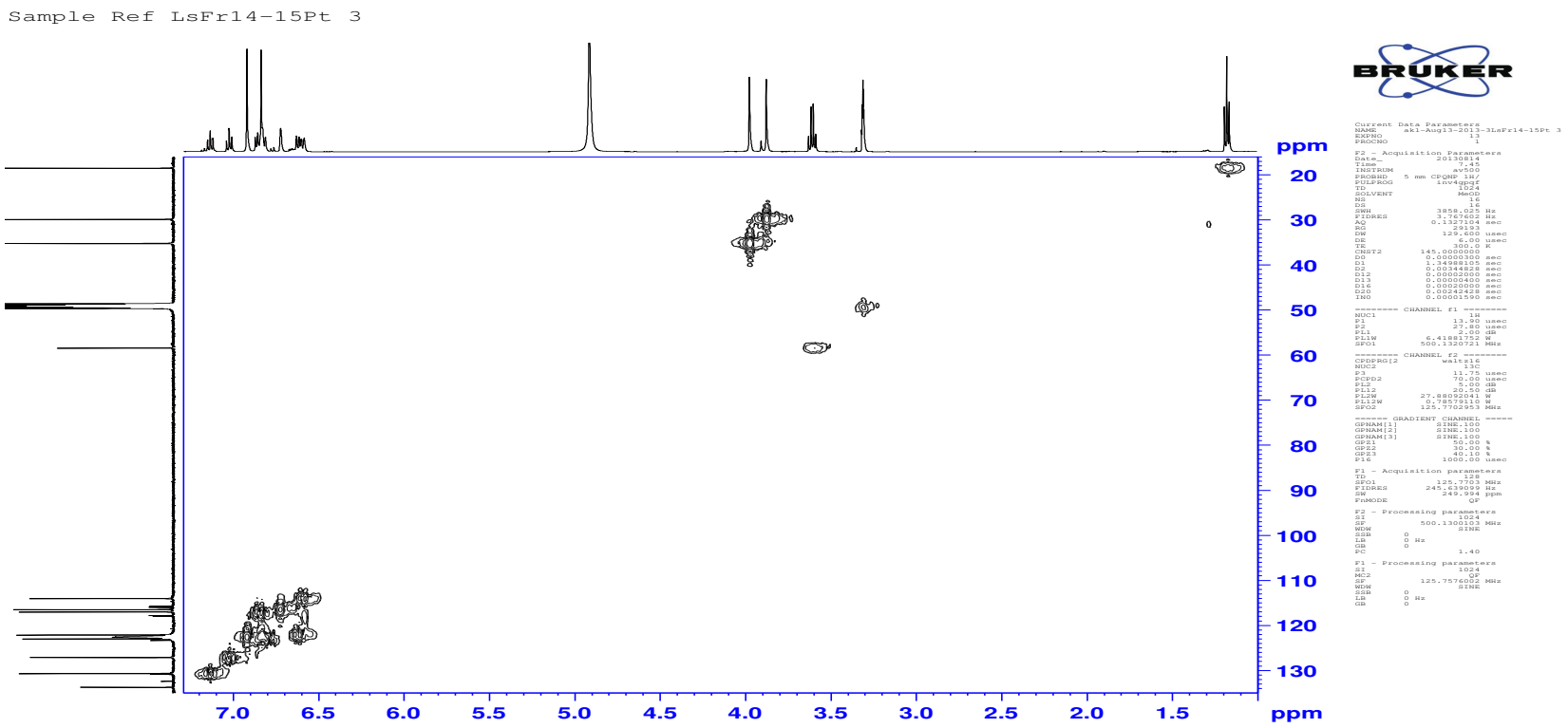

Figure A.3 HMQC spectrum for **AK-5**

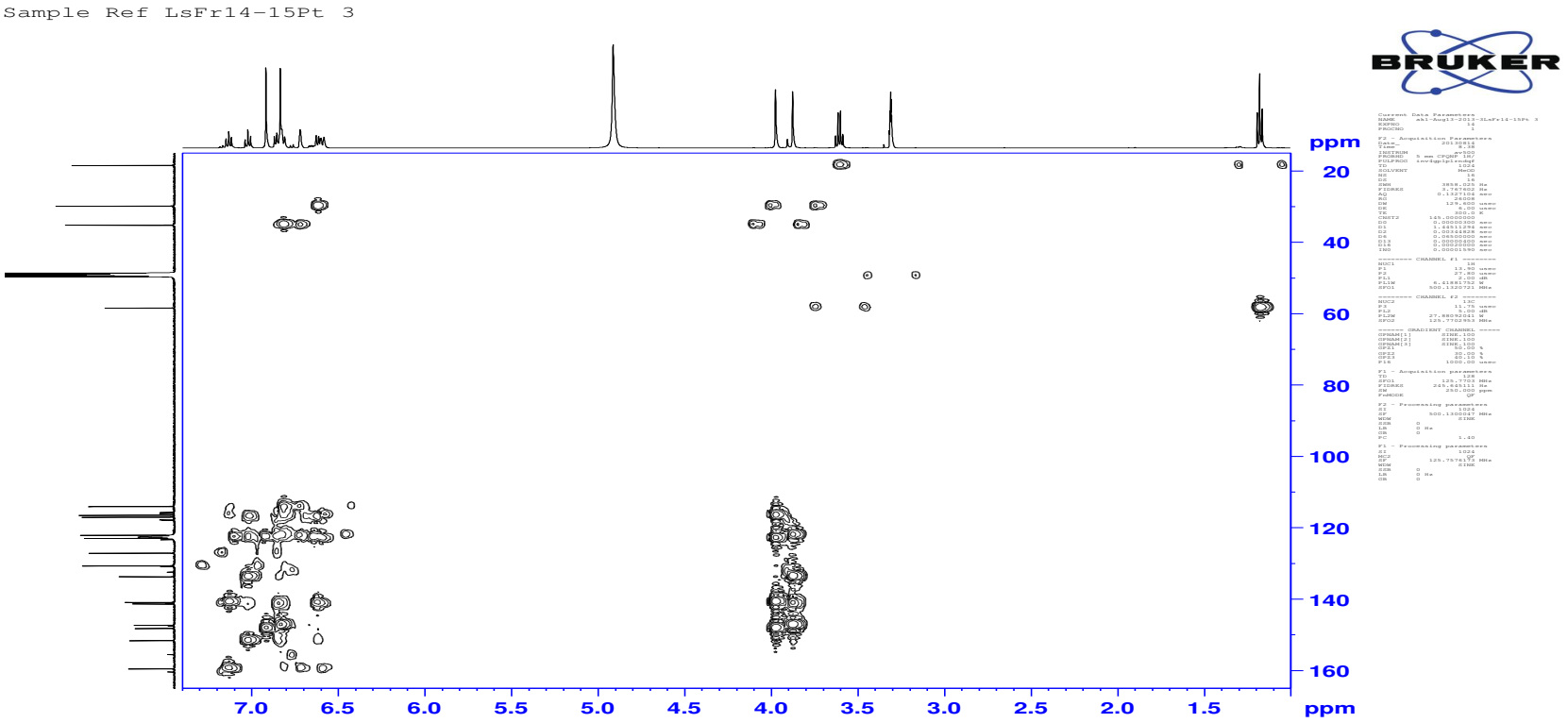

Figure A.4 HMBC spectrum for **AK-5**

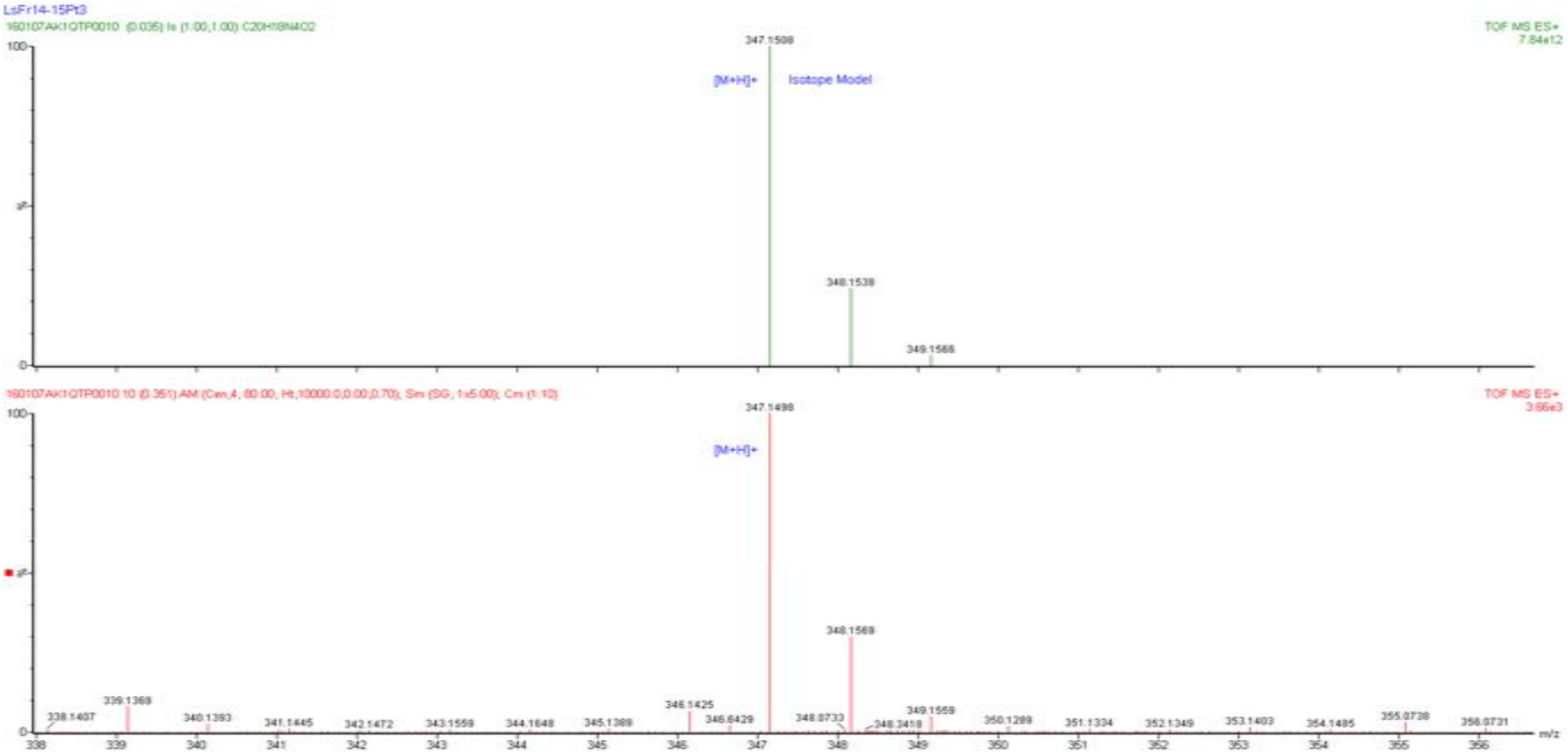

Figure A.5 HRTOFESIMS spectrum for **AK-5**

Appendix B: NMR and HRTOFESIMS spectra for AK-6

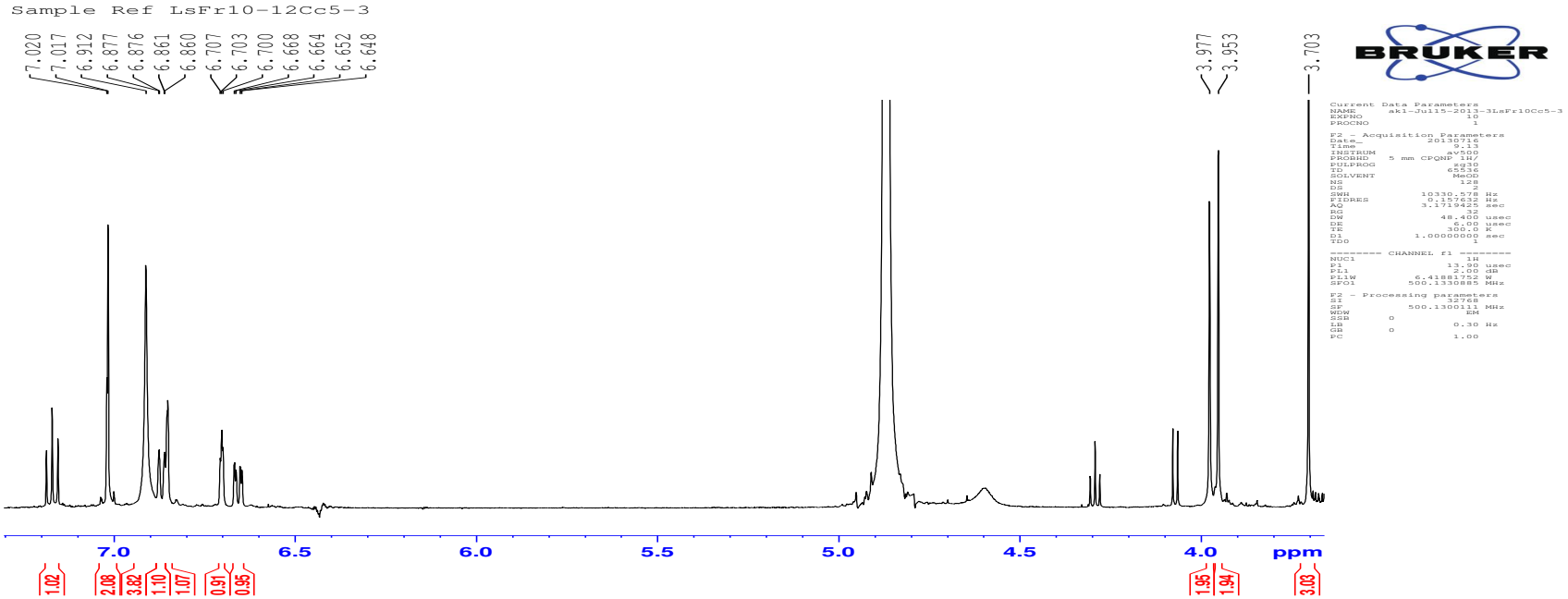

Figure A.6 ^{1}H NMR spectrum for **AK-6,** recorded in CD_3OD, 500 MHz

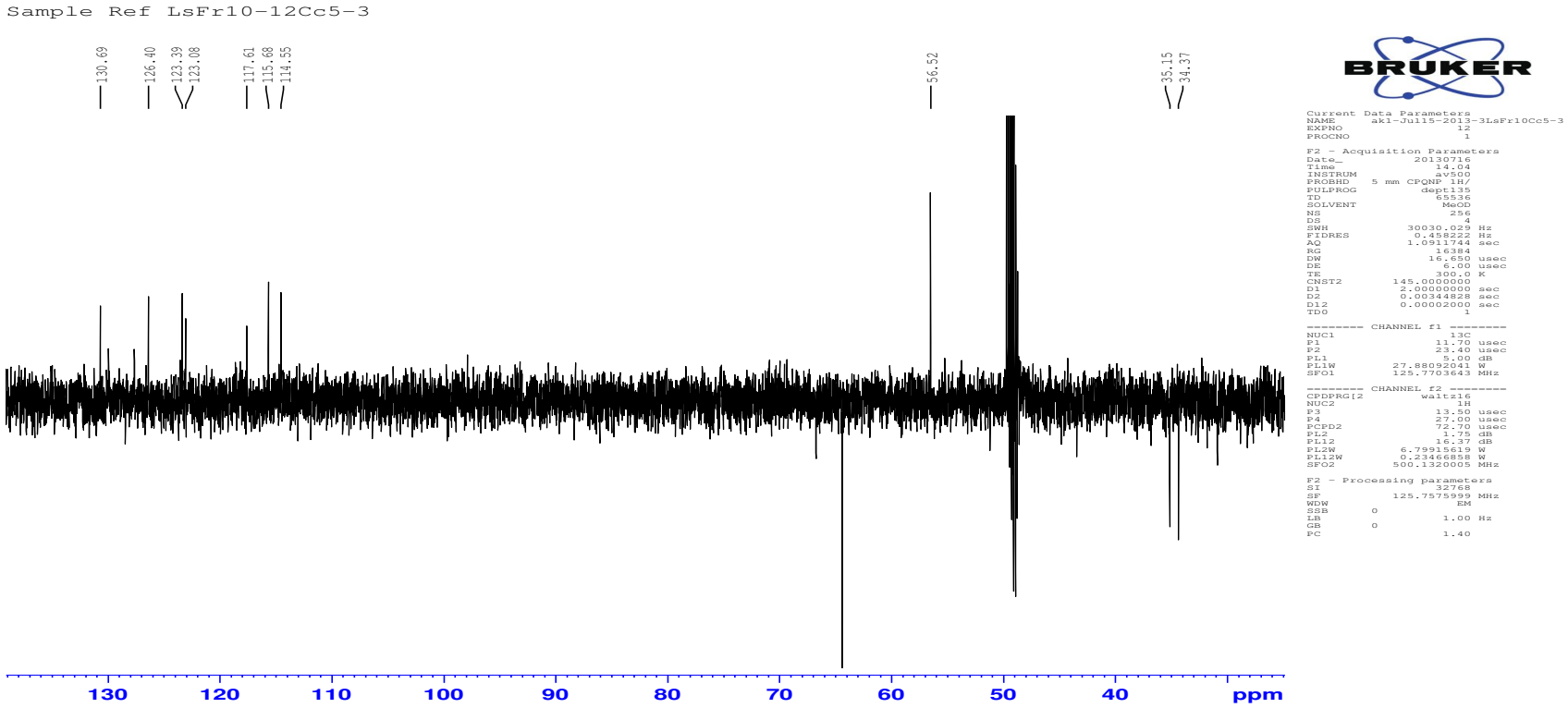

Figure A.7 DEPT-135 NMR spectrum for **AK-6**

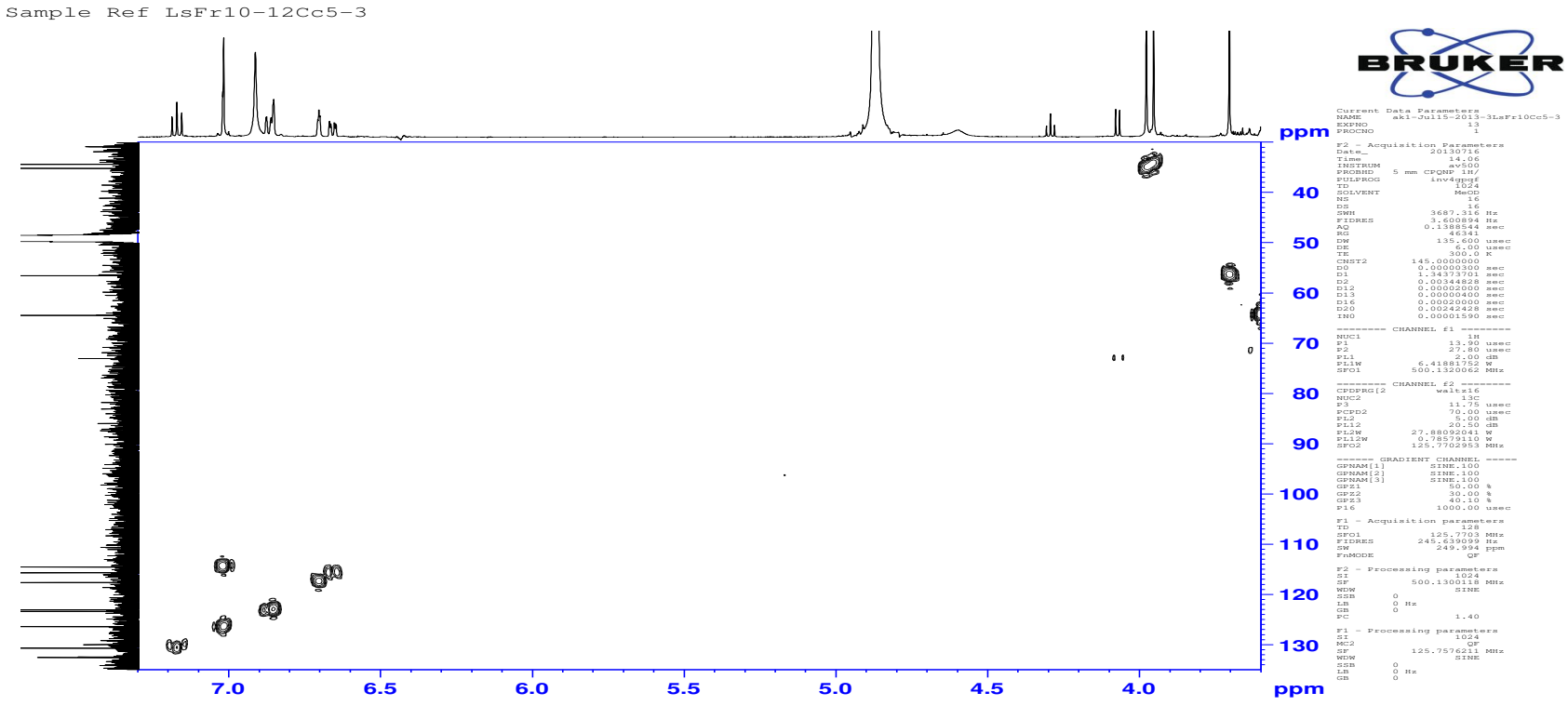

Figure A.8 HMQC NMR spectrum for **AK-6**

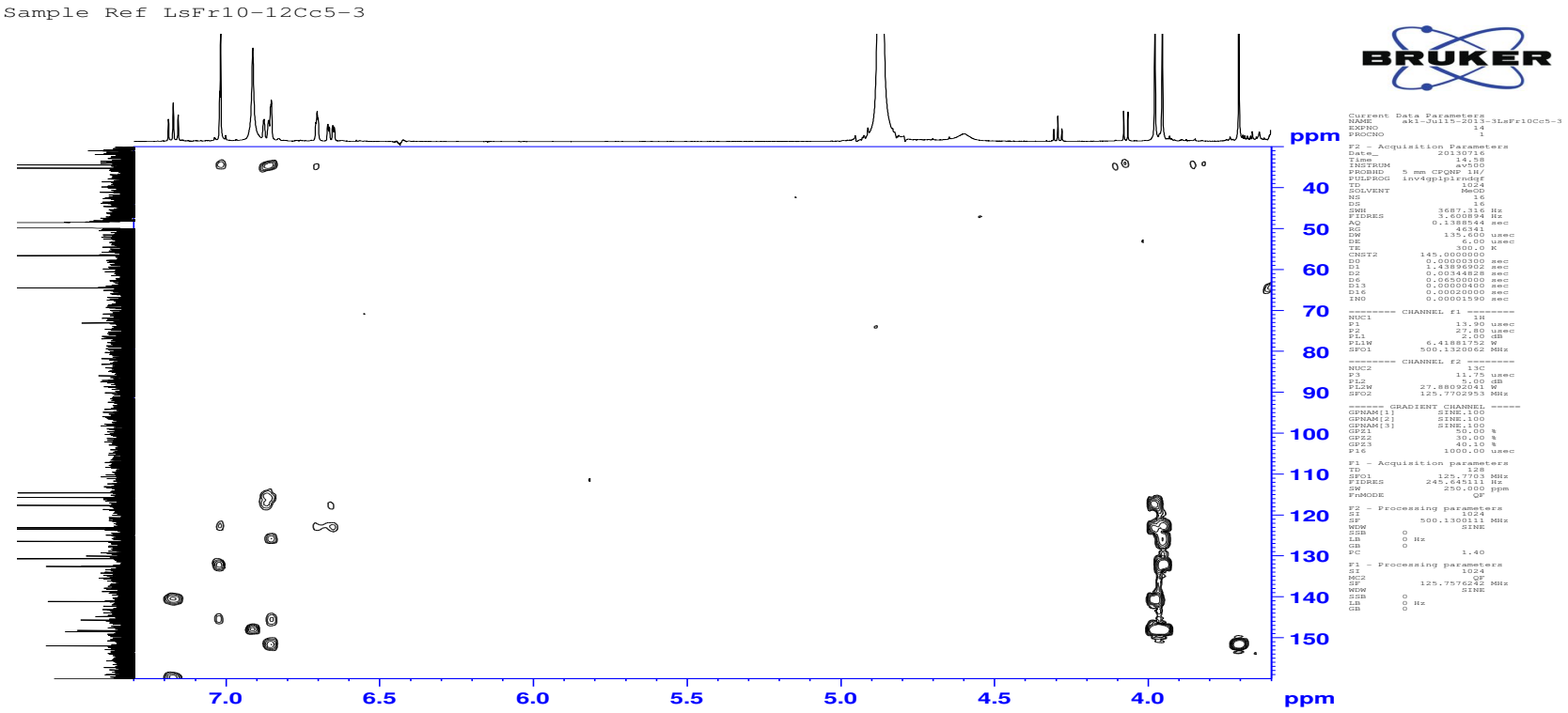

Figure A.9 HMBC NMR spectrum for **AK-6**

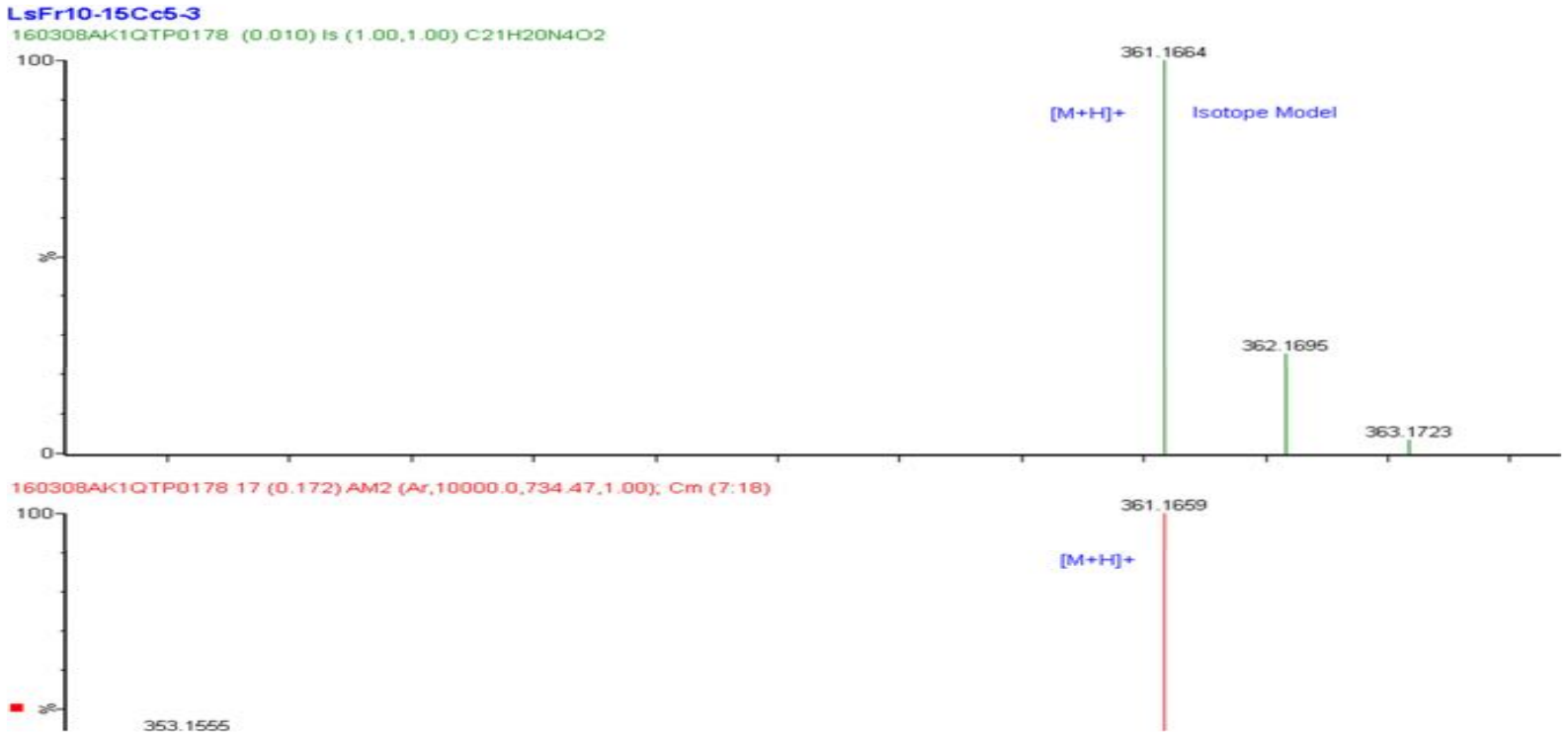

Figure A.10 HRTOFESIMS spectrum for **AK-6**

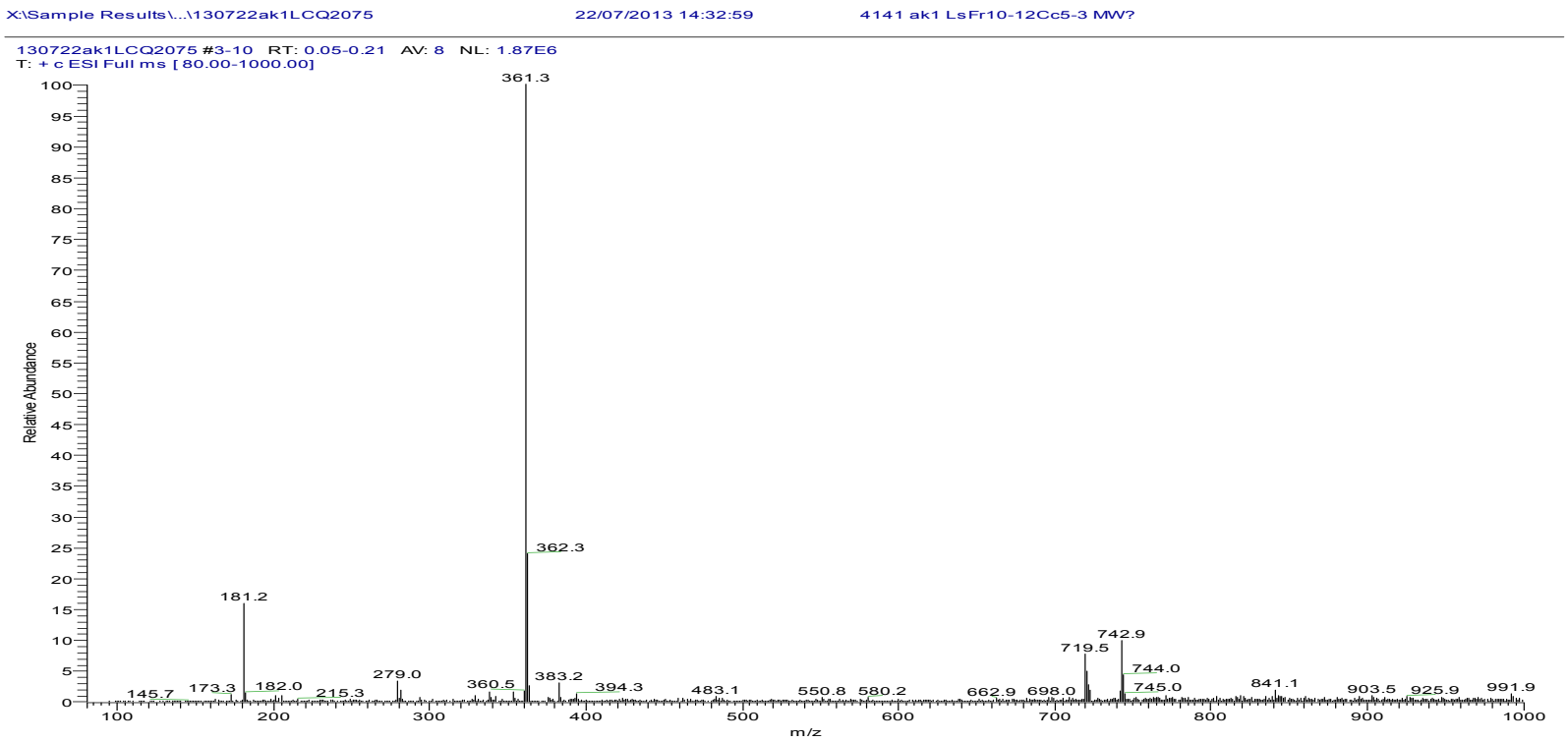

Figure A.11 ESI-MS spectrum for **AK-6**

Appendix C: NMR and HRTOFESIMS spectra for AK-7

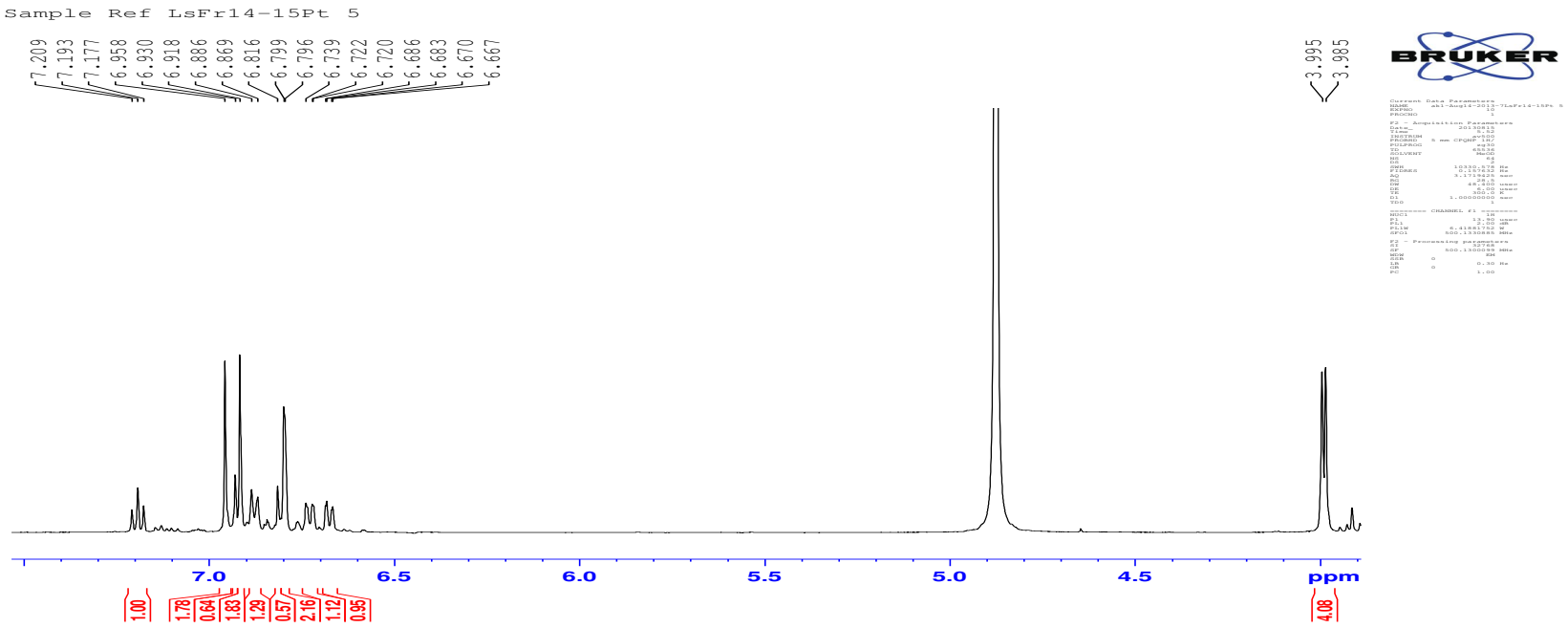

Figure A.12 ^{1}H NMR spectrum for **AK-7,** recorded in CD_3OD, 500 MHz

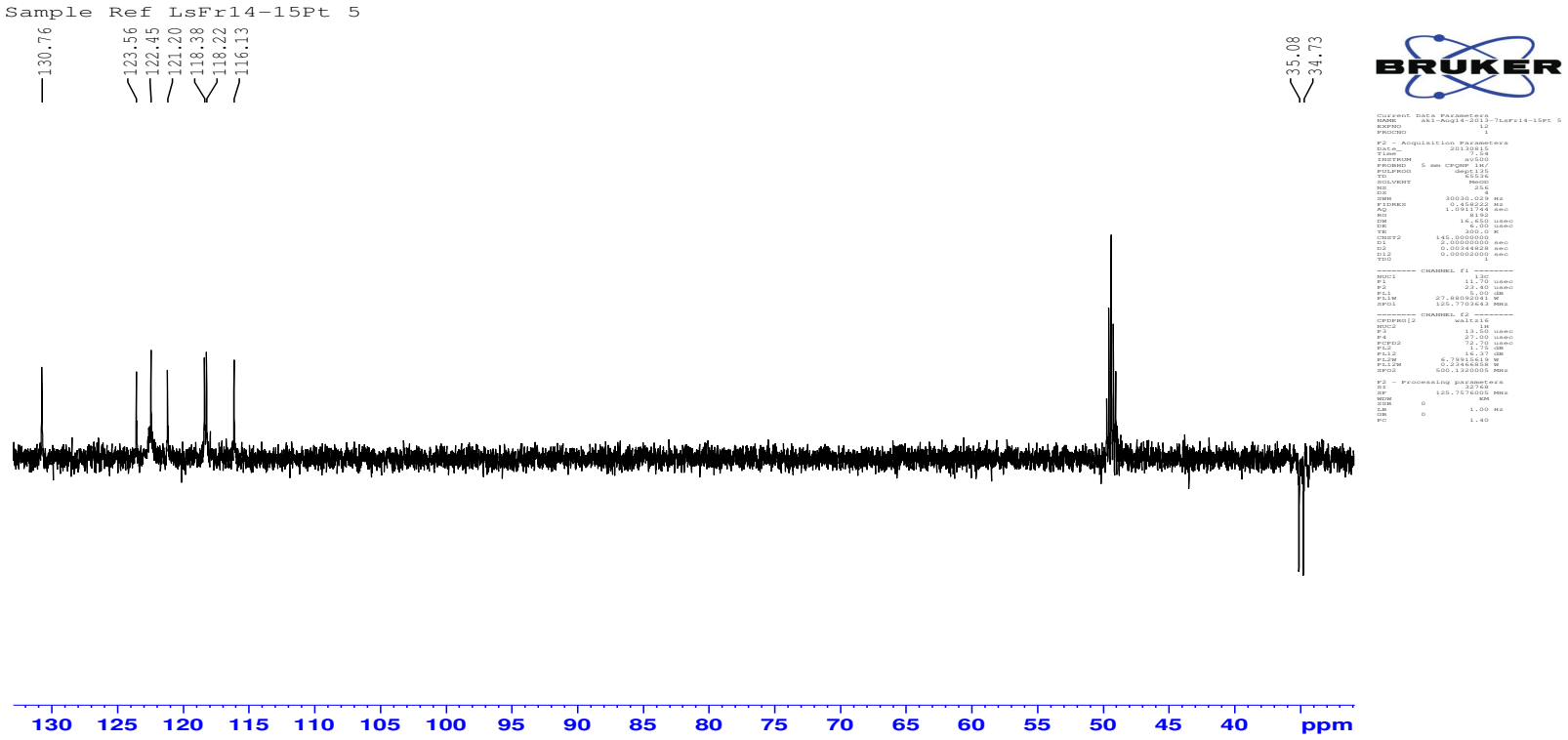

Figure A.13 DEPT-135 NMR spectrum for **AK-7**

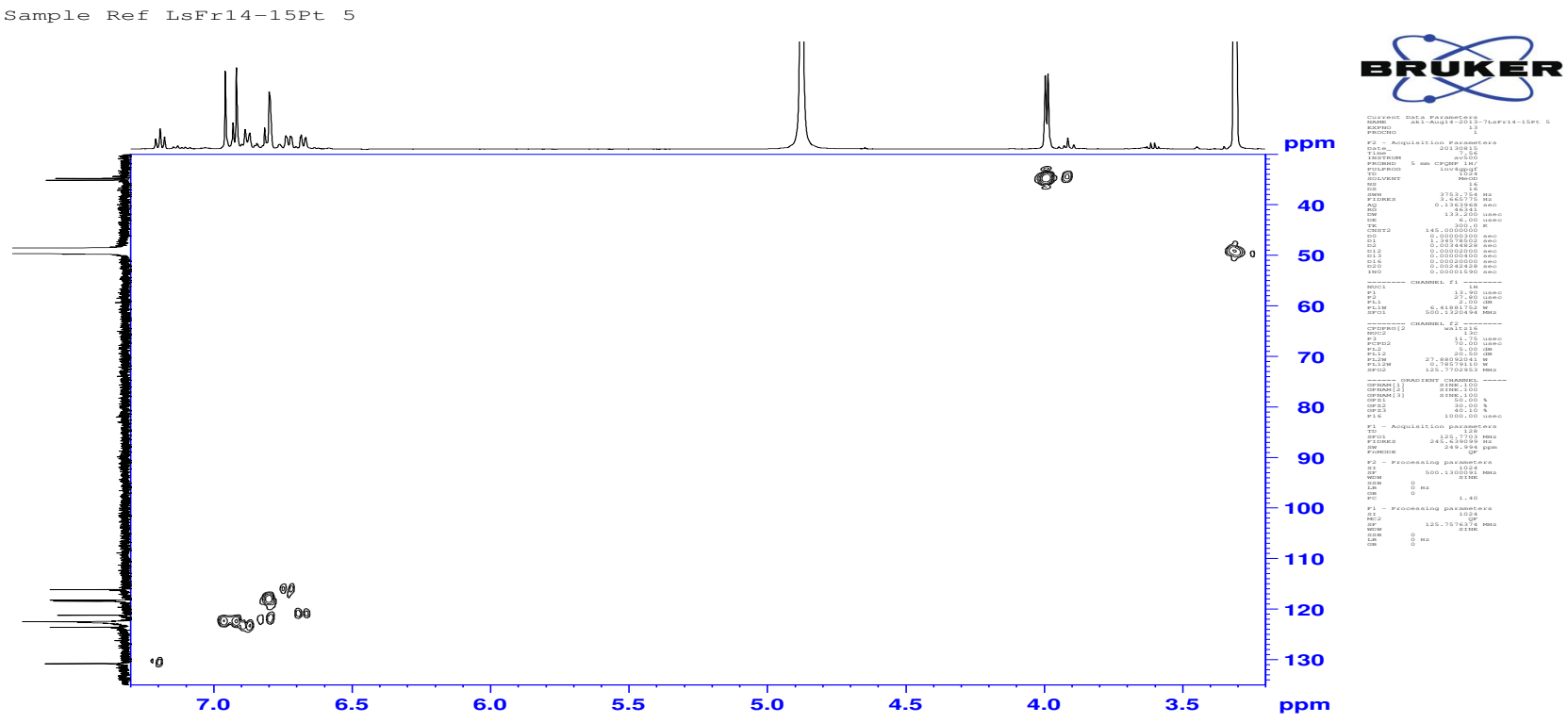

Figure A.14 HMQC NMR spectrum for **AK-7**

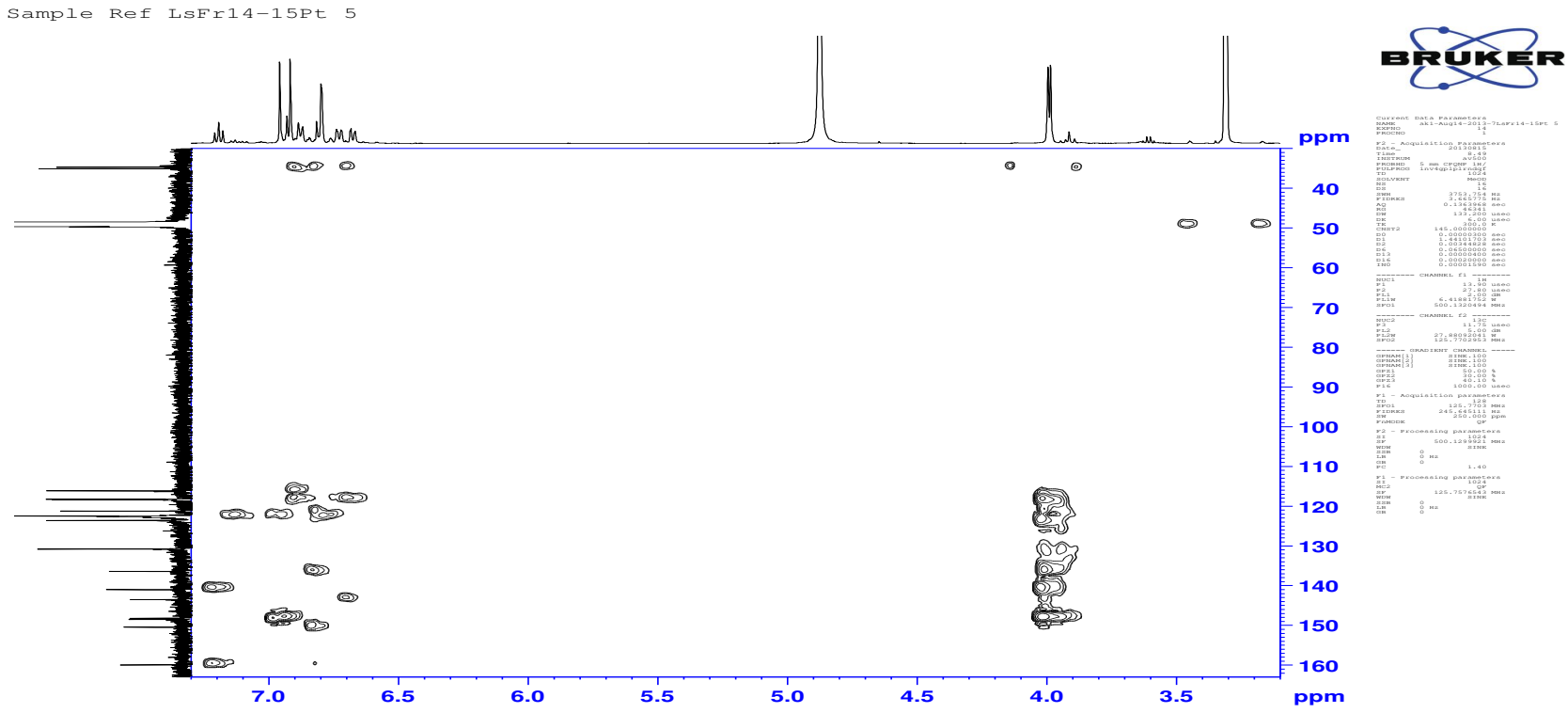

Figure A.15 HMBC NMR spectrum for **AK-7**

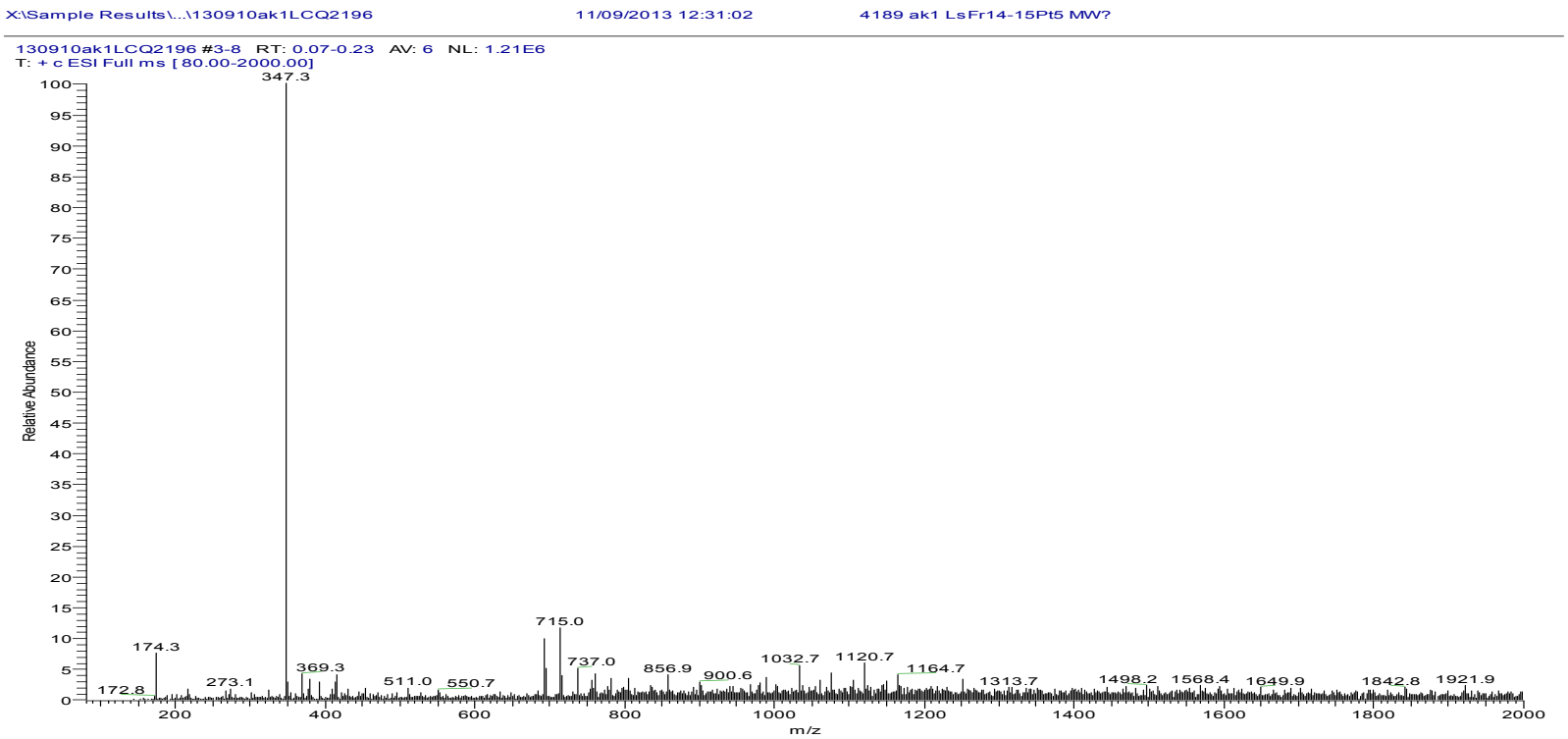

Figure A.16 ESI-MS NMR spectrum for **AK-7**

Appendix D: COSY and NOESY spectra for AK-12

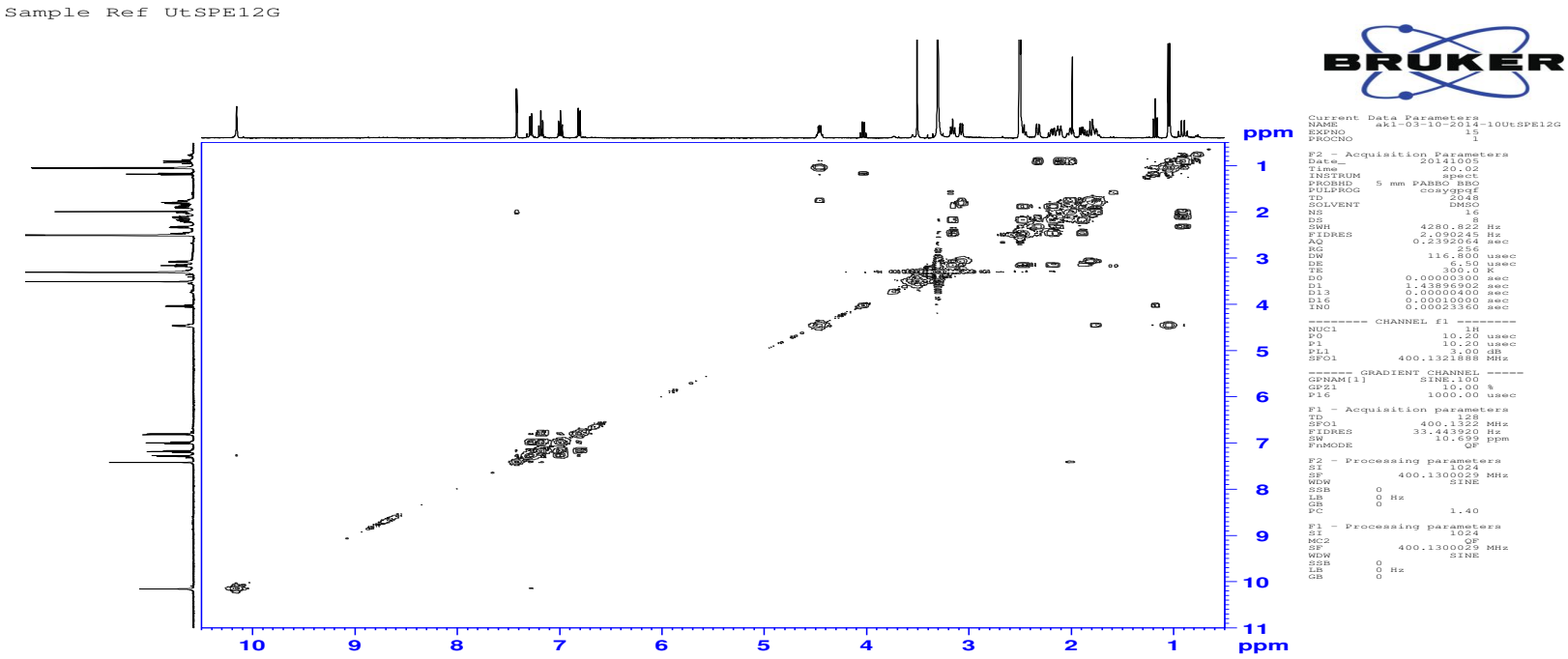

Figure A.17 COSY NMR spectrum for **AK-12**

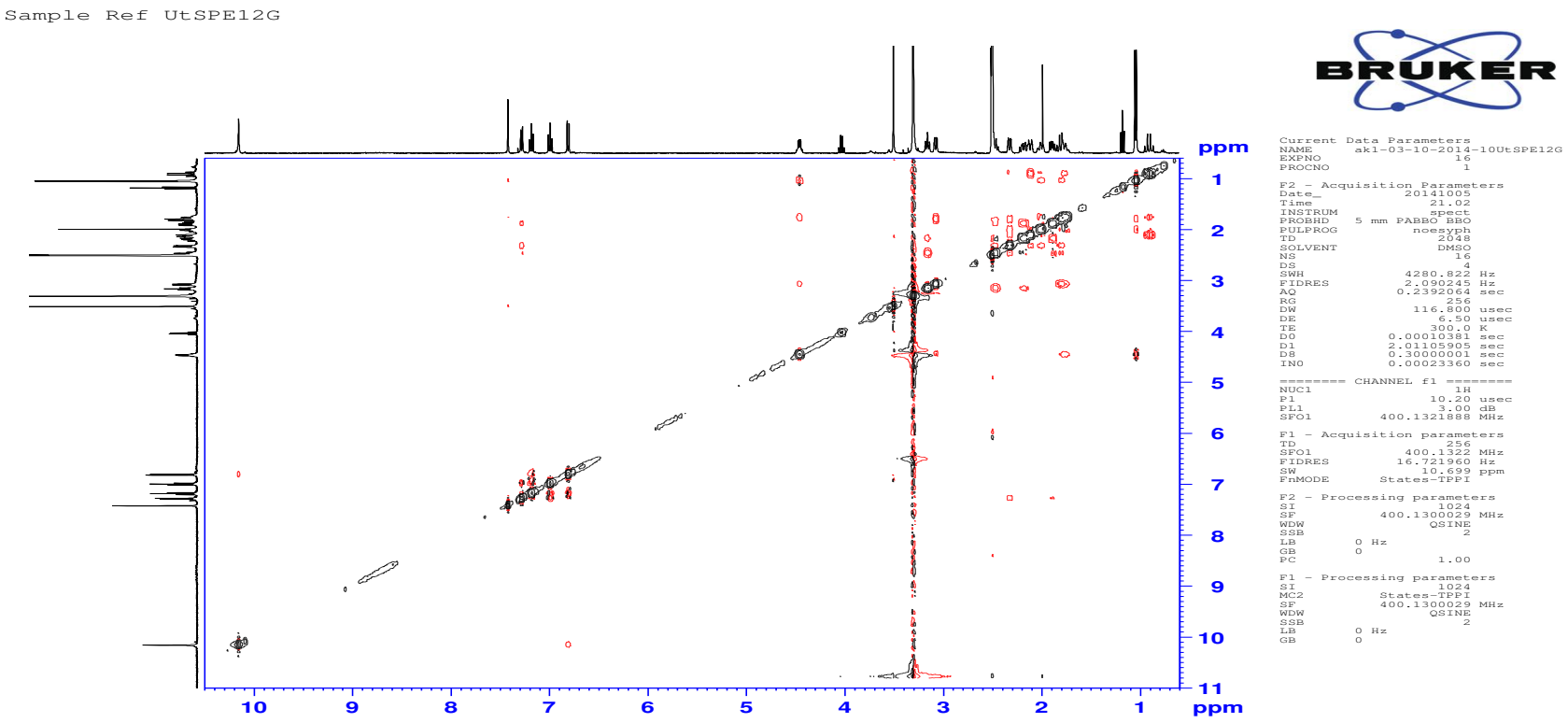

Figure A.18 NOESY NMR spectrum for **AK-12**

Appendix E: COSY and NOESY spectra for AK-13

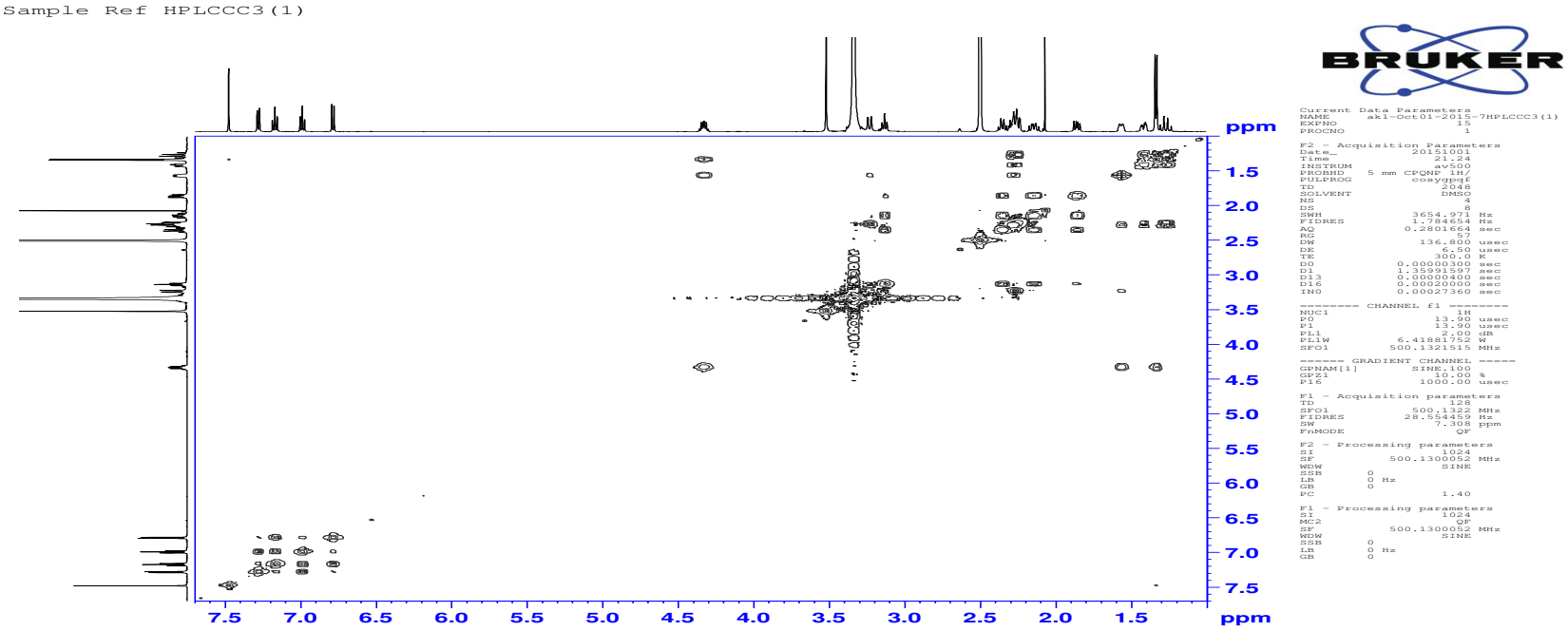

Figure A.19 COSY NMR spectrum for **AK-13**

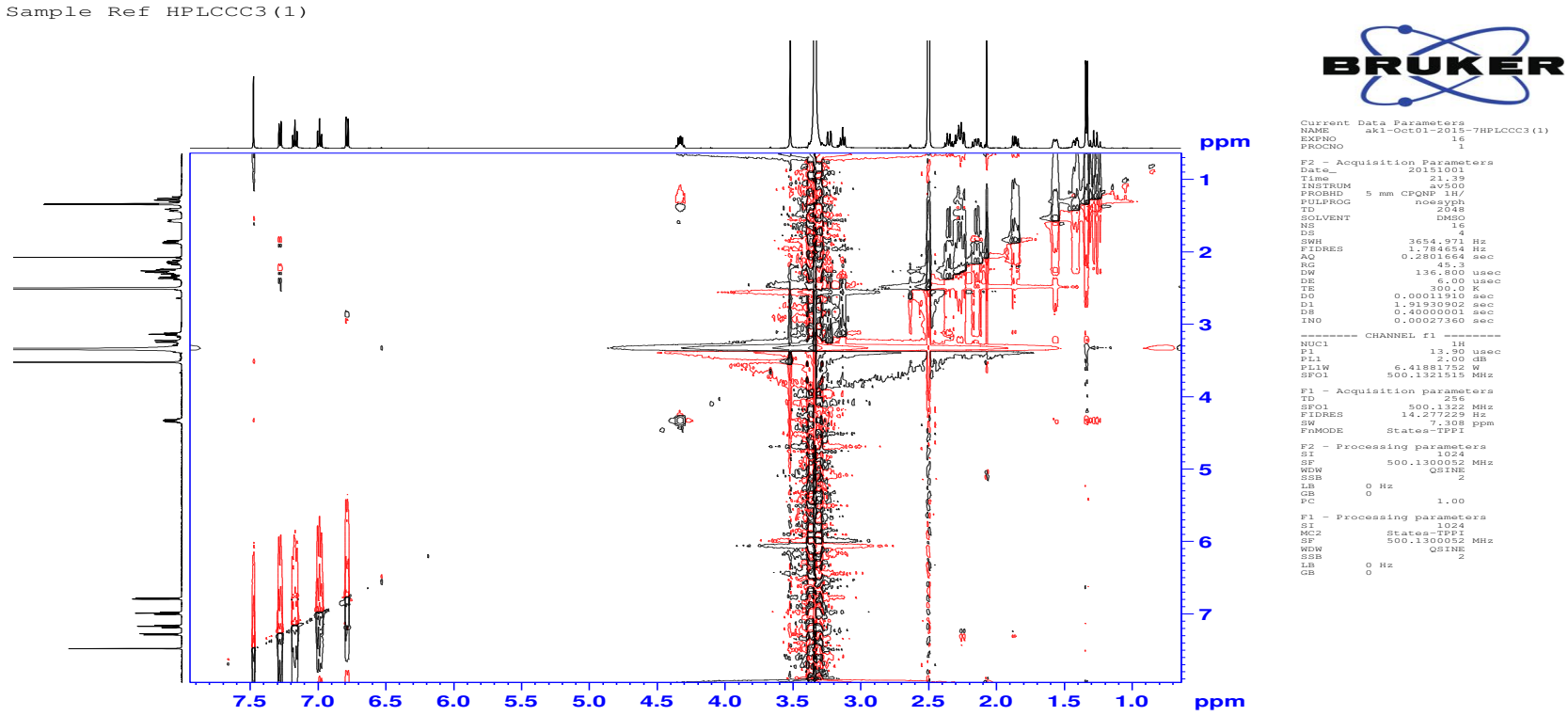

Figure A.20 NOESY NMR spectrum for **AK-13**

Appendix F: COSY and NOESY spectra for AK-14

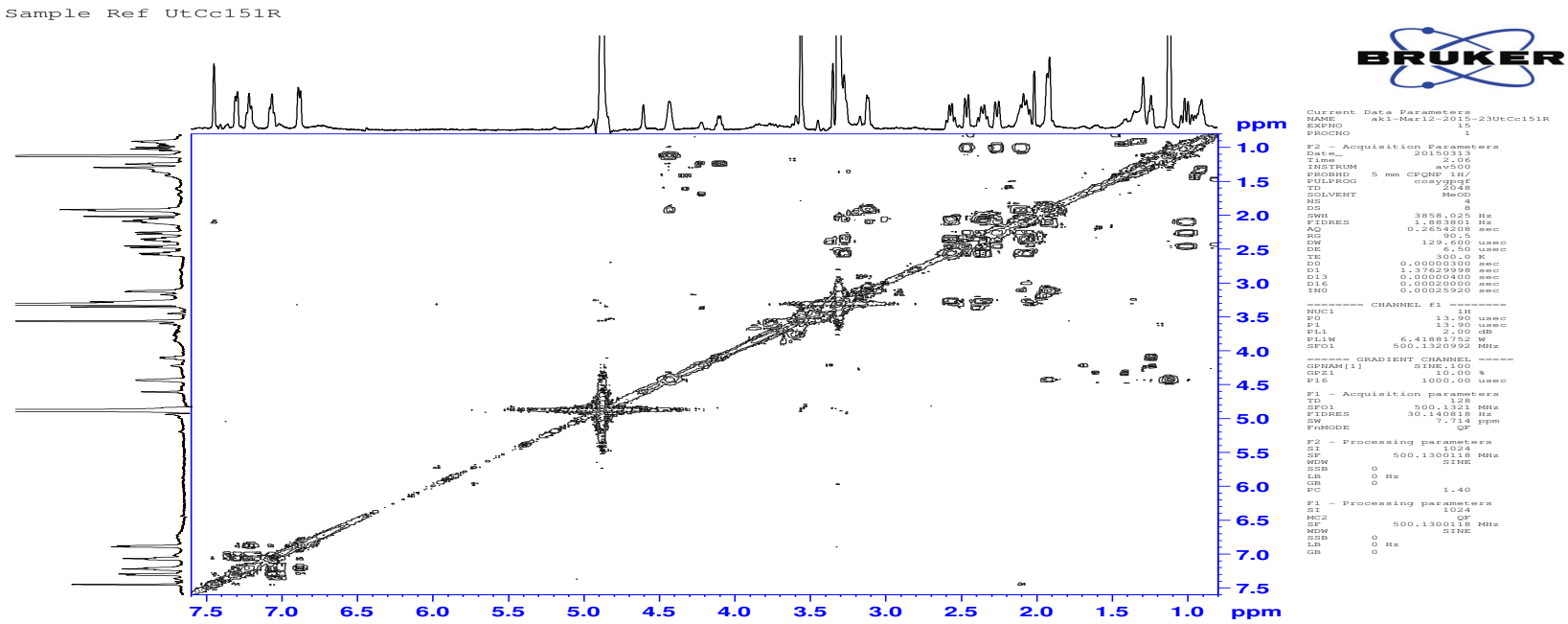

Figure A.21 COSY NMR spectrum for **AK-14**

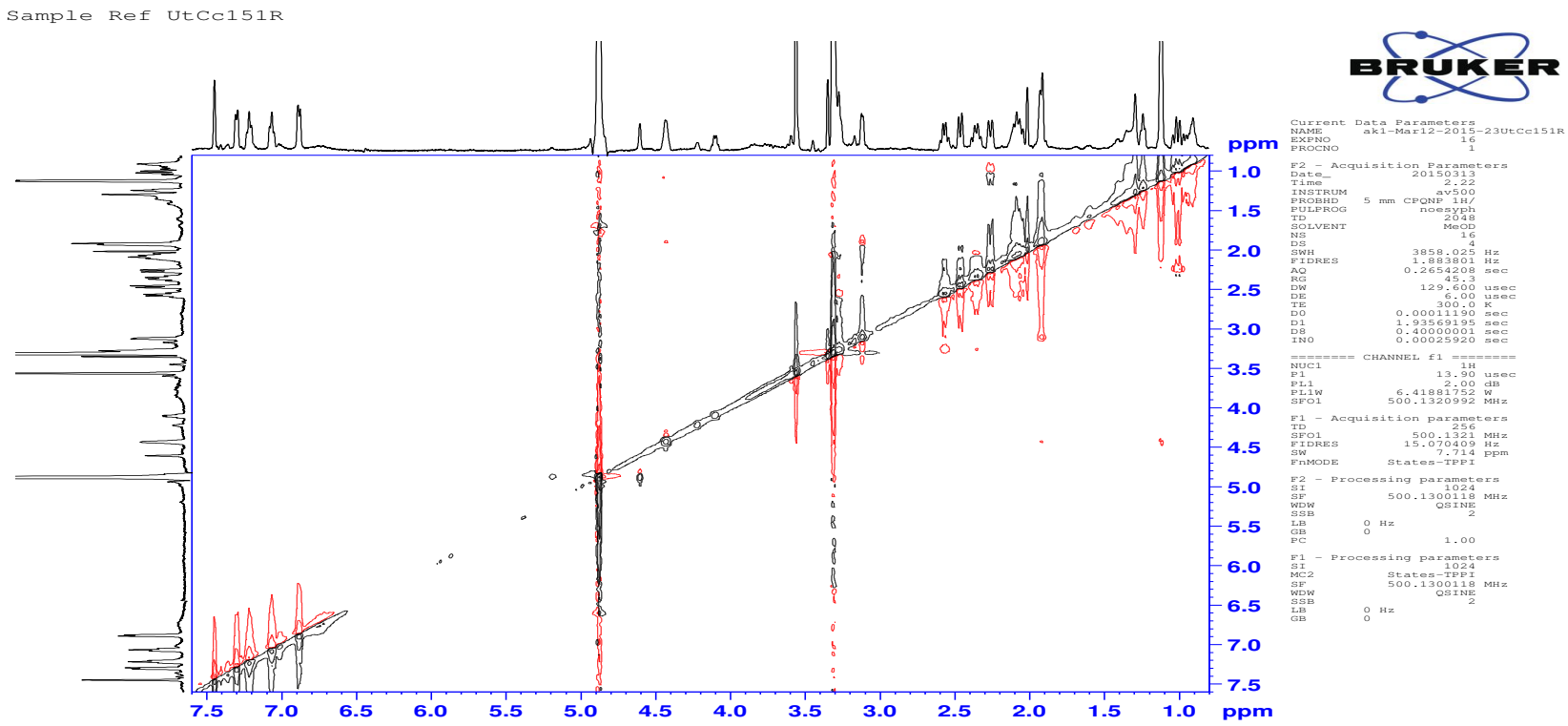

Figure A.22 NOESY NMR spectrum for **AK-14**

Appendix G: MS spectra for the isolated compounds

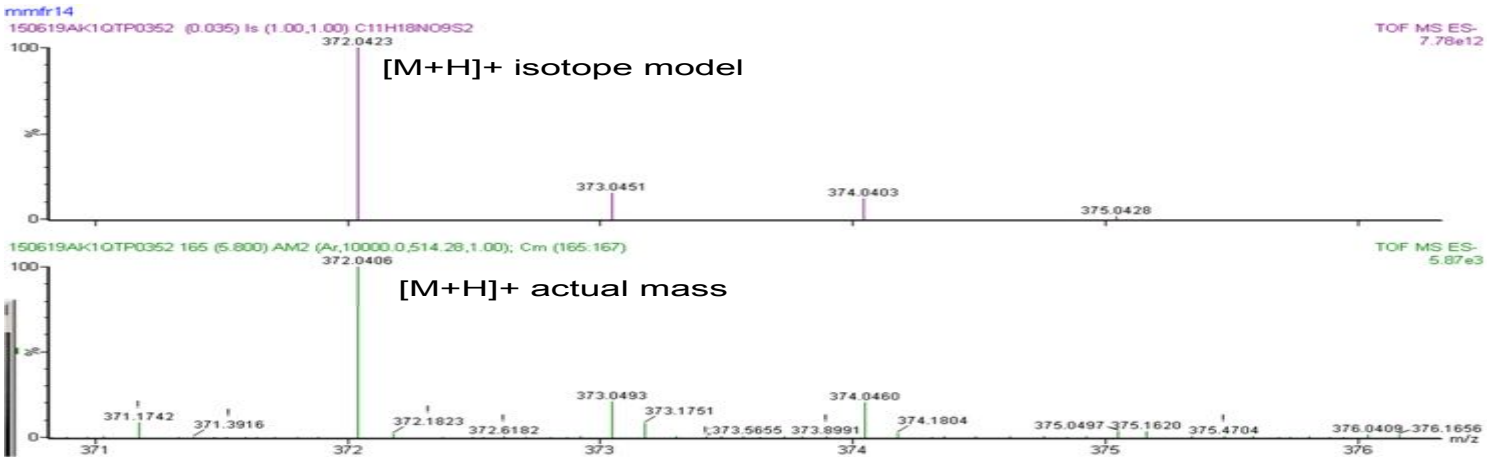

Figure A.23 HRTOFESIMS spectrum for **AK-1**

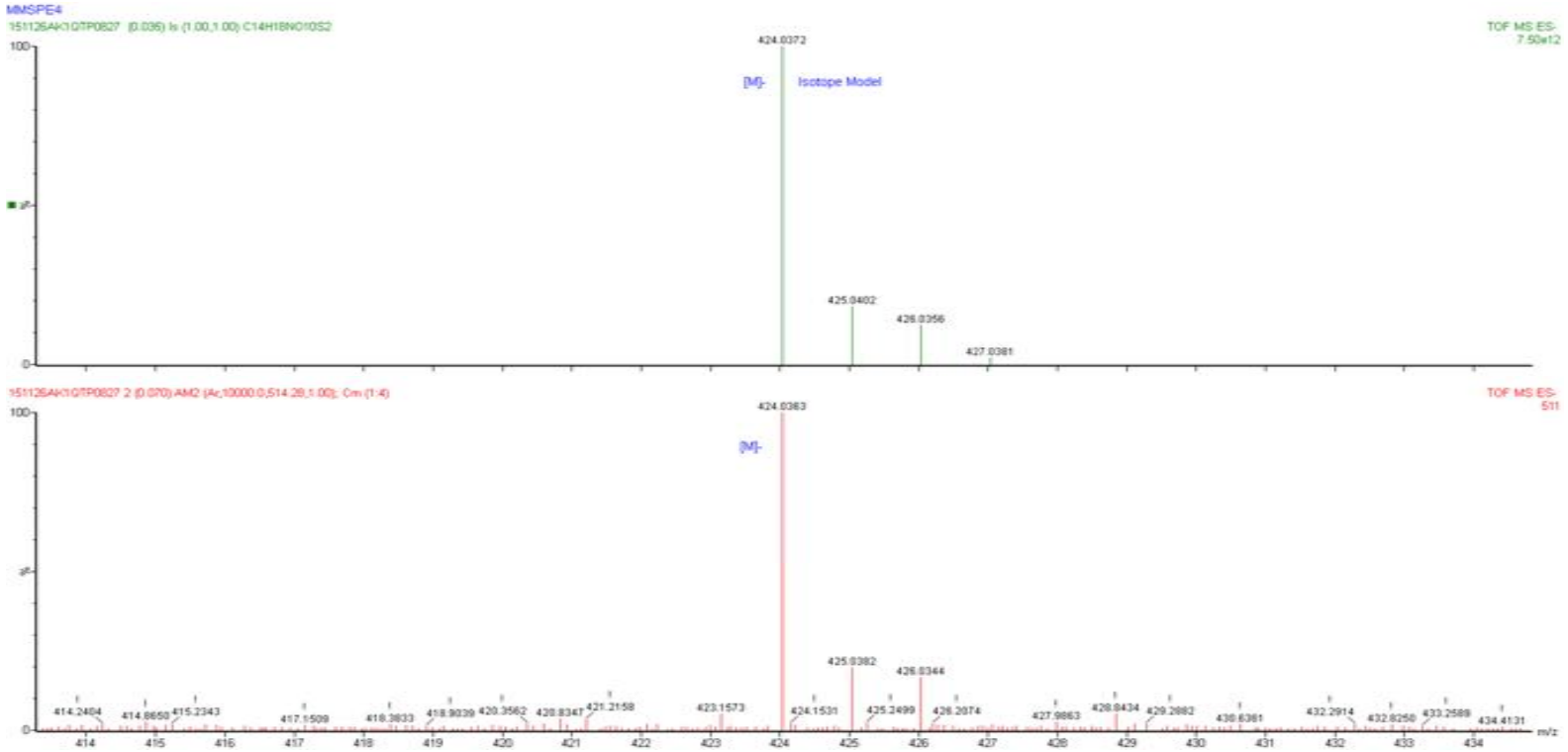

Figure A.24 HRTOFESIMS spectrum for **AK-2**

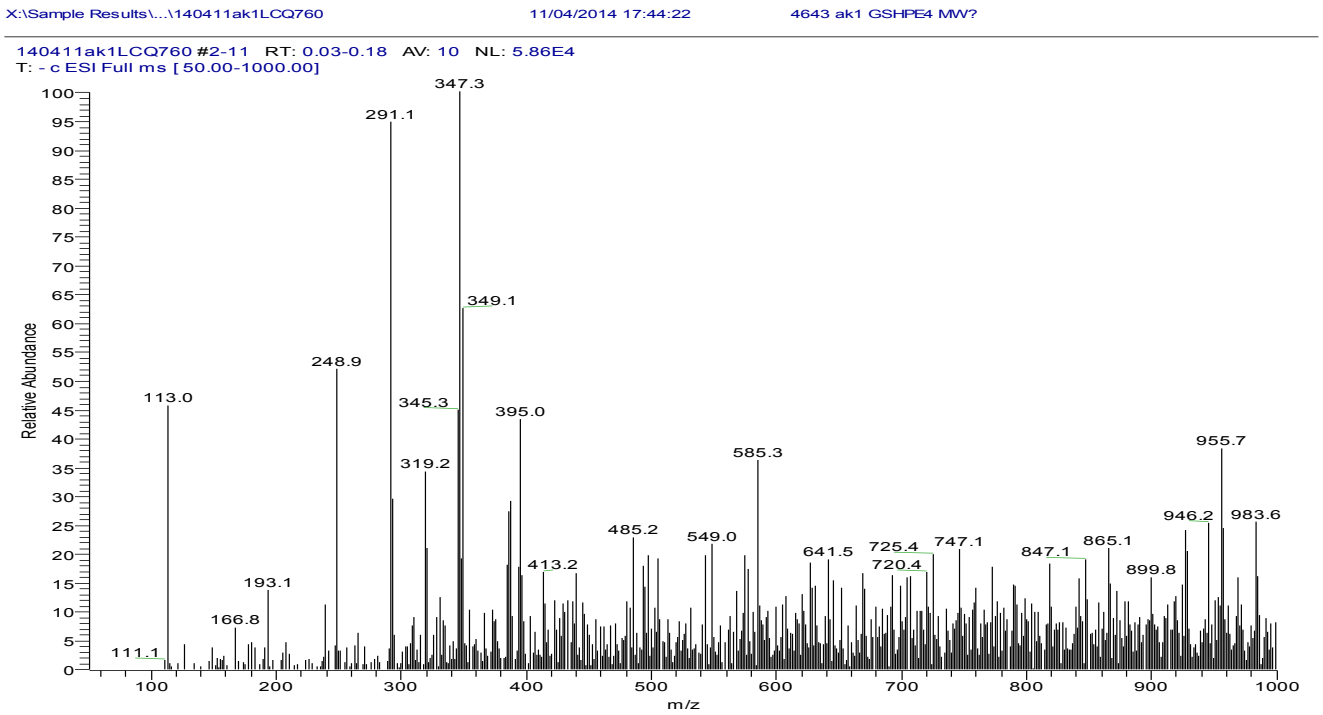

Figure A.25 ESI-MS spectrum for **AK-8**

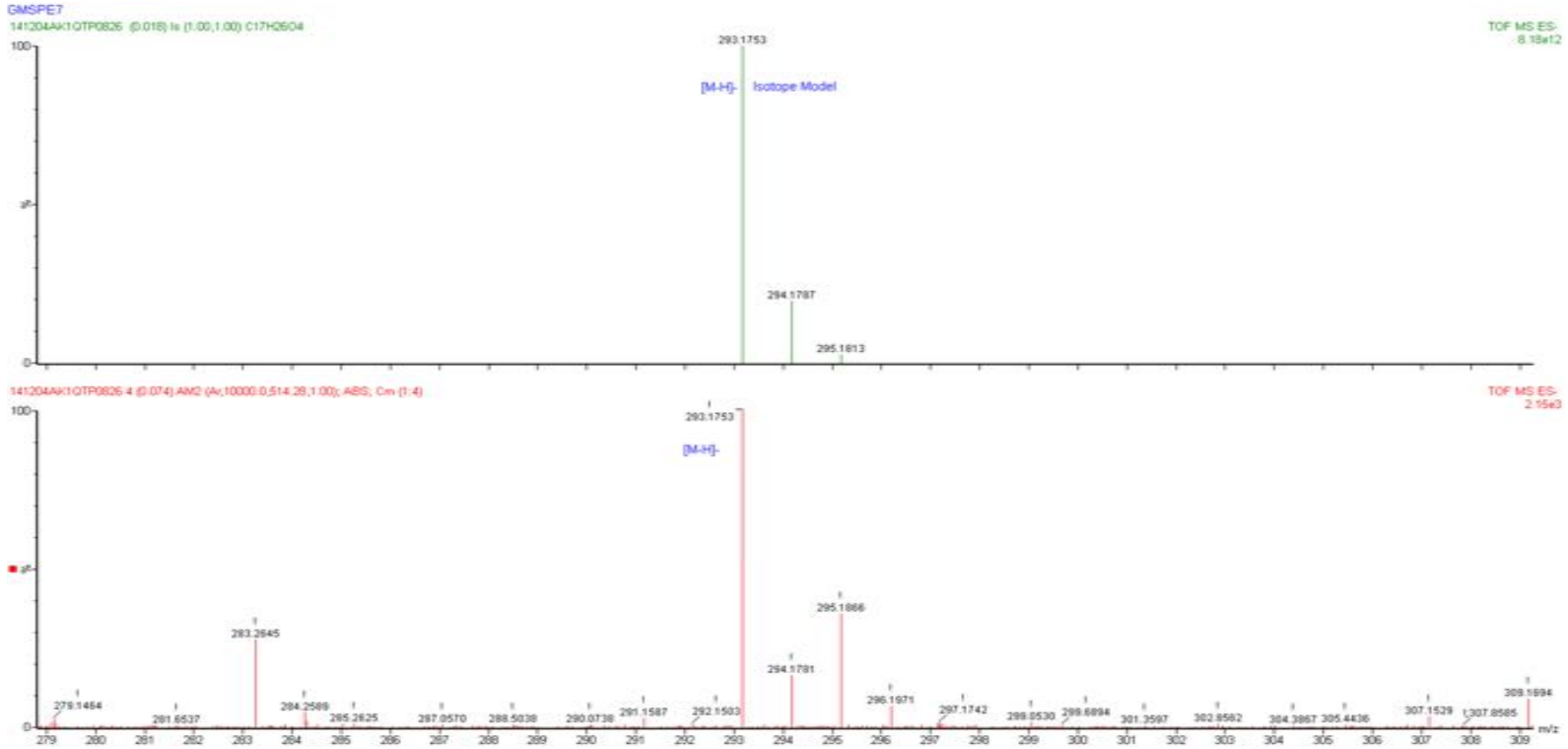

Figure A.26 HRTOFESIMS spectrum for **AK-9**

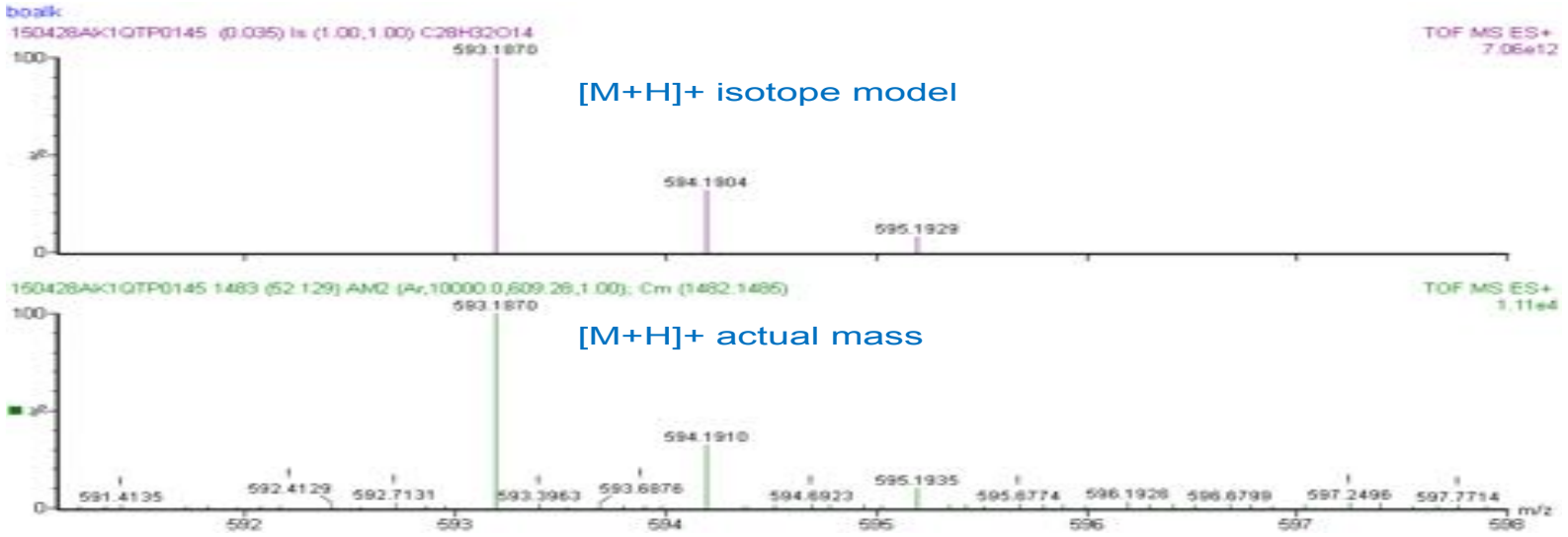

Figure A.27 HRTOFESIMS spectrum for **AK-10**

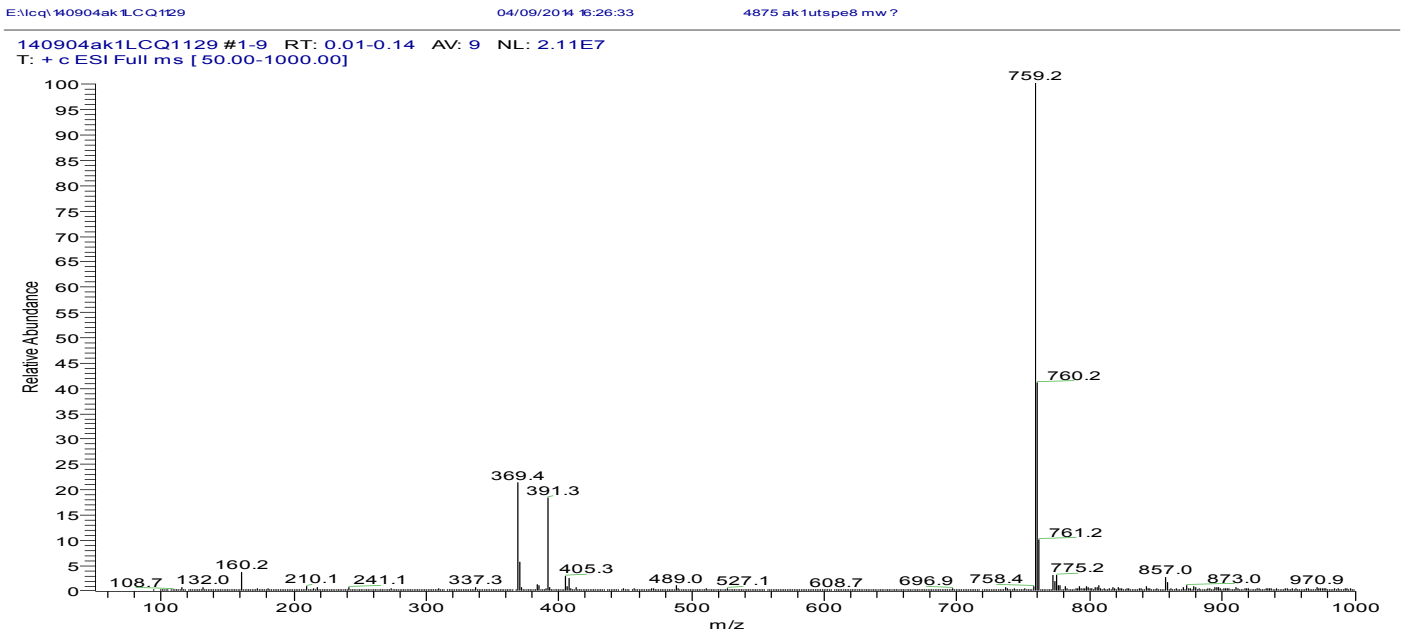

Figure A.28 ESI-MS spectrum for **AK-11**

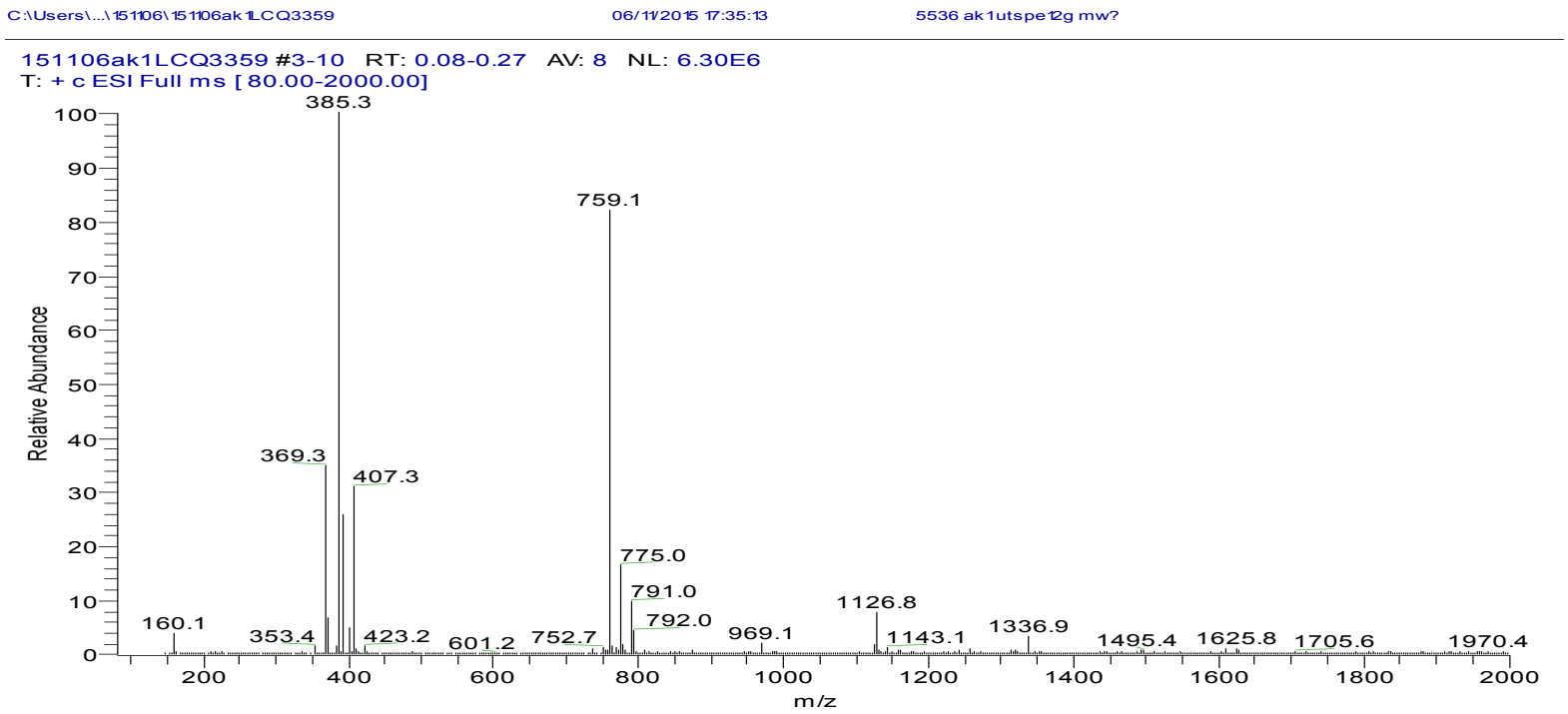

Figure A.29 ESI-MS spectrum for **AK-12**

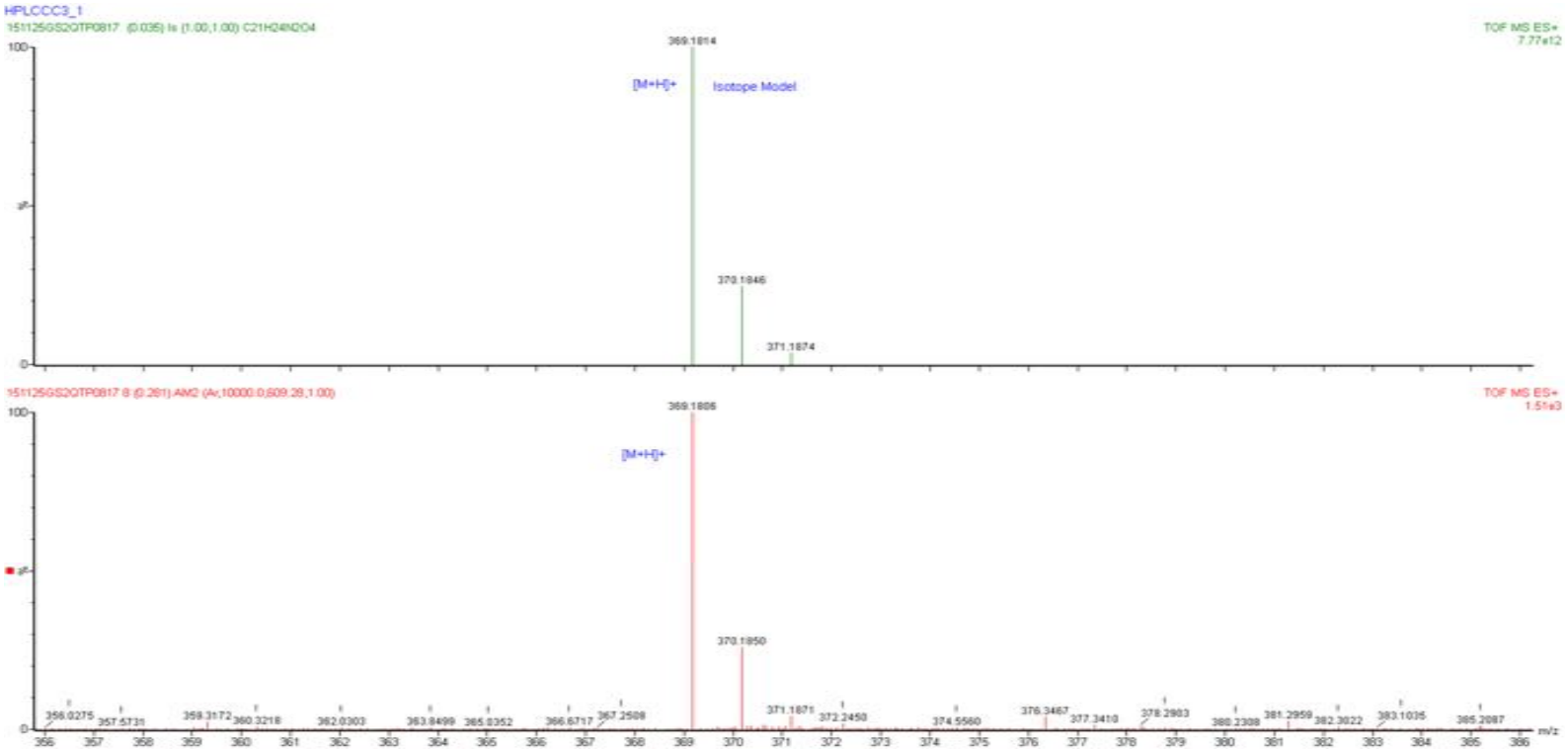

Figure A.30 HRTOFESIMS spectrum for **AK-13**

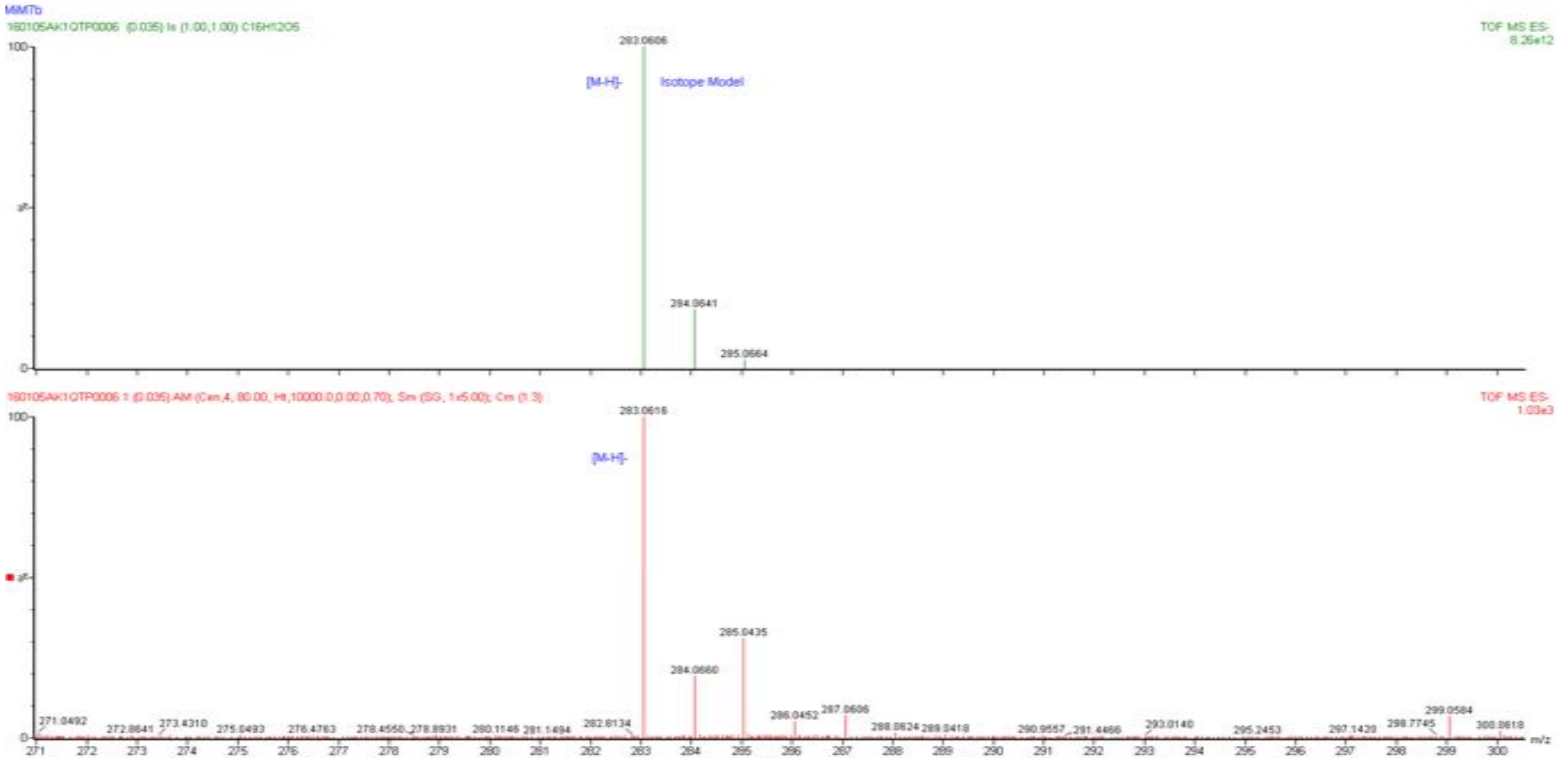

Figure A.31 HRTOFESIMS spectrum for **AK-15**

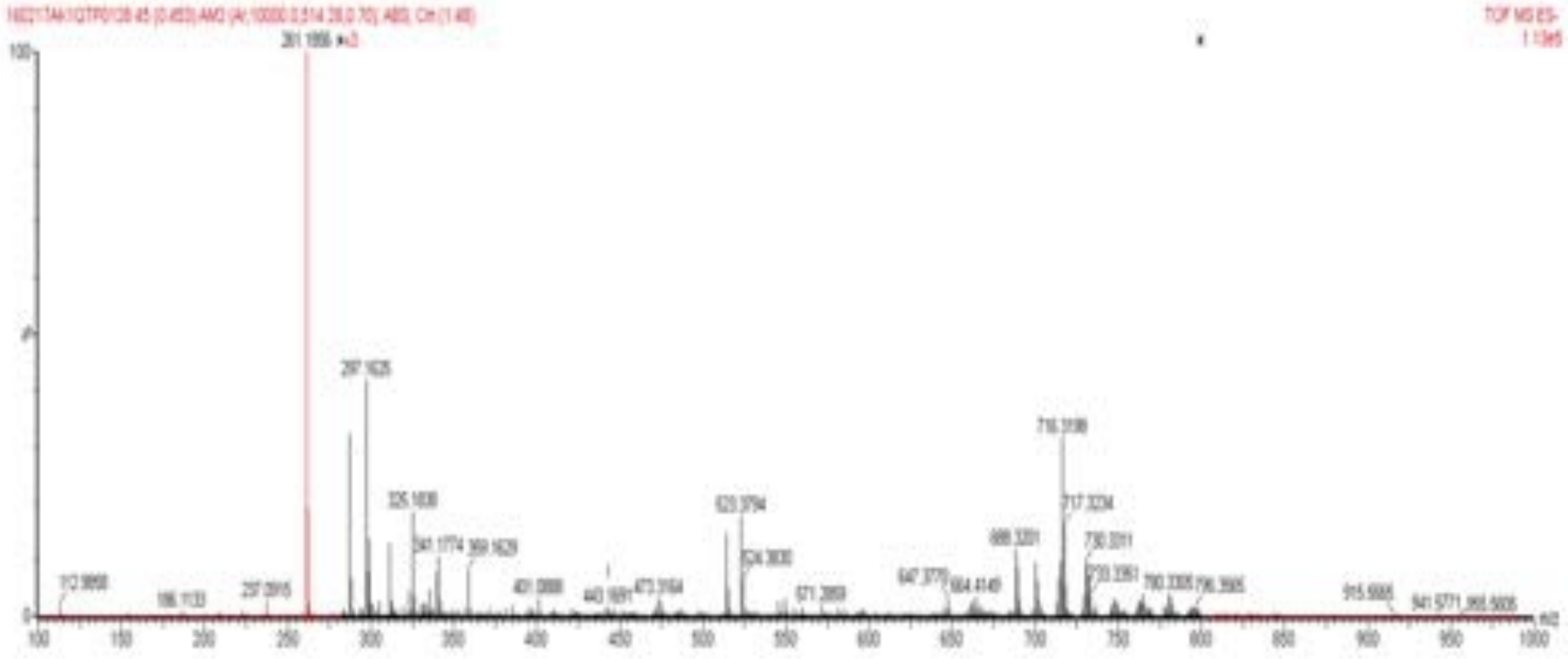

Figure A.32 HRTOFESIMS spectrum for **AK-16**

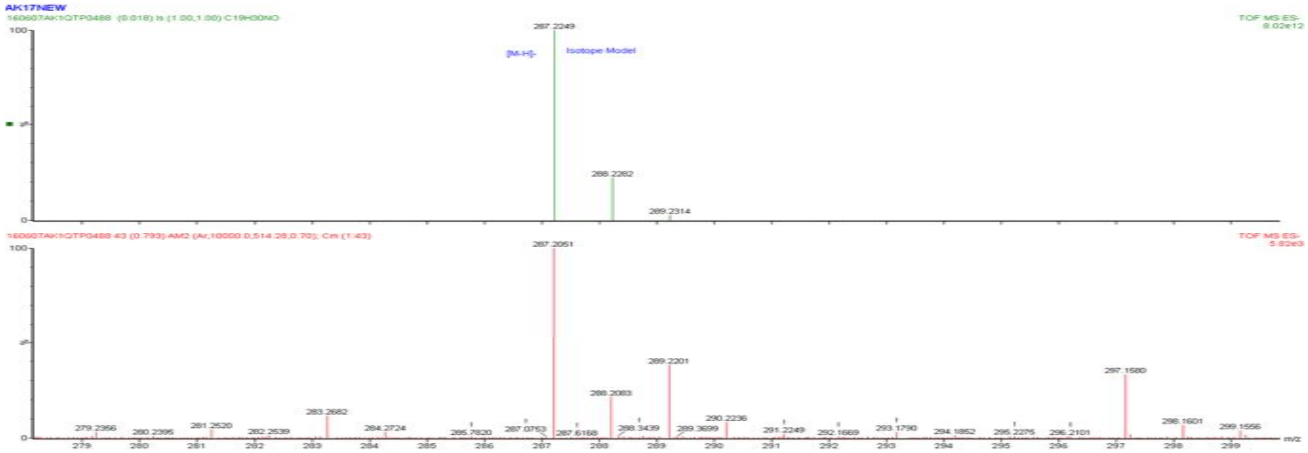

Figure A.33 HRTOFESIMS spectrum for **AK-17**

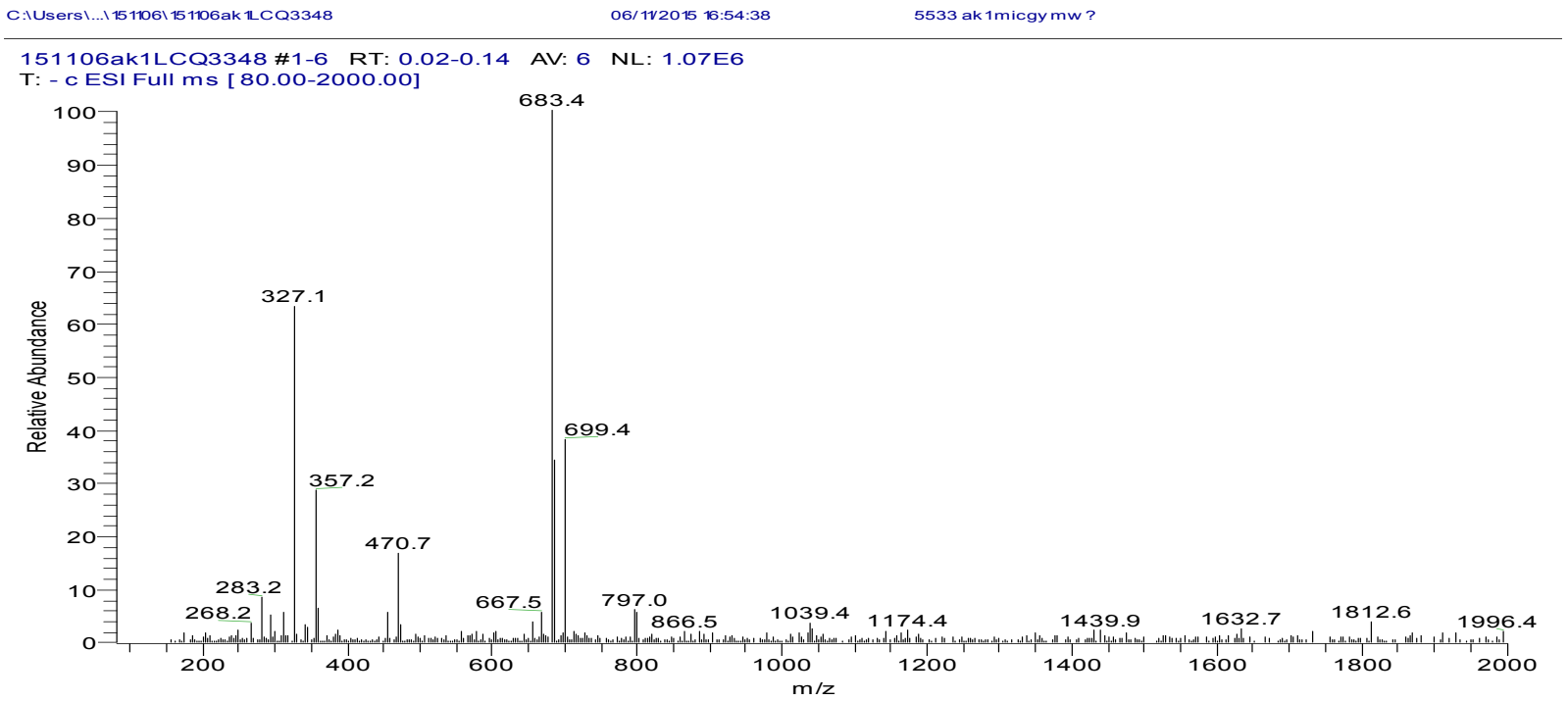

Figure A.34 ESI-MS spectrum for **AK-18**